

# Open Research Online

---

The Open University's repository of research publications and other research outputs

## Investigation of Sirtuins as Therapeutic Targets in Neurodegenerative Disorders: Studies on Mechanisms and Possible Combined Therapy

Thesis

How to cite:

Fusco, Federica (2020). Investigation of Sirtuins as Therapeutic Targets in Neurodegenerative Disorders: Studies on Mechanisms and Possible Combined Therapy. PhD thesis The Open University.

For guidance on citations see [FAQs](#).

© 2019 The Author

Version: Version of Record

Link(s) to article on publisher's website:  
<http://dx.doi.org/doi:10.21954/ou.ro.0001177d>

---

Copyright and Moral Rights for the articles on this site are retained by the individual authors and/or other copyright owners. For more information on Open Research Online's data [policy](#) on reuse of materials please consult the policies page.

---

[oro.open.ac.uk](http://oro.open.ac.uk)

**INVESTIGATION OF SIRTUINS AS  
THERAPEUTIC TARGETS IN  
NEURODEGENERATIVE DISORDERS: STUDIES  
ON MECHANISMS AND POSSIBLE COMBINED  
THERAPY**

Thesis submitted by

**Federica Fusco**

For the degree of Doctor of Philosophy

Discipline of Life and Biomolecular Sciences

The Open University, UK

Affiliated Research Centre: Istituto di Ricerche Farmacologiche  
Mario Negri IRCCS, Milan, IT - Department of Neuroscience

September 2019

## **DECLARATION**

The data presented in this thesis are original, were not previously used for any other PhD degree and were generated by myself.

During my PhD, I worked in the Genetic of Neurodegenerative Disorders Unit, Department of Neuroscience, at Istituto di Ricerche Farmacologiche Mario Negri IRCCS, Milan, Italy. My director of studies was Dr. Diego Albani and my external supervisor was Prof. Calum Sutherland from Dundee University, UK. Hydrogel formulation protocols for experiments in Chapter 5 were kindly provided by a collaboration with Prof. Carmen Giordano (Politecnico di Milano).

# Abstract

Up to now, current therapies for Alzheimer's disease (AD) can treat the symptoms with modest effect and have little impact on the overall progression. AD is a complex, multifactorial disorder, featured by aggregation of toxic proteins, inflammation, oxidative stress, synaptic deficits, and cognitive decline. Thus, the multi-target therapeutic strategy is of particular interest as it uses a combination of drugs to affect different molecular targets and converge on neuroprotection or even disease modification.

In drug discovery for neurodegenerative processes, an interesting role emerged for the histone-deacetylase enzymes Sirtuins (SIRTs), and SIRT1 and SIRT2 have been associated with neuroprotection and neurodegeneration, respectively.

The availability of SIRTs small molecule modulators allowed the achievement of good results of SIRT1 activation or SIRT2 inhibition in models of neurodegeneration and AD, as both SIRTs are actively involved, to different extent, in the regulation of amyloidogenic processing, inflammatory and oxidative cascades. A direct intervention on such molecular players could be beneficial in obtaining cognitive or pathologic phenotype improvement deriving from multiple pathways targeting.

In this work, we aimed at combining SIRT1 activation and SIRT2 inhibition to study a possible multi-target approach on AD models, both *in vitro* and *in vivo*. An initial drug dose-response and biochemical assessment was performed on the AD *in vitro* model H4-sw, focusing on the increase of the neuroprotective sAPP $\alpha$  fragment.

Next, 3xTg-AD mice received the single or the combined treatment with SIRT1 activator SRT2104 and SIRT2 inhibitor AK7 for two weeks, and the effects on cognitive performance and key biochemical parameters were assessed.

Results showed that both SIRT1 and SIRT2 single modulation independently improved cognitive performance in treated mice. Combined treatment showed complete memory recovery too. Some differences between single and double treatment emerged in biochemical assessments.

Double-treated mice had increased NRF2, sAPP $\alpha$  and reduced A $\beta$  oligomers in hippocampus, already seen upon SIRT2 inhibition, suggesting that cognitive improvement given by SIRT2 modulation could be attributed to those underlying effects.

Together with memory recovery, SIRT1 activator treated mice showed decreased hippocampal CD11b and GFAP, increased synaptophysin, SOD1, sAPP $\alpha$  and NRF2, all seen upon double treatment too.

Thus, SIRT1 and SIRT2 independent modulations could improve memory deficit acting both on peculiar or common protein targets.

In conclusion, the combined treatment resumed all the behavioural and biochemical effects of single modulations. Our data support the concept that, with a multi-target strategy, it could be possible to take full advantage of the complementarity of SIRT1/SIRT2 treatments and obtain cognitive improvement based on changes on several underlying biochemical mechanisms that with single modulation could only be partially achieved.

All these observations could open up new insights for research on SIRTs involvement in AD and neurodegeneration.

# Acknowledgments

*Firstly, I would like to express my sincere gratitude to my Supervisor Dr. Diego Albani, for encouraging my research and for allowing me to grow professionally in the Genetics of Neurodegenerative Disorders Unit.*

*Thanks also to my external Supervisor, Dr. Calum Sutherland, for his time and advice during the writing of this thesis, and to Dr. Gianluigi Forloni for giving me the opportunity to join his lab at the Mario Negri Institute for Pharmacological Research.*

*A special thanks goes to my lab team members, present and former, for their professional support, their friendship, and for lightening my path with a laugh whenever it got tough.*

*You will always find a friend in me.*

*The most important thank-you goes to my family. Thank you for supporting me for everything in my life; words cannot express how grateful I am for how much you believed in me and encouraged me throughout this experience.*

# Table of contents

DECLARATION .....	2
Abstract .....	3
Acknowledgments .....	5
Table of contents .....	6
List of figures and tables .....	9
List of abbreviations.....	14
<b>1. Introduction .....</b>	<b>17</b>
<b>1.1 Alzheimer’s disease.....</b>	<b>18</b>
1.1.1 CLINICAL SIGNS AND SYMPTOMS.....	19
1.1.2 DIAGNOSIS.....	21
1.1.3 PHYSIOPATHOLOGY.....	22
1.1.4 EPIDEMIOLOGY.....	25
1.1.5 ETIOLOGY.....	26
1.1.5.1 AD non-genetic risk factors .....	27
1.1.5.2 AD genetics.....	28
<b>1.2 AD pathogenesis: Amyloid Cascade Hypothesis.....</b>	<b>31</b>
1.2.1 Amyloid Precursor Protein (APP).....	33
1.2.2 APP PROTEOLYTIC PROCESSING.....	33
1.2.3 $\beta$ -AMYLOID PEPTIDE.....	36
1.2.3.1 A $\beta$ oligomers.....	38
1.2.4 sAPP $\alpha$ .....	41
1.2.5 sAPP $\beta$ .....	42
1.2.6 TAU PROTEIN.....	43
1.2.7 NEUROINFLAMMATION.....	46
1.2.8 OXIDATIVE STRESS.....	48
1.2.9 <i>IN VITRO</i> MODELS TO STUDY AD PATHOGENESIS.....	50
1.2.10 MOUSE MODELS TO STUDY AD PATHOGENESIS.....	53
<b>1.3 AD treatment strategies.....</b>	<b>55</b>
1.3.1 CURRENT THERAPIES.....	56
1.3.2 NEW THERAPEUTIC TARGETS.....	56
1.3.2.1 The multi-targeted approach .....	58
1.3.3 INNOVATIVE THERAPEUTIC STRATEGIES.....	60
1.3.3.1 Immune therapy.....	60

1.3.3.2 Cell-based therapy.....	61
<b>1.4 Sirtuins.....</b>	<b>62</b>
1.4.1 FUNCTIONS AND LOCALIZATION OF SIRTUINS.....	63
1.4.2 SIRT1.....	67
1.4.2.1 SIRT1 in neurodegeneration and AD.....	68
1.4.3 SIRT2.....	71
1.4.3.1 SIRT2 in neurodegeneration and AD.....	73
1.4.4 SIRT1/SIRT2 MODULATORS AND THEIR APPLICATION TO NEURODEGENERATION.....	76
1.4.4.1 SIRT1 activators.....	77
1.4.4.2 SIRT2 inhibitors.....	81
1.4.5 THE ROLE OF OTHER SIRT <sub>s</sub> IN NEURODEGENERATION AND AD.....	84
1.5 Drug-delivery Systems (DDS).....	86
1.5.1 HYDROGELS AS DDS.....	87
1.5.1.1 Hydrogels for CNS application.....	89
<b>2. Aim of the study.....</b>	<b>93</b>
<b>3. Materials and methods.....</b>	<b>97</b>
<b>3.1 In vitro experiments.....</b>	<b>98</b>
3.1.1 H4-SW CELLS.....	98
3.1.2 COMPOUNDS AND CELL TREATMENTS.....	99
3.1.3 RNA INTERFERENCE.....	99
3.1.4 MTS VIABILITY ASSAY.....	100
3.1.5 PROTEIN EXTRACTION FROM CELLS AND CULTURE MEDIA.....	100
3.1.6 SDS-PAGE AND WESTERN BLOTTING.....	101
3.1.7 Enzyme-Linked Immunosorbent Assay (ELISA).....	102
3.1.8 TOTAL RNA EXTRACTION.....	102
3.1.9 QUANTITATIVE REAL TIME PCR.....	103
<b>3.2 In vivo experiments.....</b>	<b>103</b>
3.2.1 3xTg-AD MOUSE MODEL.....	103
3.2.2 SIRT2 INHIBITOR ADMINISTRATION PROTOCOL.....	104
3.2.3 SIRT1 ACTIVATOR ADMINISTRATION PROTOCOL.....	105
3.2.4 EXPERIMENTAL TIMELINE.....	105
3.2.5 BEHAVIOURAL TEST (NORT).....	107
3.2.6 TISSUES PREPARATION FOR BIOCHEMICAL ANALYSES.....	109
3.2.7 SDS-PAGE AND WESTERN BLOTTING.....	110
3.2.8 IMMUNOHISTOCHEMISTRY.....	111
<b>3.3 Statistical analysis.....</b>	<b>111</b>



<b>3.4</b>	<b>Hydrogels for controlled release of SIRTs modulators.....</b>	<b>112</b>
3.4.1	<i>IN VIVO</i> BIOCOMPATIBILITY OF HYDROGELS: AIR POUCH MODEL .....	112
3.4.2	<i>IN VITRO</i> CONTROLLED-RELEASE: HYDROGEL COMPOSITION .....	114
3.4.3	UV-VIS SPECTROPHOTOMETRY: MODULATORS DETECTION AND STANDARD CURVE SETTING 114	
3.4.4	HYDROGEL-MEDIATED RELEASE STUDY AND DATA ANALYSIS.....	115
<b>4.</b>	<b>Results: SIRT1 activation and SIRT2 inhibition in <i>in vitro</i> and <i>in vivo</i> AD models.....</b>	<b>118</b>
<b>4.1</b>	<b><i>In vitro</i> results.....</b>	<b>121</b>
4.1.1	H4-SW CELLS.....	121
4.1.2	EVALUATION OF CYTOTOXICITY OF SIRT1 AND SIRT2 MODULATION IN H4-SW CELLS 123	
4.1.3	EFFECT OF THE DOUBLE TREATMENT ON fA $\beta$ AND sA $\beta$ LEVEL .....	125
4.1.4	SIRT2 SILENCING: EFFECT ON sA $\beta$ .....	128
4.1.5	EFFECT OF SIRT1/2 MODULATION ON AMYLOIDOGENIC PROCESSING: sA $\beta$ , A $\beta$ 40 AND A $\beta$ 42 129	
<b>4.2</b>	<b><i>In vivo</i> results.....</b>	<b>135</b>
4.2.1	3xTg-AD MICE PATHOLOGICAL PHENOTYPING .....	135
4.2.2	EFFECT OF SIRT2 INHIBITION AND SIRT1 ACTIVATION ON 3xTg-AD COGNITIVE PERFORMANCE.....	140
4.2.3	EFFECT OF SIRT2 INHIBITION AND SIRT1 ACTIVATION ON AD-RELEVANT NEUROPATHOLOGIC PATHWAYS.....	150
<b>5.</b>	<b>Results: <i>in vitro</i> set-up of a hydrogel-based controlled release system for SIRTs modulators .....</b>	<b>161</b>
<b>5.1</b>	<b>Hydrogel <i>in vivo</i> biocompatibility and matrix selection .....</b>	<b>164</b>
<b>5.2</b>	<b>Spectrophotometric analysis of SIRTs modulators .....</b>	<b>165</b>
<b>5.3</b>	<b>Release kinetic study.....</b>	<b>170</b>
<b>6.</b>	<b>Discussion and conclusions.....</b>	<b>176</b>
<b>7.</b>	<b>Bibliography .....</b>	<b>205</b>

## **List of figures and tables**

## INTRODUCTION

<b>Fig. 1.1</b> AD senile plaques and neurofibrillary tangles.....	23
<b>Fig. 1.2</b> Hyperphosphorylated tau in neuronal cell bodies.....	24
<b>Fig. 1.3</b> MRI of AD-related brain atrophy.....	25
<b>Fig. 1.4</b> Amyloid Cascade Hypothesis (ACH).....	32
<b>Fig. 1.5</b> APP processing .....	34
<b>Fig. 1.6</b> Kinetic model of A $\beta$ aggregation.....	38
<b>Fig. 1.7</b> Main effects of A $\beta$ oligomers toxicity.....	39
<b>Fig. 1.8</b> Proposed receptors for A $\beta$ oligomers.....	40
<b>Fig. 1.9</b> Physiological functions of sAPP $\alpha$ .....	41
<b>Fig. 1.10</b> Microtubules structure and tau hyperphosphorylation.....	44
<b>Fig. 1.11</b> Tau protein role in the ACH.....	45
<b>Fig. 1.12</b> Role of astrocytes and microglia in AD onset.....	46
<b>Fig. 1.13</b> Role of ROS in synaptic dysfunction.....	50
<b>Fig. 1.14</b> Four technologies for 3D AD modelling.....	53
<b>Fig. 1.15</b> Onset and progression of AD in transgenic mouse models.....	54
<b>Fig. 1.16</b> Structural domains of mammalian sirtuins.....	63
<b>Fig. 1.17</b> SIRT's deacetylase reaction.....	64
<b>Fig. 1.18</b> Changes in SIRT's brain levels during AD.....	66
<b>Fig. 1.19</b> Physiological roles of SIRT1.....	68
<b>Fig. 1.20</b> SIRT1 involvement in AD.....	69
<b>Fig. 1.21</b> Molecular targets and functions of SIRT2.....	72
<b>Fig. 1.22</b> SIRT2 involvement in AD microtubules disruption.....	75
<b>Fig. 1.23</b> Chemical structure of Resveratrol.....	77
<b>Fig. 1.24</b> Chemical structure of SIRT1 activator SRT1720.....	78
<b>Fig. 1.25</b> Chemical structure of SIRT1 activator SRT2104.....	79
<b>Fig. 1.26</b> Effects of SIRT1 activation on age-related diseases.....	81
<b>Fig. 1.27</b> Chemical structure of SIRT2 inhibitor AGK2 .....	82

<b>Fig. 1.28</b> Chemical structure of SIRT2 inhibitor AK7.....	83
<b>Fig. 1.29</b> IPN and semi-IPN hydrogel formation.....	89
<b>Table 1.1</b> AD classification.....	27
<b>Table 1.2</b> Impact of astrocytic and microglial cytokines on AD.....	48
<b>Table 1.3</b> A list of some 2D cellular models of AD developed using iPSCs...	52
<b>Table 1.4</b> Advantages and limitations of in vitro and in vivo AD modelling...	55
<b>Table 1.5</b> Localization and targets of sirtuins.....	66

## **MATERIALS AND METHODS**

<b>Fig. 3.1</b> AK7 administration protocol in 3xTg-AD mice.....	106
<b>Fig. 3.2</b> SRT2104 administration protocol in 3xTg-AD mice.....	106
<b>Fig. 3.3</b> Double treatment protocol in 3xTg-AD mice.....	107
<b>Fig. 3.4</b> NORT schematic protocol.....	107
<b>Table 3.1</b> Hydrogels composition.....	116

## **RESULTS**

<b>Fig. 4.1</b> APP-sw over-expression in H4 cells.....	121
<b>Fig. 4.2</b> SIRT1 and SIRT2 basal expression in H4-sw cells.....	122
<b>Fig. 4.3</b> AK7 toxicity scale on H4-sw cells.....	123
<b>Fig. 4.4</b> SRT1720 toxicity scale on H4-sw cells.....	124
<b>Fig. 4.5</b> Toxicity scale of combined treatment on H4-sw cells.....	125
<b>Fig. 4.6</b> flAPP level after SIRT1/SIRT2 modulation in H4-sw cells.....	126
<b>Fig. 4.7</b> sAPP level after SIRT1/SIRT2 modulation in H4-sw cells.....	126
<b>Fig. 4.8</b> sAPP $\alpha$ level after SIRT1/SIRT2 modulation in H4-sw cells.....	127
<b>Fig. 4.9</b> ADAM10 mRNA after SIRT1/SIRT2 modulation in H4-sw cells.....	128
<b>Fig. 4.10</b> sAPP $\alpha$ level after SIRT2 gene silencing in H4-sw cells.....	129
<b>Fig. 4.11</b> sAPP $\beta$ and A $\beta$ 40 ELISA assay on AK7/SRT1720 treated cells.....	130

<b>Fig. 4.12</b> sAPP $\beta$ and A $\beta$ 40 ELISA assay on AK7/SRT2104 treated cells.....	131
<b>Fig. 4.13</b> A $\beta$ 42 ELISA assay after double modulation in H4-sw cells.....	132
<b>Fig. 4.14</b> A $\beta$ 42 ELISA assay comparing SIRT2 inhibition or silencing.....	133
<b>Fig. 4.15</b> Cognitive impairment assessment in 3xTg-AD vs NTg mice.....	136
<b>Fig. 4.16</b> Temporal profile of plaques deposition in 3xTg-AD mice.....	136
<b>Fig. 4.17</b> Analysis of tau tangles in 19-months old 3xTg-AD mice.....	137
<b>Fig. 4.18</b> 55 kDa oligo-A $\beta$ in hippocampus of 3xTg-AD mice.....	138
<b>Fig. 4.19</b> CD11b, GFAP, NRF2 and Synaptophysin basal levels in 3xTg-AD mice.....	139
<b>Fig. 4.20</b> SIRT1 and SIRT2 basal levels in 3xTg-AD mice.....	140
<b>Fig. 4.21</b> 3xTg-AD body weight monitoring during AK7 treatment.....	141
<b>Fig. 4.22</b> Total exploration times in the NORT of AK7 treated mice.....	142
<b>Fig. 4.23</b> % of objects investigation in the NORT of AK7 treated mice.....	143
<b>Fig. 4.24</b> Discrimination index in the NORT of AK7 treated mice.....	143
<b>Fig. 4.25</b> 3xTg-AD body weight monitoring during SRT2104 treatment.....	144
<b>Fig. 4.26</b> Total exploration times in the NORT of SRT2104 treated mice.....	145
<b>Fig. 4.27</b> % of objects investigation in the NORT of SRT2104 treated mice..	146
<b>Fig. 4.28</b> Discrimination index in the NORT of SRT2104 treated mice.....	147
<b>Fig. 4.29</b> 3xTg-AD body weight monitoring during the double treatment.....	148
<b>Fig. 4.30</b> Total exploration times in the NORT of double-treated mice.....	149
<b>Fig. 4.31</b> % of objects investigation in the NORT of double-treated mice.....	149
<b>Fig. 4.32</b> Discrimination index in the NORT of double-treated mice.....	150
<b>Fig. 4.33</b> sAPP $\alpha$ level in SRT2104 and double-treated 3xTg-AD mice.....	151
<b>Fig. 4.34</b> 55 kDa A $\beta$ level in single and double-treated mice.....	152
<b>Fig. 4.35</b> GFAP and CD11b levels in mice treated with SRT2104 or AK7.....	154
<b>Fig. 4.36</b> GFAP and CD11b levels in double-treated mice.....	155
<b>Fig. 4.37</b> Synaptophysin level in mice treated with SRT2104 or AK7.....	156
<b>Fig. 4.38</b> Synaptophysin level in double-treated mice.....	156

<b>Fig. 4.39A</b> SOD1 and NRF2 levels in mice treated with SRT2104.....	157
<b>Fig. 4.39B</b> SOD1 and NRF2 levels in mice treated with AK7.....	158
<b>Fig. 4.40</b> SOD1 and NRF2 levels in double-treated mice.....	159
<b>Fig. 5.1</b> <i>In vivo</i> biocompatibility of collagen-based hydrogels.....	164
<b>Fig. 5.2</b> Spectrophotometric analysis of SRT1720 absorbance peak.....	165
<b>Fig. 5.3</b> Spectrophotometric analysis of AGK2 absorbance peak.....	166
<b>Fig. 5.4</b> Spectrophotometric analysis of AK7 absorbance peak.....	167
<b>Fig. 5.5</b> Spectrophotometric analysis of hydrogel degradation products.....	168
<b>Fig. 5.6</b> Calibration curves of SRT1720 and AGK2.....	169
<b>Fig. 5.7</b> SRT1720 cumulative nmol released from the hydrogel over time.....	171
<b>Fig. 5.8</b> % of SRT1720 released from the hydrogel over time.....	171
<b>Fig. 5.9</b> Korsmeyer-Peppas kinetic model for SRT1720 release.....	172
<b>Fig. 5.10</b> Spectrophotometric analysis of AGK2-loaded hydrogel .....	174
<b>Table 5.1</b> SRT1720 release kinetic data summary.....	173

## **DISCUSSION**

<b>Fig. 6.1</b> Summary of the key findings of the study.....	202
---	-----

## **List of abbreviations**

<b>ACH</b>	Amyloid Cascade Hypothesis
<b>AchE</b>	Acetylcholine Esterase
<b>AD</b>	Alzheimer's Disease
<b>ADAM10</b>	A Disintegrin And Metalloprotease 10
<b>ALS</b>	Amyotrophic Lateral Sclerosis
<b>APOE</b>	Apolipoprotein E
<b>APP</b>	Amyloid Precursor Protein
<b>A<math>\beta</math>Os</b>	A $\beta$ Oligomers
<b>BACE-1</b>	$\beta$ -site APP Cleaving Enzyme-1
<b>BBB</b>	Blood Brain Barrier
<b>CDMT</b>	Combination-drugs-multi-targets
<b>CNS</b>	Central Nervous System
<b>COLL</b>	Collagen
<b>CR</b>	Caloric Restriction
<b>DDS</b>	Drug Delivery System
<b>DI</b>	Discrimination Index
<b>EOAD</b>	Early Onset Alzheimer's Disease
<b>ESC</b>	Embryonic Stem Cells
<b>FAD</b>	Familial Alzheimer's Disease
<b>flAPP</b>	Full-length APP
<b>GSK-3<math>\beta</math></b>	Glycogen Synthase Kinase 3 $\beta$
<b>HD</b>	Huntington's Disease
<b>IPNs</b>	Interpenetrated
<b>iPSC</b>	induced Pluripotent Stem Cells
<b>LMWHA</b>	Low Molecular Weight Hyaluronic Acid
<b>LOAD</b>	Late Onset Alzheimer's Disease
<b>MAP</b>	Microtubules Associated Protein
<b>MCI</b>	Mild Cognitive Impairment
<b>MSC</b>	Mesenchymal Stem Cells
<b>MTDL</b>	Multi-target Directed Ligand



<b>NAM</b>	Nicotinamide
<b>NFTs</b>	Neurofibrillary Tangles
<b>NORT</b>	Novel Object Recognition Test
<b>NPs</b>	Nanoparticles
<b>NRF2</b>	Nuclear factor erythroid 2–related factor 2
<b>NSC</b>	Neural Stem Cells
<b>PD</b>	Parkinson’s Disease
<b>PEG</b>	Poly Ethylene Glycol
<b>PSEN1</b>	Presenilin 1
<b>PSEN2</b>	Presenilin 2
<b>ROS</b>	Reactive Oxygen Species
<b>RNS</b>	Reactive Nitrogen Species
<b>RSV</b>	Resveratrol
<b>SAD</b>	Sporadic Alzheimer’s Disease
<b>SIRTs</b>	Sirtuins
<b>SOD</b>	Superoxide Dismutase
<b>STACs</b>	Sirtuin Activating Compounds

# **1. Introduction**

## 1.1 Alzheimer's disease

Alzheimer's disease (AD), is the most frequent disease of the central nervous system (CNS) and the most common cause of dementia. As other neurodegenerative disorders, is characterized by progressive loss of functionality and specific neuronal populations' death. Given the fact that neurons cannot replicate, the disease is incurable and totally disabling. AD is characterized by memory and cognitive deterioration, has an incidence of 1-3% of the total population above 65 years-old, and an estimated prevalence of 10-30% **[Masters CL et al., 2015]**.

If we consider the sole European population, a recent metanalysis study highlighted a 5.05% (7.13% for women and 3.31% for men) prevalence of AD, and an annual incidence of 11.08 (13.25 for women and 7.02 for men) every 1000 people. These values are higher in women and tend to increase with ageing **[Niu H et al., 2017]**.

AD treatments are only able to reduce symptoms and slow down the course of the disease. Despite the huge amount of clinical trials for the identification of a cure, the search for a therapy that could arrest the disease is still ongoing **[Godiñ J et al., 2016]**. The current pharmacological approach aims at the molecular targets responsible of the two main physiopathological signs of AD:  $\beta$ -amyloid peptide and tau protein.

### 1.1.1 CLINICAL SIGNS AND SYMPTOMS

Dr. Alois Alzheimer, a German neuropathologist and psychiatrist, described AD for the first time in 1907. He described the case of a 51 years old woman with clinical signs unrelated to known diseases. The woman presented with disorientation and memory loss, with a strong paranoid behaviour **[Alzheimer A et al., 1995]**. After her death, 4 years later, Alzheimer analysed her brain and noticed two characteristic alterations, currently known as extracellular  $\beta$ -amyloid senile plaques and neurofibrillary tangles of hyperphosphorylated tau protein. These two are nowadays the typical post-mortem features for AD diagnosis confirmation **[Thal DR et al., 2005]**.

AD pathological process starts at least one decade before the appearance of the first symptoms (pre-clinical phase). Thus, it is essential to immediately recognize and diagnose early-stage AD, in order to offer the better therapeutic possibilities to patients **[Herman L et al., 2017]**.

AD clinical course can be divided in phases, with common symptoms between different patients.

Mild cognitive impairment (MCI) is considered as light memory and cognitive deficit, typical of the elderly population, which is not necessarily related with dementia. It would be very important to know whether MCI is the prodromal phase of AD to have an early diagnosis, which nowadays is often uncertain **[Tarawneh et al., 2012]**. However, MCI is currently the only chance to diagnose dementia prior to serious and irreversible cognitive decline, and usually requires multiple tests over months to rule out other non-reversible causes of the cognitive deficit.

An early AD intervention is of particular importance given the progressive nature of the disease. In fact, AD progression can be classified in three clinical phases **[De-Paula VJ et al., 2012]**:

- A pre-symptomatic AD, that can last decades before the A $\beta$  accumulates and initiate its pathological cascade.
- A pre-dementia phase, in which MCI detection is a key point, and neuropathological changes include mild neuronal dystrophy or early-stage Braak pathology. This phase can last for years depending on individual resilience.
- Dementia phase, where cognitive impairment has exceeded the dementia threshold. The patient presents accumulation of neuritic plaques and neurofibrillary tangles.

After the early stage of the disease, in the intermediate phase there is evident language deficits (aphasia), bad motor coordination and long-term memory is compromised **[Tree J et al., 2015]**.

In the advanced stage of AD, the patient is no more able to communicate and manage daily activities **[Frank EM, 1994]**. This leads to infection vulnerability, in fact pneumonia is the main cause of death in AD patients **[Glampedakis E et al., 2016]**.

AD has a variable duration, however the mean time of survival after the diagnosis is between 3.2 and 6.6 years **[Todd S et al., 2013]**.

### 1.1.2 DIAGNOSIS

AD diagnosis can be confirmed by post-mortem histological analysis on the brain tissue of patients. However, there is a 95% accuracy in the diagnosis based on patient's family anamnesis and neuropsychological tests, which allow the evaluation of cognitive functions typically compromised in AD (memory, language, perceptive and constructive abilities). These neuropsychological tests are part of the NINCDS-ADRDA criteria (National Institute of Neurological and Communicative Disorders and Stroke and the Alzheimer's Disease and Related Disorders Association), diagnostic criteria used to discriminate with >80% accuracy AD patients and subjects without dementia.

Biomarkers are measurable parameters that can be detected *in vivo*, and reflect a specific physiological or pathological process.  $\beta$ -amyloid peptide (A $\beta$ 42) and tau/phospho-tau protein can be used as CSF and plasma biomarkers in AD [Olsson B et al., 2016]. Research on novel AD biomarkers discovery is still very active as they can be of relevance for the early diagnosis. Another useful diagnostic instrument is represented by neuroimaging techniques as PET, MRI and SPECT [Pietrzak K et al., 2018]. Despite the increase in specificity, the accordance between clinical and post-mortem diagnosis is only 62% [Grandal Leiros B et al., 2018].

AD is commonly diagnosed when the patient is already in the MCI due to AD (MCI-AD) stage of the disease, using clinical and biomarkers assays. On the other hand, detection of preclinical AD stage is still a challenge for an early diagnosis that could make more effective the proposed therapeutic

interventions, improve care planning of the patient, give access to symptomatic treatments, clinical trials and innovative available therapies **[Barnett JH et al., 2014; Herman L et al., 2017]**.

### **1.1.3 PHYSIOPATHOLOGY**

As already mentioned, the two characteristic neuropathological elements of AD are  $\beta$ -amyloid senile plaques and tau protein NFTs (Figure 1.1), in the form of insoluble aggregates **[Perl DP, 2010]**. However, it is wrong to think that these elements are the unique key aspects of the disease.

AD physiopathological picture is very complex, and include a huge neuronal loss, mitochondrial dysfunction, oxidative stress, neuroinflammation and cerebral atrophy.

Amyloid plaques are extracellular spherical lesions, with a diameter generally between 10 and 200  $\mu\text{m}$ . They are composed of a central  $\beta$ -amyloid nucleus surrounded by proteins and neuronal fragments with peripheral deposits **[Takahashi RH et al., 2002]**.

A $\beta$ 42 peptide deriving from amyloidogenic processing of amyloid precursor protein (APP), is prone to auto-aggregation in two coexistent physical forms: a non-fibrillary form (non- $\beta$ sheet), composed by 2-6- units oligomers, and a fibrillary one ( $\beta$ sheet). The latter is organized in insoluble fibrils that are particularly stable and accumulate to form senile plaques **[Breydo L et al., 2016]**.  $\beta$ -amyloid core is surrounded by protein deposits (apolipoprotein E, hyperphosphorylated tau, antichymotrypsin) and fragments from dead brain cells (neurons, astrocytes and microglia). These elements are crucial for

neuronal homeostasis alteration, as energy imbalance and oxidative stress [Tramutola A et al., 2017].

Inside the brain, senile plaques are typically present in the hippocampus, frontal and temporal-parietal cortex, and cingulate gyrus. Moreover, these alterations are also present in blood vessels (vascular plaques), where they trigger a pathological cycle between A $\beta$  deposition and cerebrovascular diseases [Lee CW et al., 2014].

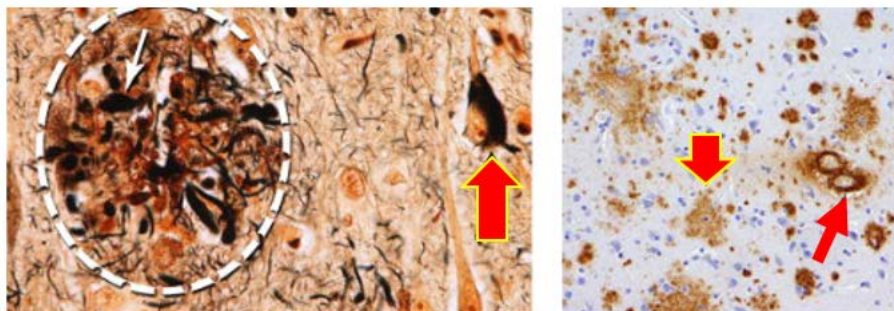


**Figure 1.1** Left: high potency microphotography of a neuritic plaque (dashed white line) in which is present a neurofibrillary tangle (black arrow). Right: immunohistochemistry of wide spread A $\beta$  plaques (thick arrows) and cerebral amyloid angiopathy (thin arrow) (modified from [Holtzman DM et al., 2011])

NFTs are mainly composed by tau protein, a microtubule associated protein with a role in their stability maintenance.

Tau protein is subject of aberrant modifications like hyperphosphorylation, and detaches from microtubules accumulating in double-helix filaments (oligomers or bigger structures) in the dendritic space (Figure 1.2) [Avila J et al., 2016].

The consequences of these events are mitochondrial dysfunction and neuronal loss, which lead to cognitive decline. NFTs extend predominantly along neuronal extensions in hippocampus and cerebral cortex.



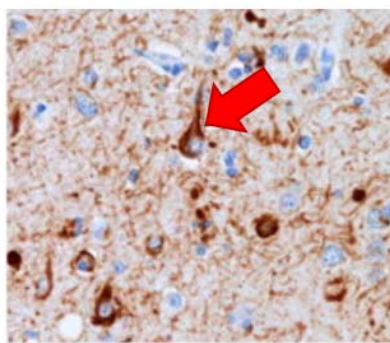


**Figure 1.2** Accumulation of hyperphosphorylated tau protein in neuronal cell bodies (arrow)  
(modified from [Holtzman DM et al., 2011])

Neuronal death can be considered as the main hallmark of AD [Spires-Jones TL et al., 2014]. The progressive loss of synapses gradually inhibits neurotransmitters release, and the amount of post-synaptic receptors decreases. In particular, the expression of the  $\alpha 7$  nicotinic subtype ( $\alpha 7$ -nAChR) is altered in AD *in vivo* models and patients, thus suggesting an important role of this receptor in the pathogenesis of the disease and a new potential pharmacological target [Shen J et al., 2015]. However, a recent study on a murine AD model has highlighted the importance of other neurotransmitter systems, such as the dopaminergic one. In fact, they noticed dopaminergic neuronal loss in the ventral-tegmental area (VTA) at a pre-plaques stage of the disease, which contributes to memory and synaptic plasticity impairment [Nobili A et al., 2017].

All these molecular pathological processes eventually lead to an extensive brain atrophy, associated with cortical and hippocampal shrinkage and ventricles dilatation (Figure 1.3).

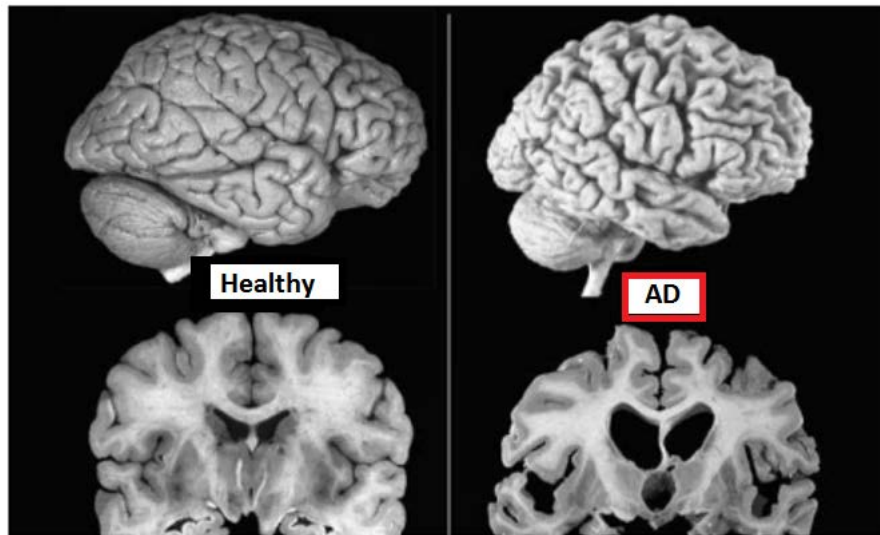


**Figure 1.3** MRI images comparing brain atrophy related to ageing (left) and AD (right).

#### 1.1.4 EPIDEMIOLOGY

Age is the most important risk factor for AD. The risk increases between 65 and 85 years of age, and beyond 65 years the incidence of the disease doubles every 5 years [Isik AT, 2010].

The rise of lifespan is a global process that proves the improvement of health in the last century. However, a negative aspect of ageing is the significant increase in the amount of senile dementia cases worldwide. It is estimated that the number of subjects with dementia could rise from the current 44 to 135 million in 2050 [Prince M et al., 2013].

Despite this, life expectancy of individuals developing the disease at the time of the diagnosis is destined to remain unchanged.

The progressive increase in the number of people affected by dementia is proportionally higher in developing countries (*Low and Middle Income Countries - LMIC*) with a young population, with respect to Western Europe or

USA (*High Income Countries – HIC*), which have an older population **[Scheltens P et al., 2016]**.

AD incidence seems to be significantly higher in women, and a recent study reported that women compose almost two-thirds of AD patients. A reason for this can be attributable to the fact that women have a longer life expectancy than men. However, it has been also highlighted that there is no difference between the two genders on the degree of disease development. A low education level is also associated to a higher AD incidence, whereas the training of cognitive abilities helps to reduce the risk to develop dementia in the early stage of the disease **[Mielke MM et al., 2014]**.

### **1.1.5 ETIOLOGY**

AD can be classified in relation to the parameter taken into consideration (Table 1.1).

If we consider age as the main parameter, AD can be classified into:

- Early Onset Alzheimer's Disease (EOAD): age of onset <65 years; 6-7% of all cases;
- Late Onset Alzheimer's disease (LOAD): age of onset >65 years; 93-94% of all cases.

If we consider instead the familial history, it is possible to define these AD forms:

- Autosomic Dominant: < 5% of EOAD cases;
- Familial (FAD): 15-25% of LOAD cases, 47% of EOAD cases;
- Sporadic (SAD): ~75% of all cases.

	Type	Details
Age of onset	Early onset (~6–7%)	<60–65 years
	Late-onset (~93–94%)	>60–65 years
Family history	Autosomal dominant (<5%)	Disease that occurs in at least three individuals in two or more generations, with two of the individuals being first-degree relatives of the third
	Familial (~15–25%)	Disease that occurs in more than one individual and at least two of the affected individuals are third-degree relatives or closer
	Sporadic (~75%)	Isolated case in the family or cases separated by more than three degrees of relationship

**Table 1.1** AD classification according to American College of Medical Genetics and National Society of Genetics Counselors (modified from [Alves L et al., 2012]).

EOAD is a familial autosomal dominant pathology (FAD) characterized by mutations in three main genes: APP, Presenilin1 and 2. LOAD is instead a heterogeneous sporadic pathology (SAD) related to ageing, genetics and environmental risk factors [Kim DH et al., 2014].

Both EOAD and LOAD are characterized by an excessive accumulation of  $\beta$ -amyloid toxic forms, resulting from an imbalance between its production and clearance. In the case of EOAD both production and clearance seem to be altered, while in LOAD it has been highlighted a decrease in elimination only [Mawuenyega KG et al., 2010].

#### 1.1.5.1 AD non-genetic risk factors

Currently, reducing the risk of developing AD depends mainly on lifestyle changes and prevention. Modifiable risk factors include age, genetics and traumatic brain injury [Ballard C et al., 2011].

Among non-genetic modifiable risk factors, instead, we can mention:

- Cardiovascular diseases: these include haemorrhagic stroke, cerebral ischemia and hypertension [O'Brien JT et al., 2014].

- Obesity and dyslipidaemia: high total plasma cholesterol and middle age BMI have been associated with development of senile dementia and AD **[Baumgart M et al., 2015]**.
- Type II diabetes mellitus: the correlation between LOAD and diabetes is not fully clear, but it may include BMI and cardiovascular mechanisms, since type II diabetes is a risk factor for stroke, hypertension and dyslipidaemia **[Reitz C et al., 2014]**.
- Smoke: its role is controversial. Some studies suggest that smoke reduces AD risk, while other studies demonstrated that AD risk is increased **[Durazzo TC et al., 2014]**.
- Alcoholism

#### **1.1.5.2 AD genetics**

There are three main genes involved in EOAD development: Amyloid Precursor Protein (APP), Presenilin 1 (PSEN1) and Presenilin 2 (PSEN2). Mutations in these genes determine abnormal amyloid  $\beta$  production, the most important cause of neuronal death, and dementia.

- APP: the gene is located on chromosome 21 and up to now 30 different mutations have been identified, of which 25 are involved in autosomic dominant EOAD development. In Down's Syndrome patients, which harbour three copies of the chromosome 21, an earlier AD development with respect to subjects without trisomy has been reported **[Bagyinszky E et al., 2014]**.

A relevant mutation of APP is the Swedish one, identified for the first time in two Swedish families. It is a double mutation resulting from the double substitution of two aminoacids: Lysine (K) and Methionine (M) with Asparagine (N) and Leucine (L) respectively (K595N/M596L). This mutation is associated with EOAD and is known to cause an abnormal APP amyloidogenic metabolism increase, with an increase in A $\beta$  peptide production and AD early onset **[Shin J et al., 2010]**.

- PSEN1: its gene is located on chromosome 14. PSEN1 mutation is the most common cause of severe form of familial EOAD, with an onset at 30 years of age. More than 180 PSEN1 mutations have been observed: the most important is a missense mutation with a substitution of an aminoacid, which causes A $\beta$ 42 abnormal accumulation **[Alonso Vilatela ME et al., 2012]**.

- PSEN2: its gene is located on chromosome 1. The missense mutation in PSEN2 is a rare cause of EOAD and the mechanism leading to brain A $\beta$  accumulation in AD patients is still unclear **[Kim DH et al., 2014]**.

Together with non-genetic risk factors, some genes involved in LOAD development have been described. Apolipoprotein E (ApoE) gene, located on chromosome 19, is the most important genetic risk factor for LOAD. ApoE is the main cholesterol carrier in the brain and is involved in neurons physiology maintenance. In the CNS, ApoE can bind different membrane receptors, which are involved in lipids transport, glucose metabolism,

neuronal communication and mitochondrial metabolism [Yu JT et al., 2014]. There are 3 different ApoE allelic variants ( $\epsilon$ 2,  $\epsilon$ 3 and  $\epsilon$ 4), which correspond to 3 different isoforms of the protein: E2, E3 and E4. The most common isoform is ApoE 3 with a global frequency of 77.9%, followed by ApoE 4 (13.7%) and ApoE 2 (8.4%) [Mahoney-Sanchez L et al., 2016]. ApoE  $\epsilon$ 4 is present in 50% of LOAD patients. The presence of a copy of the ApoE  $\epsilon$ 4 allele increases the risk of developing LOAD by about three times, while the presence of two copies of the allele increases it twelve times [Neu SC et al., 2017].

In addition to ApoE, several Genome-Wide Association Studies (GWAS) identified genes involved in LOAD development. GWAS consider the common genetic variability in the genome of big populations in order to identify correlations between specific genetic variants and AD. Some of the genes identified with this method are:

- Clusterin (CLU): is the major apolipoprotein related to inflammatory response and is expressed in all tissues. Clusterin has a protective role against apoptosis, cellular damage and oxidative stress.
  - Complement Receptor 1 (CR1) e C3b: involved in A $\beta$  clearance to prevent its aggregation.
  - PICALM, SORL1, BIN1, CTNNA3, GAB2, TREM2 and ADAM10
- [Bagyinszky E et al., 2014].

## 1.2 AD pathogenesis: Amyloid Cascade Hypothesis

The pathogenetic mechanism of AD is still unknown, and its identification is a main objective for research in this field. The Amyloid Cascade Hypothesis (ACH), formulated by Hardy and Higgins in 1992, focuses on APP,  $\beta$ -amyloid toxicity and aggregation, and tau protein (Figure 1.4). According to original ACH, the abnormal  $A\beta_{42}$  production and aggregation is crucial to determine senile plaques formation in some specific brain regions. The plaques would in turn cause neuronal damage, neurofibrillary tangles formation and finally, neuronal death and synaptic loss [**Hardy JA et al., 1992**].

During the past years, the ACH has been revised mostly because of the failure of therapies targeting  $A\beta$  deposition and aggregation. Several genetic studies demonstrated that genetic factors have an important role in AD development and progression, and that neurodegenerative processes are the result of an imbalance between  $A\beta$  production and clearance [**Tarasoff-Conway JM et al., 2015**].



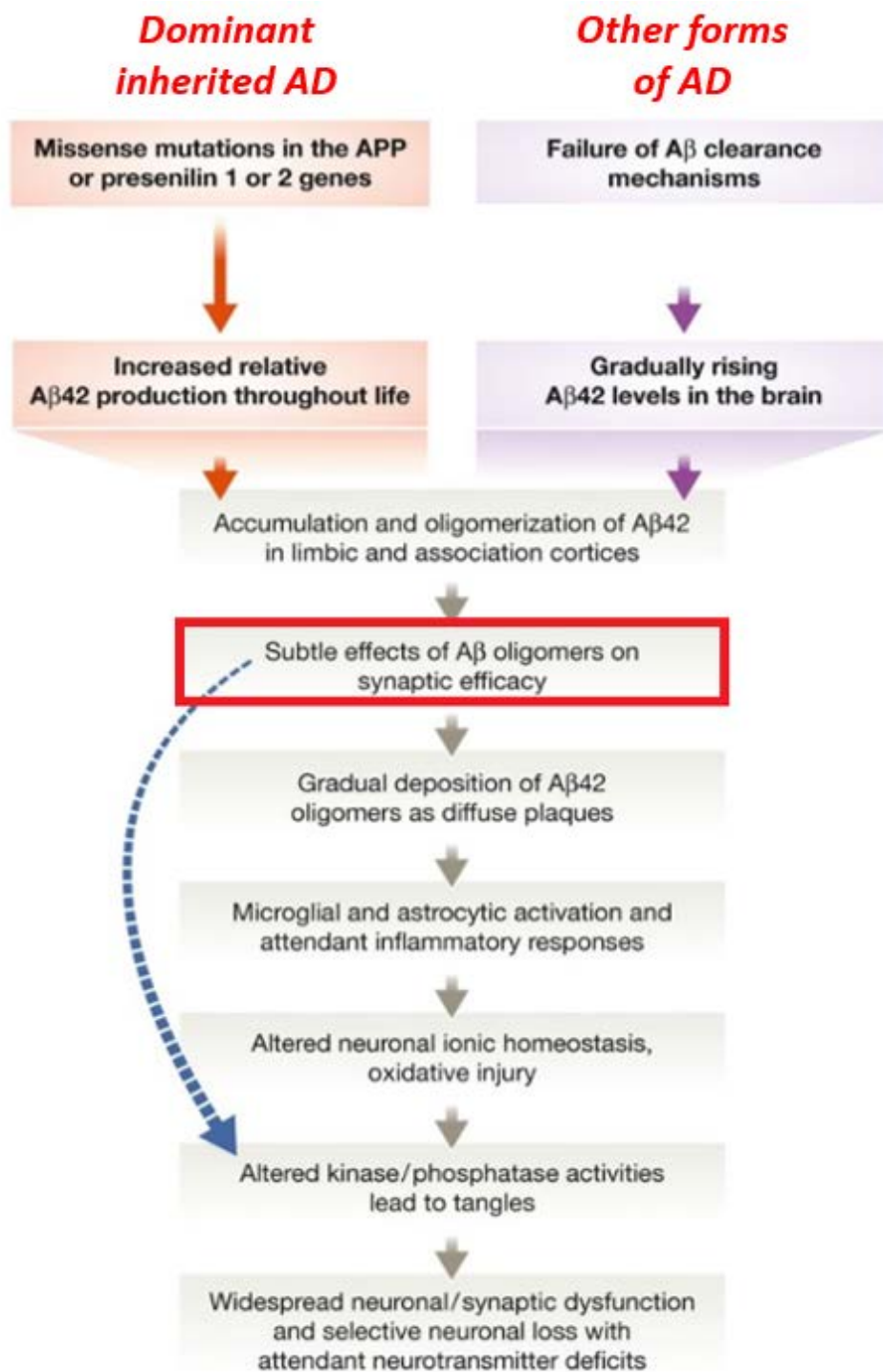


**Figure 1.4** Main pathological events according to ACH. Blue arrow indicates that A $\beta$  oligomers can directly cause synaptic damage and tau hyper-phosphorylation (from [Selkoe DJ et al., 2016]).

### 1.2.1 Amyloid Precursor Protein (APP)

APP is a transmembrane glycoprotein highly expressed in the CNS. The protein has a transmembrane hydrophobic region and a short intracellular C-terminal domain (AICD) [Zhang H et al., 2012]. APP has 8 isoforms deriving from its alternative splicing. The 695 aminoacids isoform (APP695) is mainly present in neurons, while the other isoforms (APP751, APP770) are typical of other tissues.

APP is member of a highly conserved family of APP-like proteins (APLPs): among the members of the family, APLP1 is expressed solely in mammalian brain and APLP2 is ubiquitously expressed [Nhan HS et al., 2015].

Although the pathologic role of APP in AD is well established, less is known about its physiological functions. Several recent studies suggested that APLPs are involved in CNS development, axonal growth, and synaptic functions such as plasticity, learning and memory formation [Müller UC et al., 2017].

Moreover, it seems that APP processing pathways can regulate cholesterol metabolism and sphingomyelin production, confirming a connection between lipids level and AD pathogenesis [Grimm MO et al., 2005].

### 1.2.2 APP PROTEOLYTIC PROCESSING

Neurons produce high amounts of APP that is rapidly metabolized. The protein is synthesized in the endoplasmic reticulum (ER), transported in Golgi apparatus via trans-Golgi-network (TGN) and finally sent to the synaptic terminal. A $\beta$  peptide is produced both in the ER and in the Golgi/TGN [Greenfield JP et al., 1999]. Once in the TGN, APP can be transported into

vesicles to the cell surface, where it's subjected to proteolysis or re-internalized for lysosomal degradation [Zhang YW et al., 2011].

APP processing can follow two main destinies: the amyloidogenic pathway and the non-amyloidogenic pathway (Figure 1.5).

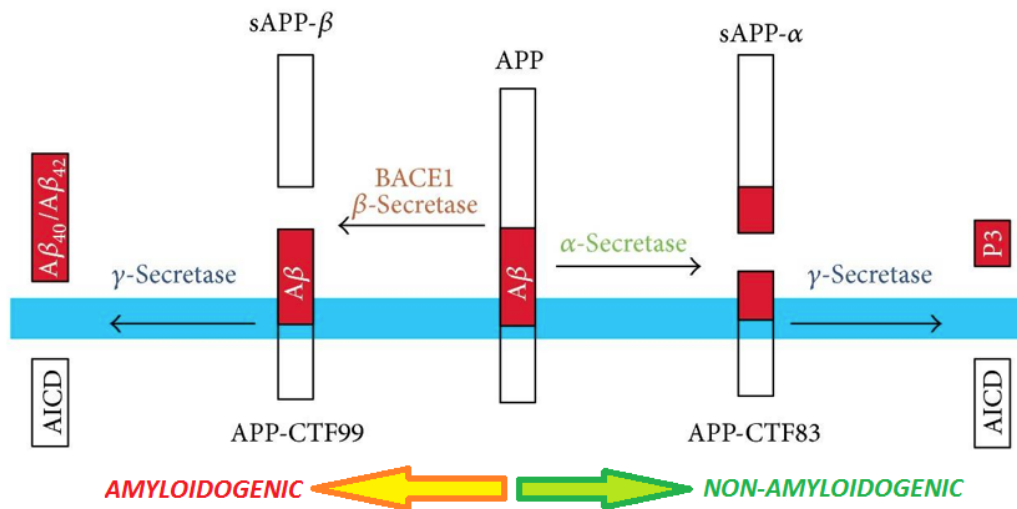


**Figure 1.5** Schematic representation of APP metabolic pathways (modified from [Pajak B et al., 2016]).

In the non-amyloidogenic pathway APP is cleaved by the enzyme  $\alpha$ -secretase at the 17<sup>th</sup> amino acid of the A $\beta$  sequence, to produce the extracellular soluble fragment sAPP $\alpha$  and a membrane-associated C-terminal fragment called CTF83.

CTF83 is subsequently cut by another enzyme, the  $\gamma$ -secretase, with the release of AICD and P3 fragments, that are rapidly degraded.

In the amyloidogenic pathway, instead, APP is cleaved at a different site of the A $\beta$  sequence by  $\beta$ -secretase, with the production of the extracellular soluble fragment sAPP $\beta$  and the membrane-bound fragment CTF99.

$\gamma$ -secretase cuts CTF99 to generate AICD fragment and the A $\beta$  peptide, which tends to aggregate in insoluble forms that initiate the amyloid plaques deposition [**Kamenetz F et al., 2003**].

As mentioned above, the enzymes responsible for APP metabolism are part of the proteases family and are called secretases:

-  $\alpha$ -secretase: the main constitutive family of  $\alpha$ -secretases is the ADAM (A Disintegrin And Metalloprotease) one. ADAM9, ADAM10, ADAM17 are the main members of the family. ADAM10 is considered the constitutive  $\alpha$ -secretase in neurons; in fact, ADAM10 deletion leads to the suppression of sAPP $\alpha$  production, an event that other ADAM members cannot compensate [**Kuhn PH et al., 2010**].

ADAM10 is a 748 amino acids protein, and is composed by an extracellular glycosylated ectodomain, a trans-membrane domain and an intracellular domain. The pro-peptide is metabolized to its active form during the transit in Golgi apparatus [**Saftig P et al., 2015; Yuan XZ et al., 2017**].

ADAM10 *in vitro* and *in vivo* over-expression increased sAPP $\alpha$  and lowered A $\beta$  production, stimulating the interest in this enzyme as therapeutic target [**Yuan XZ et al., 2017**].

-  $\beta$ -secretase: this protease is called BACE-1 ( $\beta$ -site APP Cleaving Enzyme-1) and is a type I trans-membrane protein belonging to the aspartyl-proteases. BACE-1 higher expression is in brain and pancreas, and in neurons it's localized in the pre-synaptic terminal [**Kandalepas PC et al., 2013**]. A homologue of BACE-1, BACE-2, has been identified with a 64% homology in the amino acid sequence, but this enzyme is poorly expressed in neurons [**Bennett BD et al., 2000**].

BACE-1 knock-out mice show a significant reduction in A $\beta$  production but also complex neurochemical and behavioural phenotypes [Harrison SM et al., 2003]. This suggests that the BACE-2 homologue is not able to compensate for the BACE-1 absence, but also that BACE-1 inhibitors research as AD therapeutics should be done carefully to avoid side effects related to its physiological functions block.

Since several studies have highlighted the importance of BACE-1 and APP co-localization and trafficking, interfering with the recycling of BACE1 may provide a novel approach to inhibit A $\beta$  production [Agostinho P et al., 2015; Chia PZ et al., 2011].

-  $\gamma$ -secretase: this enzyme is responsible for the production of A $\beta$  in the case of an amyloidogenic processing, while it produces P3 fragment in the case of a non-amyloidogenic processing.  $\gamma$ -secretase is composed by a complex of four proteins: Presenilin (PSEN) 1 or 2, Nicastrin (NCT, a type I trans-membrane glycoprotein), the anterior pharynx defective (APH)-1a or APH-1b, and PSEN enhancer (PEN)-2. These four proteins are requested for the functionality of the enzyme [Takasugi N et al., 2003].

APP cleavage by  $\gamma$ -secretase can produce A $\beta$  peptides with different amino acid length. In the majority of the cells A $\beta$ 1-37, 38, 39 and 42 are present in low amounts (5-20% of total A $\beta$ ), while the main species is A $\beta$ 1-40 (50% of total A $\beta$ ).

### 1.2.3 $\beta$ -AMYLOID PEPTIDE

According to ACH,  $\beta$ -amyloid generation is the first crucial event of AD pathogenesis. In 1984 Glenner and Wong isolated and purified this 4.2 kDa

peptide, hypothesizing it as a derivate of a longer precursor protein **[Glennner GG et al., 1984]**.

In physiological conditions, the ratio between A $\beta$ 42 and A $\beta$ 40 fractions is 1:10. The shift of this ratio is the first step of senile plaques formation and initiation of all the pathological AD characteristic events **[Mawuenyega KG et al., 2010]**.

The toxicity resulting from the increase in A $\beta$ 42 levels is due to its greater tendency to aggregation compared to A $\beta$ 40. In fact, all A $\beta$  monomers are soluble and harmless, but after aggregation they become neurotoxic and cause a reduction in the peptide clearance itself **[Kumar S et al., 2011]**.

It has been reported that A $\beta$ 42 oligomers accelerate further monomers aggregation to form toxic oligomers and fibrils. Furthermore, A $\beta$ 40 seems able to inhibit A $\beta$ 42 oligomerization by blocking it in stable tetrameric forms **[Irie K et al., 2005; Murray MM et al., 2009]**.

The study of A $\beta$  aggregation allowed to identify monomeric A $\beta$  structure that is composed by  $\alpha$  helix and/or disordered structures. The conformational changes that lead to  $\beta$ sheets formation, typical of disordered proteins, promote A $\beta$  oligomers formation.

Kinetic studies demonstrated that A $\beta$  monomers misfolding anticipate oligomerization and constitutes the core for fibrils growth.

The process for fibrils formation can be divided in two steps: a nucleation phase and an elongation phase.

The nucleation phase involves A $\beta$ 42 monomers self-association, a process that is thermodynamically unfavoured.

Then follows a rapid enhancement phase in which oligomers are converted to proto-fibrils and finally mature fibrils.

Fibrils formation can be kinetically represented by a sigmoid with an initial latent phase followed by a rapid growth and a final plateau [Kumar S et al., 2011] (Figure 1.6).

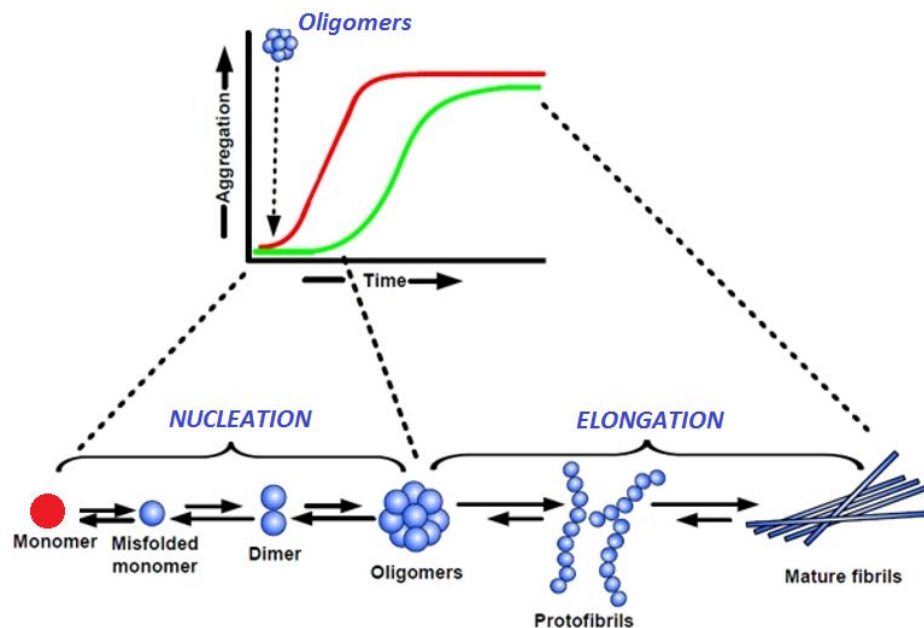


**Figure 1.6** Polymerization model of A $\beta$ : kinetic curve of fibrils formation (green) and the same kinetic curve with a shorter latency phase because of pre-formed seeds addition (red) (modified from [Kumar S et al., 2011]).

### 1.2.3.1 A $\beta$ oligomers

Even though A $\beta$  fibrils inside senile plaques have been proposed as the cause of AD for a long time, recent evidences suggest that intermediate oligomeric forms (A $\beta$ O) are the toxic factors [Verma M et al., 2015] (Figure 1.7).

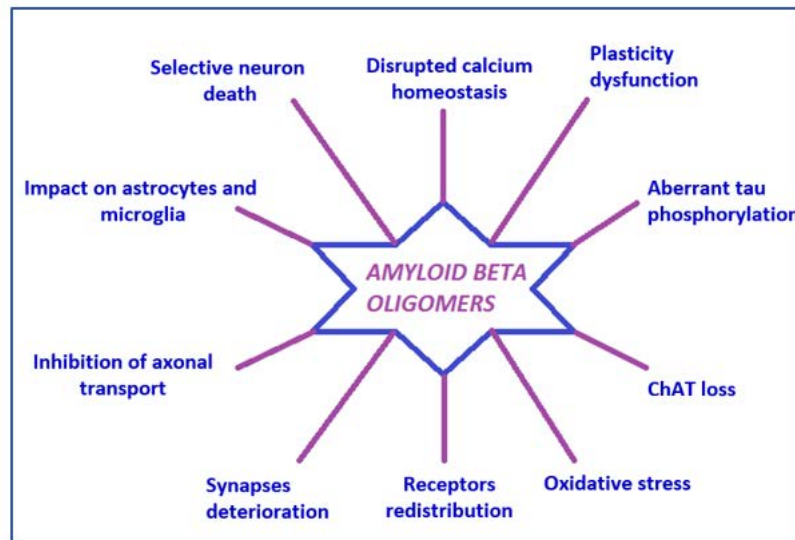


**Figure 1.7** AD-associated changes attributed to A $\beta$  oligomers (modified from [Viola KL and Klein WL, 2015]).

The levels of soluble A $\beta$ O<sub>s</sub> in human brain seem to correlate better with the severity of the disease than amyloid plaques do. Moreover, fibril-free A $\beta$ O<sub>s</sub> solutions are fundamental for memory loss, while fibrillary A $\beta$  is not the active form affecting cognition [da Rocha-Souto B, et al., 2011; Brito-Moreira J et al., 2017].

The exact localization of A $\beta$ O<sub>s</sub> is not fully clear, but there is convincing evidence of both intracellular and extracellular localizations. In particular, extracellular membrane-associated A $\beta$ O<sub>s</sub> are observable at early stages of AD, but intraneuronal A $\beta$ O<sub>s</sub> appear prior to extracellular plaques formation. It seems that there could be a dynamic exchange between the two spaces [Mroczko B et al., 2018].

A $\beta$ O<sub>s</sub> formation starts with alterations in the conformation of the monomer, resulting in low molecular weight (LMW) dimers and trimers that accumulate further monomers to form high molecular weight (HMW)



oligomers. These different conformations may be different also in their production's pathway or toxicity [Ladiwala AR et al., 2012].

A specific neurotoxic function was attributed to the dodecamer called A $\beta$ \*56. Lesnè and colleagues found an inverse relationship between the level of A $\beta$ \*56 and memory performance in Tg2576 mice. They also demonstrated that injection of young rats with A $\beta$ \*56 purified from impaired mice was able to disrupt memory [Lesnè S et al., 2006]. Another study demonstrated that A $\beta$ \*56 interacts with NMDARs in cultured neurons, increasing intracellular calcium influx and activating phosphorylation and missorting of tau protein [Amar F et al., 2017].

The toxicity of A $\beta$ O<sub>s</sub> has been correlated with the direct or indirect action on specific receptors associated with intracellular cascades, with the formation of intramembrane pores with ionic channel functions, or with non-specific perturbation of both the intra- and extracellular membrane dynamics [Forloni G et al., 2016].

Numerous candidates have been proposed as receptors for A $\beta$ O<sub>s</sub>, and are summarized in Figure 1.8.

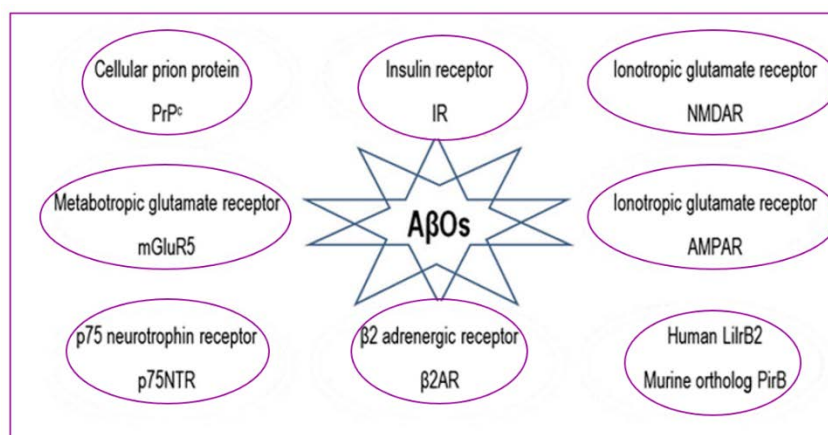


**Figure 1.8** Proposed receptors for A $\beta$ O<sub>s</sub> (modified from [Mroczko B et al., 2018]).

## 1.2.4 sAPP $\alpha$

The sAPP $\alpha$  soluble fragment is a product of APP processing through the non-amyloidogenic pathway, operated by the  $\alpha$ -secretase enzyme. The role of this fragment has been investigated over the years in order to evaluate its physiological role in the brain and its contribution to neurodegeneration and AD pathology (Figure 1.9).

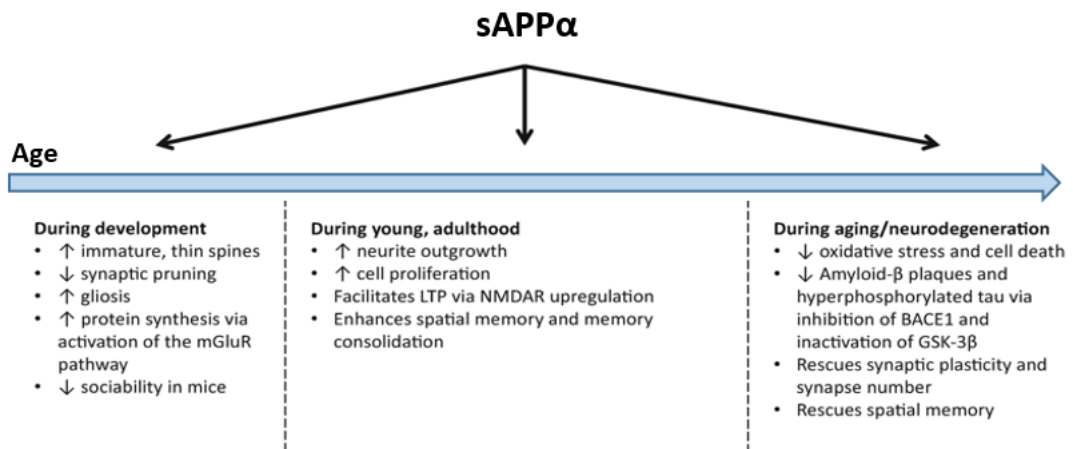


**Figure 1.9** Functions of sAPP $\alpha$  during three time-points of life: development, young adult, ageing/neurodegeneration (modified from [Corbett NJ and Hooper NM, 2018]).

sAPP $\alpha$  has been shown to have a neuroprotective role in the adult brain and during ageing or neurodegeneration. In fact, it is able to promote neuronal growth and synaptogenesis [Mattson MP, 1997] and to reduce the production of A $\beta$  by modulating the activity of BACE1 in cellular and *in vivo* models [Obregon D et al., 2012]. The viral gene transfer of sAPP $\alpha$  directly in the brain preserved synaptic loss, rescued memory impairment and decreased A $\beta$  levels in a mouse model of AD [Fol R et al., 2016]. A link between sAPP $\alpha$  and tau has been established both *in vitro* and *in vivo*: the protein was able to

decrease phosphorylated tau via glycogen synthase kinase 3 $\beta$  (GSK-3 $\beta$ ) activity modulation [Deng J et al., 2015]. Several published data demonstrated that sAPP $\alpha$  production is stimulated by low cholesterol or inhibition of cholesterol biosynthesis [Kojro E et al., 2010]. The mechanisms of action of sAPP $\alpha$  in brain are still to be fully elucidated, but some hypotheses have been raised, as for example its involvement in NMDA receptors functions [Taylor CJ et al., 2008] or its binding to p75 neurotrophic receptor [Hasebe N et al., 2013].

A recent work demonstrated that sAPP $\alpha$  functions as ligand for the GABA $_B$ R1a receptor to modulate synaptic transmission and plasticity [Rice H et al., 2019]. Besides these protective effects, too high levels of sAPP $\alpha$  can cause it to behave like a tumorigenic molecule [Nhan HS et al., 2015]. In addition, some studies suggested the importance of maintaining balanced levels of sAPP $\alpha$  during brain development as an excessive increase could be detrimental for synaptic plasticity functions [Pasciuto E et al., 2015]. This suggest that the timing, but also the amount of the protein, is critical at the synaptic level.

### 1.2.5 sAPP $\beta$

The soluble fragment sAPP $\beta$  is the product of amyloidogenic processing operated by BACE-1. Although sAPP $\alpha$  and sAPP $\beta$  differ just from 16 amino acids, sAPP $\beta$  lacks most of the neuroprotective effects of sAPP $\alpha$ . The neuroprotective effects of sAPP $\beta$  against glucose deprivation, excitotoxicity, and A $\beta$  peptide are 50- to 100-fold less potent [Furukawa et al, 1996]. In contrast with sAPP $\alpha$ , sAPP $\beta$  is not involved in LTP, suggesting that the last 16

C-terminal amino acids of sAPP $\alpha$  protein are involved in both neuroprotection and LTP [Taylor CJ et al., 2008].

A recent study suggested that sAPP $\beta$  could be cleaved to generate an N-terminal fragment. The N-terminal fragment can bind death receptor 6, activating caspase 6 which leads to further stimulation of axonal pruning and neuronal cell death [Nhan HS et al., 2015].

Overall, the functions that are related to the common domains of the two sAPP fragments are identical and are not affected by differences in the amino acidic sequence. This suggest that sAPP $\beta$  cannot be deleterious *per se*, and therapeutic strategies for AD that target A $\beta$  cleaving enzymes should aim to modulate rather than inhibit A $\beta$  generation [Chasseigneaux and Alliquant, 2012].

### 1.2.6 TAU PROTEIN

Tau protein is a microtubule-associated protein, which is abundant in neurons of the central and peripheral nervous system of vertebrates. It is part of a family called MAP (microtubules-associated proteins) and was isolated and co-purified for the first time in 1975 with tubulin, a component of microtubules, which are involved in maintaining neuronal morphology and play a fundamental role in cellular trafficking.

The gene that encodes tau protein is located on chromosome 17, and in the human brain there are six different isoforms of the protein, generated by alternative splicing [Bakota L et al., 2016].

Tau is a naturally unfolded protein with a high solubility under physiological conditions. To be susceptible to aggregation, tau must undergo a series of

post-translational modifications and conformational changes. In general, tau aggregation starts with its hyperphosphorylation, and when this happens the protein detaches from the microtubules and switches to a compact structure called “Alz50 state”. This aggregated state allows subsequent aggregation to form fibrillar structures. Furthermore, thanks to proteolytic cuts, a fragment called Tau-66 assembles into aggregates much faster than the native form. NFTs that originate at the end of this process are mostly formed by paired helical filaments (PHF-tau) [Lim S et al., 2014].

The formation of such aggregates is not typical of AD alone, but can be observed in other disorders that can be called “tauopathies”.

It is now well known that Glicogen Synthase Kinase 3 (GSK-3) uncontrolled activation is involved in tau pathologic hyperphosphorylation (Figure 1.10).

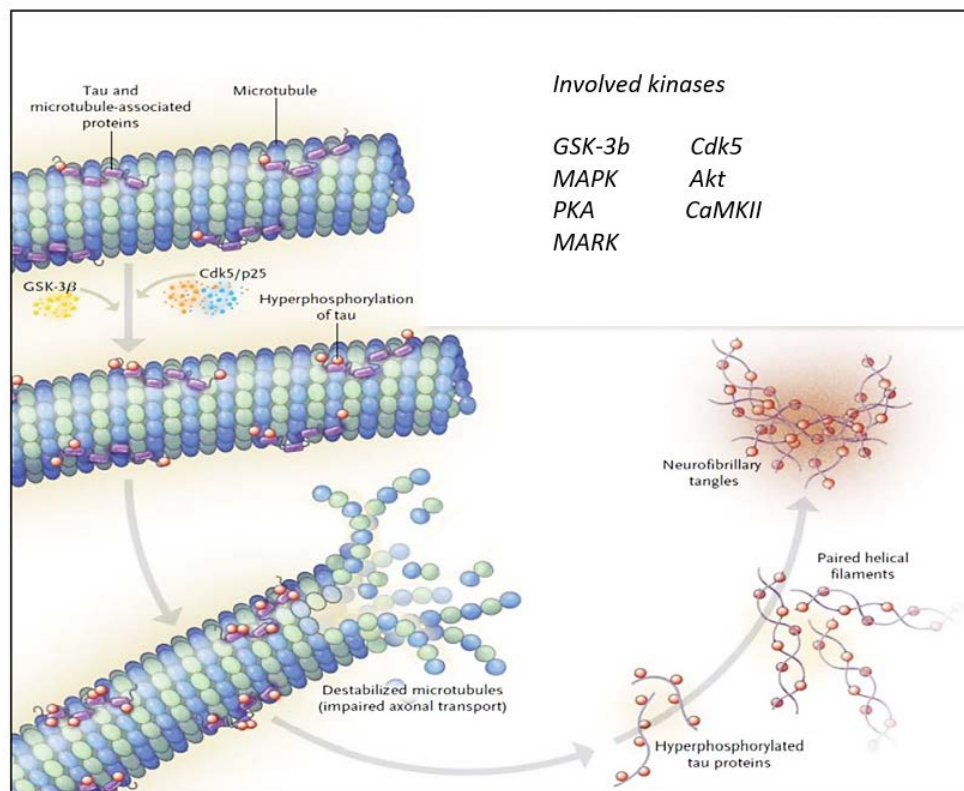


**Figure 1.10** Structure of microtubules and phosphorylation sites of tau protein. Tau hyperphosphorylation by GSK3 causes the destabilization of microtubules, followed by the detachment of Tau and its self-aggregation (modified from [Barage SH et al., 2015]).

GSK-3 is over-expressed in AD patients' brain and directly contributes to NFTs increase. For this reason, the enzyme has been studied as a specific pharmacological target for AD treatment [Gameiro I et al., 2017].

Abnormally phosphorylated tau was observed in selected subcortical areas long before its presence in the cerebral cortex, which could indicate that disease-like phosphorylation occurs already in early, preclinical disease states [Attems J et al., 2012]. In addition, tau is subjected to various other post-translational modifications including O-glycosylation, ubiquitination, methylation and acetylation. Interestingly, tau acetylation at Lys174 has been recently identified as an early modification in brains from patients with AD, which slowed down tau turnover in a mouse model and promoted tau aggregation [Min SW et al., 2015].

Figure 1.11 shows how the ACH can be influenced by tau pathologic features.

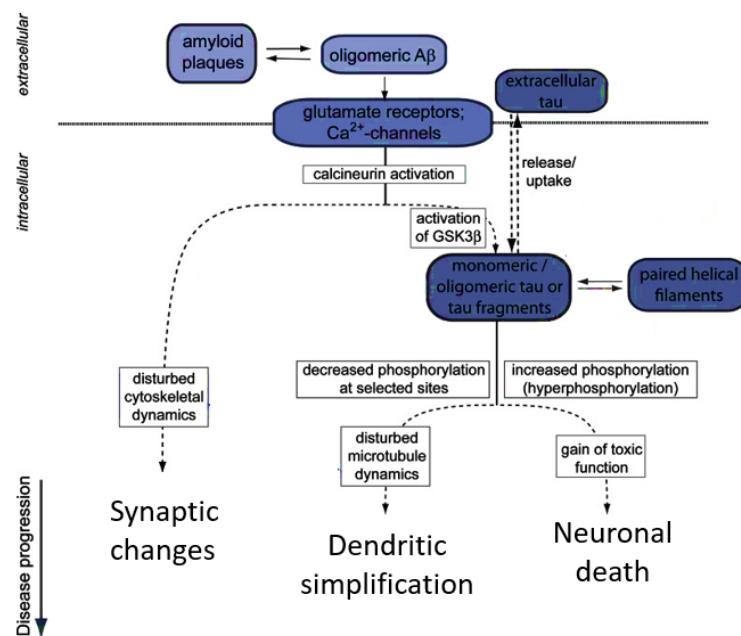


**Figure 1.11** The modified ACH where Aβ oligomers induce the synaptic changes, dendritic simplification and neuronal death via tau dependent and independent mechanisms (modified from [Bakota L and Brandt R, 2016]).

## 1.2.7 NEUROINFLAMMATION

Neuroinflammation has been evident in AD patients since the disease was first described by Alois Alzheimer. Clusters of both reactive microglia and astrocytes migrate to and surround amyloid deposits in the brain of post-mortem AD samples.

Neuroinflammation in AD is considered as a double-edged sword where the immune cells of the brain exert beneficial effects by degrading A $\beta$  deposits, as well as adverse effects by producing cytotoxic mediators that exacerbate A $\beta$  deposition resulting in neuronal dysfunction [Bhaskar M, 2016].

The two major players of the neuroinflammatory response in AD context are astrocytes and microglia (Figure 1.12).

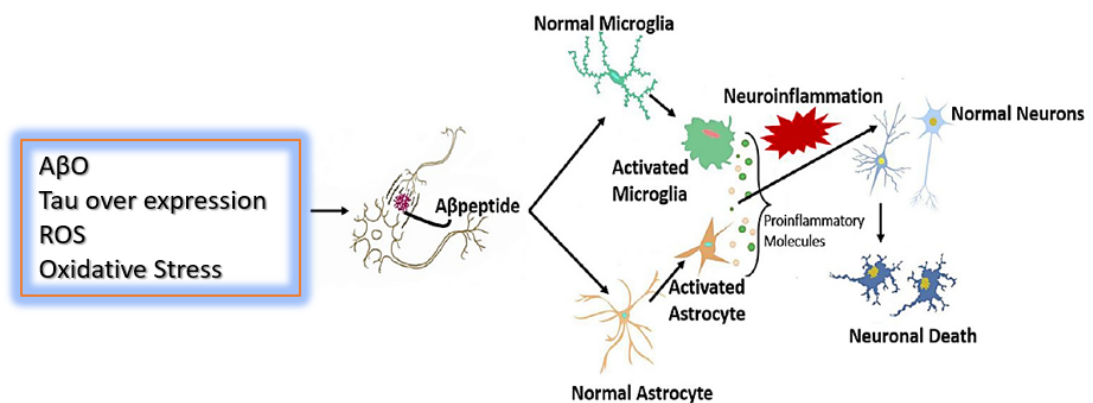


**Figure 1.12** Possible role of microglia and astrocytes in AD pathology mediated by neuroinflammatory cytokines (modified from [Ahmad MH et al., 2019]).

Microglia are the brain's resident immune cells and are found throughout the brain, spinal cord, retina and optic nerves but mainly in the hippocampus and substantia nigra.

During AD progression, microglia respond to various stimuli, including amyloid beta peptides and NFTs **[Czeh M et al., 2011]**.

It is the delicate balance between the neurotoxic and neuroprotective features that determines the role of microglial cells in AD onset and progression. In their resting form, they act on neurogenesis, synaptic pruning and neuroprotection **[Sierra A et al., 2010; Vinet J et al., 2012]**, but their prolonged over activation leads to an ineffective A $\beta$  clearance, resulting in a pro-inflammatory state **[Hickman SE et al., 2008]**. Activated microglia produce and secrete several mediators that contribute to AD pathogenesis **[Cai Z et al., 2014]**.

Astrocytes located in the CNS support the endothelial cells of the blood-brain-barrier (BBB), maintain ion balance, and provide nutrients to neurons **[Morales I et al., 2014]**. Like microglia, astrocytes release cytokines, ILs, NO, and other potential cytotoxic molecules after exposure to A $\beta$ , thereby exacerbating the neuroinflammatory response. Astrocytes damage and dysfunctions between astrocytes and the surrounding neurons can destroy the synaptic homeostasis, and initiate the cascade for neuronal injury **[Avila-Muñoz E and Arias C, 2014]**. Above all, During AD pathology, astrocytes start to express BACE-1, thus acquiring A $\beta$  producing ability **[Rossner S et al., 2005]**.

With the fact that A $\beta$  accumulation is a potent glial activator, astrocytic and microglial activation could be an early event in the pathologic process, occurring even in the absence of A $\beta$  deposition. A possible mechanism for activated astrocytes and microglia during AD pathology is described in Table 1.2 **[Ahmad MH et al., 2019]**.



<i>Mediator</i>		<i>Pathologic effect</i>
Microglia Astrocyte	TNF- $\alpha$	↑tau hyperphosphorylation ↓ nitric oxide ↑A $\beta$ synthesis; ↓A $\beta$ clearance
Microglia Astrocytes	IL-1 $\beta$	↑ tau phosphorylation ↓ tau pathology ↑ APP transcription and transduction in neurons ↑A $\beta$ synthesis ↓A $\beta$ related pathology
Microglia Astrocytes	IL-6, IL-8	↑tau hyperphosphorylation ↑production of APP ↑A $\beta$ production
Microglia Astrocytes	IL-18, IL-23	↑tau hyperphosphorylation ↓ GSK-3 $\beta$ expression ↑Cdk5 expression ↑production of APP ↑A $\beta$ production

**Table 1.2** *The impact of microglia and astrocytes in AD pathogenesis mediated by pro-inflammatory cytokines (modified from [Ahmad MH et al., 2019]).*

### 1.2.8 OXIDATIVE STRESS

In the brain, the free energy necessary to drive most cellular reactions derives from aerobic glucose oxidation. Oxidative stress is associated with increased production of reactive oxygen species (ROS) and reactive nitrogen species (RNS) such as O $_2^-$ , H $_2$ O $_2$ , NO, HO $^-$ , ONOO $^-$ , and the major contributors of this overproduction are mitochondria. Under normal conditions, ROS levels are regulated by antioxidant enzymes such as superoxide dismutase (SOD), catalase and glutathione peroxidase (GPX), and transcription factors as Nrf2, which stimulates the transcription of cytoprotective genes and antioxidant enzymes and proteins [Denzer I et al., 2016].

In AD, the balance between ROS production and antioxidant defence is impaired, and there is evidence that mitochondrial damage, resulting in ROS overproduction, contributes to the early stage of AD prior to the onset of symptoms and A $\beta$  pathology [Uttara B et al., 2009].

Several data demonstrate that in addition to mitochondrial ROS production, abnormal homeostasis of bioactive metals including iron (Fe), copper (Cu), zinc (Zn), magnesium (Mg), manganese (Mn) and aluminium (Al) could be involved in free radical production and oxidative stress influencing A $\beta$  and Tau aggregation **[Greenough MA et al., 2013; Wang P and Wang ZY, 2016]**. There is a tight connection between protein misfolding, aggregation, and metal ion homeostasis. For example, Zn affects APP processing by binding to the protein, and Al, Fe, Zn, and Cu directly bind A $\beta$  promoting its aggregation **[Lammich S et al., 1999; Tougu V et al., 2008; Mantyh PW et al., 1993]**. Similarly, the redox metals could stimulate Tau phosphorylation, its detachment from microtubules and NFTs deposition **[Sayre LM et al., 2000]**. In addition, a direct binding of A $\beta$  with Fe or Cu has been shown to generate H<sub>2</sub>O<sub>2</sub>, contributing to oxidative stress increase and extra-mitochondrial ROS production **[Huang X et al., 1999]**. Another source of ROS production directly mediated by A $\beta$  involves microglia activated in the brain in response to extracellular amyloid deposition.

Furthermore, evidences in animal models of AD and humans suggested a direct relationship between oxidative stress, A $\beta$  deposition and Tau phosphorylation, where pTau affects the activity of mitochondrial complex I, contributing to A $\beta$ -mediated dysfunction and ROS production **[Mondragon-Rodriguez S et al., 2013]**.

All these data suggest that altered mitochondria, oxidative stress, impaired antioxidant defence, production of A $\beta$  and pTau, which ultimately influence mitochondrial dynamics and ROS production, could lead to a “vicious cycle”

that with time exacerbates the pathologic process, leading to neuronal loss, as illustrated in Figure 1.13 [Tönnies E and Trushina E, 2017].

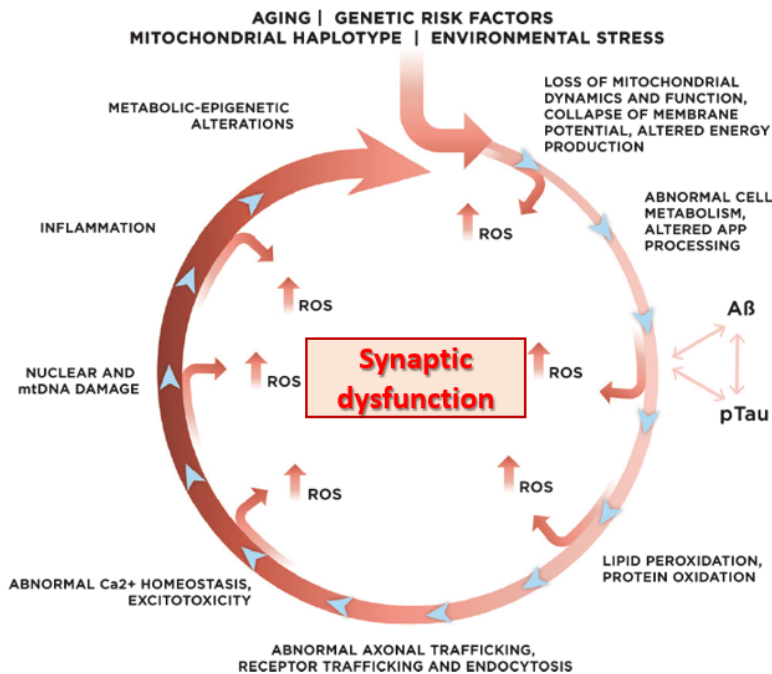


**Figure 1.13** Multiple cellular pathways and systems are affected by ROS, exacerbating ROS production, accelerating cellular damage, and leading to synaptic dysfunction (modified from [Tönnies E and Trushina E, 2017]).

### 1.2.9 IN VITRO MODELS TO STUDY AD PATHOGENESIS

Thanks to research progresses during the past years, several 2D and 3D cellular models have been proposed to study AD, combining standard culture methods with new technological platforms such as microfluidic systems and scaffolds [Ranjan VD et al., 2018].

AD *in vitro* models are usually obtained by AD-related genes transfection or treatment with synthetic compounds such as Aβ peptides. Among different types of cell cultures useful for this aim there are:

- Cell lines or primary neurons
- Induced pluripotent stem cells (iPSCs)
- 3D culture platforms

Cell lines, such as neuroblastoma SH-SY5Y cells, or primary neurons are the most common *in vitro* approach for analysing mechanisms underlying AD. Even though this approach is cheap and easy to carry out, there are some limitations, as the cultured cells are susceptible to variations in genetic or physiologic features that do not allow accurate reproducibility and disease modelling [Horvath et al., 2016]. In addition, the use of rodent cultures is limited by their differences in pathological pathways compared to human cells.

The discovery of iPSCs in 2006 opened up a new frontier in *in vitro* research and neurodegenerative disease modelling [Takahashi and Yamanaka, 2006], converting adult human cells into pluripotent stem cells that can be potentially differentiated in every cell type. This technology overcame the limits of the use of murine cells and tumor-derived cell lines, but it raised also ethical concerns of the use of human embryonic stem cells (hESCs).

A number of 2D Alzheimer's disease models have been developed using iPSCs technology, and are listed in Table 1.3.

iPSCs-based AD <i>in vitro</i> models		
FAD	Increased A $\beta$ 42 levels; $\gamma$ -secretase inhibitor treatment modulated A $\beta$ 42 levels	(Yagi et al., 2011)
FAD & SAD	Increased A $\beta$ , aGSK-3 $\beta$ , and p-tau levels; $\beta$ -secretase inhibitor treatment reduced A $\beta$ , aGSK-3 $\beta$ , and p-tau levels whereas $\gamma$ -secretase inhibitor treatment reduced A $\beta$ levels only	(Israel et al., 2012)
AD	Generation of disease specific iPSC lines from patients	(Jang et al., 2012)
FAD & SAD	Formation and accumulation of A $\beta$ oligomers inducing ER and oxidative stress; docosahexaenoic acid treatment alleviated the stress responses	(Kondo et al., 2013)
AD (DS)	Cells derived from DS patients developed AD pathologies over months in culture; production of A $\beta$ 42 peptides and hyperphosphorylated tau; $\gamma$ -secretase inhibitor treatment blocked A $\beta$ 42 production	(Shi et al., 2012)
FAD	Increased A $\beta$ 42 to A $\beta$ 40 ratios; 14 genes showing altered expressions relative to controls	(Sproul et al., 2014)
FAD	Increased APPs $\beta$ , A $\beta$ , total tau, and phosphorylated tau levels; A $\beta$ -specific antibody treatment early in culture reverses the phenotype of increased total tau levels	(Muratore et al., 2014)
FAD & SAD	Derivation of basal forebrain cholinergic neurons; increased A $\beta$ 42 to A $\beta$ 40 ratios; $\gamma$ -secretase inhibitor treatment showed altered responses in A $\beta$ 40 production with an increase seen in SAD lines	(Duan et al., 2014)
FAD	Knock-in early-onset AD mutations into iPS cells using CRISPR/Cas9 technology	(Paquet et al., 2016)

**Table 1.3** A list of some 2D cellular models of different AD forms, developed using iPSCs techniques, with their features of disease modelling (modified from [Ranjan VD et al., 2018]).

Despite their advantages, some limitations of iPSCs are to be considered, such as their heterogeneity, the variability in differentiation protocols used by different groups but also the inability of mimicking mature neurons and form complex neuronal networks present in *in vivo* conditions [Arber et al., 2017; Jorfi et al., 2017].

3D cultures that can host both cell lines and iPSCs, offer different advantages over 2D approaches, especially in terms of cell adhesion, communication, proliferation and mechanotransduction. Realizing 3D microenvironment is of vital importance for neurodegeneration modelling, allowing cell-to-cell interactions (i.e neurons-glia cells or neurons-neurons) and spatial configuration of cellular networks [Ko KR and Frampton JP, 2016]. The main 3D AD models are explant cultures, self-assembled aggregates, scaffold cultures and microfluidic organ-on-chip cultures [Ranjan VD et al., 2018], presented in Figure 1.14.

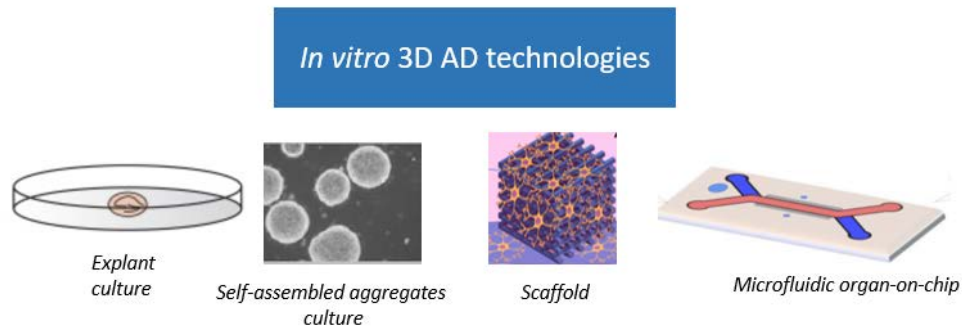


**Figure 1.14** Four technologies for 3D AD modelling: explant culture, self-assembled aggregates, scaffolds and microfluidic organ-on-chip system.

### 1.2.10 MOUSE MODELS TO STUDY AD PATHOGENESIS

Mouse models continue to play a pivotal role in AD research, taking advantage of their low cost, small size, high birth rate and easy maintenance.

Given the lack of an etiology of idiopathic AD, the majority of animal models have relied on the utilization of genetic mutations associated with FAD, with the rationale that the events downstream of the initial trigger are quite similar. Although no single mouse model recapitulates all of the aspects of the disease, each model can be useful for the analysis of one or two components of the disease [LaFerla FM and Green KN, 2012].

It has been observed that the higher the number of mutations, the faster is A $\beta$  production and accumulation [Cavanaugh SE, 2014].

Since 1995, several models overexpressing APP with FAD-related mutations have been developed, such as the Tg2576, the APP23, and the PDAPP lines. All these models overexpress APP with consequent overproduction of A $\beta$ 40 and A $\beta$ 42, and show human AD particular features such as amyloid plaques, gliosis, synaptic damage, LTP and memory impairment, with an average onset of symptoms between 9 and 12 months of age [Puzzo D et al., 2015].

The onset of the AD phenotype occurs earlier (from 3-4 months of age) in double Tg mice where the mutated APP is co-expressed with mutated PS1 or PS2 (M146L or M146V variants) [Trinchese S et al., 2004]. However, these mice do not show some aspects of the disease such as neuronal loss and tau deposition.

Oddo and colleagues generated mice harbouring 3 different mutations, the 3xTg-AD model (APP<sup>Swe</sup>, PS1 M146V, tauP301L) [Oddo S et al., 2003], with A $\beta$  pathology that precedes tau pathology with NFTs formation, LTP and memory impairment, and neuroinflammation.

There is also a 5xTg model (APP Swedish, Florida and London mutations, and PS1 M146L/L286V mutations) which presents, above other AD signs, neuronal loss in the cortical area [Jawhar S et al., 2012].

An overview of the progression of AD features in commonly used mouse models is represented in Figure 1.15.

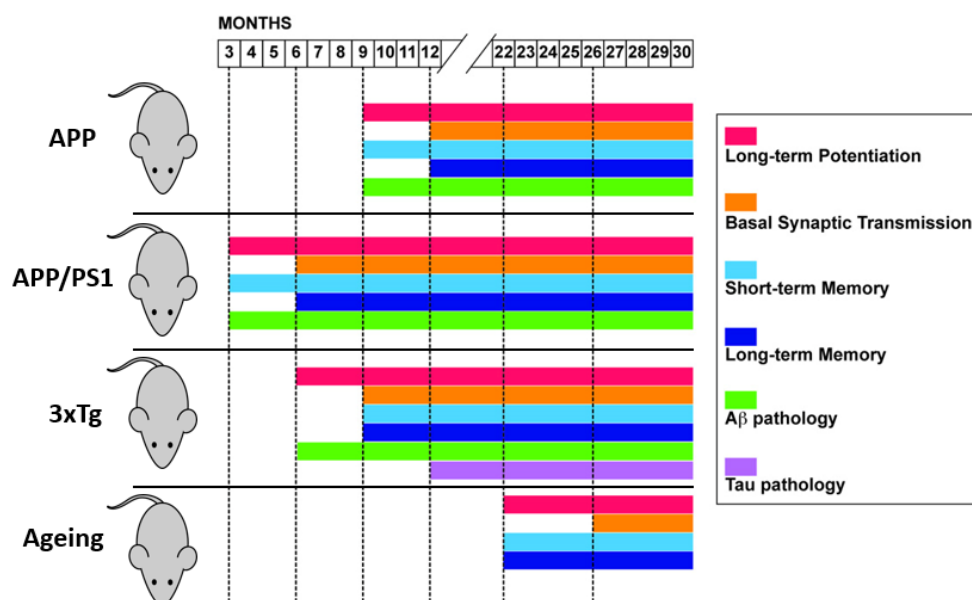


**Figure 1.15** Onset and progression of AD features in three Tg mouse models (single APP Tg<sup>2576</sup>, double APP/PS1, triple 3xTg) and in a physiological model of ageing (modified from [Puzzo D et al., 2015]).

Finally, a list of advantages and limitations of *in vivo* and *in vitro* AD models is described in Table 1.4, underlining that none of the proposed approaches is able by itself to recapitulate AD pathological picture.

AD model	Advantages	Limitations
In vitro	<ul style="list-style-type: none"> <li>▪ Use of stem cell technology making it more relevant to humans</li> <li>▪ Recapitulate both A<math>\beta</math> and tau pathology</li> <li>▪ Drug screening</li> <li>▪ Use of microfluidic platforms and scaffolds to mimick brain micro-environment</li> <li>▪ High-throughput</li> <li>▪ Elevated ER and oxidative stress levels</li> </ul>	<ul style="list-style-type: none"> <li>▪ iPSCs heterogeneity</li> <li>▪ iPSCs tumorigenicity</li> <li>▪ Lack of vascularization</li> <li>▪ Cell lines and culture protocols variability</li> <li>▪ Limited human AD cells sources</li> <li>▪ Difficulty in imaging of 3D cultures</li> <li>▪ Long-term cultures are difficult and expensive</li> <li>▪ Scalability and standardization of iPS platforms</li> </ul>
In vivo	<ul style="list-style-type: none"> <li>▪ Recapitulation of A<math>\beta</math> pathology</li> <li>▪ Possibility to assess cognitive deficits</li> <li>▪ Suitable for long-term research</li> <li>▪ Physiological relevance</li> <li>▪ Possibility of therapeutic screening</li> <li>▪ The structure and biochemistry of ageing non-human primates brain is similar to ageing human brain</li> </ul>	<ul style="list-style-type: none"> <li>▪ NFT robust pathology requires additional mutations</li> <li>▪ Dissimilarities between murine and human AD brain</li> <li>▪ Variations in phenotypes of different models</li> <li>▪ Low reproducibility</li> <li>▪ Low neuronal loss</li> <li>▪ Expensive</li> <li>▪ Ethical and legal concerns</li> <li>▪ High expression level of transgenes to induce the phenotype</li> </ul>

**Table 1.4** Advantages and limitations of *in vitro* and *in vivo* AD modelling approaches (modified from [Ranjan VD et al., 2018]).

### 1.3 AD treatment strategies

Nowadays, the available treatments for AD are symptomatic, and can only delay the need for the patient to be placed in a nursery home. In addition, the last FDA approved New Chemical Entity (NCE) for AD treatment, Memantine, dates back to 2003, as most of the “disease-modifying drugs” under study are still in clinical phase or failed the experimentation [Atri A, 2011; Small GW et al., 2015].



### 1.3.1 CURRENT THERAPIES

Current drugs for AD treatment act on the main nervous transmission systems that appear altered in the disease, the cholinergic and glutamatergic systems.

To that, is generally added a support therapy with antidepressants and antipsychotics.

The most prescribed symptomatic treatment is based on acetylcholinesterase (AChE) inhibitors: tacrine, donepezil, rivastigmine and galantamine. These molecules reduce ACh degradation inhibiting its degrading enzyme. ACh increase in the synapses leads to cholinergic stimulation in the post-synaptic compartment and memory and learning improvement **[Colović MB et al., 2013]**.

An excess of extracellular glutamate because of an increased release and decreased reuptake also characterizes AD, causing continuous stimulation of post-synaptic NMDA receptors **[Revett TJ et al., 2013]**. Memantine is a non-competitive antagonist of NMDA receptor and acts blocking its open conformation. Memantine treatment showed an improvement of learning, psychiatric symptoms and the general clinical features of the patient **[Anand R et al., 2014]**.

### 1.3.2 NEW THERAPEUTIC TARGETS

The scientific confirmation of the value of the ACh evidenced new possible therapeutic targets. One of these consists in increasing the non-amyloidogenic processing of APP. For example, BACE1 inhibitors as Verubecestat (MK-8931), showed sAPP $\beta$ , A $\beta$ 40 and A $\beta$ 42 reduction in the brain and CSF of

treated monkeys and rats, and reached the clinical phase after promising results obtained also in human patients **[Kennedy ME et al., 2016]**, but unfortunately the trial was stopped due to lack of efficacy.

The possible strategy to inhibit  $\gamma$ -secretase is limited by important side effects because of cross-interaction of the drug with other enzymes. In particular, the inhibitor Semagacestat showed plasmatic  $A\beta$  reduction together with some side effects on gastrointestinal tract and immune system **[Doody RS et al., 2015]**.

Nevertheless, it was observed that some NSAFA are able to counteract  $A\beta_{42}$  production inhibiting  $\gamma$ -secretase with minor side effects **[Tayeb HO et al., 2012]**.

Also tau protein is directly involved in AD pathogenesis, and several studies focused on its hyper phosphorylation prevention. This abnormal modification is catalysed in part by GSK-3 $\beta$ .

GSK-3 $\beta$  over-expression in mice causes tau hyper phosphorylation, while treatment with lithium, a specific GSK-3 $\beta$  inhibitor, attenuates tau phosphorylation and blocks tau-induced neurodegeneration **[Engel T Goñi-Oliver P et al., 2006]**.

Recently, a new compound able to inhibit GSK-3 $\beta$  and to induce Nuclear factor erythroid 2-related factor 2 (NRF2) has been tested. NRF2 is a transcription factor involved in anti-oxidant response and protects from oxidative damage. The tested compound showed an interesting role in neuroprotection of *in vitro* oxidative stress and AD models **[Gameiro I et al., 2017]**.

### 1.3.2.1 The multi-targeted approach

As AD is a complex and multifactorial disease, in the last few years the “one-molecule, one-target” paradigm has been exceeded by the new “multi-targeted” approach. This strategy can be based on two concepts:

- The Multi-target Directed Ligand (MTDL) approach, that aims to find a compound or a hybrid that is effective in treating complex diseases interacting with the multiple targets responsible for its pathogenesis **[Cavalli A et al., 2008]**.
- The Combination-drugs-multi-targets (CDMT) approach, that it a combination of different drugs that could act on different targets being complementary, or act on the same targets giving synergistic or additive effects.

The MTDL strategy has now been incorporated in routine therapeutic drug design, and a considerable number of compounds have been described in the last 10 years, basing on this therapeutic approach **[Oset-Gasque MJ and Marco-Contelles J, 2018]**.

In fact, as an example, the limited success of AChE inhibitors is because by improving cognitive, behavioral, and functional impairments, they seem unable to address the molecular mechanisms that underlie the pathogenic processes **[Cavalli A et al., 2008]**.

Some of the published MTDL strategies are described below.

Jeřábek and colleagues combined the structural features of the AChE inhibitor tacrine with that of resveratrol, which is known for its antioxidant and anti-neuroinflammatory activities. They found that hybrid compounds inhibited human AChE, effectively modulated A $\beta$  self-aggregation *in vitro*,

and exerted anti-inflammatory and immuno-modulatory properties in neuronal and glial AD cell models [Jeřábek J et al., 2016].

Another recent work reported the activity of hybrid compounds directed to AChE inhibition, nicotinic receptors stimulation and A $\beta$  aggregation inhibition [Simoni E et al., 2017].

Yan and colleagues fused donepezil and curcumin structures and tested their AChE inhibition, amyloid- $\beta$  aggregation inhibition and antioxidant effect with great results [Yan J et al., 2017].

Another compound developed under fusion of GSK-3 $\beta$  inhibitors and NRF2 inducers showed an interesting neuroprotective effect on inflammation, oxidative stress and neuronal death [Gameiro I et al., 2017].

Another growing approach consists of the development of BACE-1-centered compounds with a more complex mechanism of action to target different AD-related pathways [Prati F et al., 2018].

Finally, some other multi-target agents have been discovered without the fusion of two specific structures, as Quinti and colleagues did on HD models. They identified a novel thiazole-containing compound with SIRT2 inhibition and NRF2 induction properties, highlighting the potential combinatorial therapeutic effect of multi-targeted agents not only for HD, but also for other neurodegenerative diseases [Quinti L et al., 2016].

Several studies have also been developed under the CDMT hypothesis. As an example, there are some clinical trials where the combination therapy consists in AchE inhibitors and memantine administration [Matsunaga S et al., 2014]. Another study reported the beneficial role of

the combination of galantamine and cilostazol on cognition and daily living functions in AD patients with cerebrovascular disease [**Hishikawa N et al., 2017**].

Moreover, a preclinical study on an AD mouse model revealed that the combination of octyl gallate and ferulic acid improved neurodegeneration and cognition [**Mori T et al., 2017**]. Another group reported that a 2-week leptin and pioglitazone acute combined treatment resulted in cognitive, synaptic and amyloid-related improvement in a transgenic mouse model [**Fernandez Martos CM et al., 2016**].

### **1.3.3 INNOVATIVE THERAPEUTIC STRATEGIES**

Several non-conventional approaches are actually under study to counteract AD progression, and among them, we can mention immune therapy, cell-based therapy, and drug-delivery systems (DDS).

#### **1.3.3.1 Immune therapy**

Immune therapy is focused on A $\beta$  clearance to prevent toxic oligomers accumulation. It consists in A $\beta$  peptide or part of it exposure, to stimulate immune response (active immunization), or alternatively to administer a specific monoclonal antibody against A $\beta$  (passive immunization) [**Evin G, 2016**]. However, this approach has actually strong limitations; for example, the monoclonal antibody CAD106, used in a phase III clinical trial, showed serious side effects in 24.5% of patients and his approval was discontinued [**Vandenberghe R et al., 2016**].

### 1.3.3.2 Cell-based therapy

Cell-based therapies consists in implantation of new cells in damaged brain areas, to support resident neurons with neurotrophic factors and to create new neuronal networks. Stem cells are undifferentiated cells able to divide and originate several cellular subtypes.

Different types of stem cells are under study for this application, such as embryonal stem cells (ESC), mesenchymal stem cells (MSC), induced pluripotent stem cells (iPSC) and neural stem/progenitor cells (NPSC).

In animal models, stem cells were able to reduce the astrogliosis and the pro-inflammatory microglia in favour of anti-inflammatory microglia and nonreactive astrocytes, thus inhibiting the amyloid cascade through a more efficient A $\beta$  degradation. Moreover, these effects resulted in enhanced synaptogenesis, neuronal repair and increased neurotrophic factors secretion [Li XY et al., 2015; Choi SS et al., 2016; Shen Z et al., 2017].

Bone marrow-derived MSC transplant in an AD mouse model promoted functional recovery and trophic factors production, which induced survival and regeneration of host neurons [Huang B et al., 2012].

Adult mouse NSC transplant in the hippocampus of AD transgenic mice ameliorated the migration and differentiation of endogenous NSC into different brain cell types, and led to lifespan and memory functions improvement [Yamasaki TR et al., 2007].

However, cell-based therapies are source of concerns because of immune rejection and tumor development. iPSC, obtained by somatic cells re-programming, constitute a valid alternative in this sense. They have not

immunological complications, but as the ESC, there is a risk of tumorigenesis in *in vivo* transplant **[Jung YW et al., 2012]**.

ESC-derived NPC implantation in an AD mouse model ameliorated cognitive functions and preserved neuronal phenotype. In addition, 40% of ESC showed a cholinergic phenotype after transplant, and no tumor formation, indicating that this approach could be safer **[Moghadam FH et al., 2009]**.

Several clinical trials have been recently developed and two of them reached completion. Nine trials are still ongoing taking advantage of the use of different types of stem cells, assessing safety, MRI and CSF parameters **[Wang SM et al., 2019]**. A completed phase I study demonstrated the short-term and long-term safety of hippocampal intracranial injection of HUC-MSCs in patients with amyloid pathology **[Kim HJ et al., 2015]**.

## **1.4 Sirtuins**

Sirtuins (SIRTs) are a family of NAD-dependent enzymes homologues to Sir2 protein, identified for the first time in yeast. MAR1 gene (Mating-type Regulator 1) was identified in *Saccharomyces Cerevisiae* and subsequently renamed Silent Information Regulator 2 (Sir2) due to its ability to silence target genes **[Klar AJ et al., 1979]**. The first studies on *S. Cerevisiae* discovered that the presence of a supplementary copy of Sir2 gene increased survival by 50%, whereas its deletion significantly reduced it **[Kaeberlein M et al., 1999]**. Sir2 promotes yeast longevity suppressing toxic extra-chromosomal rDNA circles

(ERCs) formation [Sinclair DA et al., 1997]. Subsequent studies demonstrated that Sir2 homologues of other species can also regulate survival.

Seven SIRTs, named SIRT1-7, have been identified in mammals, and are classified as Class III Histone Deacetylases (HDACs). Every SIRT is characterized by a conserved 275 amino acids catalytic core, with a C-terminal and a N-terminal domain of variable length, differentiating the members of the protein family (Figure 1.16).

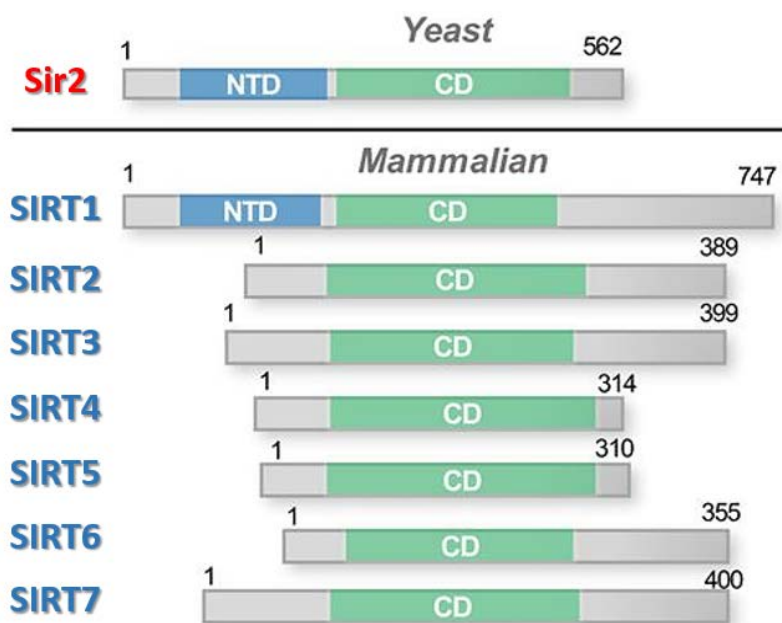


**Figure 1.16** Structural representation of mammalian SIRTs, with the catalytic domain (CD) in green (modified from [Hou X et al., 2016]).

#### 1.4.1 FUNCTIONS AND LOCALIZATION OF SIRTUINS

The main activity of SIRTs is the deacetylase one, where there is the removal of an acetyl group from the N-ε-lysine residues of the substrate. Landry and colleagues first described the mechanism of this catalytic reaction in 2000, and demonstrated that lysine deacetylation is coupled with the formation of a



product, the O-Acetyl-ADP ribose (OAADPr), and a nicotinamide (NAM) molecule [Landry J et al., 2000] (Figure 1.17).

Some SIRT6, like SIRT4 and SIRT6, have also a mono-ADP-ribosyltransferase activity, where an ADP-ribose molecule is transferred from a NAD<sup>+</sup> to a substrate protein, producing a NAM molecule and a mono-ADP-ribosylated protein [Sauve AA et al., 2006].

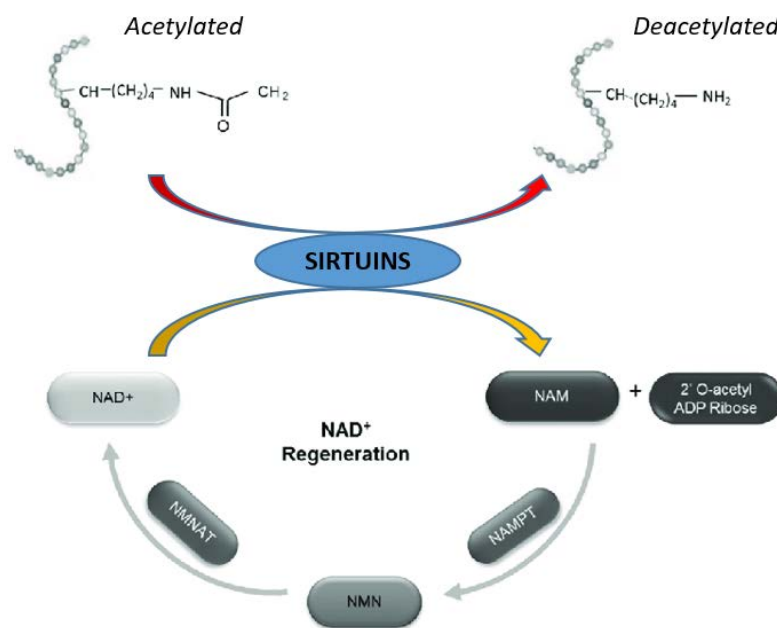


**Figure 1.17** Protein deacetylation reaction of SIRT6. Since cells cannot afford to lose NAD<sup>+</sup> after each sirtuin reaction, they operate an enzymatic mechanism to reuse NAM to re-generate NAD<sup>+</sup> (modified from [Anamika et al., 2019]).

Since SIRT6s are NAD-dependent enzymes, there is a tight correlation between their enzymatic activity and the energetic and metabolic state of the cell. NAM can operate, at high concentrations, a negative feedback on SIRT6s activity by binding in a non-competitive manner, while the OAADPr seems to be a signal mediator in the cell [Michan S and Sinclair D, 2007].

SIRT1, SIRT2 and SIRT3 have strong deacetylase activity, which is weaker for SIRT4, SIRT5 and SIRT6. In addition, SIRT4 and SIRT6 have the mono-

ADP-ribosyltransferase activity. SIRT7 activity is still under study [**Lalla R and Donmez G, 2013**].

The function of SIRT proteins reflects their sub-cellular localization.

SIRT1 is predominantly localized in the nucleus, where it deacetylates H3 and H4 histones and transcription factors. In an oxidative stress condition, a possible translocation of SIRT1 from the nucleus to the cytoplasm has been reported [**Pfister JA et al., 2008**].

SIRT2 resides predominantly in the cytoplasm, where it is associated to microtubules and deacetylates  $\alpha$ -tubulin to regulate microtubule dynamics. When the nuclear membrane disrupts during mitosis, SIRT2 is able to migrate in the nucleus and deacetylate H4 histone favouring chromatin condensation [**Vaquero A et al., 2006**].

SIRT3, SIRT4 and SIRT5 are mitochondrial sirtuins and have an important role in cellular energetic metabolism and oxidative stress response.

SIRT6 and SIRT7, like SIRT1, are nuclear proteins. In particular, SIRT6 is associated to heterochromatin, while SIRT7 is localized in the nucleolus, where it is involved in RNA polymerase I activation and DNA-association [**Pfister JA et al., 2008**].

In addition, other non-histone target proteins have been identified, which are substrate of SIRT activity, as p53, NF- $\kappa$ B and FOXOs [**Jęśko H et al., 2017**] (Table 1.5).

Sirtuin	Cell localization	Key targets/actions
Sirtuin 1	Nucleus	P53, FOXO3, RAR $\beta$ , PGC1 $\alpha$ , PPAR $\gamma$ , NF $\kappa$ B, IGF1, histones H1, H3, and H4
Sirtuin 2	Cytoplasm	NF $\kappa$ B, adipocyte differentiation, anaphase-promoting complex/cyclosome, DNA damage repair, myelin production in Schwann cells, gluconeogenesis, oligodendrocyte differentiation
Sirtuin 3	Mitochondria	Reduce ROS production, HIF-1 $\alpha$ , lipogenesis, stimulation of gluconeogenesis, activation of fatty acid oxidation, neuroprotective actions
Sirtuin 4	Mitochondria	ROS, glutamine use for energy obtaining, AMPK, increased ATP synthesis efficacy, DNA damage repair
Sirtuin 5	Mitochondria	Activate Cu/Zn SOD (SOD1)
Sirtuin 6	Nucleus	DNA repair, maintenance of genomic stability, tumor suppressor protein
Sirtuin 7	Nucleus	Promotes rDNA transcription, premature aging, cancer cells

**Table 1.5** Localization and main targets of SIRT6 (modified from [Mohamad Nasir NF et al., 2018]).

Different works highlighted the involvement of SIRT1 and SIRT2 in AD, with mRNA or protein expression decrease and increase, respectively, observed in AD human brains (Fig. 1.18). This led to stimulation of a lot of research for potential therapeutic strategies targeting these two proteins, while the involvement of other members of the family, with exception of SIRT3, is still poorly elucidated.

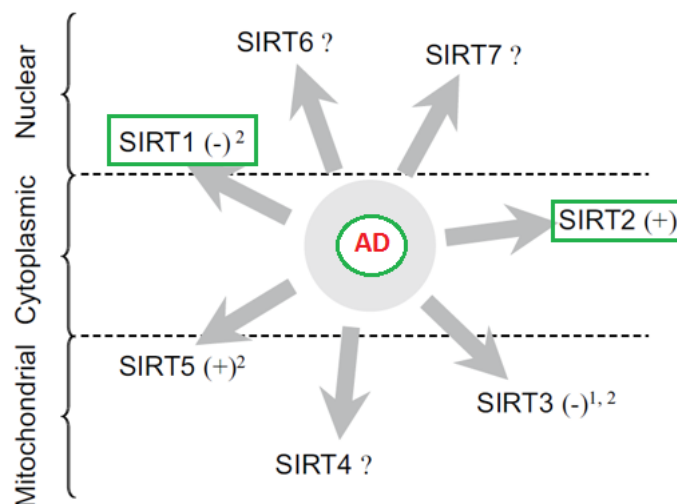


**Figure 1.18** Changes in human brain levels of various sirtuins in the course of AD. 1 mRNA expression. 2 Negative (SIRT1, SIRT3) and positive correlation (SIRT5) of hippocampal immunoreactivity with pathological staging (modified from [Jęśko H et al., 2017]).

## 1.4.2 SIRT1

SIRT1 human gene is located on chromosome 10. The protein is abundantly expressed in adipose tissue, liver, skeletal muscles and pancreas. In the brain, SIRT1 is present at high neuronal level in cerebral cortex, hippocampus, hypothalamus and cerebellum [Ramadori G et al., 2008]. Among all mammalian sirtuins, SIRT1 has been the most extensively studied due to its beneficial roles in energy metabolism by mediating caloric restriction (CR), arising the hope of extending human lifespan. SIRT1 is implicated in the regulation of multiple biological phenomena, including DNA damage repair, mitochondrial biogenesis, insulin secretion, stress response, apoptosis and genome stability (Figure 1.19).

In the white adipose tissue, SIRT1 promotes lipolysis and fatty acids mobilization with fasting state, and suppresses nuclear peroxisome proliferator-activated receptor gamma (PPAR- $\gamma$ ) activity, thus decreasing adipogenesis [Picard F et al., 2004].

In the liver, SIRT1 controls glucose production, fatty acids oxidation and cholesterol levels. During fasting, SIRT1 stimulates gluconeogenesis and suppresses glycolysis [Purushotham A et al., 2009]. The main targets of SIRT1 activity in the liver are PGC-1 $\alpha$ , PPAR- $\gamma$ , and LXR $\alpha$ , all involved in glucose and lipids metabolism.

SIRT1 is considered a pro-survival factor because it mediates p53 deacetylation preventing its transcriptional activity, and counteracts apoptosis in response to oxidative stress and DNA damage. Another SIRT1 target is NF- $\kappa$ B whose deacetylation reduces inflammatory responses.

Besides blocking apoptosis, SIRT1 increases cell survival through regulation of FOXOs transcription factors [Michan and Sinclair, 2007]. SIRT1 deacetylates FOXO1, promoting the transcription of target genes involved in gluconeogenesis [Donmez G and Outeiro TF, 2013].

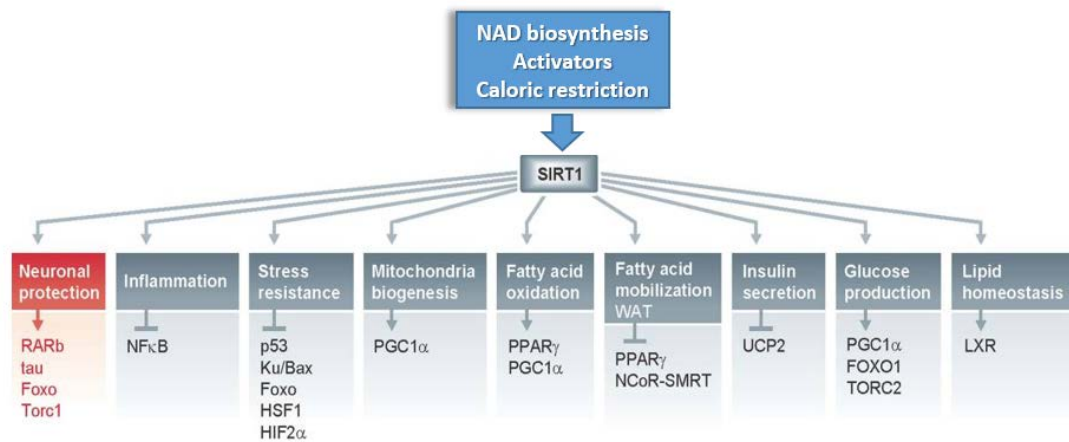


**Figure 1.19** SIRT1 plays different roles in different molecular pathways including neuronal protection, inflammation, stress resistance, mitochondrial biogenesis, fatty acid oxidation and mobilization, insulin secretion, glucose production and lipid homeostasis (modified from [Donmez G and Outeiro TF, 2013]).

#### 1.4.2.1 SIRT1 in neurodegeneration and AD

SIRT1 is highly expressed in those brain regions susceptible to neurodegeneration processes (basal ganglia, hippocampus and prefrontal cortex), and is predominantly present in neurons [Donmez G. and Outeiro TF, 2013].

There are many evidences that reported a role of SIRT1 in neurodegeneration processes related to AD (Fig. 1.20).

It has been observed a reduction in SIRT1 mRNA and protein levels with progression of AD stages, a condition that was also mimicked on SHSY5Y neuroblastoma cells treated with A $\beta$  peptide [Julien C et al., 2009; Lattanzio F et al., 2016].

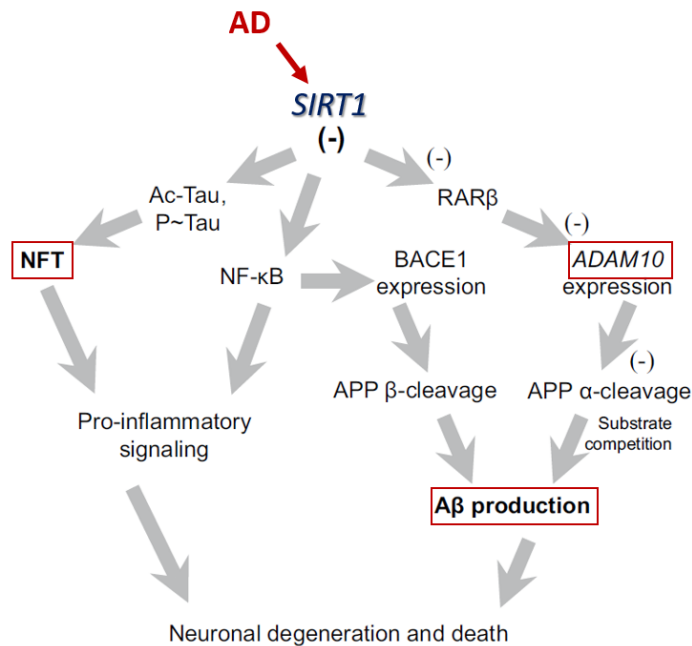


**Figure 1.20** Some of the molecular mechanisms of SIRT1 in Alzheimer's disease and consequences of reduced SIRT1-dependent effects due to AD progression (modified from [Jesko H, et al., 2017]).

The first studies on CR verified that SIRT1 over-expression reduced AD pathology [Imai S and Guarente L, 2010], and SIRT1 pharmacological activation with resveratrol reduced A $\beta$ -induced cell death and decreased cognitive impairment in a mouse model of FAD [Porquet D et al., 2014]. SIRT1 shifted the balance between amyloidogenic and non-amyloidogenic APP metabolism up-regulating the  $\alpha$ -secretase ADAM10 and down-regulating the expression of the  $\beta$ -secretase BACE1 possibly through

inhibition of NF- $\kappa$ B and activation of the retinoic acid receptors [Tippman F et al., 2009; Gao R et al., 2015; Lee HR et al., 2014].

Another study demonstrated that treadmill exercise inhibited A $\beta$  production via SIRT1 activation in AD mice, and favoured the non-amyloidogenic pathway [Koo JH et al., 2017]. *In vitro* SIRT1 over-expression reduced A $\beta$  oligomerization and oxidative stress [Wang J et al., 2010], while its activation with resveratrol in a cellular AD model was able to reduce astrocytes and pro-inflammatory mediators such as Nfkb-p65 [Scuderi C et al., 2014]. An influence on NF- $\kappa$ B signaling has also been reported upon SIRT1 activation and over-expression obtaining a reduction of microglia-mediated A $\beta$  toxicity [Chen J et al., 2005]. Moreover, PARP1 (which is overexpressed in AD, and may lead to NAD<sup>+</sup> depletion and SIRT1 activity decrease) inhibition activated SIRT1 expression in the presence of A $\beta$ 42 oligomers, and upregulated  $\alpha$ -secretase pathway [Wencel PL et al., 2018]. By deacetylation and activation of Peroxisome Proliferator-activated Receptor Gamma Co-activator 1-alpha (PGC-1 $\alpha$ ), SIRT1 also promoted mitochondrial biogenesis and prevented mitochondrial dysfunction in AD [Donmez G, 2012; Koo JH et al., 2017].

Besides A $\beta$  pathology, SIRT1 may act also on tau pathology directly deacetylating the protein. After deacetylation by SIRT1, tau may be more susceptible to ubiquitin ligases and can be degraded into multiple peptides, diminishing the formation of NFTs and suppressing the spread of tau-induced pathology *in vivo* [Min SW et al., 2010; Min SW et al., 2018]. SIRT1 and tau also share upstream regulators such as AMPK and

microRNA-132, supporting the inverse correlation between SIRT1 levels in AD brain and abnormal tau deposit [**Julien C et al., 2009; Salminen A et al., 2012; Kim HS et al., 2015**].

SIRT1/retinoic acid receptor  $\beta$  pathway is also able to activate Notch cleavage, mediating neuroprotection, neurogenesis, synaptic plasticity, learning and memory functionality [**Costa RM et al., 2005; Bonda DJ et al., 2011**].

Other possible SIRT1 molecular partners involved in AD could be the FOXO transcription factors, that are able to modulate protein turnover and oxidative stress [**Perez FP et al., 2014**]. FOXO1 level is altered with AD progression, and FOXO3a could be the mediator of A $\beta$ -induced inhibition of the neuroprotective PI3K/Akt signaling [**Gòmez Ravetti M et al., 2010; Akhter R et al., 2014**].

Another recent study also highlighted the critical role of SIRT1 in the BBB permeability/leakage. In this study, the age-dependent modification of SIRT1 expression, its knockdown or overexpression, affected BBB integrity, thus proposing SIRT1 as a promising target for reducing BBB hyperpermeability associated with ageing or neurodegenerative disorders [**Stamatovic S et al., 2018**].

### **1.4.3 SIRT2**

SIRT2 human gene is located on chromosome 19. The protein is preferentially cytosolic, co-localizes with microtubules and is responsible of  $\alpha$ -tubulin deacetylation [**North BJ et al., 2003**]. SIRT2 transiently shuttles to the nucleus during the G2/M transition of the cell cycle, where it has a strong preference for histone H4 lysine 16, thereby regulating chromosomal condensation during



mitosis [Inoue T et al., 2007]. Despite this target preference, SIRT2 interacts with and regulates numerous histone and non-histone protein substrates, and the variety of endogenous targets is correlated with the different biological functions modulated by this deacetylase [de Oliveira RM et al., 2012] (Figure 1.21).

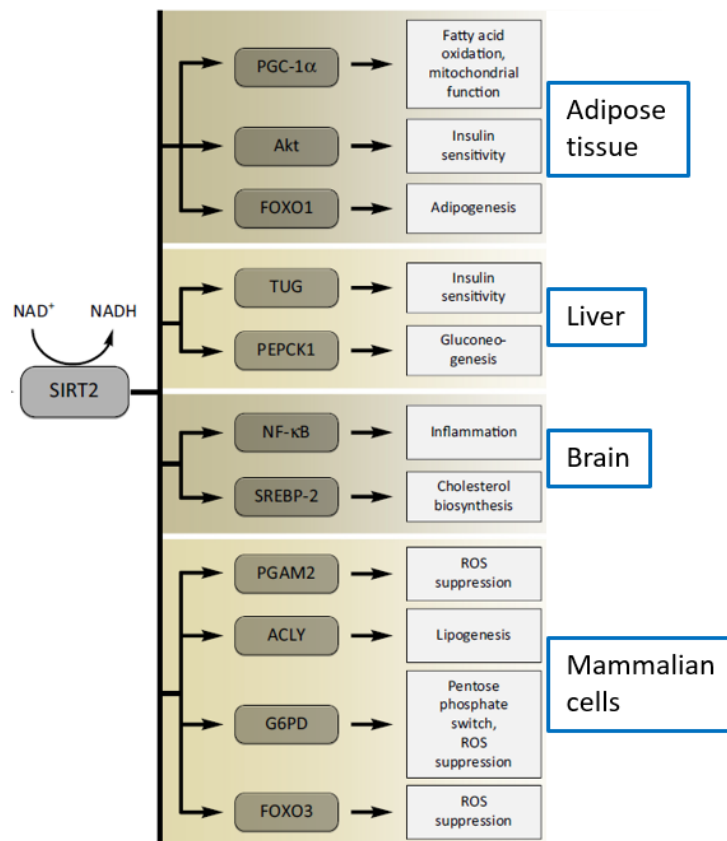


**Figure 1.21** A list of selected protein targets of SIRT2 in different organs, and the involved metabolic pathways (modified from [Gomes P et al., 2015]).

SIRT2 is expressed in a wide range of tissues and organs and has been detected in metabolically relevant tissues, including the brain, muscle, liver, testes, pancreas, kidney and adipose tissue [Wang F et al., 2007; Kim HS et al., 2011; Maxwell MM et al., 2011]. In these tissues, SIRT2 exerts its function

on cell cycle regulation, energy metabolism, oxidative stress and inflammation, among others.

Some of the non-histone targets of SIRT2 are p65, FOXO3 and FOXO1 and NRF2.

Numerous evidences implied a role for SIRT2 in pathological processes such as tumorigenesis, where there are still contradictory results about its tumorigenic or tumor-suppressor functions [**Chen J et al., 2013; Wang F et al., 2007**].

With respect to SIRT1, whose beneficial role is well established, the implication of SIRT2 in pathological and protective functions is less clear, raising the question of whether activation or inhibition of SIRT2 is beneficial or detrimental under specific circumstances.

#### **1.4.3.1 SIRT2 in neurodegeneration and AD**

SIRT2 is highly expressed in the brain, especially in oligodendrocytes, glial cells and post-mitotic neurons, and is involved in numerous cerebral functions. In neurons and oligodendrocytes, SIRT2 is localized in the cytosol. At neuronal level, its expression can be detected in all neurites and growth cones. Among SIRT2 functions in the brain there are the alteration of cones and neurites growth dynamics (acting on acetylated- $\alpha$ -tubulin), and oligodendrocytes arborization and differentiation [**Pandithage R et al., 2008**]. Several published data demonstrated an association between SIRT2 activity and neurodegenerative processes and ageing [**Maxwell MM,et al., 2011**], giving rise to a growing interest in the

use of SIRT2 inhibitors on models of AD and other disorders [**Donmez G and Outeiro TF, 2012**].

A link between SIRT2 and AD pathology has been provided by genetic studies, which demonstrated an association between the SNP rs10410544 in *SIRT2* gene and AD susceptibility in a case-control study on a Caucasian population, a result that was confirmed in a meta-analysis too [**Polito L et al., 2013; Wei W et al., 2014**].

SIRT2 was associated with the aggregation of amyloidogenic proteins such as  $\alpha$ -synuclein and huntingtin [**Outeiro TF et al., 2007; Luthi-Carter R et al., 2010**] that share some of their characteristics with A $\beta$ .

In addition, SIRT2 was indirectly associated with neurodegenerative processes such as inflammation, apoptosis, microtubules destabilization, autophagy and oxidative stress [**De Oliveira RM et al., 2012**].

The work from Biella et al demonstrated that SIRT2 specific inhibition was able to stimulate non-amyloidogenic pathway, suppress the amyloidogenic one, and improve cognitive function in two transgenic mouse models (3xTg-AD and APP23) [**Biella et al., 2016**].

Microtubules instability and altered autophagy are also two important mechanisms that result affected by SIRT2 activity in AD. Silva and colleagues demonstrated that in AD patient's brain there is mitochondrial dysfunction, that leads to SIRT2 over-activation and consequently to microtubules disruption and autophagic-lysosomal pathway (ALP) impairment. Through SIRT2 inhibition they propose an approach to stabilize microtubules and improve autophagic traffick through tubulin acetylation, preventing ALP dysfunction and consequent toxicity given by

accumulation of A $\beta$  and tau protein aggregates (Figure 1.22). Increased acetylated tubulin/ $\alpha$ -tubulin ratio was also reported in samples of AD brains [Silva DF et al., 2017].

Another study pointed out that SIRT2 inhibition-dependent  $\alpha$ -tubulin acetylation, a process that is linked to more stable microtubules, improves microtubules dynamics increasing tau/tubulin binding and consequently decreasing its accumulation and aggregation [Esteves AR et al., 2018].

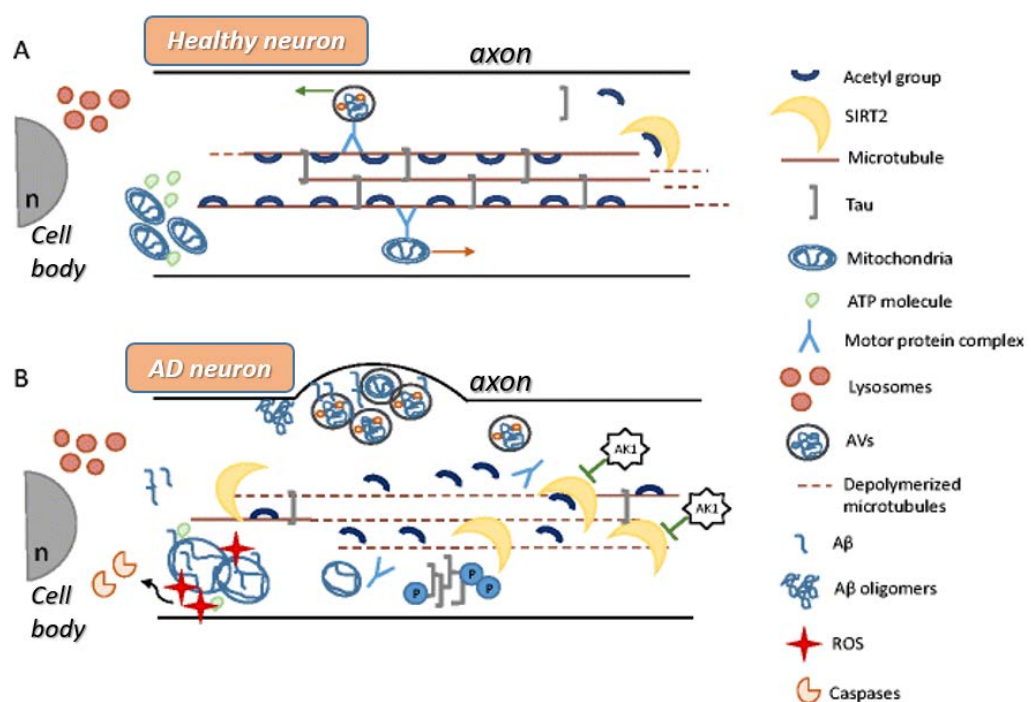


**Figure 1.22** The proposed mechanism of SIRT2-dependent microtubule acetylation and its regulation. A) Healthy neuron in basal conditions: microtubules stabilization is reached in a dynamic manner through SIRT2-dependent acetylation and tau binding. Autophagic vacuoles (AVs) are transported to lysosomes side for digestion and other cargo proteins are transported along microtubules bidirectionally; B) AD neuron when mitochondrial metabolism fails: ROS production and SIRT2 over-activation lead to microtubules disruption, tau dissociates and is prone to phosphorylation and aggregation. AVs are not transported and accumulate in the cell, favouring A $\beta$  release and aggregation into oligomers. Autophagic flux impairment and metabolic disregulation lead to caspases activation and cell death. SIRT2 inhibition with AK1 could partially reverse some of these features (modified from [Silva DF et al., 2016]).

Of notice, in the context of oxidative stress that characterizes AD, SIRT2 was also reported as deacetylase of NRF2, reducing its cellular and nuclear levels. This NRF2 reduction is associated with a decrease in transcription of its target gene *Fpn1*, which leads to a reduction in iron efflux from the cell, increasing intracellular iron level. An excessive intracellular iron is associated with oxidative stress and cellular damage **[Yang X et al., 2017]**.

Another molecular player that is influenced by SIRT2 inhibition is SREBP-2, involved in sterol biosynthesis at neuronal level, and whose nuclear translocation seems to be inhibited by tubulin acetylation, conferring neuroprotection **[Luthi-Carter R et al., 2010]**.

Wang and colleagues demonstrated that SIRT2 is required for LPS-induced neuroinflammation by microglial activation, and SIRT2 inhibition rescued this process also preventing nuclear translocation of NF- $\kappa$ B and TNF $\alpha$  and IL-6 levels **[Wang B et al., 2016]**.

Given all the evidences of SIRT2 contribution to neurodegeneration, in particular for HD and PD models, there is rising interest in elucidating the effects and possible mechanisms through which SIRT2 influence AD pathology.

#### **1.4.4 SIRT1/SIRT2 MODULATORS AND THEIR APPLICATION TO NEURODEGENERATION**

The greater knowledge of the functions of SIRT1 and SIRT2 and their implication in gene expression, cellular metabolism, inflammation and

neuroprotection, has pushed the scientific community to search for molecules able to modify their activity. The use of SIRT modulators have broadened the knowledge of the molecular and biological functions of these proteins, and identified new lead compounds for the treatment of different pathological conditions.

#### 1.4.4.1 SIRT1 activators

Most of the Sirtuin Activating Compounds (STACs) act on SIRT1. Their action is to decrease the  $K_m$  of SIRT1 catalytic reaction. STACs bind the SIRT1-peptide complex on an allosteric site on the catalytic domain, increasing the enzyme's affinity for the acetylated substrate [Milne JC et al., 2007].

The first generation of STACs is represented by polyphenolic metabolites [Howitz KT et al., 2003]. The most potent natural STAC is resveratrol (RSV) (Figure 1.23), a polyphenolic compound able to produce a 10-fold increase in SIRT1 activity. RSV is present in red wine, and was already known for its antioxidative properties on human health [Bhat KPL et al., 2001].

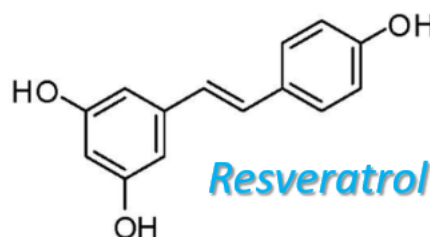


**Figure 1.23** The chemical structure of resveratrol (modified from [Smith JJ et al., 2009]).

RSV and other STACs can mimic CR, increasing survival [Wood JG et al., 2004], and its beneficial effect was recently confirmed in the context of senile dementias and AD [Sawda C et al., 2017].

The second generation of STACs is composed of synthetic molecules with an imidazole-derived structure: some of these compounds are SRT1720, SRT1460, SRT2104 and SRT2183.

Despite the similar mechanism of action to natural compounds, synthetic STACs are much more potent. SRT1720 is a potent and selective SIRT1 activator, with an  $EC_{50} = 0.16 \mu\text{M}$  (Figure 1.24), that showed beneficial effects against oxidative stress, insulin-resistance [Milne JC et al., 2007], and neurodegeneration.

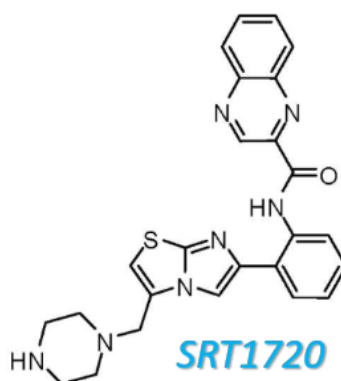


**Figure 1.24** The chemical structure of SRT1720 (modified from [Smith JJ, et al., 2009]).

SRT1720 also preserved mitochondrial biogenesis [Hansen LW et al., 2016], reduced oxidative damage in interstitial fibrosis models [Ren Y et al., 2017], and showed a protective effect against age-

related disorders in mice fed both a high-fat and a standard diet [Minor RK et al., 2011; Mitchell SJ et al., 2014].

In neurological context, this modulator showed neuroprotection during *in vivo* cerebral oxidative stress [Gueguen C et al., 2014], significantly improved outcomes after spinal cord injury acting on inflammation [Chen H et al., 2017], and reversed ROS excess, inflammation and endothelial dysfunction in aged mice [Gano LB et al., 2014].

Another new STAC with promising proof-of-concept efficacy data is SRT2104 (Figure 1.25), which reached fourteen clinical trials [Dai H et al., 2018]. SRT2104 was well tolerated in humans and produced beneficial effects on serum cholesterol, LDL levels and triglycerides, both in healthy volunteers and diabetic patients [Libri V et al., 2012; Baksi A et al., 2014]. Another clinical trial demonstrated a beneficial effect of SRT2104 administration in patients with moderate-to-severe psoriasis [Krueger JG et al., 2015].

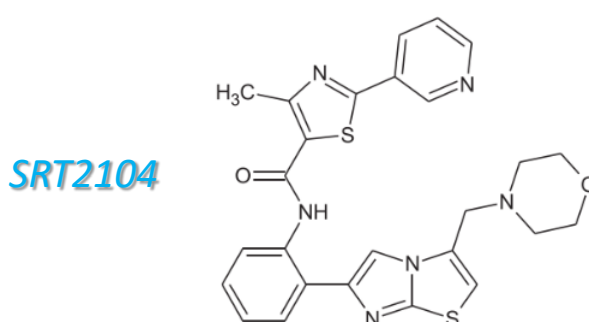


**Figure 1.25** The chemical structure of SRT2104 (modified from [Dai H et al., 2018]).



SRT2104 is also under study at preclinical level, and demonstrated interesting properties.

Mercken and colleagues demonstrated that SRT2104 extends survival of male mice on a standard diet, improving motor coordination and insulin sensitivity, increasing mitochondrial content and decreasing inflammation. In the same study, SRT2104 short-term treatment preserved bone and muscle mass in a model of atrophy **[Mercken EM et al., 2014]**.

Another recent study demonstrated the beneficial effect of SRT2104 hippocampal injection on stress-induced depressive-like behaviors and microglial phenotype switch in mice **[Duan C et al, 2020]**.

SRT2104 was also tested in neurodegeneration context, where it was demonstrated that it penetrates the BBB, attenuates brain atrophy, improves motor function, and extends survival in a mouse model of HD **[Jiang M et al., 2014]**.

A summary of STACs effects in ageing and age-related disorders is presented in Figure 1.26.

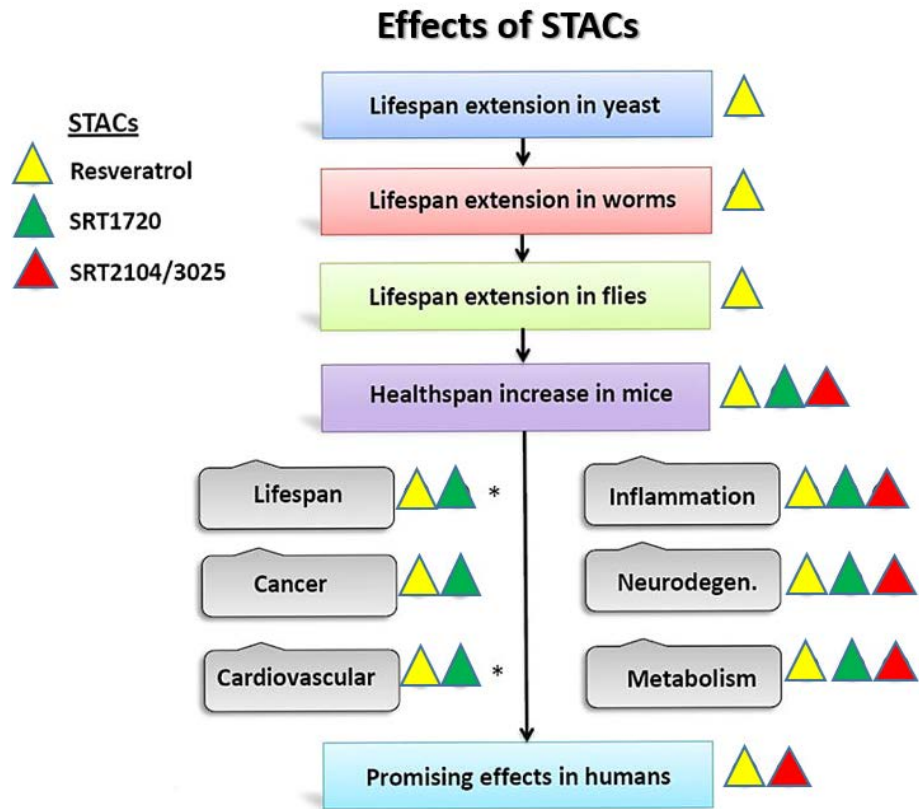


**Figure 1.26** Effects of SIRT1 activation by RSV, SRT1720 and SRT2104 on ageing and neurodegenerative diseases. Stars indicate ongoing studies (modified from [Hubbard and Sinclair, 2014])

#### 1.4.4.2 SIRT2 inhibitors

Several studies highlighted that SIRT2, whose cellular levels are altered in senile dementias, promotes neurodegeneration. Its pharmacological inhibition antagonised this pathological process, conferring neuroprotection.

SIRT2 inhibition has been investigated in AD models. Rat primary astrocytes treated with AGK2 had a reduction in their activation and pro-inflammatory mediators' production [Scuderi C et al., 2014].

AGK2 is a SIRT2 reversible, potent inhibitor ( $IC_{50} = 3.5 \mu M$ ) (Figure 1.27), able to protect SIRT2-overexpressing SHSY5Y cells from oxidative damage induced by rotenone and diquat toxins [**Singh P et al., 2017**].

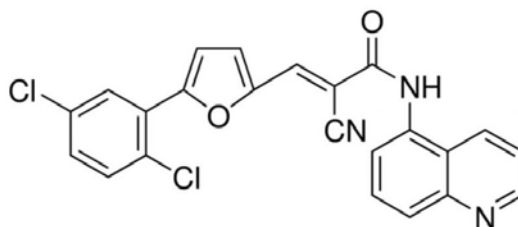


**Figure 1.27** The chemical structure of the SIRT2 inhibitor AGK-2.

AGK2 treatment protected neuronal cultures and reduced microglial activation in PD models with dopaminergic degeneration and microglial infiltration [**Harrison IF et al., 2018**].

In cellular and invertebrate HD models, AGK2 treatment down-regulated genes involved in sterol biosynthesis, leading to neuroprotection [**Luthi-Carter R et al., 2010**].

Taylor and colleagues observed that sulfobenzoic acid derivatives exerted high SIRT2 inhibition and screened such derivatives in order to select a new, potent, selective and brain-permeable SIRT2 inhibitor.

The compound named AK7 (Figure 1.28) was developed based on the structure of its analogue AK1 [Spires-Jones TL et al., 2012] and was able to satisfy those requirements.

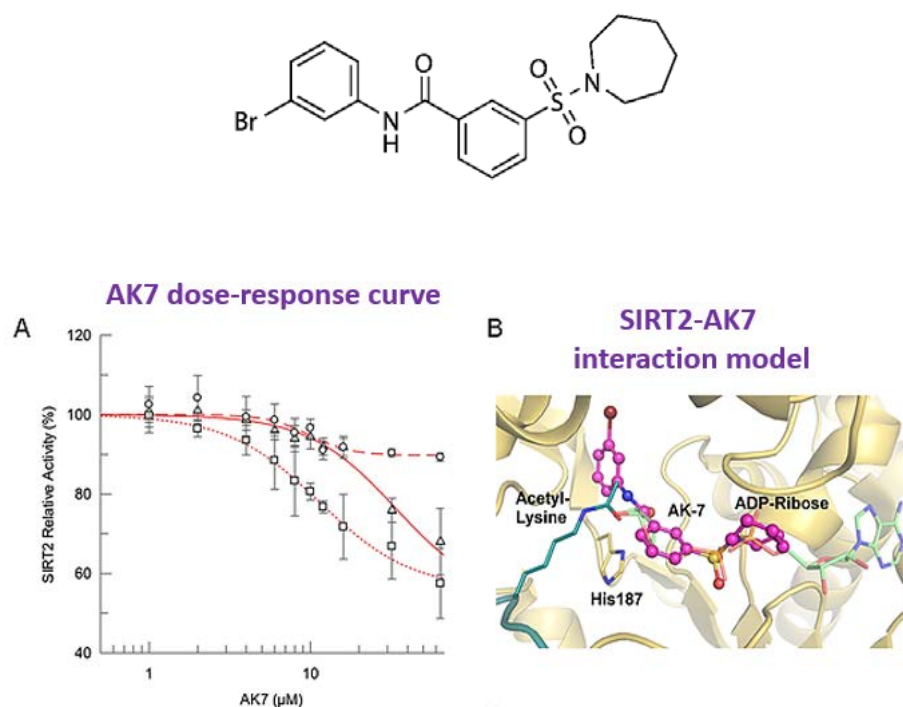


**Figure 1.28** The chemical structure of the SIRT2 inhibitor AK7 (top), a dose-response curve (A) and a three-dimensional model for AK7 and SIRT2 interaction (modified from [Chen X et al., 2015]).

Our group investigated AK7 application in two AD models (3xTg-AD and APP23 mice), and demonstrated that AK7 administration recovered their cognitive deficit and acted on APP processing increasing the neuroprotective fragment sAPP $\alpha$  and decreasing sAPP $\beta$  [Biella G et al., 2016].

Silva and colleagues investigated SIRT2 inhibition with the compound AK1 in AD context demonstrating protection against microtubule disruption and autophagy dysfunction [Silva DF et al., 2017].

Treatment of an *in vitro* model of HD with AK7 showed neuroprotection, reducing the aggregation and number of polyglutamine neuronal inclusions and cholesterol levels [Taylor DM et al., 2011].

In a mouse model of HD, AK7 was able to ameliorate motor deficits, extend survival and reduce cerebral atrophy [Chopra V et al., 2012]. Positive results have been obtained also on PD models, where AK7 reduced *in vitro*  $\alpha$ -synuclein toxicity and *in vivo* MPTP-induced neuronal loss [Chen X et al., 2015]. Other studies demonstrated neuroprotection by AK7 treatment on a rotenone-induced PD rat model and on MPTP-treated mice, acting on aging-related neurochemical and behavioural deficits and dysfunction of redox network [Wang X et al., 2015; Guan Q et al., 2016].

#### **1.4.5 THE ROLE OF OTHER SIRT<sub>s</sub> IN NEURODEGENERATION AND AD**

Besides SIRT1 and SIRT2, whose role in neurodegenerative diseases is the most studied, other members of the protein family are now a target of interest. In fact, all SIRT<sub>s</sub> are present in the brain in a highly regulated pattern and are able to influence the course of ageing and age-related disorders [Wątroba M and Szukiewicz D, 2016].

The expression of SIRT3-SIRT7 undergoes changes in the ageing brain and during AD pathology [Jęśko H et al., 2017].

SIRT5 is induced in activated microglia of AD brains [Lutz MI et al., 2014], and overexpression of APP and PS1 has led to a reduction in SIRT3 mRNA and protein in a mouse model [Yang W et al., 2015].

It has been found that short-term treatment with A $\beta$ 42 oligomers stimulated SIRT4 expression and a prolonged treatment influenced all mitochondrial SIRTs (SIRT3, SIRT4, SIRT5), suggesting a complex link between SIRTs and A $\beta$ /APP pathology [Cieslik M et al., 2015].

SIRT6 activity declines with age and AD, with a concomitant accumulation of DNA damage. Furthermore, brain-specific SIRT6-KO mice have behavioral and learning impairments and hyperphosphorylated tau, possibly through increased activation of GSK3 $\alpha/\beta$  [Kaluski S et al., 2017].

The most relevant results in AD context were recently produced on SIRT3. A natural SIRT3 activator named Honokiol exerted antioxidant activity, mitochondrial energy regulation and decreased A $\beta$  levels in APP/PS1 CHO cells [Ramesh S et al., 2018].

Another study showed that SIRT3 has a role in hippocampal synaptic plasticity and adaptations to intermittent fasting in a mouse model of AD [Liu Y et al., 2019].

Li and colleagues demonstrated that SIRT3 could be involved in tau protein acetylation and consequent accumulation [Li S et al., 2019].

The rising interest in SIRTs involvement in neurodegenerative diseases stimulates the search for new, specific, brain-permeable small inhibitors/activators, an objective that for most of the members of this protein family is still challenging.

## 1.5 Drug-delivery Systems (DDS)

DDS are a useful solution for those molecules that have promising therapeutic potentialities but poor pharmacokinetic parameters or the impossibility to cross the BBB.

DDS could increase brain bioavailability of new compounds giving a chance to AD treatment **[Choonara YE et al., 2016]**.

Among all DDS, three main categories can be mentioned in relation to the mechanism that allows the drug release from a polymeric system: release controlled by chemical reaction, solvent-mediated activation, and diffusion-dependent release.

Another interesting type of delivery system is the one based on nanoparticles (NPs) as carriers for active compounds (NPDDS). NPs are able to cross the BBB and can be functionalized to release the drug in the target site **[Nguyen KT et al., 2017]**.

Repeated intraperitoneal injection of small nanoparticles carrying phosphatidic acid/cardioplipin reduced brain A $\beta$  level in APP/PSEN1 mice **[Ord3n3ez-Guti3rrez et al., 2015]**.

NPDDS also constitute an interesting approach for delivery of already approved symptomatic drugs, such as rivastigmine **[Leszek J et al., 2017]**.

Besides their interesting potential, nanotechnologies have some limitations related to the cost/benefit ratio and processability of NPDDS, generally neglected factors **[Wen MM et al., 2017]**.

In addition, the most effective NPs formulations for the transport of drugs in brain accumulate significantly in other regions of the body, such as liver,

spleen and kidney, before being eliminated. It is important to design nanoformulations that only after reaching the brain are activated to release the drug [Li W et al., 2015] instead of doing it elsewhere in the body [Saraiva C et al., 2016].

In the last decades, bioengineering developed new sophisticated DDS, the injectable hydrogels, which have mechanical features similar to brain tissue [Khaing Z et al., 2014]. These materials can be injected in the brain in liquid form and can gelate *in situ*. Their biocompatibility avoids inflammatory reactions, and their biodegradability makes it possible to eliminate them without requiring additional surgery [Pakulska MM et al., 2012]. Thus, injectable hydrogels are promising as DDS in the CNS and could offer new therapeutic possibilities for AD treatment.

### 1.5.1 HYDROGELS AS DDS

Hydrogels are three-dimensional hydrophilic networks able to absorb great water or biological fluids volumes without dissolving in it. The presence of chemical or physical networks, indeed, makes these materials insoluble [Peppas NA et al., 2000]. This feature is important as hydrogels mimic human tissues and are highly biocompatible [Kopecek J et al., 2007].

Hydrogels can be ideally composed by any hydrophilic polymer, so they exist in a wide range of chemical compositions and mechanical properties. They can be classified according to different characteristics, such as the ionic charge of the side groups, the physical structure, the method of preparation and the reversible or irreversible nature of the cross-linking. Moreover, it is possible to formulate hydrogels in different physical forms, such as micro particles, NPs,



plates and films, peculiarities that make them suitable for applications in different fields.

In the biomedical field, they have been used as:

- systems for the delivery of bioactive molecules **[Hoare et al., 2008]**
- vehicles for cell-based therapies **[Munarin F et al., 2012]**
- tools for the creation of 3D models of pathologies **[Choi SH et al., 2014]**
- scaffolds in regenerative medicine **[O'Loughlin A et al., 2013]**
- supports for stem cell growth and differentiation **[Ou L et al., 2011]** and for tissue engineering **[Billiet T et al., 2012]**.

Hydrogels can be classified by their preparation method, in homopolymeric, copolymeric, multipolymeric, and interpenetrated (IPNs).

IPNs hydrogels are of particular interest because of the co-existence of two polymers that are physically independent. In IPN hydrogels there is the co-existence of a reticulated matrix polymer (main matrix) with a second polymer which can be dispersed within the meshes of the main matrix or cross-linked to form a secondary matrix. The formation of the IPN polymeric network occurs when a pre-polymerized hydrogel is immersed in a solution of monomers, a polymerization initiator and an agent that promotes the second network (cross-linker). In the absence of the cross-linker, the linear polymers do not cross-link, but remain trapped in the main matrix, generating semi-interpenetrated hydrogels (semi-IPNs), as illustrated in Figure 1.29.

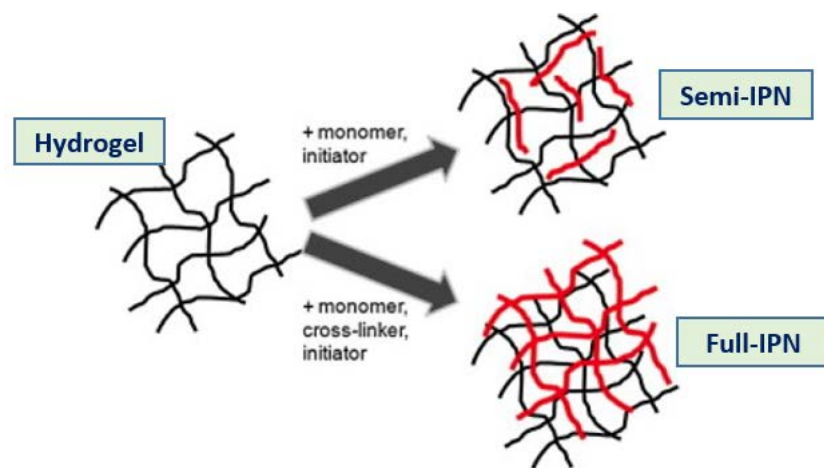


**Figure 1.29** IPN and semi-IPN hydrogel formation (modified from [Hoare TR et al., 2008])

The interest in these structures is due to the possibility of combining the favorable properties of each component to produce a new system with properties that often differ from those of the single polymer [Zoratto N et al., 2018].

Semi-IPNs hydrogels are more efficient in preserving release kinetics at varying pH and temperature. They also possess many of the benefits of IPNs hydrogels, such as pore size control, the ability to slowly release an active molecule and good mechanical properties [Hoare TR et al., 2008].

### 1.5.1.1 Hydrogels for CNS application

As mentioned above, the main applications of hydrogels are injectable devices. Exogenous materials that are supposed to be implanted under the skin, unfortunately, can evoke an undesired response by the host tissue, like inflammation, tumorigenesis and immune response. Therefore, the essential requirement for such materials is the bioavailability, a feature

that completely characterizes hydrogels, in addition to other peculiar properties including minimal irritation following *in vivo* application, possibility of loading drugs with different hydrophilicity and size, possibility of adjusting the release kinetics by modulating the pore size of the network. Furthermore, the study of the polymers used for the production of injectable hydrogels has led to the development of biodegradable systems, which do not require further surgery for the removal after the complete release of the drug **[Cho CS et al., 1999]**.

CNS targeting therapies have some peculiar limitations, such as the possibility that the active molecule, systemically administered, does not reach efficiently the target tissue because of the presence of the BBB. In fact, in physiological conditions BBB does not allow passive diffusion of molecules and immune cells from the blood to the brain.

Further critical elements are the skull which makes any intervention extremely invasive, the mechanical properties of the brain that do not allow the use of rigid scaffolds, the cicatrization of the glia that prevent the correct tissue regeneration and the accurate endogenous immune mechanisms.

Tunesi and colleagues have extensively analysed the rheological properties of collagen/PEG semi-IPNs injectable hydrogels, in cellular and murine neurodegeneration models. Their results highlighted the *in situ* gelation, the neuronal viability preservation, cell line proliferation maintenance, and the absence of inflammatory reaction after subcutaneous injection. In addition, no inflammation or tissue damage was detected after intracranial injection **[Tunesi M et al., 2013]**.

Li and colleagues, after having identified the neuroprotective potential of activin B in PD, overcame the limitations related to its short half-life developing an injectable and thermo-sensible hydrogel as vehicle for a prolonged release. Stereotactic injection of such hydrogel in a PD *in vivo* model revealed an increase in tyrosine hydroxylase, neuroinflammation reduction and cognitive improvement **[Li J et al., 2016]**.

Intracranial injectable hydrogels are also included among the innovative therapeutic strategies for neuro-regeneration following traumatic spinal cord injury **[Kumar P et al., 2015]**. Injecting a thermo-sensible hydrogel into a clinically relevant spinal cord injury model promoted remodelling of the extracellular matrix, eliminating cystic cavities. Hydrogels could potentially be used, therefore, as a form of natural filling of defects and body cavities **[Hong LTA et al., 2017]**.

Finally, in a recent study, an IPN chitosan hydrogel was used for prolonged local administration of a chemotherapeutic agent and a radiopharmaceutical in an *in vitro* glioblastoma model. The results showed a reduction in tumor size and an increase in the survival of the treated cells compared to the control group **[Puente P et al., 2018]**.

Injectable hydrogels are an excellent vehicle for the delivery of active molecules in brain and an innovative therapeutic strategy for many CNS diseases.

One promising approach for a local and minimally-invasive brain drug delivery was the epi-cortical positioning of a scaffold containing a hyaluronan-metilcellulose hydrogel. This approach allowed CNS delivery

of EGF without tissue damage and good results in the stroke-injured mouse brain [**Cooke MJ et al., 2011**].

## **2. Aim of the study**

Although our knowledge of AD pathology has increased enormously in recent years, we do not yet have effective therapies for its treatment. Given the high number of people affected by AD throughout the world, a prevalence destined to rise according to estimates, the development of therapies capable of modifying the course of the disease remains a very urgent need. In fact, the available therapies for AD are still symptomatic and do not arrest the progression of the pathology.

Over the years, new molecular players are emerging, involved in a neuroprotective or neurodegenerative sense in pathogenetic mechanisms linked to AD, such as inflammation, oxidative stress, aggregation of toxic proteins, synaptic deficits, and others.

In this context, an interesting role also emerged for Sirtuins (SIRTs), enzymes with deacetylase activity that regulate a high number of cellular processes, such as energetic metabolism, epigenetic mechanisms and cell cycle. Numerous works highlighted the involvement of SIRTs in neurodegenerative processes, particularly because both epigenetic and metabolic deregulation rise with ageing, and can promote the onset and progression of neurodegeneration. SIRT1 and SIRT2 are the most studied in neurodegenerative disorders, where SIRT1 has been associated with neuroprotective properties, while SIRT2 seems to be involved in neurodegenerative mechanisms.

Active research on small molecules able to modulate the activity of these enzymes has led to studies aimed at activating SIRT1 or inhibiting SIRT2 in models of AD, demonstrating a protective effect of these two approaches.

It has now been established that AD is a very complex multifactorial pathology, and it is interesting to notice that therapeutic strategies aimed at a single molecular target, such as AchE inhibitors or BACE inhibitors, have proved to be ineffective as disease-modifying drugs. The multi-targeted therapeutic approach, in which a single or a combination of drugs is able to target different molecular players of a disease to obtain an enhanced therapeutic effect, is currently of particular importance, and studies on this strategy are steadily growing.

The work presented in this thesis aims to study a possible multi-target approach involving SIRT1 and SIRT2, on AD *in vitro* and *in vivo* models. The rationale is that, starting from positive data for the sole activation of SIRT1 and the sole inhibition of SIRT2, we could combine these two modulations at the same time. This can potentially allow us to act on different molecular pathways and pathologic features that can be linked to the activity of one or both enzymes (APP-derived metabolites, inflammatory and antioxidative pathways) and attack the pathology from multiple points, converging on a pro-cognitive general effect obtained with the union of the two approaches.

The characterization of this new strategy was achieved through the development of the following points:

- The first part of the work will focus on an AD cellular model, the H4-sw neuroglioma cell line expressing human Swedish APP. The aim is to evaluate the feasibility of a combined treatment with SIRT1 activators SRT1720 or SRT2104 and SIRT2 inhibitor AK7 in terms of potential cytotoxicity, and to explore the effects on APP metabolism, a characteristic parameter of the selected model. In particular, the focus



of the experiments will be to evaluate a possible effect on sAPP $\alpha$  production and A $\beta$  levels, following the molecular hypothesis of a role of SIRT1/2 in non-amyloidogenic processing stimulation and A $\beta$  production decrease.

- The second part of the work will target the single and the double treatment with SIRT1 activator SRT2104 and SIRT2 inhibitor AK7 on a transgenic AD mouse model, the 3xTg-AD. The main purpose is to achieve cognitive improvement of 6-months old mice receiving the single and the combined treatment following an acute protocol of two weeks. After behavioural assessment, biochemical analyses will be performed to define the effect on sAPP $\alpha$  production, A $\beta$  oligomers, inflammation markers CD11b and GFAP, oxidative stress response proteins NRF2 and SOD1, and synaptic density marker Synaptophysin, in order to detect some changes in AD-related molecular pathways. As both SIRT1 and SIRT2 are involved with different extent in neurodegenerative features, the effects seen upon single treatments will clarify the contribution of each SIRT to the potential cognitive effect obtained combining SIRT1 and SIRT2 modulation.

### **3. Materials and methods**

## 3.1 *In vitro* experiments

### 3.1.1 H4-SW CELLS

For *in vitro* experiments we used H4 human neuroglioma cell line harbouring a plasmid containing human mutated APP (Swedish mutation KM595/596NL). The over-expression of mutated APP makes H4-sw cells able to produce high amounts of A $\beta$  in culture medium.

Cells were cultured in Dulbecco's Modified Eagle's Medium (DMEM) supplemented with foetal bovine serum to a final concentration of 10%, 2mM L-glutamine, 100 U/mL penicillin and 100 $\mu$ g/mL streptomycin. For stable transfection maintenance, 300  $\mu$ g/mL Hygromycin B and 10  $\mu$ g/mL Blasticidin S were freshly added to plated cells.

Cells were incubated at 37°C in 5% CO<sub>2</sub> humidified atmosphere and were split two times per week from sub confluent flasks. In details: after washing with PBS to remove any trace of serum, cells were incubated with 500 $\mu$ L of trypsin/EDTA solution (0.005% trypsin and 0.02% EDTA in PBS) for 3-5 min at 37°C. After inhibiting trypsin with DMEM, the cells were collected and centrifuged. The supernatant was discarded and fresh medium was added to dilute the pellet at the appropriate cell concentration. For the experiments, cells were counted with a Burker chamber and seeded in the appropriate multi-well at the desired density:

- 96-well plate: 8000 cells/well
- 6-well plate: 120000 cells/well

### **3.1.2 COMPOUNDS AND CELL TREATMENTS**

To obtain the inhibition of SIRT2 cells were exposed to the specific inhibitor AK7 (Sigma-Aldrich) at 20  $\mu\text{M}$  for 24 hours. AK7 is a brain-permeable selective SIRT2 inhibitor with an  $\text{IC}_{50}$  = 15.5  $\mu\text{M}$ .

To obtain the activation of SIRT1 cells were exposed to the potent activator SRT1720 ( $\text{EC}_{50}$  = 160 nM; Cayman Chemicals) at 0.5  $\mu\text{M}$ , or SRT2104 (MedChem Express;  $\text{EC}_{50}$  =  $\mu\text{M}$  range) at 3  $\mu\text{M}$ , for 24 hours.

All the compounds were purchased in powder form and dissolved in DMSO to obtain a stock solution. Working dilutions were made in fresh complete culture medium and added directly to the corresponding well.

### **3.1.3 RNA INTERFERENCE**

To reach SIRT2 silencing in H4-sw cells, we used a specific siRNA (Silencer® Select siRNA – Ambion®) and a commercial scrambled sequence as negative control siRNA.

Cells were transfected using Lipofectamine™ 3000 (Invitrogen) as transfection agent. In detail: cells were plated on 6-well plates and let reach almost 80% confluence. The medium was replaced with antibiotic-free medium 1 hour before transfection. After mix preparation according to manufacturer's instructions, the siRNA-Lipofectamine complex was added to the corresponding wells. 5 hours post transfection, the medium was replaced again to avoid liposomes excessive toxicity. Cells were incubated for 48 hours to reach effective gene silencing, then culture media were collected and cells were lysed for biochemical tests.

### **3.1.4 MTS VIABILITY ASSAY**

Cellular viability of H4-sw cells was evaluated using the CellTiter 96® AQueous One Solution Cell Proliferation Assay (Promega).

Briefly, cells were plated on 96-well plates, treated with SIRT's modulators for 24 hours, and finally the medium was replaced with fresh medium containing 1:10 MTS solution. After 3 hours of incubation, absorbance was read with Tecan Infinite® M200 instrument at 490 nm.

Results were expressed as % cellular viability vs control.

### **3.1.5 PROTEIN EXTRACTION FROM CELLS AND CULTURE MEDIA**

Proteins for Western blotting and ELISA analyses were extracted as follows. Proteins released in the culture medium were obtained with media centrifugation at 21000 rcf for 5 minutes at 4°C, and then the supernatant was frozen at -20°C until use.

For whole cell lysates, H4-sw were washed with cold PBS 1X and lysed on ice with a scraper using a pH 7.4 Ice Cold Lysis Buffer (50mM Tris/HCl, 150mM NaCl, 0.5mM EDTA and 1% Triton X-100) with 1% broad-range Proteases Inhibitor Cocktail (Sigma-Aldrich). Lysed cells were centrifuged at 21000 g for 5 minutes at 4°C. Pellets were discarded and supernatants were stored at -20°C. Small aliquots were taken for protein quantification by Pierce™ BCA Protein Assay Kit (Thermo Scientific).

### 3.1.6 SDS-PAGE AND WESTERN BLOTTING

Equal amounts of proteins (10-20  $\mu\text{g}$  depending on the protein of interest) from cell lysates were denatured by boiling in SDS sample buffer (125mM Tris-HCl pH 6.8, SDS 1%, glycerol 10% and bromophenol blue 0.006%) added with 50 mM DTT at 95°C for 5 minutes. For secreted proteins, equal volumes of medium were processed in the same way and normalized to BCA protein content of the corresponding cell lysate.

Proteins were separated on 8% poly-acrylamide gels using a molecular weight marker (Biorad). Electrophoresis was carried out in 1X Tris Glycine-based Running Buffer, at 180 V. Proteins were then transferred to a nitrocellulose membrane in 1X Transfer Buffer for about 2 hours at 300 mA. The membrane was blocked for 1 hour in 5% non-fat dry milk or Bovine Serum Albumin (BSA) dissolved in Tris-Buffer Saline supplemented with 0.1% Tween 20 (TBS-T). After blocking, membranes were incubated overnight with the specific primary antibody diluted in 5% non-fat dry milk/TBS-T solution at 4°C, with gentle shaking. The following primary antibodies were used: 2C11 (not commercial IgG2a for full length APP, from Dr. Alessio Colombo), 22C11 (Millipore MAB348), 6E10 (Biolegend 803001), SIRT1 (Abcam ab32441), SIRT2 (Sigma-Aldrich S8447),  $\alpha$ -tubulin (Abcam ab7291).

The following day, membranes were washed three times for 10 minutes in TBS-T and incubated with the appropriate secondary HRP-conjugated Ig antibody for 1h at room temperature with gentle shaking. Membranes were then washed again with TBS-T as described above and covered with ECL substrate reagent (Millipore) for 3min. At the end, membranes were exposed to ChemiDoc™ Imaging System (BioRad) for signal detection.

Quantitative densitometric analyses were performed on digitalized images of immunoblots and band intensities were measured using ImageJ software. The obtained values were normalized to the corresponding  $\alpha$ -tubulin band intensity or to the protein concentration of the sample in the case of secreted proteins.

### **3.1.7 Enzyme-Linked Immunosorbent Assay (ELISA)**

$\beta$ -amyloid peptides and sAPP $\beta$  fragment were assessed in the conditioned culture media of H4-sw cells, using Human Amyloid  $\beta$ (1-40)/ $\beta$ (1-42) Assay Kit and Human sAPP $\beta$  Assay Kit (IBL) according to the manufacturer instructions. Briefly, media were appropriately diluted and added to the pre-coated plate for antigen capture. After overnight incubation and several washing steps, the secondary antibody was added to the samples and the colorimetric reaction was detected with Tecan Infinite® M200 (450 nm) after adding TMB substrate. Obtained values, expressed in pg/ml, were finally normalized on BCA protein content of every sample.

### **3.1.8 TOTAL RNA EXTRACTION**

Total RNA extraction from H4-sw cells was performed with Maxwell® 16 LEV simplyRNA Cell Kit (Promega). According to the manufacturer instructions, cells were seeded on 6-well plates and processed for automated RNA extraction after loading into the Maxwell® 16 instrument (Promega). The eluted RNA was quantified with NanoDrop 1000 (Thermo Scientific) and stored at -80°C in small aliquots.

### 3.1.9 QUANTITATIVE REAL TIME PCR

A total of 500 ng RNA from treated H4-sw samples were reverse transcribed into cDNA in a 20  $\mu$ L reaction mixture using the High-Capacity cDNA Reverse Transcription Kit (Applied Biosystems).

RT-PCR assay run on the Applied Biosystem 7300 RT-PCR System. RT-PCR was prepared using 80 ng of cDNA, 2x TaqMan® Master Mix and 20x TaqMan® gene expression assays. The reference gene used for the experiment was human  $\beta$ -actin. The fluorescence emitted after each cycle was measured and plotted (in log scale) against the cycle number. The raw data (threshold cycle CT) were used for the analysis of mRNA expression. The relative expression of each gene was calculated by the  $\Delta\Delta$ Ct method according to the following formula:

$$\text{Amount of target} = 2^{-\Delta\Delta\text{Ct}}$$

$$\Delta\Delta\text{Ct} = [(C_{\text{target gene}} - C_{\text{reference gene}})_{\text{Q}} - (C_{\text{target gene}} - C_{\text{reference gene}})_{\text{CB}}]$$

Q= Sample (treatment condition) and CB= Calibrator (control condition).

All samples run in triplicate in the same 96-well plate.

## 3.2 *In vivo* experiments

### 3.2.1 3xTg-AD MOUSE MODEL

Homozygous 3xTg-AD mice were generated from a C57BL/6-129SV mixed background. A PSEN1 mutant (M146V) mouse embryo was transfected with two expression plasmids, one containing a cDNA encoding the AD linked



Swedish double mutation of APP (K595M/N596L) and the other a cDNA encoding a tau mutation (P301L) that causes frontotemporal lobar dementia, both under the control of the Thy-1 promoter. Originally developed 3xTg-AD mice display both plaques and NFTs. A $\beta$  deposition is progressive, with massive intracellular immunoreactivity detected as early as three to four months of age. Extracellular A $\beta$  deposits appear visibly by twelve months. Hyperphosphorylated tau and NFTs occur later, by 12 to 15 months. Cognitive impairment, gliosis, LTP and synaptic plasticity deficiency appear at an early stage (4-6 months of age) [Oddo S et al, 2003; Billings LM et al, 2005; Stover KL et al., 2015].

Treatments were performed on 6 months old animals, while phenotypic characterization was conducted on multiple time-points (6,12,18 and 22 months). As 3xTg-AD mice and Non-Tg (NTg) mice had the same genetic background but were not littermates, high attention was paid in housing all the animals in the same room and subjecting them to the same environmental conditions and manipulations.

Procedures involving animals and their care were conducted in conformity with the institutional guidelines at the Istituto di Ricerche Farmacologiche Mario Negri IRCCS, in compliance with national and international laws and policies. Mice were housed in a SPF animal facility, at 23°C room temperature, with food and water *ad libitum* and a 12 hours light/dark cycle.

### **3.2.2 SIRT2 INHIBITOR ADMINISTRATION PROTOCOL**

AK7 (Sigma Aldrich, code SML0152) is a SIRT2 selective reversible inhibitor, and it is a brain-permeable sulfobenzoic acid derivate, with IC<sub>50</sub>= 15.5  $\mu$ M.

AK7 powder was dissolved in DMSO to obtain the stock solution, and stored at -80°C.

Mice received an intraperitoneal injection twice daily (AK7 half-life= 2 h).

For treated group, AK7 was diluted at a dose of 20 mg/kg in a vehicle composed by  $\beta$ -hydroxypropyl-cyclodextrin (Sigma Aldrich) 10% in sterile water.

Control group received the vehicle solution alone.

### **3.2.3 SIRT1 ACTIVATOR ADMINISTRATION PROTOCOL**

SRT2104 (MedChem Express; EC50 =  $\mu$ M range) is a SIRT1 selective and brain-permeable activator.

SRT2104 powder was dissolved in DMSO with warming and sonication to obtain a stock solution, and stored at -80°C.

Mice received an oral gavage once daily.

For treated group, SRT2104 was diluted at a dose of 100 mg/kg in a vehicle composed by  $\beta$ -hydroxypropyl-cyclodextrin (Sigma Aldrich) 10% in sterile water.

Control group received the vehicle solution alone.

### **3.2.4 EXPERIMENTAL TIMELINE**

Sex and age balanced 3xTg-AD mice were divided in two groups of treatment (8 mice per group) and subjected to the following experimental timelines.

In AK7 experiment, mice were treated with AK7 or vehicle twice daily for 15 days. Before sacrifice, mice were assessed for cognitive impairment with Novel Object Recognition Test (NORT) (Figure 3.1).

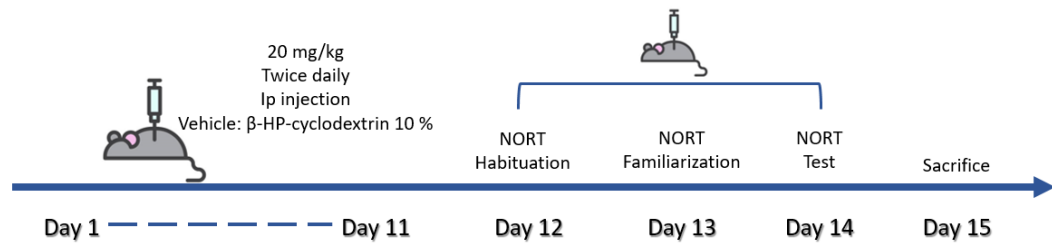


**Figure 3.1** Timeline for AK7 experiment on 3xTg-AD mice

In SRT2104 experiment, mice were treated with SRT2104 or vehicle for 15 days once daily. Before sacrifice, mice were assessed for cognitive impairment with NORT (Figure 3.2).

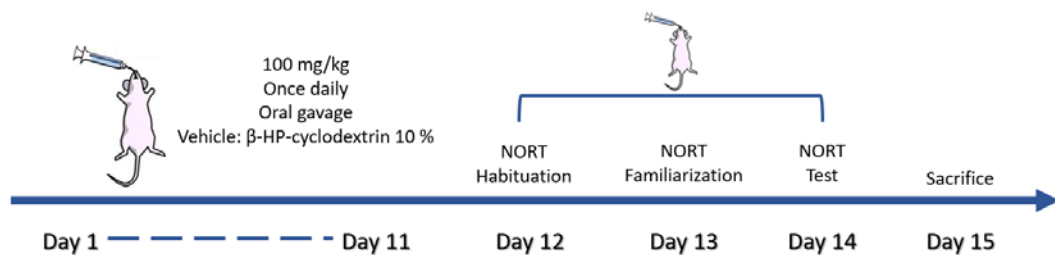


**Figure 3.2** Timeline for SRT2104 experiment on 3xTg-AD mice

For combined treatment, mice were treated with the combination of AK7 and SRT2104 or with vehicle, for 15 days. Before sacrifice mice were tested for cognitive impairment with NORT (Figure 3.3)

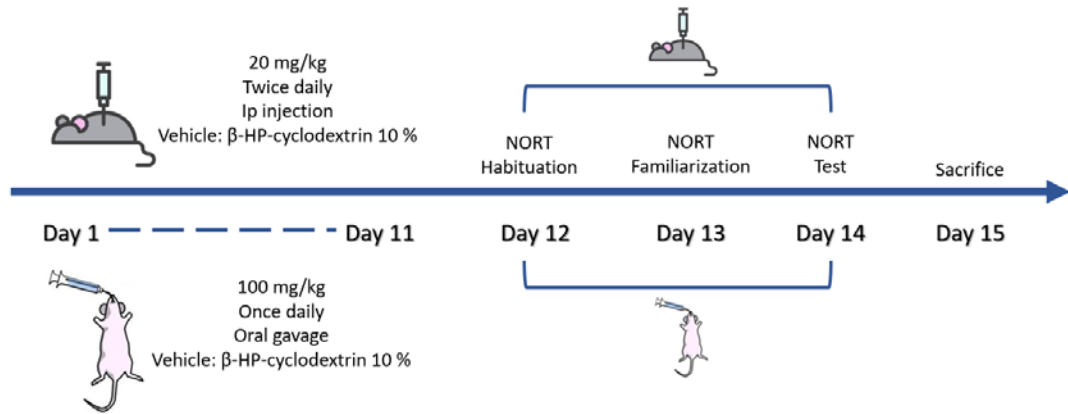


**Figure 3.3** Timeline for AK7 and SRT2104 combined treatment experiment on 3xTg-AD mice

All mice involved in the experiments were genotyped and monitored for excessive stress behaviour and changes in body weight during the experiment. Mice were weighed on day 1, day 7 and day 15 of treatment.

### 3.2.5 BEHAVIOURAL TEST (NORT)

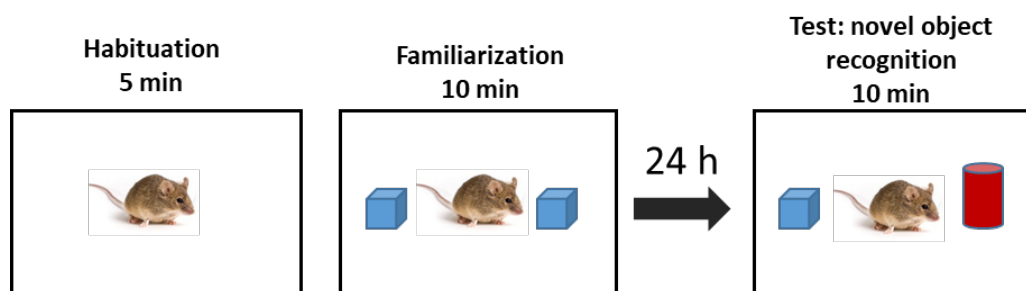


**Figure 3.4** Schematic representation of NORT protocol

Mice were tested in an open-square grey arena (40 x 40), 30 cm high (Figure 3.4).

The following objects were used for the test: a black plastic cylinder, a glass vial with a white cup, a metal cube, and a holed black plastic cone.

The protocol started with a habituation trial during which the animals were placed in the empty arena in the absence of any specific stimulus for 5 minutes, and their movements were videorecorded in terms of distance travelled within the arena, and average speed, using the Ethovision XT software.

The next day, mice were placed in the same arena containing two identical objects (training phase) placed at opposite corners of the arena. Exploration time was recorded in a 10 minutes trial. Sniffing, touching and stretching the head toward the object at a distance not more than 2 cm were considered as object investigation.

The third day, mice were placed again in the arena containing one familiar object from the training phase, and a novel object, different from the familiar one. Time spent exploring the two objects was videorecorded in a 10 minutes trial and analysed by an investigator blinded to the treatment assigned to the mouse.

Memory was expressed as a discrimination index (DI) with the following formula:

$$\text{Discrimination Index (DI)} = \frac{(\text{Seconds on novel object} - \text{Seconds on familiar object})}{(\text{Seconds on novel object} + \text{Seconds on familiar object})}$$

The positions of the objects were randomly changed for each animal and both the arena and the objects were cleaned with ethanol diluted in water between trials.

Total exploration times in the training and in the test days were calculated for each mouse, in order to verify any significant difference between the two groups in the exploration activity.

An NTg mice group was included in each trial to obtain the baseline physiologic cognitive performance value.

### **3.2.6 TISSUES PREPARATION FOR BIOCHEMICAL ANALYSES**

The day after behavioural assessment, mice received the last dose of the treatment and were sacrificed 4 hours later by decapitation after a mild anaesthesia. Brains were removed from the skull and laid on an ice chilled dish. Hippocampi were dissected from the brain and fresh frozen on dry ice.

Ice-cold Lysis buffer pH 7.4 (50 mM Tris/HCl, 150 mM NaCl, 0.5 mM EDTA and 1% Triton X-100) was prepared and 2% of broad-range Proteases Inhibitor Cocktail (Sigma-Aldrich) was added. Tissues were homogenized by a Teflon-on-glass homogenizer with 500  $\mu$ L of lysis buffer. Lysates were then passed through a 29-gauge needle to disrupt DNA, and were then cleared by centrifugation at 21000 rcf for 5 minutes at 4°C. Supernatants were collected and stored at -80°C, and small aliquots were taken for protein quantification by BCA assay.

Soluble fractions were prepared by clearing the total homogenate by centrifugation at 21000 rcf for 5 minutes at 4°C, and then ultracentrifugating the resulting supernatant at 100000 rcf for 1h. The obtained supernatants were taken as the soluble protein extract and protein concentrations were determined.

Where histology was required, one brain hemisphere was collected and post-fixed in 4% paraformaldehyde overnight, dehydrated for 24h in 30% sucrose in PBS 1X, and frozen in N-pentane for histology analyses. 30µm-thick coronal sections were cut from post-fixed brains using a cryostat and placed in 24-well plates containing PBS 1X.

### **3.2.7 SDS-PAGE AND WESTERN BLOTTING**

20 µg of proteins from brain homogenates and soluble fractions were denatured by boiling in SDS sample buffer added with 50 mM DTT at 95°C for 5min. Proteins were separated on 8% or 12% poly-acrylamide gels (depending on the protein of interest). Electrophoresis and immunoblotting protocols were carried out as described in 3.1.6 paragraph.

The following primary antibodies were used: 2C11 (not commercial IgG2a for full length APP, from Dr. Alessio Colombo), 22C11 (Millipore MAB348), 6E10 (Biolegend 803001), SIRT1 (Sigma-Aldrich S5196), SIRT2 (Sigma-Aldrich S8447),  $\alpha$ -tubulin (Abcam ab7291), GFAP (Millipore MAB3402), CD11b (Abcam ab75476), SOD1 (StressMarq SPC-206), Synaptophysin (SYSY 101002), NRF2 (Abcam ab137550).

### **3.2.8 IMMUNOHISTOCHEMISTRY**

Free-floating sections were incubated in 0.6% H<sub>2</sub>O<sub>2</sub> solution in PBS 1X for 10 minutes to inactivate endogenous peroxidases. After washing in PBS 1X, the slices were blocked for 1h in 0.1% Triton x-100, 3% normal goat serum with gentle shaking, then the slices were incubated overnight at 4°C with the specific primary antibody with gentle shaking. The following primary antibodies were used: 6E10 (Biolegend 803001), AT8 (Thermo Fisher MN1020).

The next day after washing the slices with PBS 1X, the sections were incubated with biotinylated secondary antibody for 1h at room temperature. At the end of this incubation, another washing step was carried out with TBS 1X, and then 1% avidin-biotin horseradish peroxidase complex in TBS 1X (Vectastain ABC HRP kit – Vector Laboratories) was added for 1h. Peroxidase activity was determined by reaction with a solution containing diaminobenzidine (DAB). The sections were washed with TBS 1X and mounted on gelatinated slides, dried, dehydrated and covered with mounting medium.

### **3.3 Statistical analysis**

All the analyses reported in this chapter were processed with GraphPad Prism® V. 7.0 software.

For the *in vitro* analyses, Kruskal-Wallis with Dunn's post hoc test was used to compare groups of cellular viability, mRNA, SIRTs silencing and ELISA assays, Mann-Whitney test was used for H4-sw characterization, one-way



ANOVA followed by Tukey's post hoc test was used for APP metabolism Western blotting analyses.

For the *in vivo* analyses, Student's t test or Mann-Whitney test were used for 3xTg-AD characterization, one way or two way ANOVA with Tukey's post hoc test were used for behavioural data and body weights, whereas Student's t test was used for Western blotting protein analyses.

Before applying the parametric statistics, D'Agostino-Pearson normality test was performed as recommended by GraphPad Prism® V. 7.0 software, to check for normal distributions of experimental groups.

Data shown in the graphs correspond to the value of each experimental group (mean  $\pm$  SEM) with respect to the correspondent control group.

Two-tailed levels of significance were used in all the above analyses and  $p < 0.05$  was the cut-off for statistical significance.

### **3.4 Hydrogels for controlled release of SIRT's modulators**

#### **3.4.1 *IN VIVO* BIOCOMPATIBILITY OF HYDROGELS: AIR POUCH MODEL**

An air pouch is obtained by subcutaneous injection of sterile air into the back of a mouse, and mimics the synovial cavity providing an environment permeable to circulating inflammatory cells.

We used this model to test the inflammatory potential of hydrogel biomaterials.

Two hydrogels, kindly provided from Politecnico di Milano, were tested:

1) Collagen 1.2 mg/mL + Low Molecular Weight Hyaluronic Acid (LMWHA) 2.5 mg/mL (pH 7.0)

2) Collagen 1.8 mg/mL + PEG2000 0.6 mg/mL (pH 7.0)

The hydrogels were prepared, loaded in a 1 mL syringe, and left at 37 °C for 1 hour to obtain solidification prior to the injection in the air-pouch animal model. The extent of inflammatory response reflected the amount of inflammatory cells in the air-pouch after the injection of the tested compound (LPS was used as positive control, sterile saline as negative control).

The experiment was conducted on CD-1 male mice.

- Day 1 – air pouch formation: 5 mL of sterile air were injected subcutaneously on the back of the mouse, forming an air pouch.
- Day 4 – air pouch maintenance: 5 mL of sterile air were re-injected inside the first air pouch.
- Day 5 – positive stimulus and test biomaterials injection: positive control group received 0.5 µg LPS injection, negative control group received 1 mL sterile saline injection, and test groups received 1 mL of the hydrogel.
- After 4 hours, LPS injected mice were sacrificed, 1 mL saline was injected into the air-pouch and the exudate was collected.
- After 24 hours, exudates were collected from saline and biomaterial-injected mice.
- Exudates were diluted and cells were counted with a Burker chamber using Trypan Blue dye.

### **3.4.2 *IN VITRO* CONTROLLED-RELEASE: HYDROGEL COMPOSITION**

The selected hydrogel for *in vitro* experiments was a type I collagen (COLL) and PEG2000-based semi-IPN polymeric system.

The COLL 2.4 mg/mL stock solution was prepared as follows:

- 80% Bovine Collagen 3 mg/mL (Sigma-Aldrich)
- 10% PBS 10x (Phosphate Buffered Saline Solution, Sigma-Aldrich)
- 10% NaOH 0.1 N

The PEG2000 2.4 mg/mL stock solution was prepared dissolving the polymer in saline and autoclaving for 20 minutes at 121°C.

The final hydrogel composition was COLL 1.8 mg/mL and PEG2000 0.6 mg/mL obtained mixing three parts (v/v) of COLL stock solution with one part (v/v) of PEG2000 stock solution in PBS 1X.

All the process was done on ice to prevent hydrogel polymerization during preparation. Ultimately, a final 500 µL mix was dispensed in 48-well plates and incubated at 37°C for polymerization. After 1 hour, 750 µL of supernatant (PBS 1X) was added to polymerized hydrogels.

### **3.4.3 UV-VIS SPECTROPHOTOMETRY: MODULATORS DETECTION AND STANDARD CURVE SETTING**

UV-VIS spectrophotometry was used to quantify SIRTs modulators concentration in solution at a specific absorbance wavelength ( $\lambda_{ax}$ ). The absorbance peak for SRT1720, AK7 and another SIRT2 inhibitor, AGK2 (Sigma-Aldrich code A8231; IC<sub>50</sub>=3.5 µM), was investigated with an

explorative analysis ( $\lambda$  range = 209.6-800 nm) of the compound in PBS 1X solution using a UV-VIS spectrophotometer with a quartz cuvette. The solution was analysed in parallel with a negative control containing DMSO instead of the compound.

To avoid interference given by the natural degradation of the hydrogel, the same explorative analysis was performed with supernatants (PBS 1X) derived by control hydrogels.

To obtain the linear range between concentration of the compound and absorbance value at the corresponding peak, several modulator solutions with known concentration in PBS 1X were prepared. All the solutions were then analysed with Tecan Infinite® M200 at the maximum absorbance wavelength of the compound.

The analysis was done in triplicate and the absorbance values were elaborated after subtraction of the blank (DMSO in PBS 1X) value.

#### **3.4.4 HYDROGEL-MEDIATED RELEASE STUDY AND DATA ANALYSIS**

For each sample, a 500  $\mu$ L mix of hydrogel containing SIRTs modulator or DMSO (control) was prepared in triplicate in a 48-well plate, with 750  $\mu$ L PBS 1X as supernatant (Table 3.1).

Hydrogel solution components for COLL 1,8 mg/mL + PEG2000 0,6 mg/mL final concentrations	Volumes ( $\mu$ L) for each sample (total volume 555,56 $\mu$ L)
<b>COLL 2.4 mg/mL</b>	<b>375</b>
<b>PEG2000 1.8 mg/mL</b>	<b>125</b>
<b>PBS 1X + compound/ DMSO</b>	<b>55.56</b>

**Table 3.1** Hydrogel composition for each sample.

The compound was loaded into the hydrogel in three increasing concentrations to assess the possibility of a load-dependent release kinetic. Hydrogels covered with supernatant were placed on an orbital shaker (35 rpm) at 37°C.

At selected time points (from 1 hour up to 7 days from hydrogels incubation), the supernatant was collected and replaced with 750  $\mu$ l of fresh PBS 1X. Collected supernatants were analysed with Tecan Infinite® M200 at the maximum absorbance wavelength of the compound.

The concentration of the compound was measured interpolating the obtained absorbance values, after blank subtraction, with the corresponding standard curves. The amount of modulators released in the supernatant at each time point was obtained by summing the concentrations acquired from the analysis of the supernatants taken at earlier time points.

Once the concentration of the compound was obtained, we calculated the released moles.

Finally, the percentage of modulator released as a function of time was calculated with the following formula:

$$\% \text{ modulator} = [(\text{released nmol}/\text{loaded nmol}) * 100]$$

## **4. Results: SIRT1 activation and SIRT2 inhibition in *in vitro* and *in vivo* AD models**

## Introduction

Despite the continuous effort to find an effective therapeutic strategy for AD, still no therapy able to modify the course of the disease has been discovered. In recent years, the concept of multi-target therapy has increasingly developed, stimulating the research of hybrids or combination of drugs that can modify different molecular mechanisms of AD pathogenesis, obtaining cognitive improvement. In fact, AD presents a complex set of neuropathological alterations such as A $\beta$  and aggregation and toxicity, neuroinflammation, synaptopathy, oxidative stress, and others, which makes it suitable for a multi-target intervention.

In this perspective, the aim of the work presented in this thesis was to try a multi-target approach on AD models, with a combination of drugs able to modulate SIRT1 and SIRT2. These two proteins, members of a deacetylase enzymes family, were reported as opposite players in neurodegeneration, with a marked neuroprotective role of SIRT1 and a neurodegenerative one of SIRT2.

As these two enzymes have different preferential localizations and different molecular targets, our hypothesis was that the contemporary activation of SIRT1 and inhibition of SIRT2 on AD models could provide a new strategy to attack the pathology from different but converging points, obtaining cognitive improvement.



## **Specific aims**

In the first part of the work, the combined treatment was tested on the H4-sw cellular AD model to assess the cytotoxicity and impact on APP metabolism, as these cells are a suitable model to assess APP production and processing. Starting from previous evidences of our laboratory on *in vivo* SIRT2 inhibition, a SIRT1 activator and SIRT2 inhibitor were given both alone and in combination to 6-month old 3xTg-AD mice, following an acute 2-weeks protocol. AD mice were characterized for cognitive impairment and specific pathological alterations, such as neuroinflammation, synaptic and antioxidant deficiency and A $\beta$  toxic oligomers presence. All those parameters were re-assessed on treated mice to verify cognitive deficit rescue, in order to characterize the pathway-specific contribution of the two SIRTs modulations to the overall cognitive effect, and to what extent each SIRT could be involved in the pathology.

## 4.1 *In vitro* results

### 4.1.1 H4-SW CELLS

H4-sw cell line was previously developed in our laboratory with the aim to create a cellular system suitable for APP production and processing analyses. Despite its limits due to immortalized neuroglioma origin, this cellular model is able to offer an indication of treatments effects on APP parameters and has been already used in literature [Czvitkovich S et al., 2011; Colombo A et al., 2008; Colombo A et al., 2013; Shin J et al., 2010]. As *in vitro* experiments were aimed at preliminary evaluation of combined treatment feasibility, we decided to use this available and easy to use cellular tool.

In order to characterize our *in vitro* model, we first verified the presence of the Swedish double mutation KM595/596NL, and then evaluated full-length APP (flAPP) over-expression in H4-sw cells, with respect to H4 native cells. We confirmed that H4-sw cells had a high over-expression of APP (Fig. 4.1), while in H4 native cells endogenous APP protein level was poorly detectable.

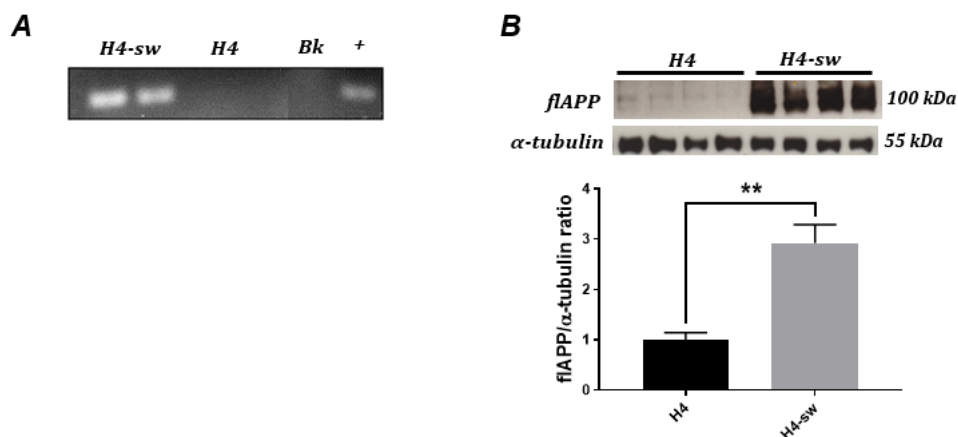


**Figure 4.1** A) PCR analysis to confirm the presence of the APP-Sw mutation in H4-sw cells. H4 native cells were used as negative control. B) Western blotting analysis of whole cell lysates from H4 and H4-sw cells, assessing flAPP protein level with 2C11 antibody, normalized with α-tubulin (right). Results are reported as Mean±SEM (n=4; Mann-Whitney test, \* p<0.05).

Before treating H4-sw cells with SIRT1 activator and SIRT2 inhibitor, we also verified the basal expression of the two SIRTs in this model, in order to elucidate if the over-expression of APP-sw could interfere with expression of our targets of interest [Shin et al., 2010]. Figure 4.2 shows a representative Western blotting where SIRT2 is significantly increased in H4-sw cells, while SIRT1 expression level has a not significant trend towards a decrease, suggesting the lack of a link between APP-sw presence and SIRT1 protein level, even if the specific cellular model or the small sample size of the experiment could have contributed to this result.

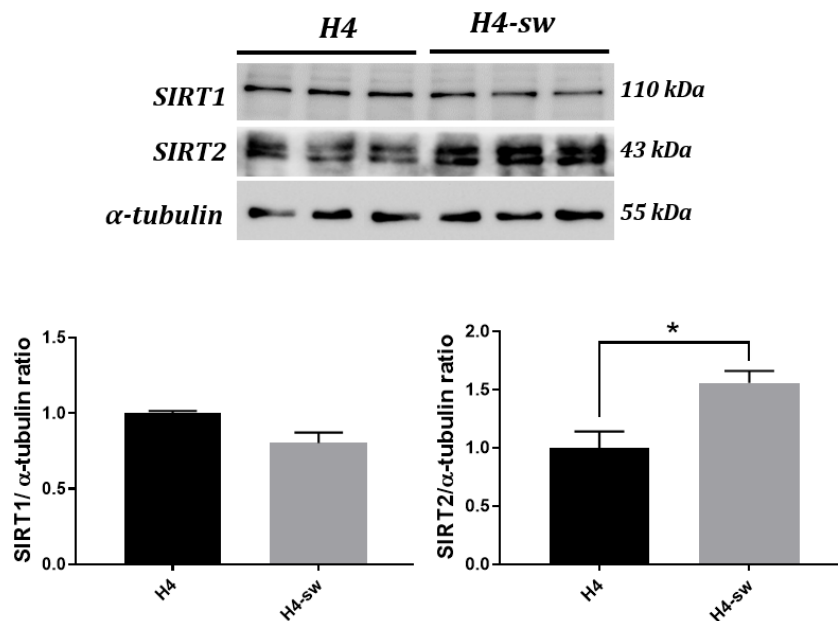


**Figure 4.2** Representative Western blotting analysis of three independent experiments on whole cell lysates from H4 and H4-sw cells, assessing SIRT1 and SIRT2 protein levels, normalized to  $\alpha$ -tubulin. Results are reported as Mean $\pm$ SEM ( $n=3$ ; Mann-Whitney test, \*  $p<0.05$ ; SIRT1  $p=0.1$ , SIRT2  $p=0.045$ ).

#### 4.1.2 EVALUATION OF CYTOTOXICITY OF SIRT1 AND SIRT2 MODULATION IN H4-SW CELLS

In order to proceed with the combined treatment on SIRT1 and SIRT2, it was necessary to assess its potential cytotoxicity, so we did viability assays after the single and the double treatment and determined the proper concentration for *in vitro* experiments.

AK7 is a brain-permeable and selective SIRT2 inhibitor, whose structure was derived from its analogue AK1. The concentration range of AK7 for cellular treatments was selected referring to available literature [Chen X et al., 2015; Wang X et al., 2015].

The analysis of cellular viability with increasing concentrations of the SIRT2 inhibitor AK7 showed that the modulator is not toxic in the 10-20  $\mu\text{M}$  concentration range (AK7  $\text{IC}_{50}$ = 12.5  $\mu\text{M}$ ) (Fig. 4.3).

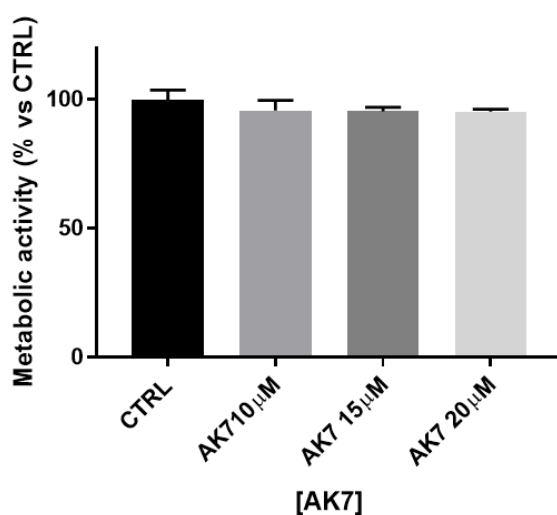


**Figure 4.3** MTS assay on H4-sw cells treated for 24 hours with increasing concentrations of the SIRT2 inhibitor AK7. CTRL= DMSO. Results are reported as Mean $\pm$ SEM (n=4; Kruskal-Wallis and Dunn's post hoc test).

For the SIRT1 activator SRT1720, we did the analysis of cellular viability with increasing concentrations of the compound in the 0.3-2  $\mu\text{M}$  range ( $\text{EC}_{50}$ = 0.16  $\mu\text{M}$ ), as our previous experiments and literature data showed that this was the efficacy concentration interval for *in vitro* treatments [Nishida K et al., 2018; Minor RK et al., 2011]. In H4-sw cells, starting from 2  $\mu\text{M}$ , SRT1720 leads to significant cytotoxicity (Fig. 4.4).

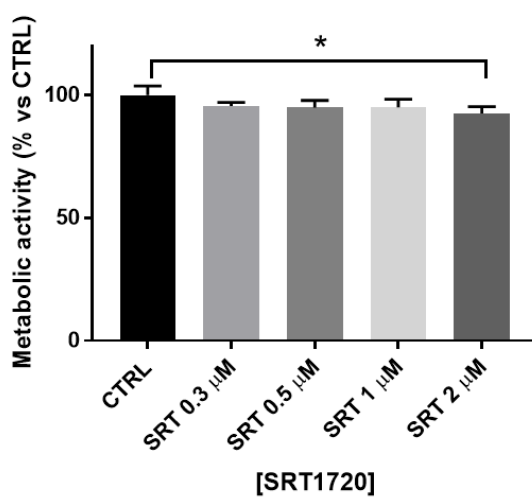


**Figure 4.4** MTS assay on H4-sw cells treated for 24 hours with increasing concentrations of the SIRT1 activator SRT1720. CTRL= DMSO. Results are reported as Mean $\pm$ SEM ( $n=4$ ; Kruskal-Wallis and Dunn's post hoc test, \*  $p<0.05$ ).

Next, we decided to combine the higher non-toxic dose of AK7 (20  $\mu\text{M}$ ) with increasing concentrations of SRT1720, which was the one that showed slight toxicity in the considered range. Analysis of cellular viability after 24 hours treatment revealed that the higher concentration that does not produce significant cellular mortality is 20  $\mu\text{M}$  AK7 and 0.5  $\mu\text{M}$  SRT1720 (Fig. 4.5).

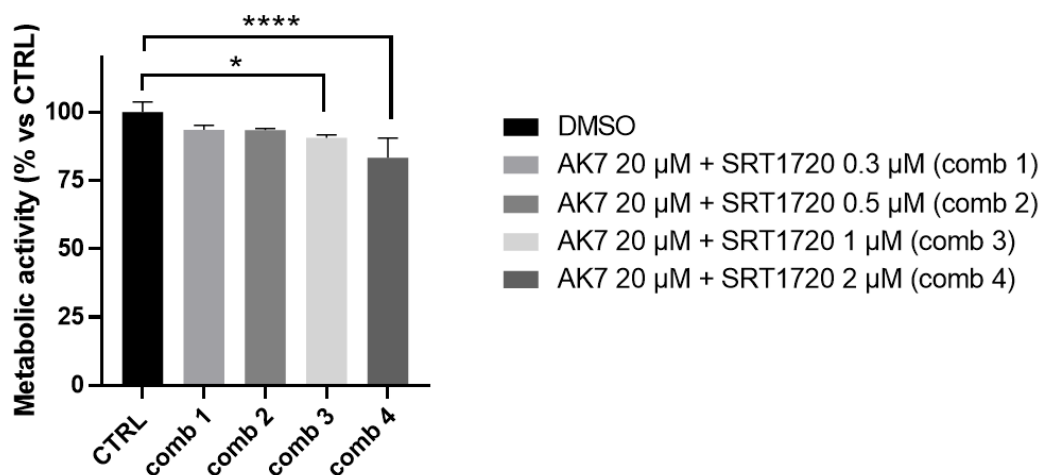


**Figure 4.5** MTS assay on H4-sw cells treated for 24 hours with 20  $\mu$ M AK7 together with increasing concentrations of SRT1720. CTRL= DMSO. Results are reported as Mean $\pm$ SEM ( $n=4$ ; Kruskal-Wallis and Dunn's post hoc test, \*  $p<0.05$ , \*\*\*\* $p<0.0001$ ).

#### 4.1.3 EFFECT OF THE DOUBLE TREATMENT ON flAPP AND sAPP $\alpha$ LEVEL

H4-sw cells have a high amyloidogenic APP metabolism and A $\beta$  production [Colombo et al., 2008].

We decided to analyse if our single or double treatments could exert an effect both on the production of flAPP protein and on its proteolytic processing fragments. Western blotting analysis on flAPP showed no change between untreated and treated cells, both with one or two combined modulators (Fig. 4.6), suggesting that SIRT1 activation and SIRT2 inhibition don't affect APP expression.

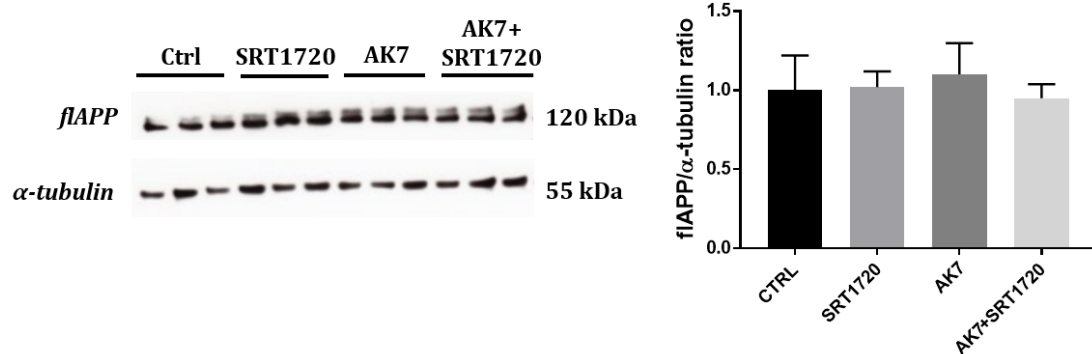


**Figure 4.6** Representative Western blotting analysis on H4-sw cells treated for 24 hours with 20  $\mu$ M AK7, 0.5  $\mu$ M SRT1720, and the combination of the two modulators, assessing flAPP protein level with 2C11 antibody, normalized to  $\alpha$ -tubulin. CTRL= DMSO. Results are reported as Mean $\pm$ SEM (n=6; One-way ANOVA and Tukey's post-hoc test).

After we verified that our treatment did not affect flAPP production, we analysed its metabolism by assessing the total pool of soluble fragments (sAPP $\alpha$  and sAPP $\beta$ ) released in H4-sw conditioned media. Western blotting analysis on cell supernatants after the single and the combined treatments showed a significant increase of total sAPP protein (Fig. 4.7).

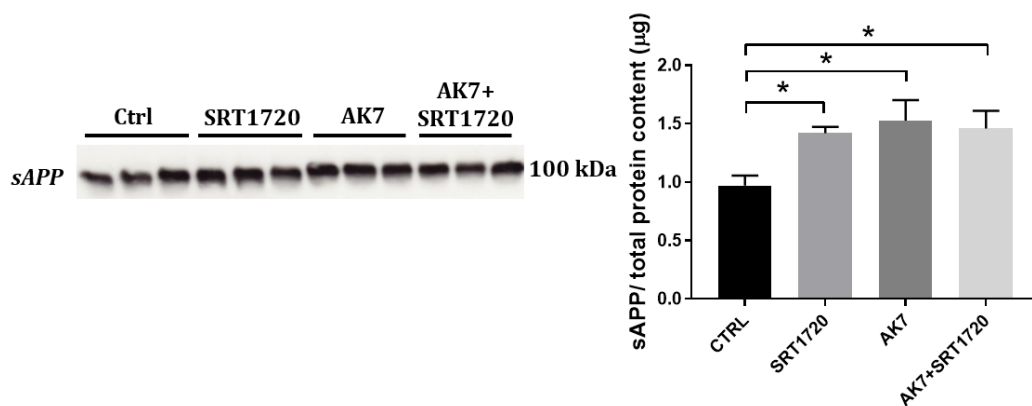


**Figure 4.7** Representative Western blotting analysis on conditioned media from H4-sw cells treated for 24 hours with 20  $\mu$ M AK7, 0.5  $\mu$ M SRT1720, and the combination of the two modulators, assessing sAPP protein level with 22C11 antibody, normalized to the total protein content of the sample. CTRL= DMSO. Results are reported as Mean $\pm$ SEM (n=6; One-way ANOVA and Tukey's post-hoc test; CTRL vs SRT1720 \*p=0.03, CTRL vs AK7 \*p=0.011, CTRL vs AK7+SRT1720 \*p=0.047).

As the total pool of soluble APP increased but no indication was given on specific proteolytic pathway involvement, we proceeded with the analysis of the sAPP $\alpha$  fragment, to assess if sAPP increase could be related to the non-amyloidogenic processing activation. Both AK7 and SRT1720 produced a significant increment of this neuroprotective protein. Moreover, with the double treatment we obtained a larger increase of sAPP $\alpha$  (Fig. 4.8) with respect to single modulators, suggesting that we could observe an additive effect of the two modulations.

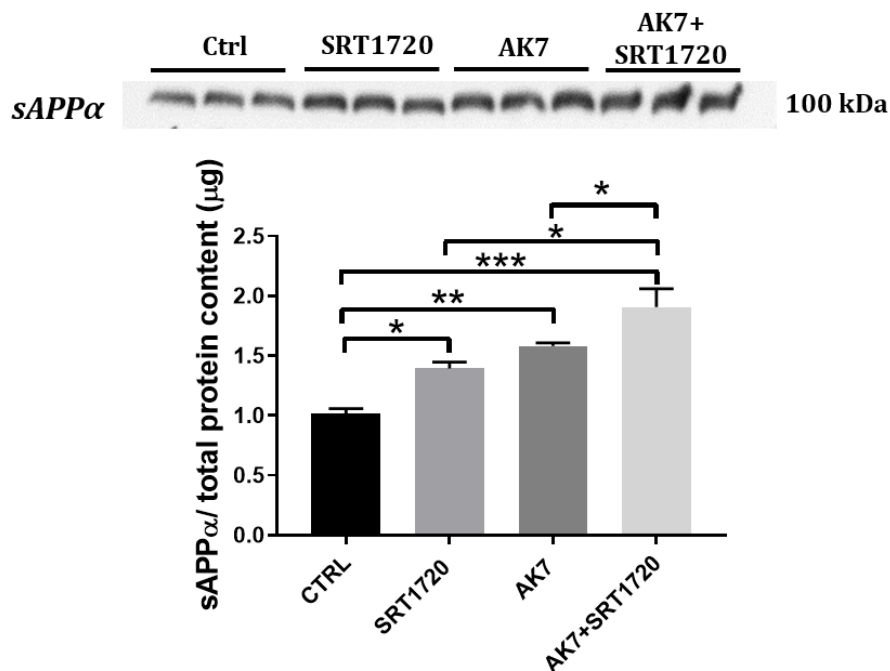


**Figure 4.8** Representative Western blotting analysis on conditioned media from H4-sw cells treated for 24 hours with 20  $\mu$ M AK7, 0.5  $\mu$ M SRT1720, and the combination of the two modulators, assessing sAPP $\alpha$  with 6E10 antibody, normalized to the total protein content of the samples. CTRL= DMSO. Results are reported as Mean $\pm$ SEM (n=6; One-way ANOVA and Tukey's post-hoc test; \* $p$ <0.05, \*\* $p$ <0.01, \*\*\* $p$ <0.001; CTRL vs SRT1720 \* $p$ =0.036, CTRL vs AK7 \*\* $p$ =0.0068, CTRL vs AK7+SRT1720 \*\*\* $p$ =0.0004, SRT1720 vs AK7+SRT1720 \* $p$ =0.010, AK7 vs AK7+SRT1720 \* $p$ =0.049).



We checked if sAPP $\alpha$  increase could be due to enhanced  $\alpha$ -secretase (ADAM10) mRNA, as this fragment is the result of  $\alpha$ -secretase activity, but the Real Time PCR result unexpectedly showed that the treatments were ineffective on ADAM10 gene expression (Fig. 4.9), a result that is also in contrast with some literature data. In this case too, the data could suggest the hypothesis of a model-dependent effect or an effect on ADAM10 activity and membrane availability rather than on its mRNA level.

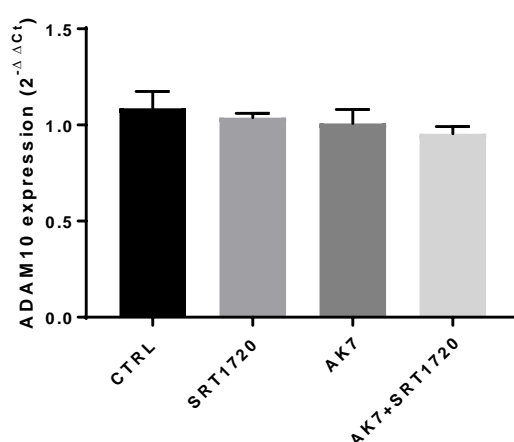


**Figure 4.9** ADAM10 mRNA levels in H4-sw cells treated for 24 hours with 20  $\mu$ M AK7, 0.5  $\mu$ M SRT1720, and the combination of the two modulators, assessed by quantitative Real time PCR. CTRL= DMSO. Data were calculated with the  $2^{-\Delta\Delta C_t}$  method, using  $\beta$ -actin as reference endogenous gene. Results are reported as Mean $\pm$ SEM (n=4; Kruskal-Wallis and Dunn's post hoc test).

#### 4.1.4 SIRT2 SILENCING: EFFECT ON sAPP $\alpha$

In order to deepen the relationship between sAPP $\alpha$  increase and SIRT2 modulation and to verify AK7 specificity whose *in vitro* data are less represented in literature, we decided to analyse sAPP $\alpha$  parameter after transient small interfering RNA silencing (siRNA) of SIRT2 to replicate AK7 effect.

SIRT2 silencing produced an increase in the neuroprotective sAPP $\alpha$  fragment, in accordance with SIRT2 pharmacological inhibition with AK7 (Fig. 4.10).

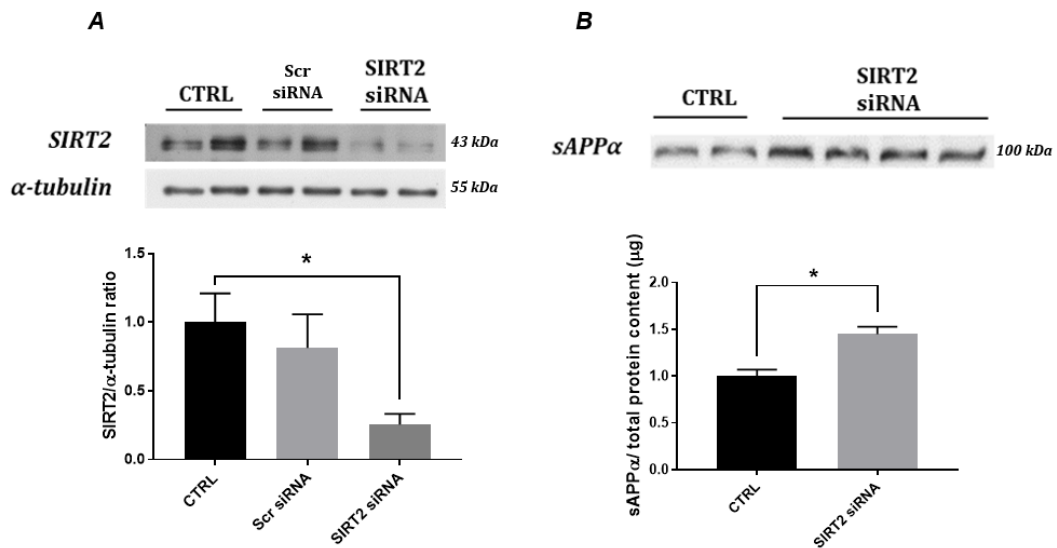


**Figure 4.10** A) Representative Western blotting analysis on H4-sw cells treated for 48 hours with SIRT2 siRNA or a negative control siRNA (Scr siRNA=scrambled sequence with no match in human gene database), assessing SIRT2 protein level, normalized to  $\alpha$ -tubulin. B) sAPP $\alpha$  protein analysis on H4-sw conditioned media, after 48 hours treatment with SIRT2 siRNA. Results are reported as Mean $\pm$ SEM (n=4; Kruskal-Wallis and Dunn's post hoc test; Mann-Whitney test; \*p<0.05; sAPP $\alpha$  \*p=0.028).

#### 4.1.5 EFFECT OF SIRT1/2 MODULATION ON AMYLOIDOGENIC PROCESSING: sAPP $\beta$ , A $\beta$ 40 AND A $\beta$ 42

The total sAPP increase in treated cells correlated with neuroprotective sAPP $\alpha$  increase. To draw a complete picture of APP processing, we focused our analyses also on the amyloidogenic pathway by assessing sAPP $\beta$  fragment and  $\beta$ -amyloid peptides (A $\beta$ 40 and A $\beta$ 42) generation.

The double treatment produced a significant decrease of sAPP $\beta$  level, while the single treatments did not affect this  $\beta$ -secretase cleavage product. The same effect was evident for A $\beta$ 40 peptide (Fig. 4.11).

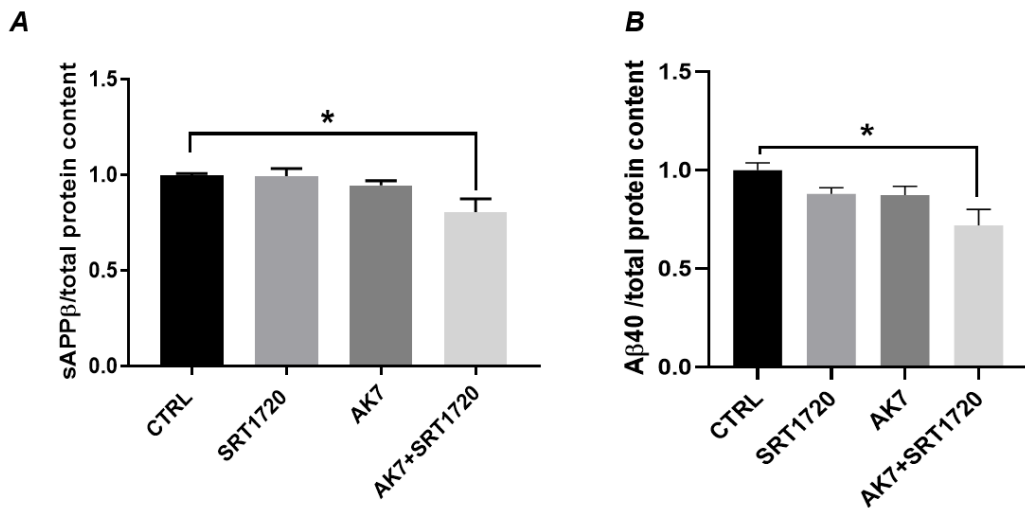


**Figure 4.11** sAPPβ (A) and Aβ40 (B) ELISA assay on conditioned media from H4-sw cells treated for 24 hours with 20 μM AK7, 0.5 μM SRT1720, and the combination of the two modulators. CTRL= DMSO. Data were normalized to the total protein content of the sample. Results are reported as Mean±SEM (n=4; Kruskal-Wallis and Dunn's post hoc test, \*p<0.05; sAPPβ CTRL vs AK7+SRT1720 \*p=0.0306, Aβ40 CTRL vs AK7+SRT1720 \*p=0.021).

The same experiment was performed with another SIRT1 activator, SRT2104, which is brain-permeable and has been subsequently introduced for *in vivo* treatments in the following part of the thesis. SRT2104 cytocompatibility in H4-sw cells was previously assessed both for single and combined treatment (data not shown).

In this case too, the double treatment decreased both sAPPβ and Aβ40, a change that was not significant in the case of single modulations (Fig. 4.12).

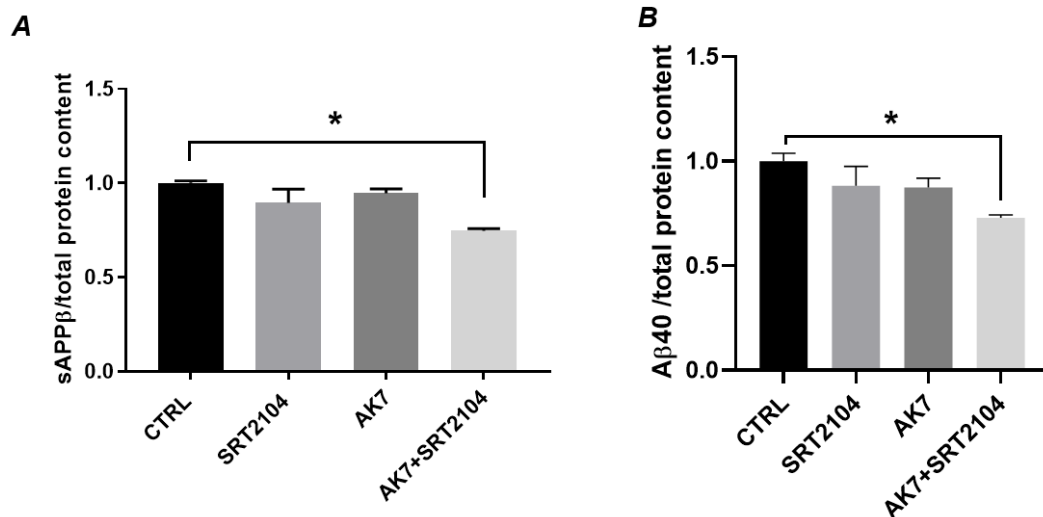


**Figure 4.12** sAPPβ (A) and Aβ40 (B) ELISA assay on conditioned media from H4-sw cells treated for 24 hours with 20 μM AK7, 3 μM SRT2104, and the combination of the two modulators. Data were normalized to the total protein content of the sample. CTRL= DMSO. Results are reported as Mean±SEM (n=4; Kruskal-Wallis and Dunn's post hoc test, \*p<0.05; sAPPβ CTRL vs AK7+SRT1720 \*p=0.039, Aβ40 CTRL vs AK7+SRT1720 \*p=0.048).

The results obtained on sAPPβ and Aβ40 suggest that the combination of the two treatments is necessary to produce a significant change of these parameters.

We examined the effect of the treatment on Aβ42 peptide too, and the result was surprisingly in contrast with the previous one. In particular, the presence of AK7 in both the single and the double treatment conditions produced a significant increase in Aβ42 levels. The experiment was replicated twice, and performed with SRT2104 activator too, as for Aβ40 (Fig. 4.13).

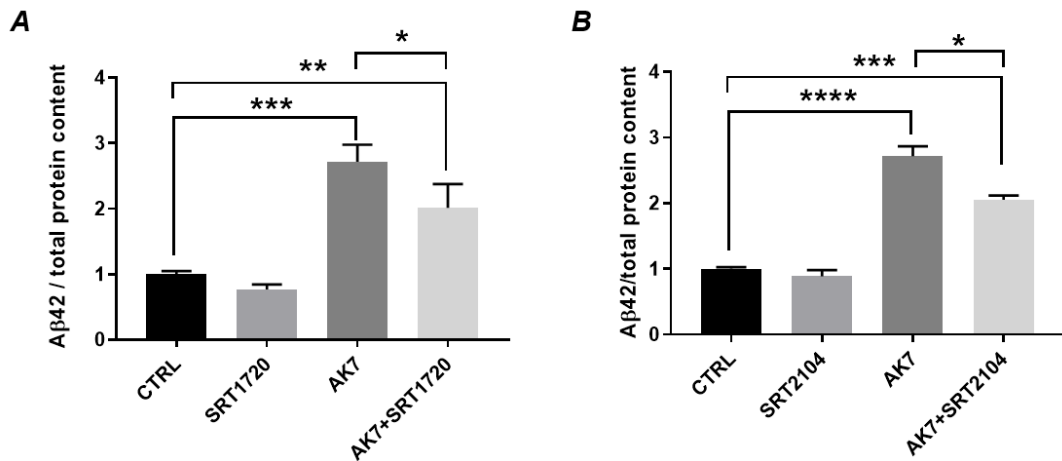


**Figure 4.13** Aβ42 ELISA assay on conditioned media from H4-sw cells treated for 24 hours with A) 20 μM AK7, 0.5 μM SRT1720, AK7+SRT1720 and B) 20 μM AK7, 3 μM SRT2104, AK7+SRT2104. Data were normalized to the total protein content of the sample. CTRL= DMSO. Results are reported as Mean±SEM (n=4; Kruskal-Wallis and Dunn's post hoc test, \*p>0.05, \*\*p<0.01, \*\*\*p<0.001, \*\*\*\*p<0.0001).

Interestingly, Aβ42 level in the double-treated cells was lower than that observed on AK7-treated cells, suggesting that the presence of the SIRT1 activator could interfere with this unexpected increase of Aβ42.

To check if this AK7 effect was dependent on its action on SIRT2, Aβ42 assay was repeated with conditioned media from H4-sw cells treated either with the inhibitor AK7 or with SIRT2 siRNA. The result showed that only AK7 was able to increase Aβ42, while SIRT2 siRNA did not affect its level. This suggests that the elevated Aβ42 monomer fraction is due to a direct interaction between AK7 molecule and Aβ forms, which could interfere with the ELISA assay result without SIRT2 involvement (Fig. 4.14).

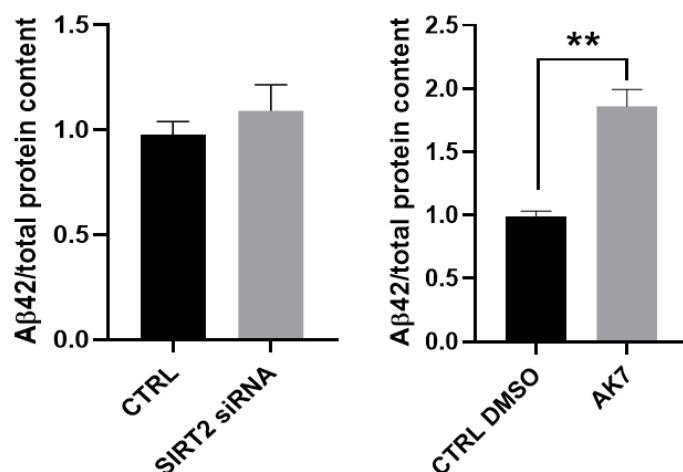


**Figure 4.14** Aβ42 ELISA assay on conditioned media from H4-sw cells treated either with SIRT2 siRNA and control siRNA (left), or with AK7 and DMSO as control (right). Data were normalized to the total protein content of the sample. Results are reported as Mean±SEM (n=4; Mann-Whitney test, \*\*p<0.01 AK7 vs Ctrl DMSO).

Different hypotheses can be formulated on this result. The first can be a side effect of the molecule, which could lead to reconsideration of its potential clinical use, even if we demonstrated that such effect was not dependent on SIRT2 inhibition, therefore such unspecific mechanism would still be unknown. We formulated another possible hypothesis that considers AK7 reacting with oligomeric Aβ42 through a chemical, SIRT2-independent mechanism, directly acting on oligomers that form in cell culture medium [Reed MN et al., 2011; Walsh DM et al., 2002] of H4-sw cells. We hypothesized a dissolving effect on oligomers leading to monomeric fraction increase, but further studies are needed to explore this hypothesis, as for now we found some literature considerations to support our idea (see Discussion section).

### ***In vitro* results: general conclusions**

The data obtained from our *in vitro* experiments demonstrated that the approach of combining the inhibition of SIRT2 with activation of SIRT1 is feasible, as it did not negatively influence the viability of the selected H4-sw cellular model. The main aim of this section was to obtain some indications of the beneficial effect of the treatment on APP proteolytic processing. We demonstrated that the double treatment is able to modulate the non-amyloidogenic processing through increase of sAPP $\alpha$  protein fragment, known for its neuroprotective properties. Moreover, the combined modulation of SIRT1/2 showed a greater effect compared to single treatments. The assessment of amyloidogenic processing supported the use of the combination too, as the single treatments were not effective on both sAPP $\beta$  and A $\beta$ 40 peptide, while the double treatment decreased those two parameters. However, some contradictory results emerged, as the assessment of A $\beta$ 42 revealed a paradoxical increase with SIRT2 inhibitor treatment, an effect that we hypothesized to be related to an antiaggregant property, but that could also constitute a potential side effect of the molecule that needs careful investigation.

## 4.2 *In vivo* results

### 4.2.1 3xTg-AD MICE PATHOLOGICAL PHENOTYPING

For *in vivo* experiments, we selected 3xTg-AD mice between 6 and 7 months of age, balancing experimental groups for sex, age and weight. The selected age could allow to treat early-stage AD mice, harbouring a cognitive deficit and neuropathological alterations in a pre-plaque status, where the pathology is mainly related to intraneuronal A $\beta$  accumulation and oligomers toxicity, thus mimicking an early intervention strategy in humans .

At this age, mice present a significant cognitive deficit, measured by NORT, where the mean discrimination index (DI) of NTg mice (see Materials and Methods 3.2.5) is between 0.3 and 0.4, while the mean discrimination index of 3xTg-AD mice is close to zero (Fig. 4.15).

A phenotypic characterization of these mice showed that both extracellular and intraneuronal A $\beta$  are detectable in hippocampus, while a very low detectability was obtained in the cortex, so we decided to focus our neuropathological analyses on brain samples of hippocampal origin.

This feature is partially in line with what has been described by other research groups that characterized the temporal and regional progression of pathology in 3xTg-AD model [**Oddo S et al., 2006; Belfiore R et al., 2018**]. With respect to what was reported previously [**Mastrangelo and Bowers, 2008**] in the original model characterization, there is some temporal delay in the development of the pathology, as pointed out by Belfiore and colleagues [**Belfiore R et al., 2018**].



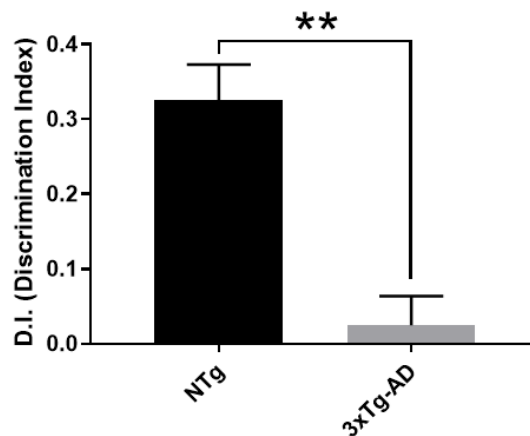


**Figure 4.15** Discrimination Index of 3xTg-AD and NTg mice at 6 months of age, measured by the Novel Object Recognition Test (NORT). Results are reported as Mean±SEM (n=8; Student's t test, \*\*p=0.0011).

Prior to plaques formation, A $\beta$  accumulates intracellularly mostly at hippocampal level, at the age of 6 months.

Mice show A $\beta$  senile plaques deposition starting from 12 months of age, detectable in hippocampus but not in cortex (Fig. 4.16).

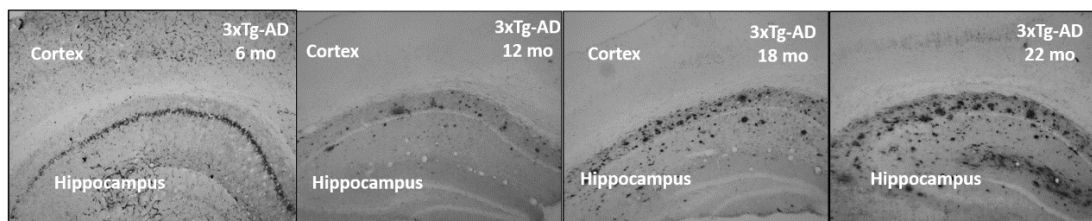


**Figure 4.16** Immunohistochemistry for A $\beta$  plaques using 6E10 antibody on coronal 30  $\mu$ m-thick brain sections from 3xTg-AD mice. The panel shows the temporal profile of intracellular A $\beta$  at 6 months and plaques deposition from 12 to 22 months of age.

Some immunoreactivity for NFTs is detectable in the hippocampus from 19 months of age, while 6-months old 3xTg-AD mice do not show the presence

of PHF-tau (Fig. 4.17), accordingly to literature data about a late development of tau tangles in transgenic AD mice **[Belfiore R et al., 2018]**.

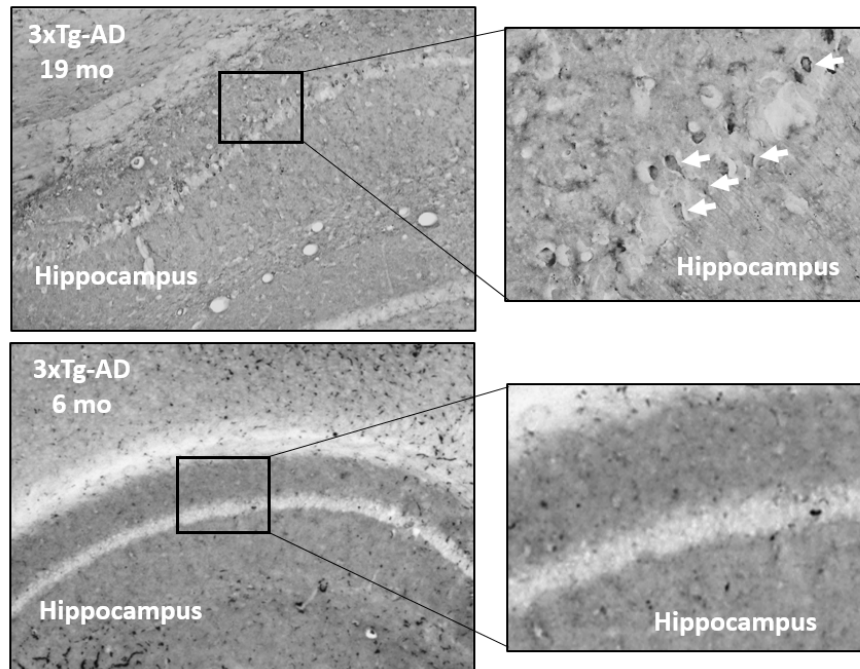


**Figure 4.17** Immunohistochemistry for tau tangles (PHF tau) using AT8 antibody on coronal 30  $\mu\text{m}$ -thick brain sections from 3xTg-AD at 19 and 6 months of age. The panel shows magnifications of the hippocampal regions, highlighting some signal at the age of 19 months but not at 6 months. The white arrows point to positive hippocampal neurons that accumulate phospho-tau in their soma.

Then, we evaluated the detectability of hippocampal soluble  $\text{A}\beta$  oligomers in samples from 3xTg-AD mice with the widely used human  $\text{A}\beta$  antibody 6E10. This commercial antibody has been used for  $\text{A}\beta\text{O}$  detection by other groups **[Amar F et al., 2017]** despite some concerns could be raised on its potential cross-reactivity with mouse tissue samples due to its mouse IgG nature, as well as on its inability to detect all the  $\text{A}\beta$  forms **[Hunter S and Brayne C, 2017]**.

We were able to detect a high molecular weight signal at 55 kDa, absent in NTg hippocampus, possibly representing A $\beta$ \*56 form, which is an oligomeric form related to the presence of cognitive impairment [Lesnè S et al., 2006; Billings LM et al., 2007]. A low molecular weight signal was visible near 15 kDa, which could represent a smaller aggregate form. Other specific signals were not detectable with this method (Fig. 4.18).

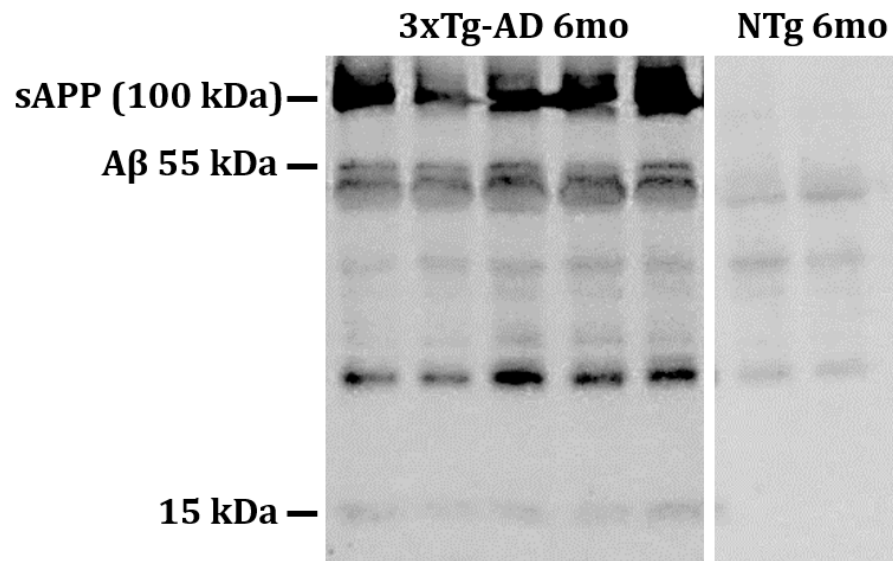


**Figure 4.18** Western blotting analysis on hippocampal soluble fractions of 3xTg-AD and NTg mice at 6 months, assessing A $\beta$  soluble oligomers with 6E10 antibody. One clear specific signal was detected, possibly representing a high-molecular weight aggregate form (55 kDa). Another weaker signal was present near 15 kDa, corresponding to the expected molecular weight of a trimeric aggregate. Other signals were attributable to unspecific binding.

At hippocampal level, 3xTg-AD mice show also an increase in neuroinflammation markers GFAP and CD11b, and a decrease in the presynaptic marker Synaptophysin. We also assessed the level of NRF2, a master regulator of oxidative stress response, and detected a trend towards the decrease of this transcription factor (Fig. 4.19).

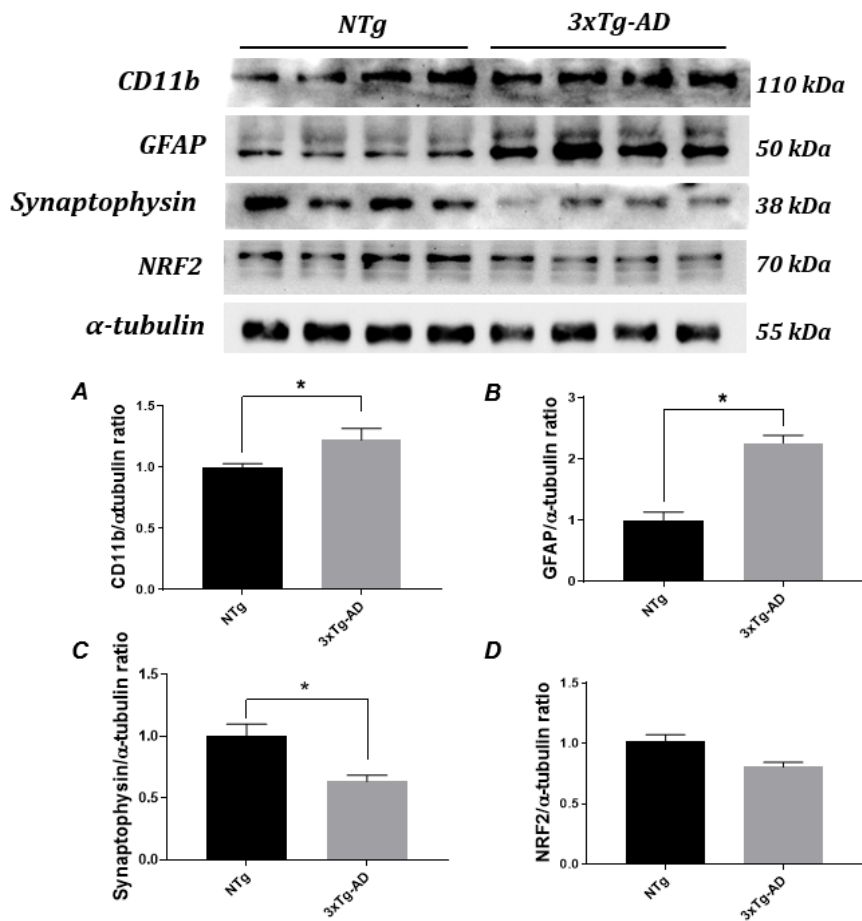


**Figure 4.19** Western blotting analysis on hippocampal lysates of 3xTg-AD and NTg mice at 6 months, assessing (A) CD11b, (B) GFAP, (C) Synaptophysin and (D) NRF2. Data were normalized to  $\alpha$ -tubulin and are presented as Mean $\pm$ SEM (n=4; Mann-Whitney test, \* $p$ <0.05; A \* $p$ =0.050, B \* $p$ =0.028, C \* $p$ =0.04, D  $p$ =0.0571).

We also assessed the basal expression of SIRT1 and SIRT2 in our model. As shown in Figure 4.20, SIRT1 expression was not different between 3xTg-AD and NTg mice. Differently, hippocampal SIRT2 basal expression in 3xTg-AD mice is higher than NTg mice. This corroborates our rationale of inhibiting SIRT2 for pathological phenotype improvement, while it seems that in our experimental model we are not in the condition of a SIRT1 deficiency and the treatment should boost its neuroprotective activity.

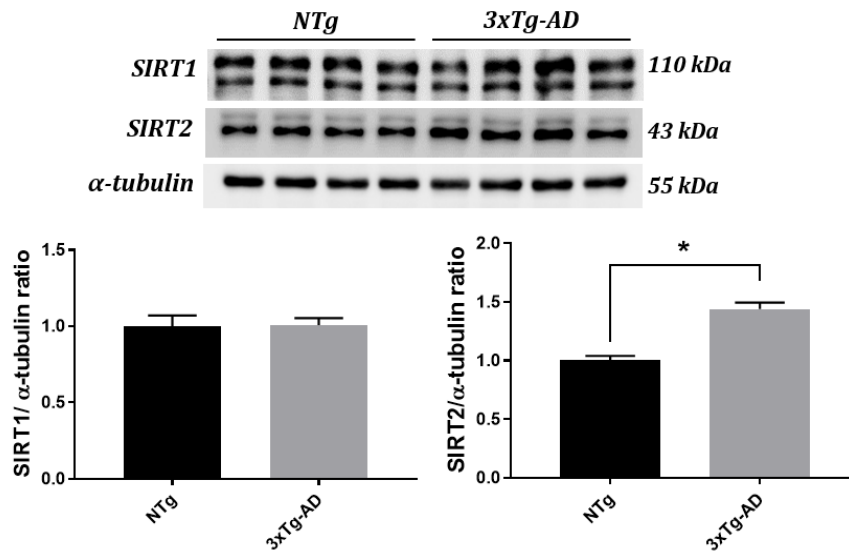


**Figure 4.20** Western blotting analysis on hippocampal lysates of 3xTg-AD and NTg mice at 6 months, assessing SIRT1 and SIRT2. Data were normalized to  $\alpha$ -tubulin and are presented as Mean $\pm$ SEM ( $n=4$ ; Mann-Whitney test  $*p>0.05$ ; SIRT2 NTg vs 3xTg-AD  $*p=0.029$ ).

All the characterization results suggest that our 3xTg-AD mice have a group of neuropathological alterations including neuroinflammation and an indication of synaptic deficit, which with the presence of high intracellular A $\beta$  and oligomers could contribute to cognitive impairment establishment and memory loss.

#### 4.2.2 EFFECT OF SIRT2 INHIBITION AND SIRT1 ACTIVATION ON 3xTg-AD COGNITIVE PERFORMANCE

As already demonstrated by **Biella et al. in 2016**, 2 weeks treatment of 3xTg-AD mice at 6-8 months with AK7 leads to cognitive deficit improvement. In addition, AK7-treated mice had an increased non-amyloidogenic and decreased amyloidogenic APP processing, in the hippocampus. We replicated the NORT behavioural data on 6 months-old mice (8 mice per group) in order

to assess the reproducibility of the protocol and move on with the combined treatment approach.

First, we verified that AK7 treatment was well tolerated, as assessed by body weight monitoring during the experiment (Fig. 4.21). Body weight was not significantly different between treated and untreated mice.

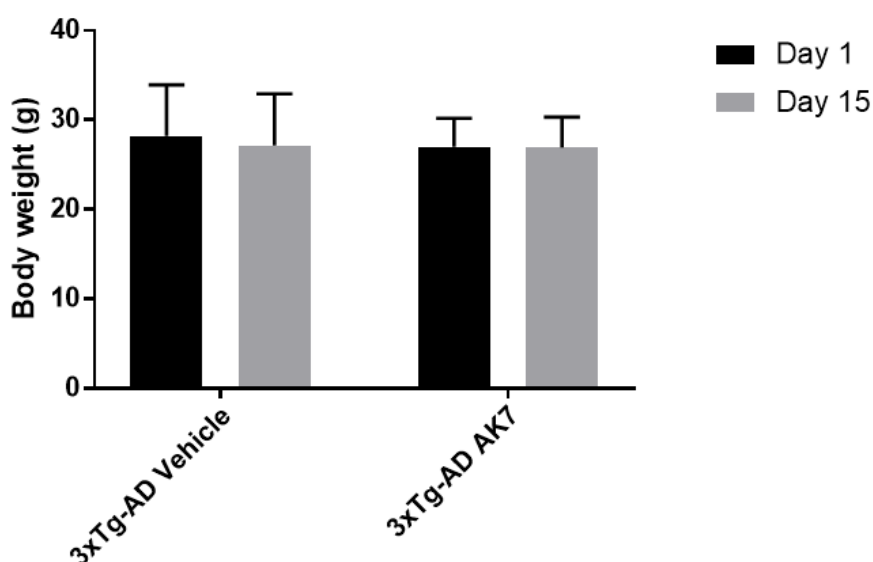


**Figure 4.21** Body weight monitoring of 3xTg-AD mice treated with AK7 or vehicle, assessed on day 1 and day 15. Data are presented as Mean±SEM (n=8; Two-way ANOVA and Tukey's post hoc test;  $p>0.05$ ).

We decided to treat 3xTg-AD mice only, as we focused our objective on closely detecting an improvement of the pathologic phenotype dependent on mutated human transgenes expression, favouring this aspect over the assessment of an effect on the healthy mouse phenotype. Our decision was also supported by the fact that SIRT2 inhibition with AK7 did not show pro-cognitive effect on NTg mice [Biella G et al., 2016]. However, it could be possible that SIRT1 treatment or the combined one boost cognitive functions in NTg mice too, as in our experimental set-up we are masking the contribution given by genotype

to our treatment effects. This could be a limit of our experiment's design, and a complete assessment on both a treatment- and genotype-dependent basis should be taken into consideration for future experiments.

Treated and untreated 3xTg-AD mice, together with a NTg control group taken for baseline measurement, were tested for cognitive impairment with the NORT as described in Methods.

Total exploration time of the training and testing phases was calculated and was not significantly different among groups (Fig. 4.22).

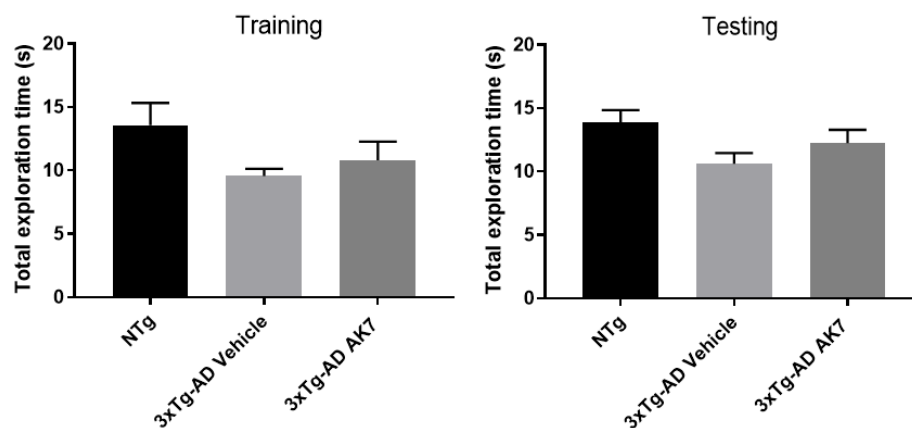


**Figure 4.22** Total exploration time of training and testing phases for each experimental group. Data are presented as Mean $\pm$ SEM ( $n=8$ ; One-way ANOVA and Tukey's post hoc test;  $p>0.05$ ; NTg vs 3xTg-AD Vehicle  $p=0.115$  for Training,  $p=0.08$  for Test).

The % of investigation on the familiar and the novel object during the test phase was calculated. As shown in Figure 4.23, the vehicle-treated 3xTg mice did not show a difference in the % of investigation between the familiar and the novel object, suggesting no preference for a specific object. The AK7-treated mice, instead, spent more time exploring the novel object, as NTg mice did.

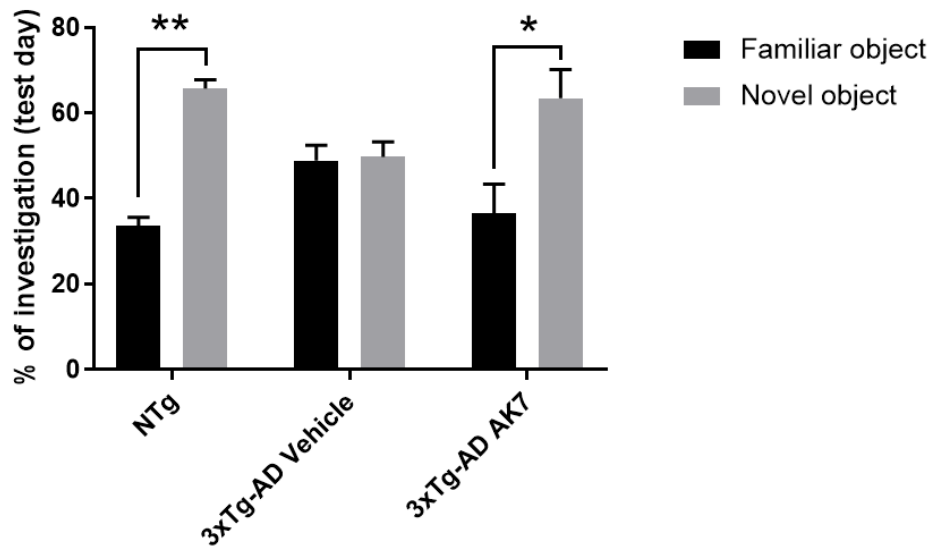


**Figure 4.23** % of investigation on the familiar and the novel object for each experimental group, during the test phase. Data are presented as Mean±SEM (n=8; Repeated measures Two-way ANOVA and Tukey's post hoc test; \*p<0.05, \*\*p<0.001).

AK7 treatment produced the recovery of memory deficit in 3xTg-AD mice (DI 3xTg AK7 vs. DI 3xTg vehicle \*p<0.05) (Fig. 4.24), that had a mean DI similar to NTg mice.

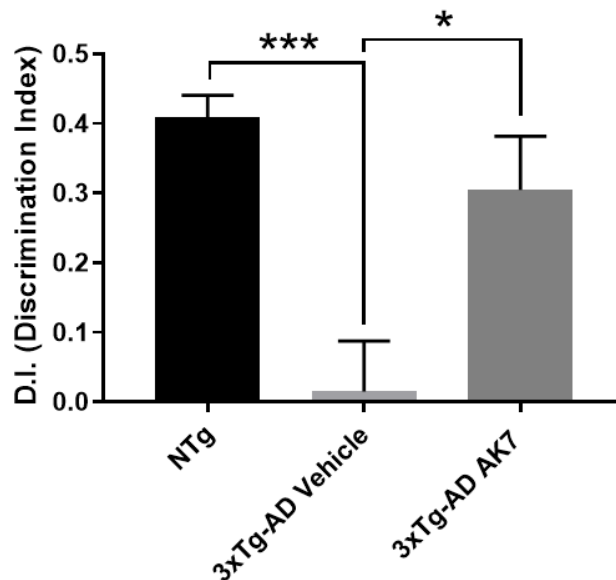


**Figure 4.24** Discrimination Index of 3xTg-AD mice treated with AK7 or vehicle, measured by the Novel Object Recognition Test (NORT). Results are reported as Mean±SEM (n=8; One-way ANOVA and Tukey's post hoc test, NTg vs 3xTg-AD Vehicle \*\*\*p<0.001, 3xTg-AD Vehicle vs 3xTg-AD AK7 \*p=0.0114).



We selected another group of 6-months old 3xTg-AD mice to be treated with the SIRT1 activator SRT2104, for two weeks, by oral gavage (8 mice per group).

SIRT1 activator administration was well tolerated, as assessed by body weight monitoring during the treatment (Fig. 4.25).

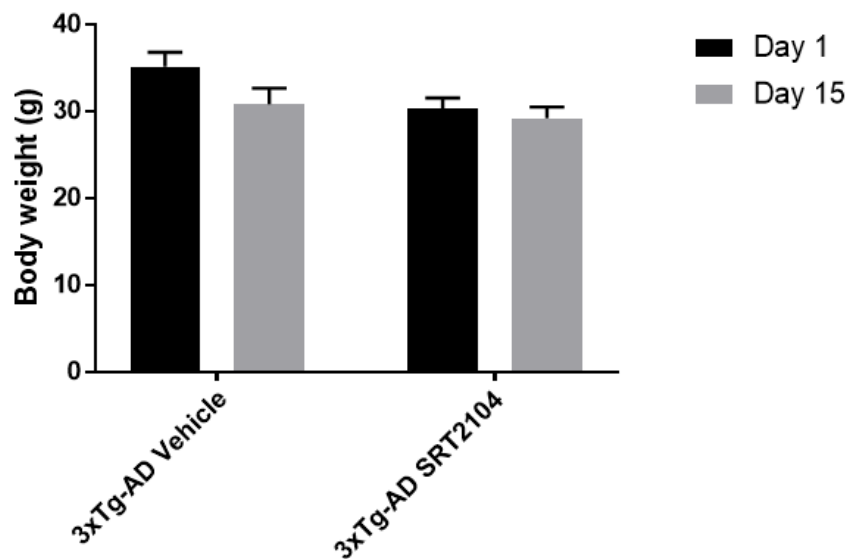


**Figure 4.25** Body weight monitoring of 3xTg-AD mice treated with SRT2104 or vehicle, assessed on day 1 and day 15. Data are presented as Mean±SEM (n=8; Two-way ANOVA and Tukey's post hoc test,  $p>0.05$ ).

As we did for AK7 experiment, we assessed cognitive performance with NORT, together with the NTg control group. Again, total exploration time of the training and testing phases was not significantly different between groups (Fig. 4.26).

It is worth to notice a substantial difference in exploration times between this experiment and the one in Figure 4.22. In fact, AK7 treatment resulted in total exploration times below 15 seconds, while Figure 4.26 shows longer

explorative activity both in training and testing phase of SRT2104 treatment. As an explanation for the oscillations between the experiments and experimental groups, one point to clarify is that these animals do not show long exploratory activity as a characteristic of the 129SV strain, which is quite sensitive to anxious situations [van Bogaert MJ et al., 2006]. In general, the exploratory activity presents some variability depending on the animals, the treatment protocol, the operator and the handling. In the AK7 experiment, which was the first of the set, a handling factor could have influenced the propensity of the animals to move and explore, a factor that with operator training and further experiments became less evident.

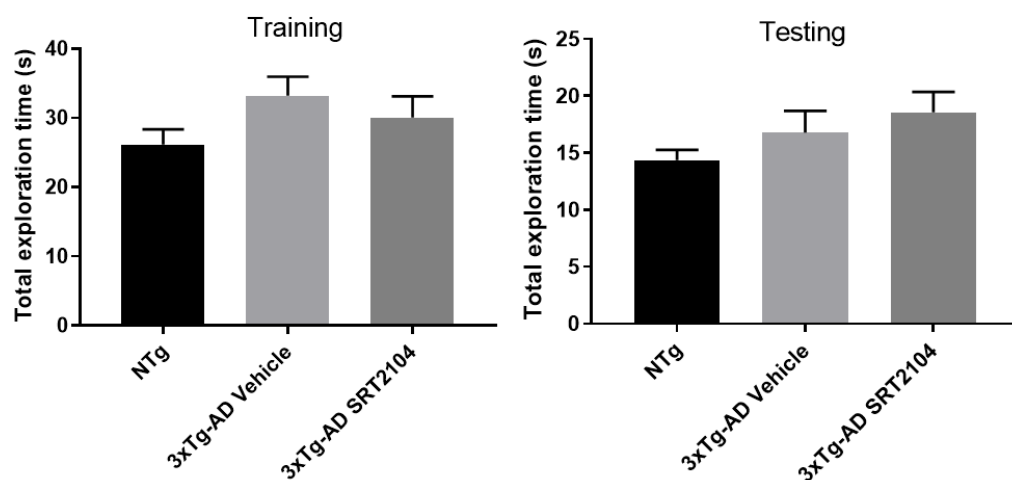


**Figure 4.26** Total exploration time of training and test phases for each experimental group. Data are presented as Mean±SEM (n=8; One-way ANOVA and Tukey's post hoc test; p>0.05).

As shown in Figure 4.27, vehicle-treated 3xTg mice did not show a difference in the % of investigation between the familiar and the novel object, while SRT2104-treated and NTg mice spent more time exploring the novel object.

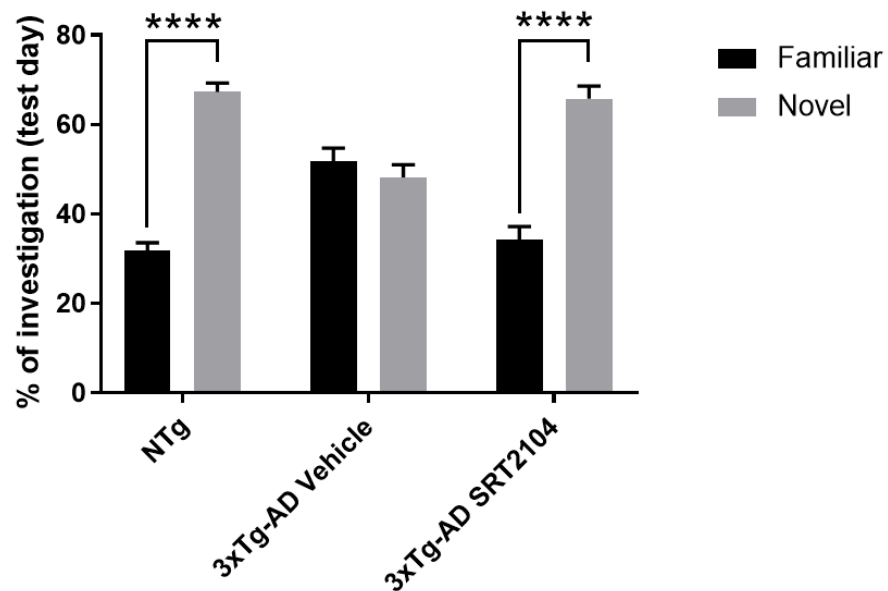


**Figure 4.27** % of investigation on the familiar and the novel object for each experimental group, during the test phase. Data are presented as Mean±SEM (n=8; Repeated measures Two-way ANOVA and Tukey's post hoc test; \*\*\*\*p<0.0001).

Like SIRT2 inhibition, SIRT1 activation was able to recover cognitive deficit of 3xTg-AD mice (DI 3xTg SRT2104 vs. DI 3xTg vehicle \*\*p<0.01), as shown by DI calculation in Figure 4.28, where the mean DI of SRT2104-treated mice was tendent to that of NTg group.

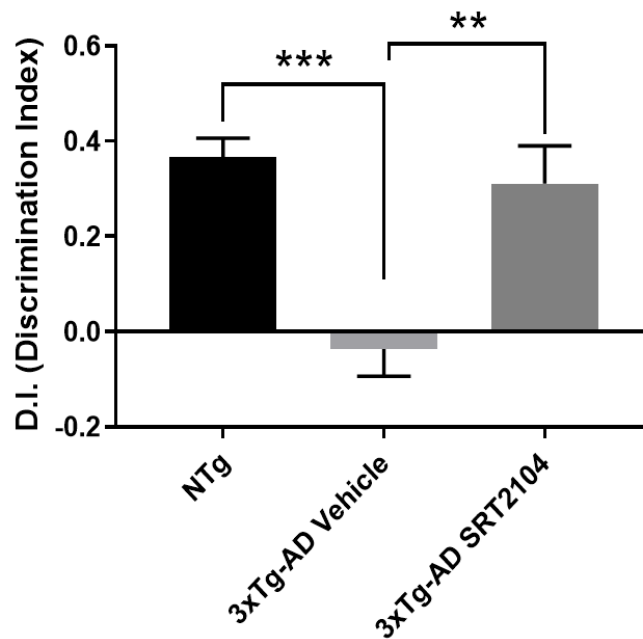


**Figure 4.28** Discrimination Index of 3xTg-AD mice treated with SRT2104 or vehicle, measured by the Novel Object Recognition Test (NORT). Results are reported as Mean±SEM (n=8; One-way ANOVA and Tukey's post hoc test, NTg vs 3xTg-AD Vehicle \*\*\*p<0.001, 3xTg-AD Vehicle vs 3xTg-AD AK7 \*\*p=0.002).

Considering the behavioural results presented above, the two single treatments on SIRT1 and SIRT2 were able to favour cognitive damage recovery of 3xTg-AD mice, so we decided to move on with our overall objective combining these two approaches. We treated 6 months-old 3xTg-AD mice with intraperitoneal SIRT2 inhibitor and oral SIRT1 activator, for 2 weeks.

Before the experiment, we performed a preliminary evaluation of the stress related to the procedure and of DMSO potential toxicity. Mice's general health status and body weight were constantly monitored during a one-week trial with vehicle containing DMSO both for intraperitoneal and oral dosing, and were not affected by the double treatment (data not shown).

As we did for the single treatments, during AK7/SRT2104 protocol we monitored mice's general health state and body weight (Fig. 4.29). No difference in body weight was evident.

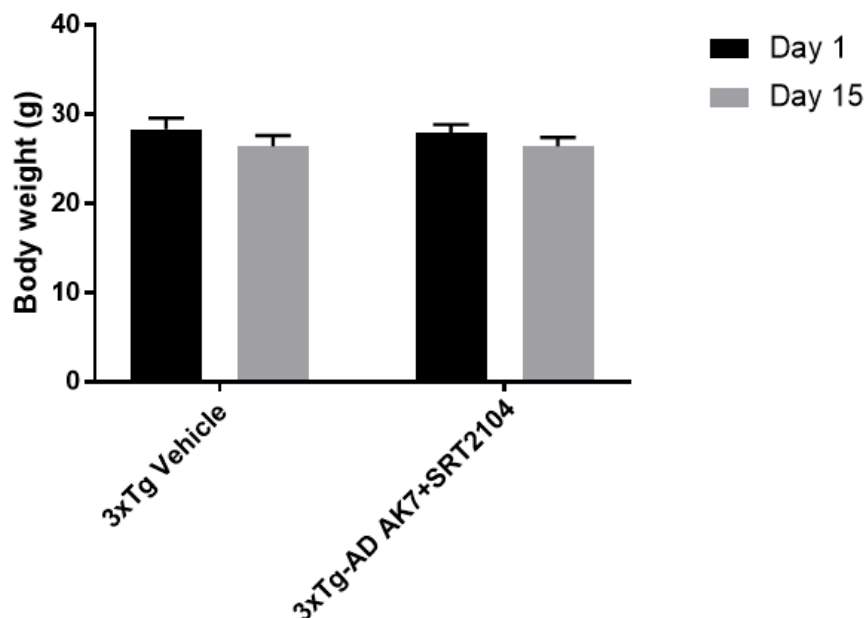


**Figure 4.29** Body weight monitoring of 3xTg-AD mice treated with AK7+SRT2104 or vehicle, assessed on day 1 and day 15. Data are presented as Mean $\pm$ SEM ( $n=8$ ; Two-way ANOVA and Tukey's post hoc test,  $p>0.05$ ).

Animals were subjected to NORT protocol for cognitive assessment, following the same timeline of the previous experiments.

Total exploration time of the training and testing phases was calculated and was not significantly different among groups (Fig. 4.30).

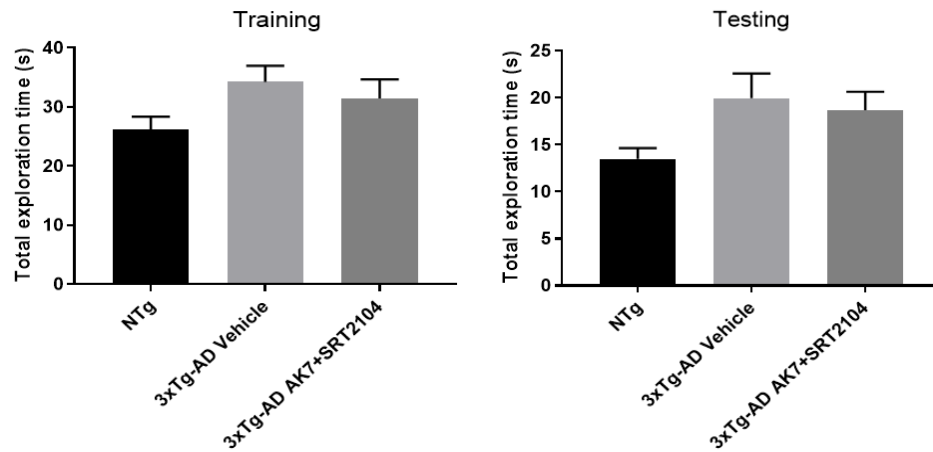


**Figure 4.30** Total exploration time of training and testing phases for each experimental group. Data are presented as Mean±SEM (n=8; One-way ANOVA and Tukey's post hoc test; p>0.05).

As shown in Figure 4.31, the vehicle-treated 3xTg mice showed no significant difference in the % of investigation between the familiar and the novel object, while AK7/SRT2104-treated mice spent more time exploring the novel object.

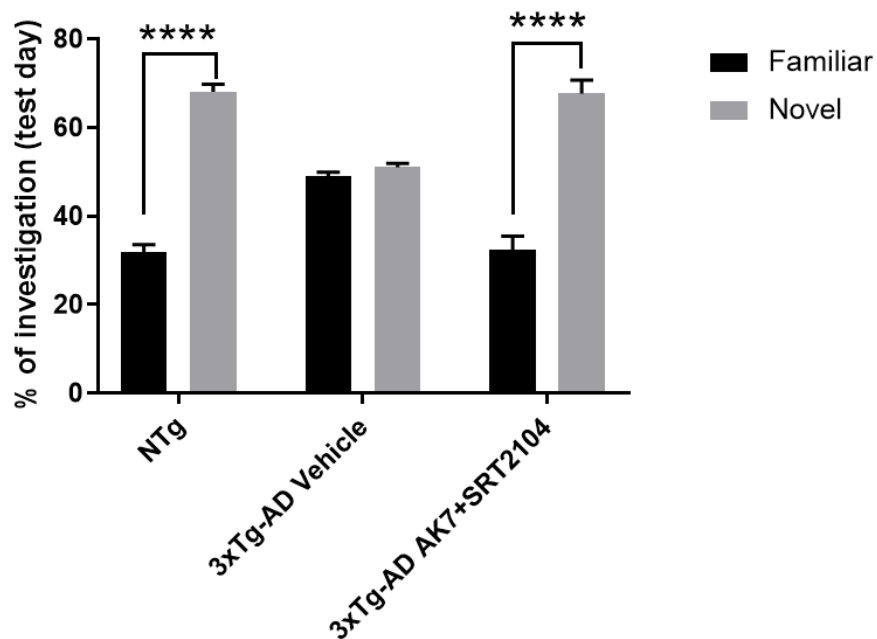


**Figure 4.31** % of investigation on the familiar and the novel object for each experimental group, during the test phase. Data are presented as Mean±SEM (n=8; Repeated measures Two-way ANOVA and Tukey's post hoc test; \*\*\*\*p<0.0001).

The double treatment significantly improved the cognitive performance of 3xTg-AD mice (DI 3xTg AK7+SRT2104 vs. DI 3xTg vehicle \*\*\*\* $p < 0.0001$ ), which had a mean DI comparable to that of NTg mice (Fig. 4.32).

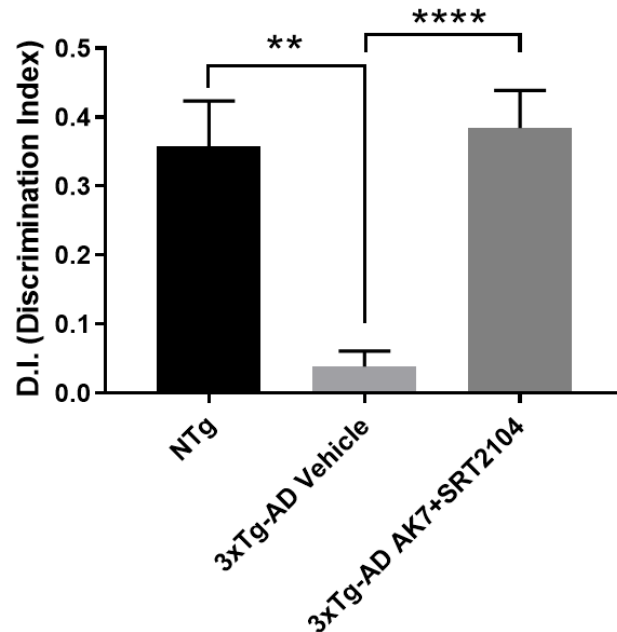


**Figure 4.32** Discrimination Index of 3xTg mice treated with AK7+SRT2104 or vehicle, measured by the Novel Object Recognition Test (NORT). Results are reported as Mean $\pm$ SEM ( $n=8$ ; One-way ANOVA and Tukey's post hoc test, \*\* $p < 0.0015$ , \*\*\*\* $p < 0.0001$ ).

This result confirms that when AK7 and SRT2104 modulators are given in combination are still able to lead to complete cognitive deficit recovery.

#### 4.2.3 EFFECT OF SIRT2 INHIBITION AND SIRT1 ACTIVATION ON AD-RELEVANT NEUROPATHOLOGIC PATHWAYS

AK7 treatment acted on APP metabolism *in vivo*, leading to sAPP $\beta$  decrease and sAPP $\alpha$  increase, as previously reported [Biella G et al., 2016] and suggested by *in vitro* data obtained in this thesis. Starting from this point, we checked sAPP $\alpha$  level in SRT2104 treated mice too, and we detected a

significant increase of this protein in hippocampus (Fig. 4.33A). sAPP $\alpha$  level resulted significantly increased also in double-treated mice (Fig. 4.33B).

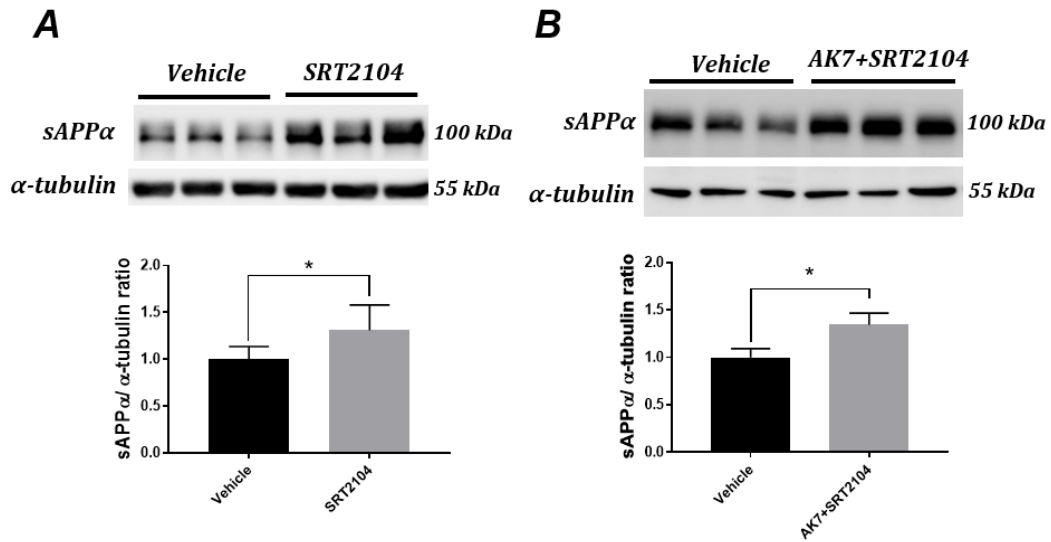


**Figure 4.33** Representative Western blotting analysis on hippocampal soluble fractions of 3xTg-AD mice treated with SRT2104 (A) or AK7+SRT2104 (B), assessing sAPP $\alpha$  protein normalized to  $\alpha$ -tubulin. Data are presented as Mean $\pm$ SEM (n=8; Student's *t* test, \**p*<0.05; Vehicle vs SRT2104 *p*=0.0168, Vehicle vs AK7+SRT2104 *p*=0.04).

As mentioned previously we were able to identify, in hippocampal soluble fractions of 3xTg-AD mice, a 55 kDa SDS-resistant form of A $\beta$ , that we assume to be the called A $\beta$ \*56, whose presence was correlated to cognitive deficits [Lesnè S et al., 2006; Cheng IH et al., 2007; Amar F et al., 2017].

We performed Western blotting on hippocampal soluble fractions from treated 3xTg-AD mice and assessed the level of the 55 kDa A $\beta$ . The results in Figure 4.34A-B show that AK7 treatment significantly reduced 55 kDa A $\beta$ , with respect to the vehicle-treated group, while SIRT1 activation with SRT2104 was ineffective on this A $\beta$  aggregate.

Again, in double-treated mice there was a significant reduction of 55 kDa A $\beta$  (Fig. 4.34C), reflecting the result obtained with single modulations.



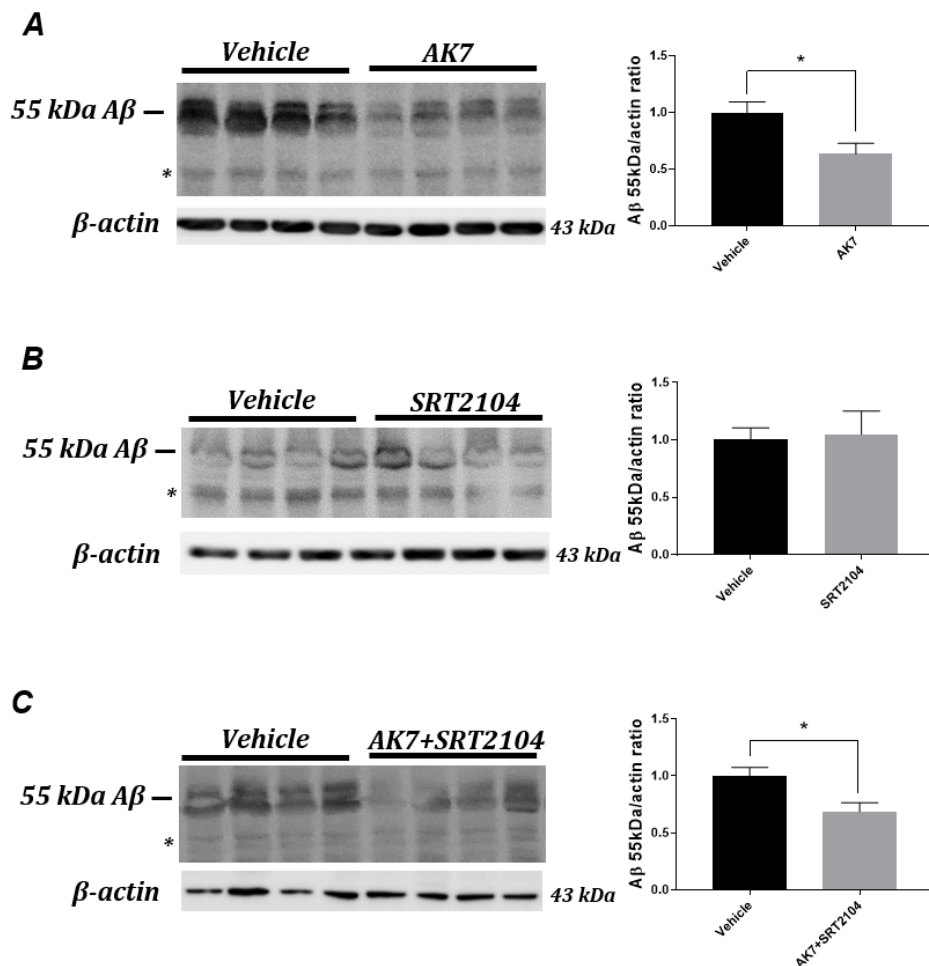


**Figure 4.34** Representative Western blotting analysis on 55 kDa A $\beta$  aggregates, assessed with 6E10 antibody in the hippocampus of 3xTg-AD mice treated with AK7 (A), SRT2104 (B) or the combination of the two modulators (C). Target proteins were normalized to  $\beta$ -actin. The stars point to unspecific bands. Data are presented as Mean $\pm$ SEM (n=8; Student's *t* test, \**p*<0.05; Vehicle vs AK7 *p*=0.0186, Vehicle vs AK7+SRT2104 *p*=0.0113).

This result could support the hypothesis that AK7 exerts its effect on A $\beta$  aggregation, reducing oligomers fraction and contributing to cognitive recovery.

At this point, we decided to move beyond the investigation of APP metabolism and shift our attention to other relevant pathways of AD neuropathology, such as neuroinflammation, oxidative stress and synaptic physiology.

First, we evaluated GFAP and CD11b as neuroinflammation markers of astrocytes and microglia, respectively. These two markers were over-

expressed in the hippocampus of 6-months old 3xTg-AD mice, as shown in 4.2.1 section.

Western blotting analysis revealed that both GFAP and CD11b were reduced by SRT2104 treatment (Fig. 4.35A-B), while no significant change was detected in mice treated with AK7 (Fig. 4.35C-D).

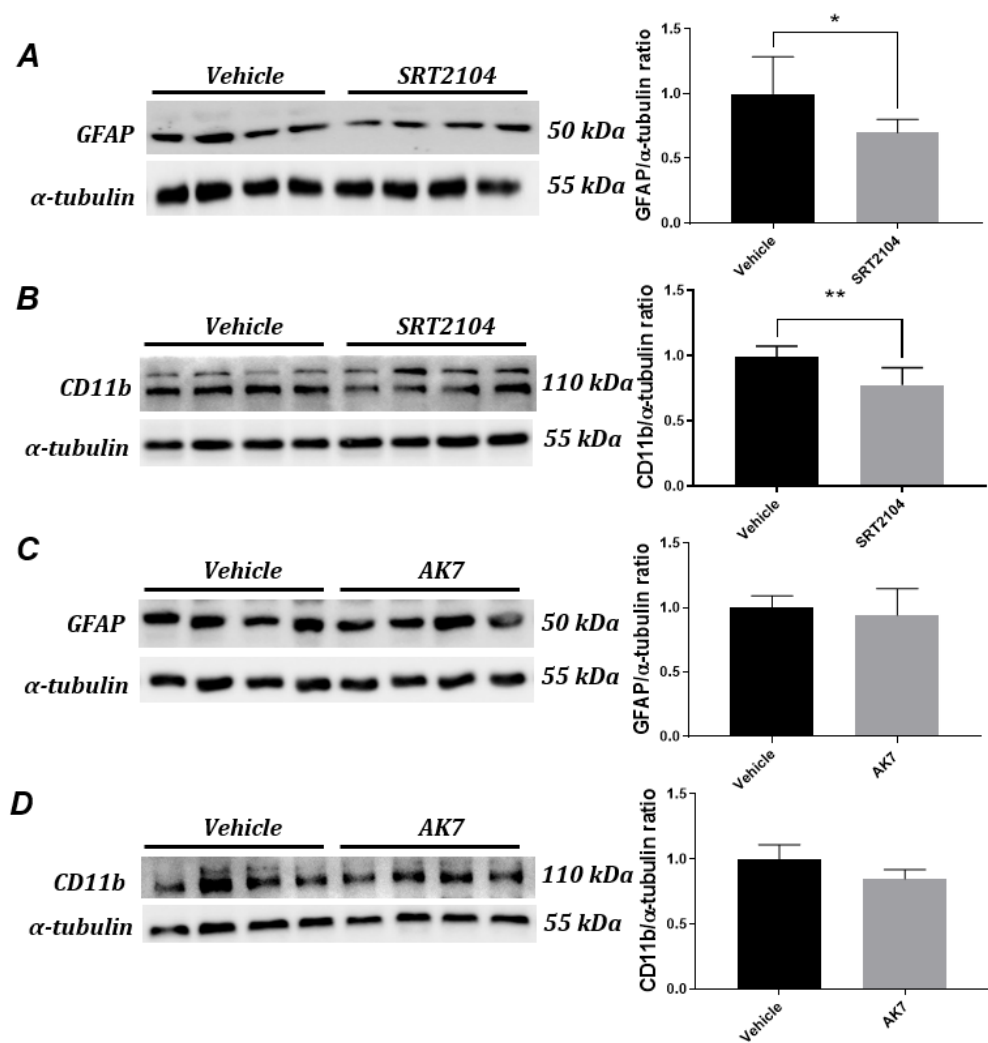


**Figure 4.35** Representative Western blotting analysis on GFAP and CD11b, assessed in the hippocampus of 3xTg-AD mice treated with SRT2104 (A-B), or AK7 (C-D). Target proteins were normalized to  $\alpha$ -tubulin. Data are presented as Mean $\pm$ SEM (n=8; Student's *t* test, \**p*<0.05, \*\**p*<0.01; CD11b Vehicle vs SRT2104 \**p*=0.048, GFAP Vehicle vs SRT2104 \*\**p*=0.0038).

The reduction of neuroinflammation markers was confirmed in double-treated mice, where SRT2104 and AK7 were given together. In fact, both GFAP and CD11b were significantly reduced (Fig. 4.36).

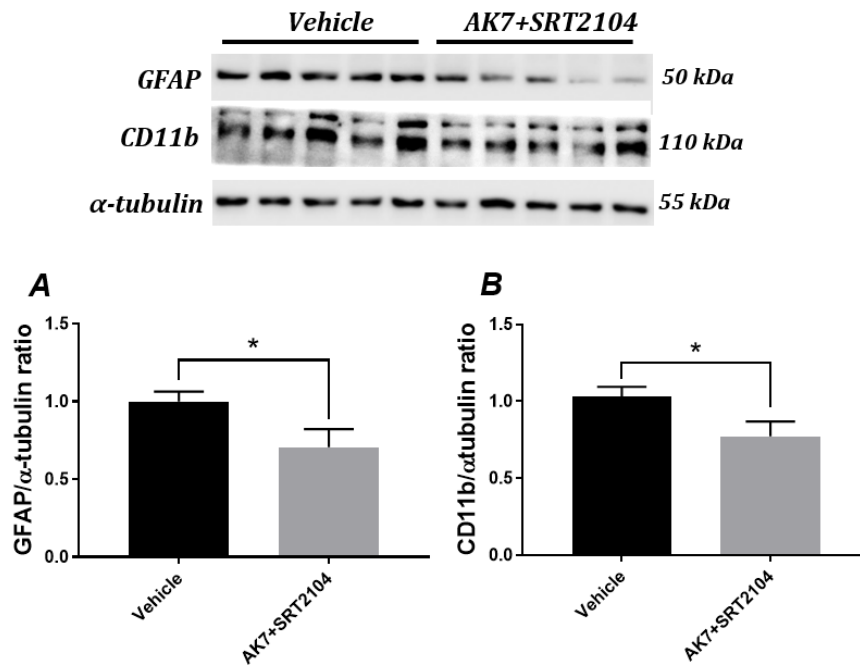


**Figure 4.36** Representative Western blotting analysis on (A) GFAP and (B) CD11b, assessed in the hippocampus of 3xTg-AD mice treated with SRT2104 together with AK7. Target proteins were normalized to α-tubulin. Data are presented as Mean±SEM (n=8; Student's *t* test, \**p*<0.05; GFAP \**p*=0.0343, CD11b *p*=0.042).

As previously shown (Fig. 4.19) Synaptophysin hippocampal level was significantly reduced in 3xTg-AD mice at the age of 6 months. We found that SIRT1 activation with SRT2104 was able to significantly increase Synaptophysin level (Fig. 4.37A), while no effect was seen with SIRT2 inhibition (Fig. 4.37B).

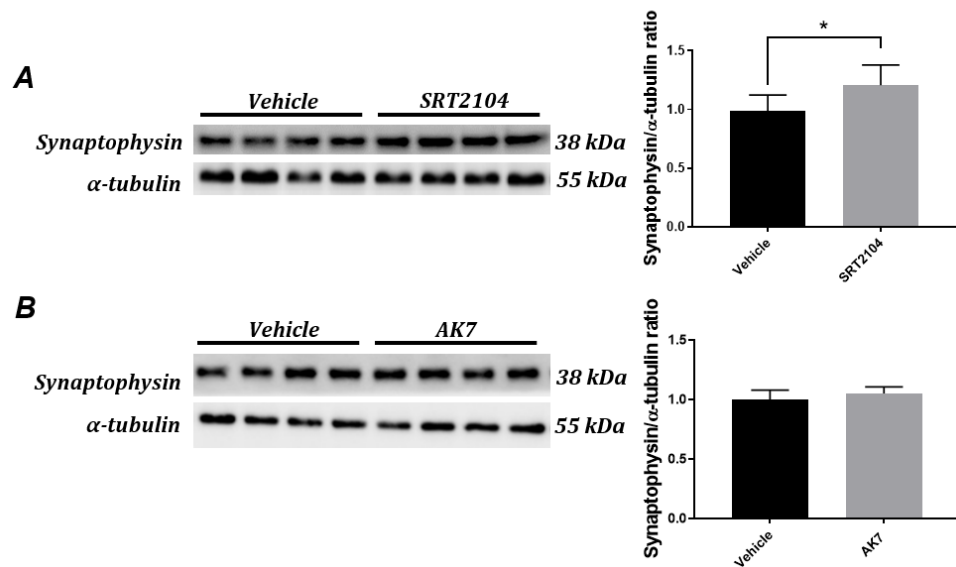


**Figure 4.37** Representative Western blotting analysis on Synaptophysin, assessed in the hippocampus of 3xTg-AD mice treated with SRT2104 (A) or AK7 (B). Target proteins were normalized to  $\alpha$ -tubulin. Data are presented as Mean $\pm$ SEM (n=8; Student's *t* test, \**p*<0.05; Vehicle vs SRT2104 \**p*=0.021).

This positive modulation was confirmed in double-treated mice, where SRT2104 and AK7 were administered together (Fig. 4.38).

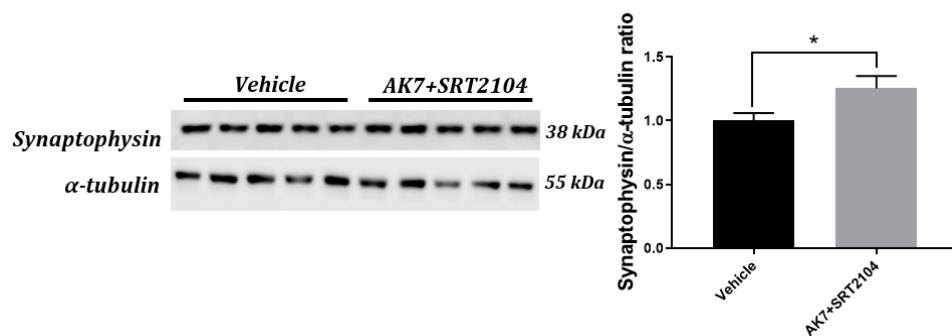


**Figure 4.38** Representative Western blotting analysis on Synaptophysin, assessed in the hippocampus of 3xTg-AD mice treated with SRT2104 together with AK7. Target proteins were normalized to  $\alpha$ -tubulin. Data are presented as Mean $\pm$ SEM (n=8; Student's *t* test, \**p*=0.0363).

A clear connection has been established between APP protein misfolding, aggregation and ROS production [Mondragon-Rodriguez S et al., 2013].

Provided that, we evaluated the hippocampal level of two antioxidant proteins: the transcription factor NRF2, whose levels were slightly reduced in 3xTg-AD mice, and the enzyme SOD1, an important player of the antioxidant machinery that was reported to be connected to NRF2 pathway [Park EI and Rho HM, 2002; Mota SI et al., 2015]. NRF2 defects were also correlated to AD pathology and SIRT1/2 activities [Xue F et al., 2016; Yang X et al., 2017]. Western blotting analysis revealed that SIRT1 activation significantly increased both NRF2 and SOD1 (Fig. 4.39A), while SIRT2 inhibition did not affect the level of the two proteins (Fig. 4.39B).

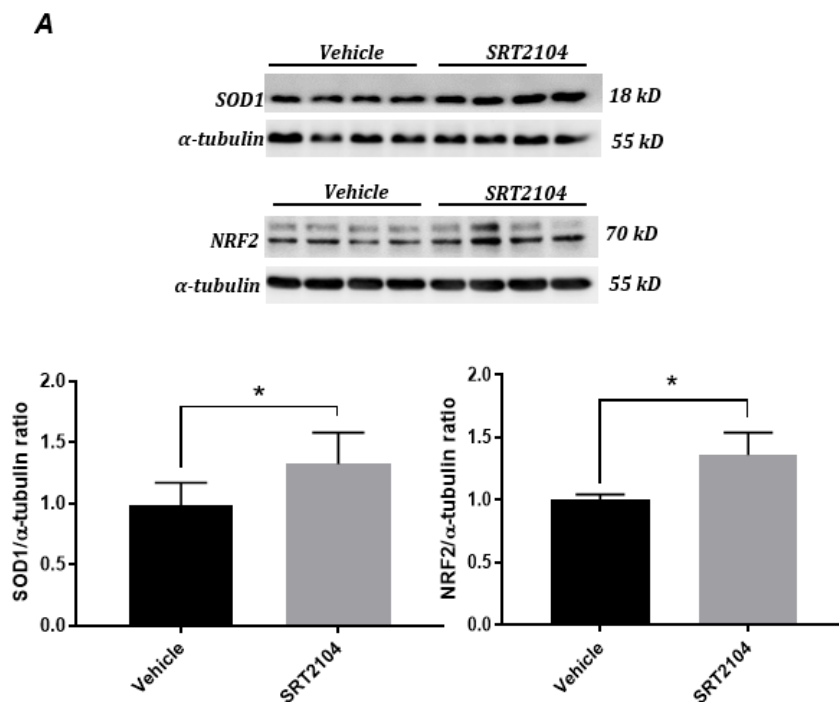


**Figure 4.39A** Representative Western blotting analysis on SOD1 and NRF2, assessed in the hippocampus of 3xTg-AD mice treated with SRT2104. Target proteins were normalized to  $\alpha$ -tubulin. Data are presented as Mean $\pm$ SEM ( $n=8$ ; Student's  $t$  test,  $*p<0.05$ ; SOD1 Vehicle vs SRT2104  $p=0.037$ , NRF2 Vehicle vs SRT2104  $p=0.035$ ).

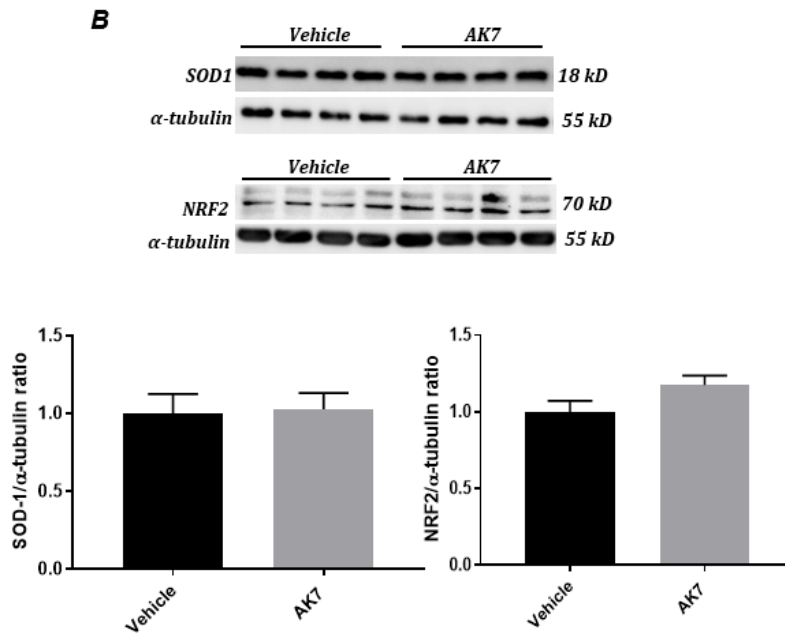


**Figure 4.39B** Representative Western blotting analysis on SOD1 and NRF2, assessed in the hippocampus of 3xTg-AD mice treated with AK7. Target proteins were normalized to  $\alpha$ -tubulin. Data are presented as Mean $\pm$ SEM ( $n=8$ ; Student's  $t$  test,  $*p<0.05$ ; NRF2 Vehicle vs AK7  $p=0.056$ ).

The combined treatment with SRT2104 and AK7 confirmed a significant increase of both hippocampal SOD1 and NRF2 (Fig. 4.40).

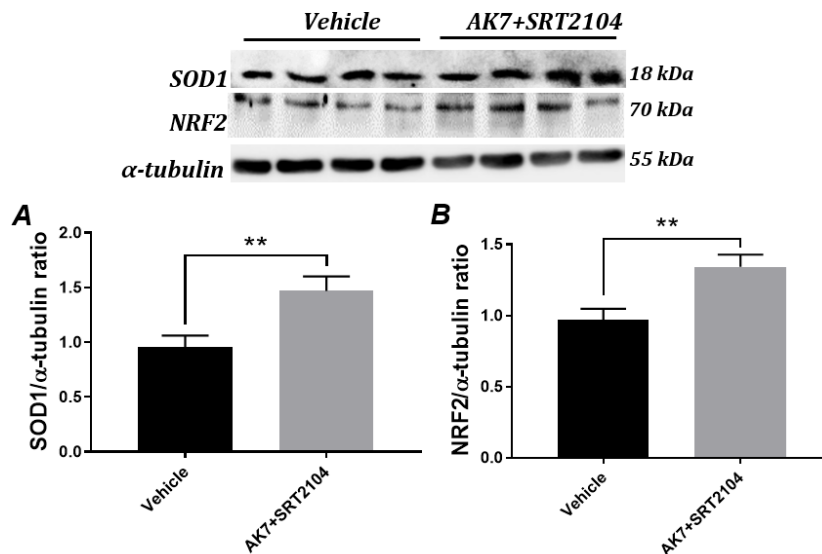


**Figure 4.40** Representative Western blotting analysis of (A) SOD1 and (B) NRF2, assessed in the hippocampus of 3xTg-AD mice treated with SRT2104 together with AK7. Target proteins were normalized to  $\alpha$ -tubulin. Data are presented as Mean $\pm$ SEM ( $n=8$ ; Student's  $t$  test,  $**p<0.01$ ; SOD1 Vehicle vs AK7+SRT2104  $p=0.0072$ , NRF2 Vehicle vs AK7+SRT2104  $p=0.0051$ ).

### ***In vivo* results: general conclusions**

Overall, *in vivo* results are supportive of our hypothesis about the beneficial effect of SIRT1/2 modulation both at cognitive and biochemical level. NORT behavioural assay resulted in a recovery of the cognitive impairment measured on 3xTg-AD mice through the visual recognition task. All treatments led to improved cognitive performance, and biochemical results defined the contribution of each of the two modulations to the effects on different molecular targets. While both SIRT1 activation and SIRT2 inhibition seem involved in the increase of sAPP $\alpha$ , as already demonstrated in cellular experiments, SIRT1 activation could be more active on antioxidative response stimulation, synaptic density and neuroinflammation, while SIRT2 inhibition could affect mostly



amyloid-related parameters with milder effect on other pathways, at least in these experimental conditions. The use of the combined treatment could not only ensure cognitive recovery, but also integrate some disease-modifying molecular effects that are dependent by the single modulations and could influence each other's. A direct comparison between the single and the double treatments is mandatory to evaluate whether the extent of the cognitive and biochemical effect could be synergic or not, in parallel with a more complete drawing of the cognitive picture, measurable through multiple memory tasks and multiple time-points of testing.

**5. Results: *in vitro* set-up of a hydrogel-based controlled release system for SIRTs modulators**

## Introduction

Although SIRT2 modulators, including those used in this work, have interesting pharmacological properties in AD models, there are limits to their administration in complex systems, including *in vivo* models of pathology. These limits are mainly the inability to pass through the BBB by passive diffusion or their rapid clearance, or even both. For these reasons, we considered the characterization of a hydrogel matrix loaded with SIRT2 modulators, in search of a controlled release delivery system of these neuroactive molecules. For this preliminary study, we considered the SIRT2 inhibitor AK7 because it possesses one of the aforementioned limitations. Despite the brain permeability and SIRT2 selectivity, AK7 has a short half-life (2 h) and  $IC_{50}$  of 15.5  $\mu$ M that makes it moderately potent. Thus, it could be considered for a controlled release from the periphery to the CNS using the hydrogel, avoiding repeated administrations, but also a direct CNS prolonged administration to minimize periphery loss [Li J and Mooney DJ, 2016]. In parallel with AK7, we decided to include in the analysis another well documented SIRT2 inhibitor, called AGK2, that we used in previous work [Villalba JM and Alcaín FJ, 2012; Biella G et al., 2016]. This choice was supported by the fact that AK7 showed some paradoxical results during *in vitro* experiments on A $\beta$ 42 that cannot completely exclude a potential side effect. In addition, AGK2 has an  $IC_{50}$  of 3.5  $\mu$ M, thus suggesting better potency. As a limit, AGK2 is not brain-permeable, which makes it a good candidate for a controlled-release system directly in the target site (CNS).

A controlled release of SIRT1 activator was evaluated too, using SRT1720 as candidate instead of SRT2104, both because of its higher potency ( $EC_{50}$

ranging in nM interval respect to EC<sub>50</sub> in μM range for SRT2104) and its inability to cross the blood-brain barrier, supporting the use of the hydrogel for controlled CNS release.

For controlled release, fundamental characteristics of the selected polymeric system are injectability, biocompatibility and biodegradability.

Injectable hydrogels are excellent vehicles for the specific site release of drugs (drug delivery) in the CNS as they can be implanted with minimally invasive techniques. In fact, these materials can be injected in liquid form and gelate in situ. Biocompatibility avoids post implantation inflammatory reactions, while biodegradability, finally, makes it possible to eliminate it from the organism without requiring additional surgical intervention [**Pakulska MM et al., 2012**].

These preliminary tests will allow having an idea about the potentiality of using hydrogel-based systems for the administration of SIRTs modulators with pharmacokinetic and chemical characteristics varying case by case.

### **Specific aims**

In this part of the work, a hydrogel matrix was selected basing on the *in vivo* biocompatibility and SIRTs modulators capability to gelate inside the formulation.

Next, a SIRT1 activator and a SIRT2 inhibitor were analysed by spectrophotometric technique to obtain a maximum absorbance peak ( $\lambda_{\text{max}}$ ), and their release kinetic from the hydrogel matrix was assessed.

## 5.1 Hydrogel *in vivo* biocompatibility and matrix selection

To test the potential release system for SIRTs modulators, we initially considered two different semi-synthetic semi-IPN hydrogels, and tested their inflammatory potential after peripheral implantation in the air-pouch model described in Materials and Methods section 3.4.1:

1) Collagen 1.2 mg/mL + Low Molecular Weight Hyaluronic Acid (LMWHA) 2.5 mg/mL (pH 7.0)

2) Collagen 1.8 mg/mL + PEG2000 0.6 mg/mL (pH 7.0)

After the injection of LPS, saline or the two biomaterials in the air pouch, the exudates were collected, and inflammatory cells were counted. The count revealed that neither of the two hydrogels produced a significant inflammatory reaction at the site of injection, suggesting that *in vivo* implantation of these biomaterials could be safe (Fig. 5.1).

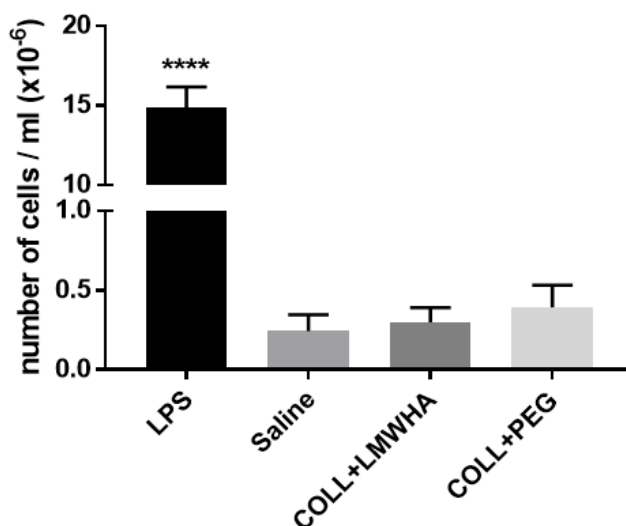


**Figure 5.1** Cell count in the exudates collected from air pouches containing LPS, saline, COLL+LMWHA hydrogel, and COLL+PEG hydrogel. Data are presented as Mean±SEM (n=5, One-way ANOVA and Tukey's post hoc test; \*\*\*\*p<0.0001).

Of the two available hydrogels, we chose the COLL+PEG2000 formulation. In fact, in a preliminary test SRT1720, AK7 and AGK2 compounds were loaded into both hydrogels, but the COLL+HA hydrogel was not able to gelate after 1 hour incubation. We hypothesized that the cause could be an interference of DMSO with the hydrogel components. On the other hand, COLL+PEG2000 biomaterial easily gelled after loading and incubation with all modulators.

## 5.2 Spectrophotometric analysis of SIRTs modulators

Known concentrations of SRT1720, AGK2 and AK7 were analysed by an explorative assay ( $\lambda$  range = 209.6-800 nm) with an UV-Vis spectrophotometer, looking for an absorbance peak of the molecule.

The manufacturer indicated the absorbance peak of SRT1720, and we confirmed this parameter, detecting a maximum absorbance peak at 244 nm ( $\lambda_{\text{max}}$ ) (Fig. 5.2).

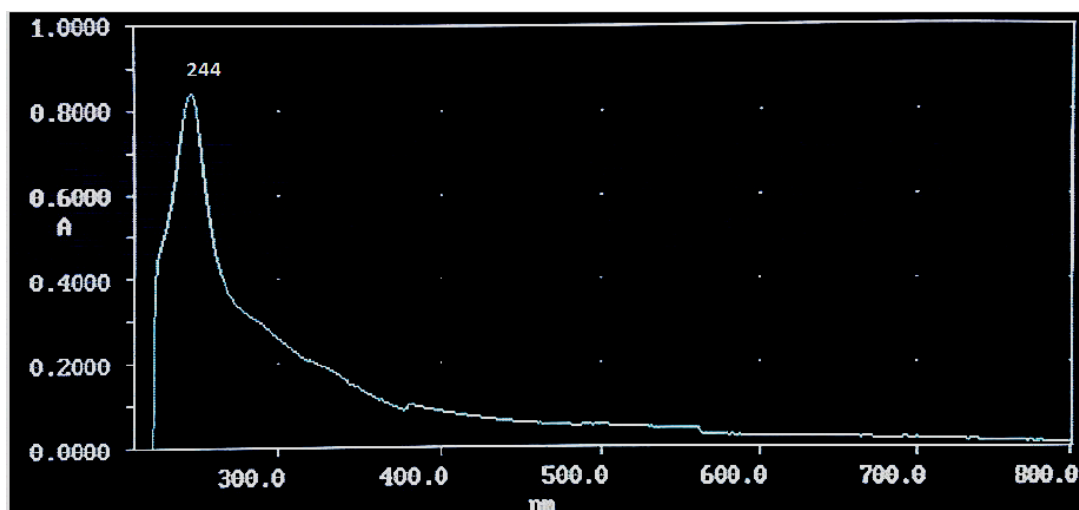


**Figure 5.2** Spectrophotometric analysis of a 25  $\mu\text{M}$  solution of SRT1720 in PBS 1X vs blank (PBS 1X with DMSO in equivalent volume). The maximum absorbance peak at 244 nm is  $A \approx 0,820$ .

The  $\lambda_{\text{max}}$  of AGK2 was unknown, so two different concentrations of the modulator were prepared from DMSO stock solutions. Dilutions in PBS 1X or H<sub>2</sub>O were prepared in ratios that not affect solubility in an aqueous solvent, which is essential for spectrophotometric analysis.

Two peaks were detected, at 233 nm and 359 nm (Fig. 5.3).

The  $\lambda_{\text{max}}=359$  nm was selected for AGK2 quantification analysis, and PBS 1X was chosen as supernatant as the peak intensity (pink and green lines) was higher than that obtained with H<sub>2</sub>O (blue and yellow lines). The peak intensity was also proportional to the concentration of the modulator.

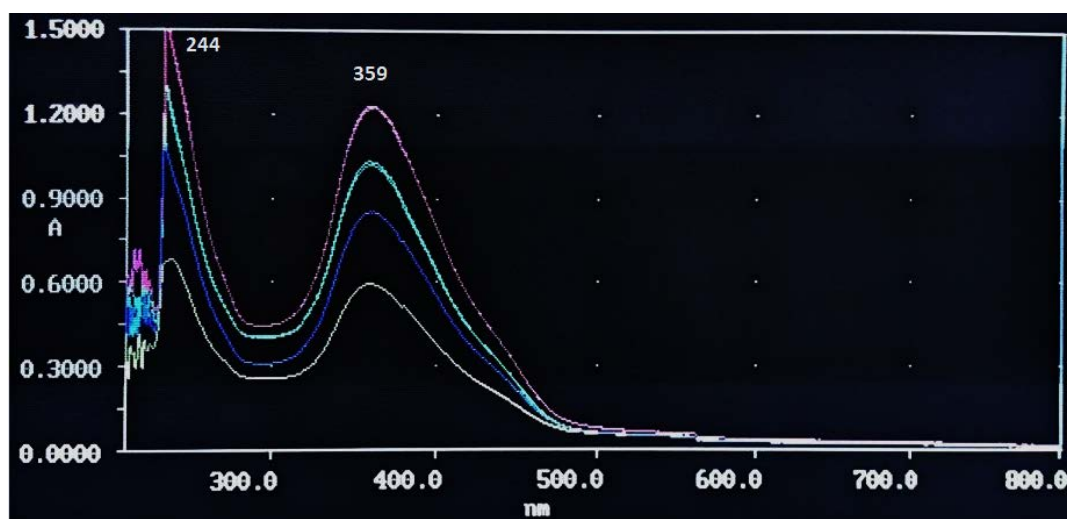


**Figure 5.3** Spectrophotometric analysis of 100  $\mu\text{M}$  AGK2 in PBS 1X (pink) and in H<sub>2</sub>O (green) or 75  $\mu\text{M}$  AGK2 in PBS 1X (blue) and in H<sub>2</sub>O (yellow) vs blank (PBS 1X and H<sub>2</sub>O with DMSO in equivalent volume). The maximum absorbance peak at 359 nm for PBS 1X solutions is  $A \approx 1.210$  for 100  $\mu\text{M}$  AGK2 and  $A \approx 0.880$  for 75  $\mu\text{M}$  AGK2.

The same spectrophotometer scan was performed with AK7, as no information was available regarding the presence of a chromophore in its chemical structure. Unfortunately, no peak was detectable for this molecule, suggesting that AK7 need another type of analytical technique for quantification (Fig. 5.4).

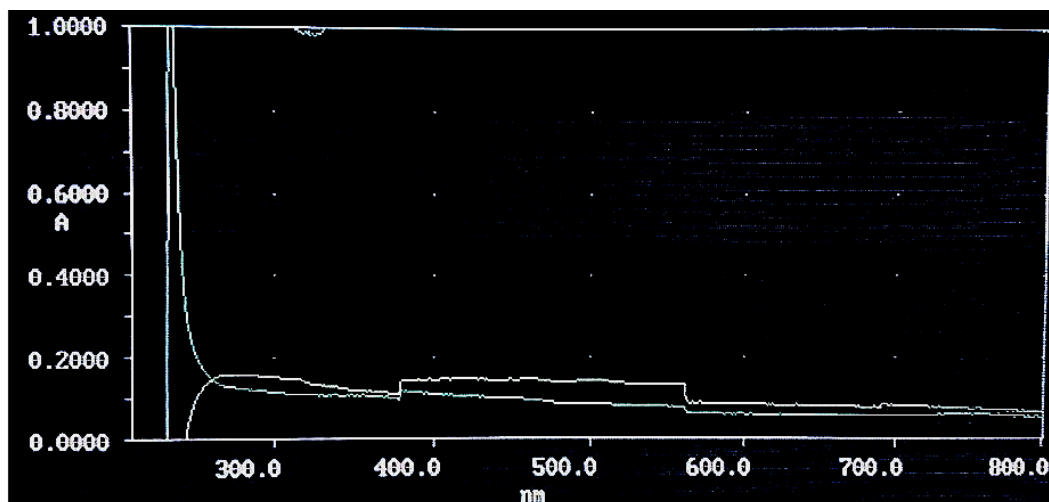


**Figure 5.4** Spectrophotometric analysis of 40  $\mu$ M AK7 in PBS 1X vs blank (PBS 1X with DMSO in equivalent volume). No peak was detectable, using both a quartz (yellow) or a plastic (green) cuvette.

The hydrogelic matrix where SIRT's modulator are to be loaded is biodegradable, and for this reason, any interference in spectrophotometric readings due to gel components leakage was investigated.

The analysis of supernatants from unloaded COLL+PEG2000 hydrogels, after 24 - 48 - 72 hours of incubation, revealed no peaks at the  $\lambda_{\text{max}}$  of SRT1720 and AGK2 (Fig. 5.5).



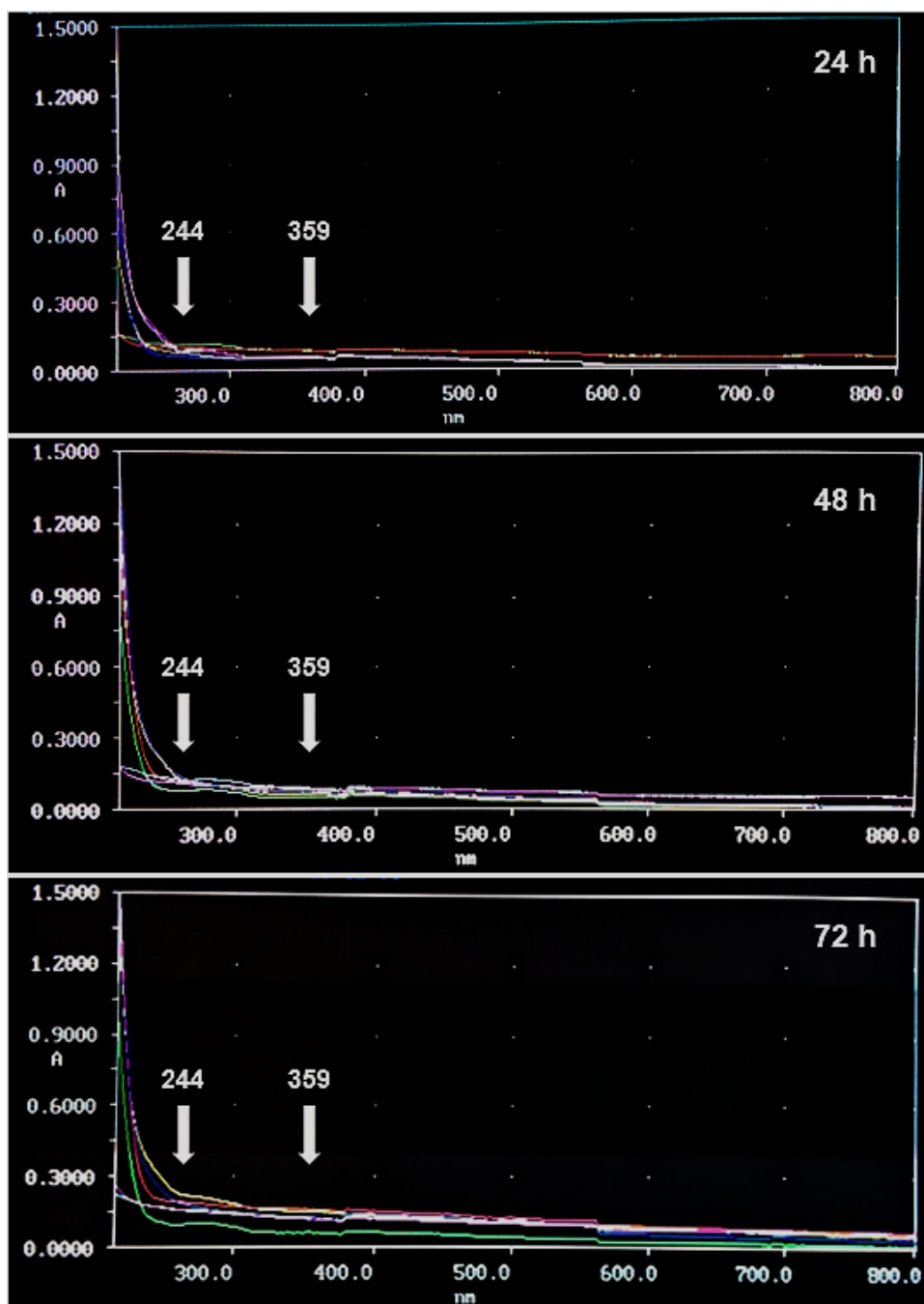


**Figure 5.5** Spectrophotometric analysis of unloaded hydrogel supernatants collected at 24, 48 and 72 hours. No peak was detectable at the absorbance wavelength of AGK2 and SRT1720 (359 nm and 244 nm, respectively).

After the determination of the  $\lambda_{\text{max}}$  for AGK2 and SRT1720, we verified the linear correlation between their concentration and the absorbance.

We obtained two calibration curves (Fig. 5.6) to use in the release kinetic study to extrapolate the unknown concentrations of modulators released at increasing time points.

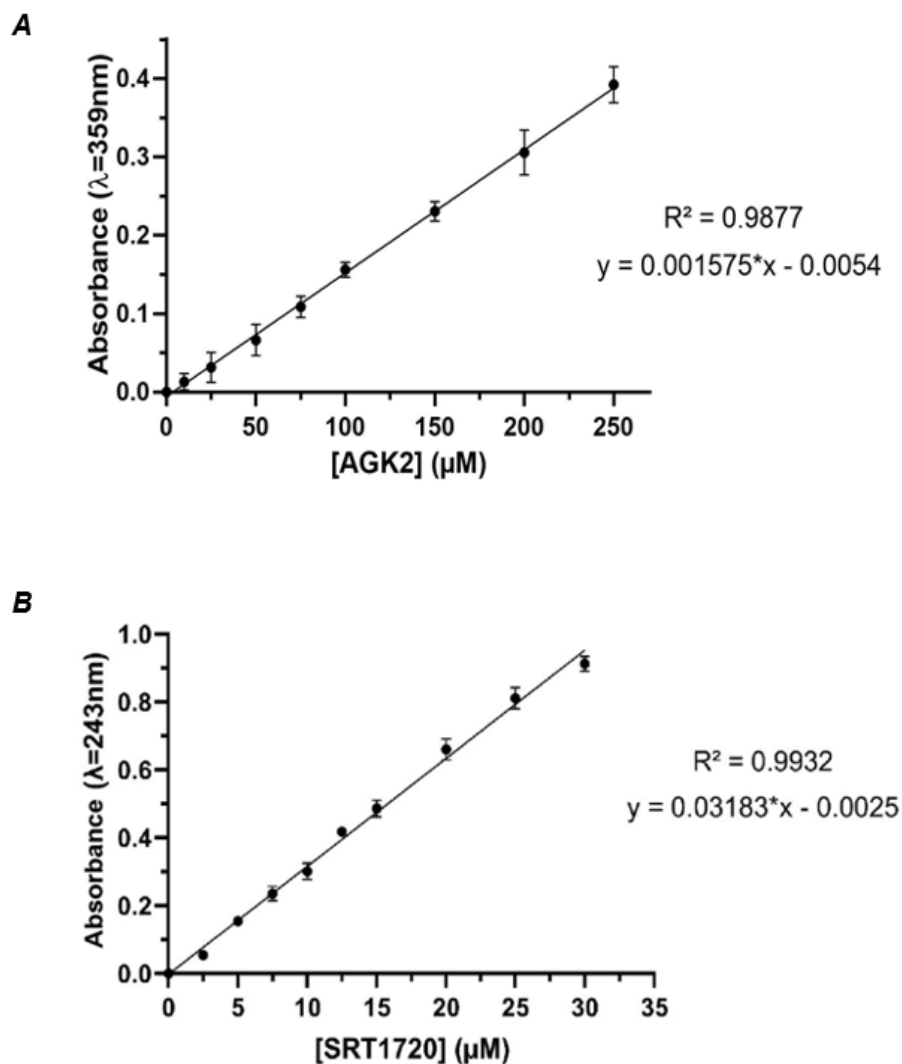


**Figure 5.6** Concentration-absorbance correlation for (A) AGK2 and (B) SRT1720, assessed by spectrophotometric analysis at the absorbance  $\lambda_{\text{max}}$  (Linear regression;  $n=3$  for each point).

### 5.3 Release kinetic study

As described in Materials and Methods section 3.4.4, the supernatants from AGK2- and SRT1720-loaded hydrogels were collected at different time points and analysed to determine the concentration of the released SIRT's modulator.

- **SRT1720**

30, 60 and 90  $\mu\text{M}$  SRT1720, corresponding to 15-30-45 nmol, were loaded in the hydrogel of COLL 1.6 mg / mL + PEG2000 0.6 mg / mL. After each time point, the supernatant was replaced with fresh PBS 1X and the amount of released modulator was calculated by adding the amounts acquired from the supernatants taken from previous time points.

SRT1720 was released at decreasing rate with time (Fig. 5.7). Moreover, there was a correlation between the modulator's released nanomoles and the initial load (15-30-45 nmol). Independently from the starting hydrogel loading, the % of released modulator over time was the same. After 168 h from hydrogel loading, the % of released SRT1720 was  $92.8\% \pm 5.2\%$  of total loading (Fig. 5.8).

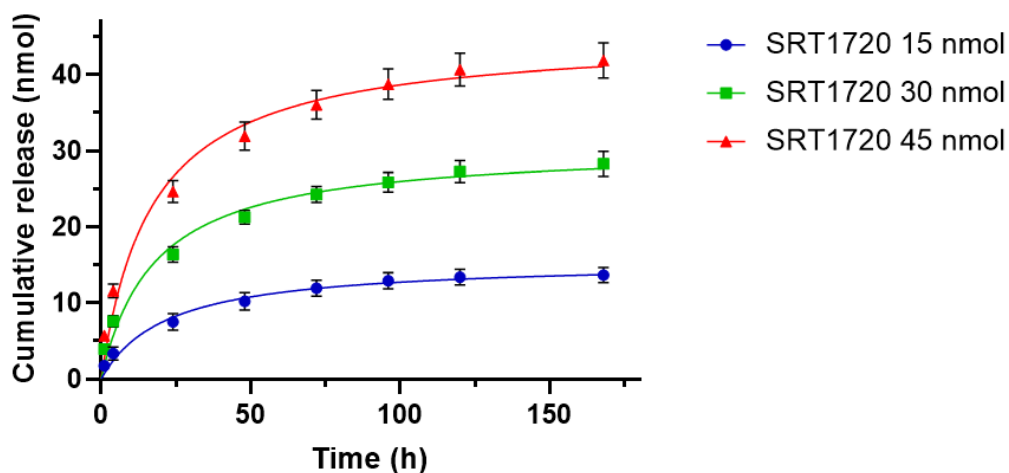


**Figure 5.7** Spectrophotometric analysis of supernatants collected from hydrogels loaded with 15 (blue), 30 (green), 45 (red) nmol SRT1720. The graph represents the released nmol over time (0-168 hours). (Nonlinear regression, curve fit;  $n=4$ ).

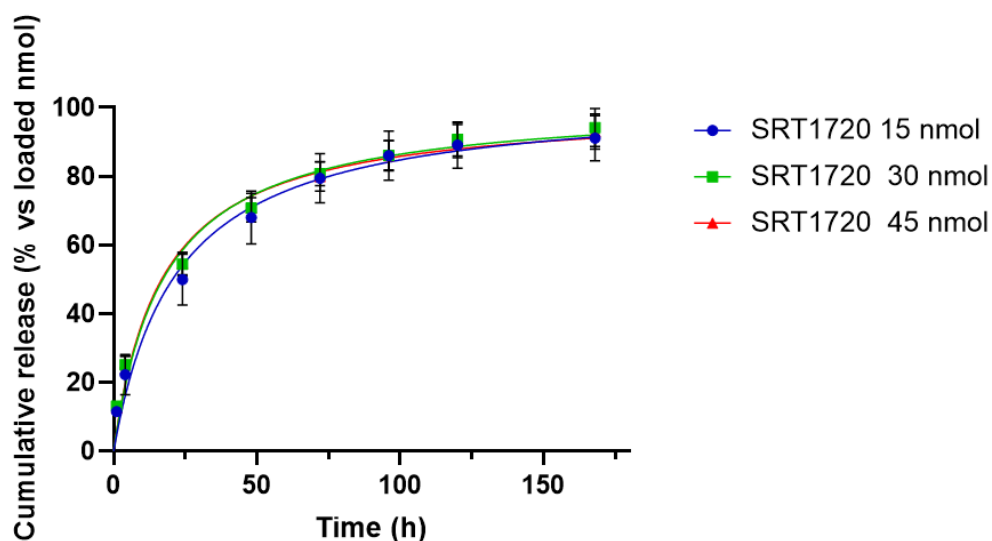


**Figure 5.8** Spectrophotometric analysis of supernatants collected from hydrogels loaded with 15 (blue), 30 (green), 45 (red) nmol SRT1720. The graph represents the % SRT1720 released by the hydrogel over time, with respect to the total loading. (Nonlinear regression, curve fit;  $n=4$ ).

The release mechanism of SRT1720 was then studied taking in consideration four different kinetic models: zero order, first order, Korsmeyer-Peppas and

quadratic. The rate constants ( $k$ ) and the determination coefficients ( $R^2$ ) were obtained through linear regression (best fitting).

The zero order and the first order models produced  $R^2$  values of 0.768 and 0.81, respectively.

The best correlation values (best fitting) were obtained with the quadratic kinetic model ( $R^2 = 0.925$ ) and with the Korsmeyer-Peppas model ( $R^2 = 0.976$ ), suggesting an active release mechanism from the hydrogelic matrix controlled by diffusion and little influenced by matrix swelling (Fig. 5.9).

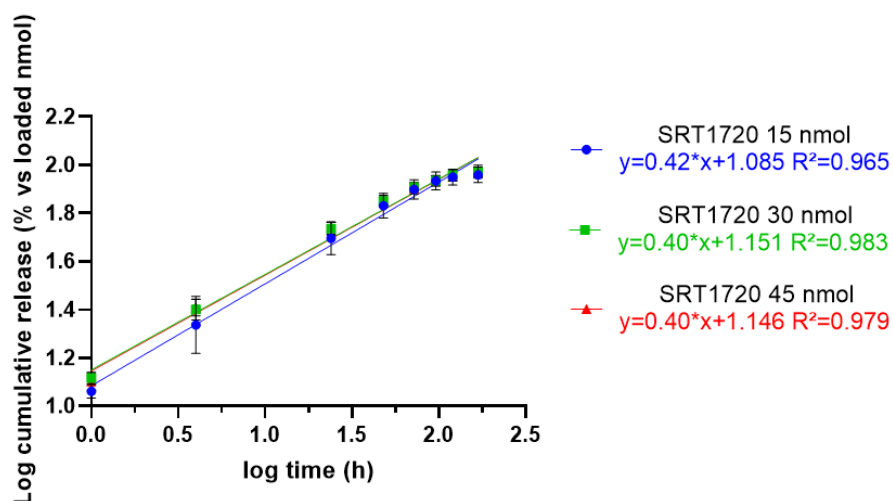


**Figure 5.9** Korsmeyer-Peppas model: logarithmic transformation of SRT1720 cumulative release (Linear Regression;  $n=4$ ).

A summary of data elaboration is presented in the table below (Table 5.1).

Time point (h)	Cumulative Absorbance			SRT1720 ( $\mu\text{M}$ ) in supernatant			% release vs loading ( $\mu\text{M}$ )	SRT1720 (nmol) in supernatant			Mean % release vs loading (nmol)
1	0.07	0.16	0.24	2.3	5.2	7.6	8.3	1.7	3.9	5.7	12.4
4	0.14	0.32	0.49	4.5	10.1	15.4	16.3	3.3	7.6	11.6	24.4
24	0.32	0.69	1.04	10.0	21.8	32.8	35.4	7.5	16.3	24.6	53.0
48	0.43	0.90	1.35	13.6	28.3	42.5	46.6	10.2	21.2	31.9	69.9
72	0.50	1.03	1.53	15.9	32.3	48.0	53.4	11.9	24.2	36.0	80.1
96	0.55	1.09	1.64	17.2	34.4	51.6	57.4	12.9	25.8	38.7	86.1
120	0.57	1.15	1.72	17.8	36.3	54.2	60.1	13.4	27.2	40.6	90.1
168	0.58	1.20	1.77	18.2	37.7	55.8	61.9	13.7	28.3	41.9	92.8

- SRT1720 30  $\mu\text{M}$  – 15 nmol
- SRT1720 60  $\mu\text{M}$  – 30 nmol
- SRT1720 90  $\mu\text{M}$  – 45 nmol

**Table 5.1** Mathematical elaboration of recorded cumulative absorbance values. For each time point, mean values are reported in the table. % data are reported as the mean value of all the considered loading concentrations.

In summary, these experiments have shown that the controlled release of the SIRT1 activator SRT1720 by a biocompatible collagen-based hydrogel is feasible.

#### • AGK2

AGK2 was loaded into the hydrogel of COLL 1.6 mg/mL + PEG2000 0.6 mg/mL in three concentrations: 300-600-900  $\mu\text{M}$ , corresponding to 150-300-450  $\mu\text{mol}$  of modulator.

As in the case of SRT1720, the aim was to avoid obtaining a release not detectable by spectrophotometry.

Unfortunately, the absorbance values recorded at each load concentration examined were close to zero (Fig. 5.10).

The result suggests that the molecule is not released from the matrix, and the reasons need further investigation. A hypothesis could be the presence of a sufficiently strong, maybe covalent, interaction between the molecule and the matrix components.

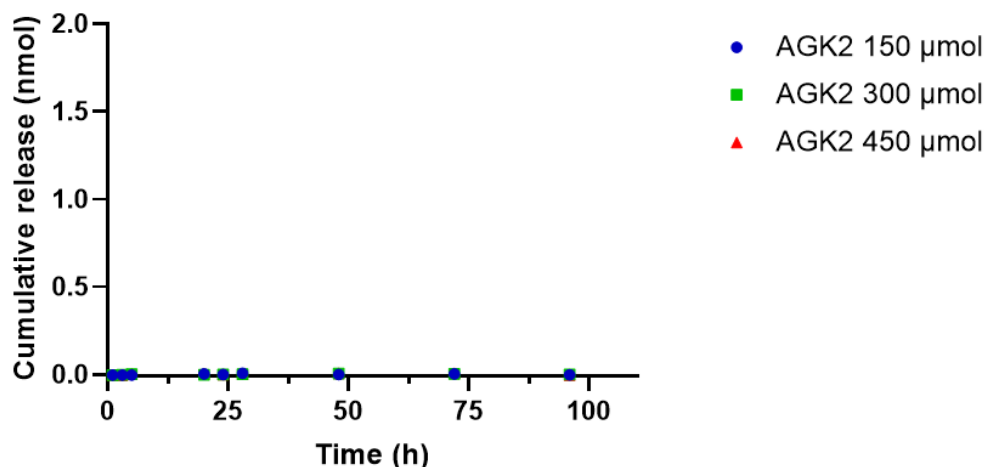


**Figure 5.10** Spectrophotometric analysis of supernatants collected from hydrogels loaded with 150 (blue), 300 (green), 450 (red)  $\mu\text{mol}$  AGK2. ( $n=4$ ).

## General conclusions

The data presented in this last section are still preliminary, but supported the idea of the potential usefulness of hydrogels as DDS for SIRT's modulators, in accordance with available literature. Our results showed *in vivo* biocompatibility of a Type I collagen/PEG2000 semi-interpenetrated hydrogel, and its potential application to the characterization of SIRT's modulators controlled-release, based on the assumption that some of those compounds possess pharmacokinetic issues that require non-conventional administrations. Unfortunately, the optimization of such complex systems needs deep study, as only one of the chosen compounds, the SIRT1 activator

SRT1720, was suitable for controlled-release detection and analysis in our experimental conditions. This suggests that, despite the potentialities of hydrogel-based DDS, their use for SIRTs modulators loading and release is still far from the application to *in vivo* models and clinic, and needs further investigation.



## **6. Discussion and conclusions**

AD is a frequent neurodegenerative pathology affecting the central nervous system, characterized by deterioration of memory and other cognitive processes. AD generally occurs in the elderly population, as its incidence doubles every 5 years after 65 years of age. This disease finds its pathophysiological basis in the progressive loss of some specific neuronal populations, which then causes typical symptoms such as memory impairment, linguistic and motor disorders, and behavioural changes [**Herman L et al., 2017; Tree J et al., 2015**].

AD still lacks a precise pathogenic mechanism, and for most of the past years research has been based on the concept of ACH. This hypothesis focuses on the pivotal role of A $\beta$ 42 production and aggregation in determining senile plaques formation, causing neuronal damage, tau neurofibrillary tangles accumulation and finally, neuronal death and synaptic loss [**Hardy JA et al., 1992**].

Although there are approved pharmacological treatments able to alleviate AD symptoms, there is an urgent need to improve the understanding of its pathogenesis to allow the development of therapies capable of modifying the course of the disease. In fact, no drug for the symptomatic treatment of AD has been approved by FDA since 2003, and compounds proposed as "disease-modifying drugs" are still in the clinical phase with no certainty of their actual effectiveness, a fundamental aspect given the amount of failures obtained over the years [**Small GW, et al., 2015**].

Of relevance, several preclinical and clinical trials are progressing but with no success as "one-molecule-one-target" single therapies. Most of the AD drugs that failed have been developed against amyloid pathology, but it is now well

established that AD is more than an amyloid-centred pathology. In fact, it can be defined as a complex, multifactorial disease, in which several other pathologic processes are involved, and most of them still need to be identified. The major etiologic features leading to neuronal death can be summarised in four groups **[Weinstein JD, 2018]**:

- Mitochondrial dysfunction that is linked to energetic metabolism impairment, ROS production and cerebrovascular hypoperfusion.
- Abnormal protein deposits: in addition to A $\beta$  protein, whose oligomeric aggregates are the most toxic species for neurons, some other proteins with amyloidogenic behaviour have been proposed in AD context (e.g. tau,  $\alpha$ -synuclein, TDP43).
- Oxidative stress, where ROS are not neutralized and the oxidation-defence mechanisms are impaired.
- Neuroinflammation, where overactivation of astrocytes and microglia leads to destructive inflammatory processes in a vicious cycle.

In a context of such complexity, the research for an effective therapy for AD is increasingly moving to support the concept of both multi-targeted and combination therapies. While the former requires the development of a new drug or the implementation of an existing chemical entity able to affect different targets of the pathology, the latter takes advantage of existing molecules that can work in combination, giving synergistic, additive or complementary effects on pathologic or neuroprotective mechanisms.

SIRT6 is a rational target for AD combined therapy. In fact, they have been studied as therapeutic targets for neurodegenerative diseases, with many positive results but no strong indication supporting clinical trials. Drug

development of molecules able to modulate SIRT's activity delivered several data about their involvement in neurodegenerative pathologies, including AD. The SIRT's protein family is composed of seven mammalian members (SIRT1-SIRT7), NAD-dependent enzymes with deacetylase activity and a fundamental role in gene expression regulation, cellular homeostasis, energetic metabolism, inflammation and senescence **[Wątroba M et al., 2017]**.

The interest in SIRT's is due to their involvement in molecular neurodegenerative processes. In fact, in the ageing population, metabolic impairment and epigenetic deregulation increase, and can influence the initiation or progression of neurodegeneration **[Silberman DM, 2018]**.

SIRT1 and SIRT2 are the most interesting targets in this context, as they seem to possess opposite roles, neuroprotective for SIRT1 and neurodegenerative for SIRT2 **[Donmez G and Outeiro TF, 2013]**.

SIRT1 over-expression or pharmacological activation with RSV resulted in reduced AD pathology, A $\beta$ -induced cell death and cognitive impairment improvement in a mouse model **[Imai S and Guarente L, 2010; Porquet D et al., 2014]**. In addition, other studies demonstrated that SIRT1 activation via treadmill exercise and via CR favoured APP non-amyloidogenic pathway and reduced A $\beta$  production **[Koo JH et al., 2017; Wang J et al., 2010]**, and RSV treatment reduced reactive gliosis and pro-inflammatory mediators *in vitro* **[Scuderi C et al., 2014]**. By acting on PGC-1 $\alpha$  and NF- $\kappa$ B, SIRT1 also promotes mitochondrial biogenesis and prevents mitochondrial dysfunction in AD **[Donmez G, 2012; Gan L and Mucke L., 2008]**. Moreover, SIRT1 overexpression acted also on tau pathology promoting its degradation and reducing the spread of tau-induced pathology *in vivo* **[Min SW et al., 2018]**.

Some studies suggested that, possibly via NF- $\kappa$ B inhibition and activation of the retinoic acid receptors, SIRT1 could shift the balance between alpha and beta secretases expression and activity [Tippman F et al., 2009; Gao R et al., 2015; Lee HR et al., 2014].

Some data exist implicating SIRT2 changes in AD, while several data have suggested a neurodegenerative role of SIRT2 in ageing, PD and HD.

SIRT2 high expression level was detected in brain cells of AD patients, and SIRT2 inhibition with the synthetic inhibitor AK1 led to microtubules stabilization, improved autophagy and A $\beta$  oligomers elimination in AD models [Silva DF, et al., 2017]. In addition, the SIRT2 intronic SNP rs10410544 was associated with sporadic AD in two genetic studies [Polito L et al., 2013; Wei W et al., 2014].

SIRT2 specific inhibition with the compound AK7 (a brain-permeable AK1 analogue) resulted in neuroprotective effects both in PD and HD models, preventing  $\alpha$ -synuclein and huntingtin toxicity and aggregation, and improving motor functions [Chen X et al., 2015; Chopra V et al., 2012].

A study from our laboratory demonstrated the efficacy of SIRT2 inhibition with AK7 in two AD mouse models, resulting in improved cognitive function and increased APP non-amyloidogenic processing [Biella G et al., 2016].

Esteves and colleagues reported that  $\alpha$ -tubulin acetylation dependent on SIRT2 inhibition improves microtubules stabilization and increases tau/tubulin binding decreasing tau detachment and aggregation [Esteves AR et al., 2018].

Regarding inflammatory processes, Wang and colleagues demonstrated that SIRT2 is involved in microglial activation, and its inhibition rescued this process acting on NF- $\kappa$ B translocation cytokines levels [Wang B et al., 2016].

On this basis, SIRT1 activation coupled to SIRT2 inhibition could represent a still unexplored potential multi-target approach for AD neuropathology.

The rationale of the work presented in this thesis is to combine SIRT1 and SIRT2 modulations, and better understand SIRT1/2 involvement in AD molecular mechanisms, eventually allowing us to act on different pathologic features dependent on one or both enzymes, under the hypothesis that attacking the pathology at different targets could improve the final neuroprotective effect.

We started implementing this approach with an *in vitro* model, the H4-sw cells. H4-sw are human neuroglioma cells over-expressing the Swedish mutated APP gene (K595N/M596L), which makes these cells an ideal model for high A $\beta$  peptides production and investigation of APP metabolism. We considered also the use of primary neurons from 3xTg-AD mice, but the problem with those primary cultures was that the transgenes are under the control of the Thy1.2 promoter that starts its activity only after postnatal day 6. Given this limitations we chose the H4-sw model for our preliminary analyses. Interestingly, in these cells we observed an increase of SIRT2 basal expression, as depicted by literature, while no SIRT1 reduction was detected. The reason for the absence of SIRT1 reduction could be model-dependent, or could be due to the small sample size taken into consideration. Another

hypothesis could be that SIRT1 expression is not affected by the APP-sw presence but its enzymatic activity instead is. Given this observation, it could be interesting to investigate a link between the APP-sw and imbalanced catalytic activity of SIRT1s.

First, we assessed the feasibility of the double treatment *in vitro*, assessing the potential cytotoxicity, as SIRT1s targets are proteins and transcription factors with an important role in cellular physiology.

The results showed that the single and double treatments were safe for our model, in a range of doses similar to those used in the literature [Nishida K et al., 2018; Minor RK et al., 2011; Chen X et al., 2015; Wang X et al., 2015].

After the optimization of the double treatment protocol, we decided to assess APP, and the effect of our treatment on its processing.

While no effect of both the single and the double treatment was found on total APP production, we detected an increase in the soluble fragments pool, released by cells after APP cleavage. The increase of total sAPP showed no difference between the single and the double modulation. As total sAPP detection is not specific for single APP metabolic pathways, we focused our attention on the non-amyloidogenic one, assessing specifically sAPP $\alpha$  in conditioned media from treated cells.

H4-sw cells showed a significant increase in sAPP $\alpha$  when treated with SIRT1 activator or SIRT2 inhibitor. Moreover, when the two compounds were given in combination, the increase in sAPP $\alpha$  was higher, suggesting a possible synergic effect.

An increase in sAPP $\alpha$  protein is actually considered an important goal for AD treatments, as this fragment shows neuroprotective properties able to

counteract neurodegeneration. It can promote neuronal growth and synaptogenesis, reduce A $\beta$  production, and contrast synaptic loss when directly injected in brains of AD mouse models [Obregon D et al., 2012; Fol R et al., 2016].

A possible link between SIRT1-2 and sAPP $\alpha$  could be the fact that SIRT1 activation or over-expression was already reported to increase APP non-amyloidogenic processing [Koo JH et al., 2017; Qin W et al., 2006], while we previously demonstrated that SIRT2 inhibition led to increased sAPP $\alpha$  *in vivo* [Biella G et al., 2016], with a mechanism that is still unclear.

Some published data demonstrated that sAPP $\alpha$  production is stimulated by low cholesterol or inhibition of cholesterol biosynthesis [Kojro E et al., 2010]. Since Taylor and colleagues reported that SIRT2 inhibition with AK7 was neuroprotective in HD models through reduced cholesterol levels [Taylor DM et al., 2011], an association between cholesterol, SIRT2 and APP processing could be a hypothesis also for AD.

sAPP $\alpha$  increase was persistent after SIRT2 silencing, in agreement with AK7 treatment, confirming that pharmacological SIRT2 inhibition led to specific biological effects.

Another interesting point was that ADAM10 mRNA levels were unaltered by treatment, despite the increase in sAPP $\alpha$  that is the product of its secretase activity. A possible explanation for this result could be an increased activation or membrane trafficking of the secretase, rather than its over-expression. In fact, ADAM10 activity is also regulated by its intracellular trafficking, where the membrane localization is associated with its activation [Marcello E et al., 2013]. Since some evidences point to an involvement of SIRTs in intracellular



trafficking, it could be interesting to undertake further studies on the SIRT1-2 influence on ADAM10 membrane localization [Budayeva HG and Cristea IM, 2016]. Another point could be also the choice of the model of study, that could produce some contradictory results, suggesting the need to move to more reliable models as neuronal cultures.

As for the APP amyloidogenic processing, conditioned media from H4-sw treated cells were analysed for sAPP $\beta$ , A $\beta$ 40 and A $\beta$ 42. At this stage the brain-permeable SRT1720 analogue called SRT2104, selected for subsequent *in vivo* treatments, was assessed in parallel for single and combined treatments. Both sAPP $\beta$  protein and A $\beta$ 40 peptide were significantly reduced by the double treatment condition only, supporting the importance of using both compounds to obtain significant molecular effects on this pathway. This result suggests that the double treatment could act on both APP processing pathways, with a greater weight on the non-amyloidogenic one. This is in accordance with the total sAPP increase measured in the double-treated condition that is not different from the single modulations, maybe because of the compensation between sAPP $\alpha$  increase and sAPP $\beta$  decrease.

A paradoxical result emerged when we found A $\beta$ 42 levels were significantly increased in SIRT2 inhibition condition and double modulation, but not with SIRT1 activation. This result is clearly inconsistent with that obtained on A $\beta$ 40 and sAPP $\beta$ , and we assumed a SIRT2-independent effect of the AK7 compound. This hypothesis was confirmed by comparing A $\beta$ 42 levels after AK7 treatment or after SIRT2 silencing with specific siRNA. The unexpected A $\beta$ 42 increase was evident only after AK7 treatment, while with SIRT2 silencing there was no effect, consistently with A $\beta$ 40 result. We tried to

formulate some hypotheses for this unexpected result. First, it must be taken into account that the characterization and potential clinical use of this molecule is in its infancy, so it is possible that some side or off-target effects could emerge upon its pre-clinical use in disease models. This observation highlights the attention to be paid to a more cautious use of these compounds.

Another interesting hypothesis that we formulated was that AK7 directly interacts with A $\beta$ 42 in cell-conditioned medium. We support the concept that AK7 could act as a disaggregating or anti-aggregating compound on A $\beta$ 42 oligomers, increasing the monomeric fraction that we detect in ELISA assay. Our theory is based on some evidences about the anti-aggregating effect of AK7, its analogue AK1 and other sulfobenzoic acid derivates, on poly-glutamine aggregates [**Chopra V, et al., 2012; Khanfar MA, et al., 2014**].

In addition, AK7 chemical structure has some similarities with compounds screened for their direct A $\beta$ 42 binding capability and anti-aggregating effect. Some of these similarities are the high hydrophobicity, the presence of aromatic groups and the presence of bromine substitution on one aromatic ring [**McKoy AF et al., 2014**]. Another point to be addressed is the discrepancy between A $\beta$ 40 and A $\beta$ 42 results. Since the two peptides have very different kinetic and propensity to aggregation [**Qiu T et al., 2015; Zheng W et al., 2017**], it is reasonable to expect that a disaggregating effect in the short time-frame of our cell model will occur preferentially on A $\beta$ 42 rather than on A $\beta$ 40. The perspective of an anti-aggregating effect, not attributable to the inhibition of SIRT2, could constitute an additional property of the molecule on an important target of the pathology. In fact, numerous efforts are underway to counteract the aggregation of toxic proteins in AD, since they seem directly

responsible for the major neuropathological damaging effects [Verma M et al., 2015; Brito-Moreira J et al., 2017].

However, as mentioned previously, it is possible that the AK7 effect is simply model or assay-dependent, or even a side effect making this drug not safe, and specific analyses will be required to verify and confirm our hypothesis on its anti-aggregating properties. Some of those analyses could for example include an aggregation kinetic study of A $\beta$ 42 oligomers in the presence of AK7, or the measurement of other peptides downstream of the amyloidogenic processing, as C99 fragment, whose level should be unchanged if the antiaggregating hypothesis is supported.

Overall, the *in vitro* data suggest that contemporary SIRT1 and SIRT2 modulation is compatible with cellular viability and is effective in modulating APP metabolism improving the neuroprotective pathway through sAPP $\alpha$  increase and sAPP $\beta$  decrease, thus stimulating further analyses using this combined strategy.

Taking advantage of the *in vitro* evidence, and to better explore the relevance of the combined SIRT1 activation and SIRT2 inhibition as multi-target approach, we moved to an *in vivo* mouse model of AD, the 3xTg-AD [Oddo S et al., 2003]. We decided to select mice at 6-7 months of age to mimic an early disease stage and approximate a clinical situation where patients are diagnosed for the first time with memory impairment and biomarkers alterations in biological fluids.

At this age, 3xTg-AD mice have a marked cognitive deficit, without A $\beta$  plaques and tau tangles, which appear after 12 and 18 months, respectively. Despite the absence of the two major pathological features, these animals have other

alterations that could contribute to the observed cognitive impairment. They consist primarily of accumulation of intracellular A $\beta$  in the hippocampus, which was already associated with the onset of the early cognitive deficit in 3xTg-AD mice **[Billings LM et al., 2005]**.

Moreover, a 55 kDa A $\beta$  species, that could represent a highly toxic oligomer much discussed in literature and called A $\beta$ \*56 **[Chiang ACA et al., 2018; Lesnè SE et al., 2006; Billings LM et al., 2007; Amar F et al., 2017; Lesnè SE et al., 2013]**, was detected by 6E10 antibody in hippocampal soluble lysates of our 6 month-old 3xTg-AD mice. 6E10 is a commercial antibody widely used for human APP and A $\beta$  species detection and reported for recognition of A $\beta$ \*56 too **[Chiang ACA et al., 2018]**. However, some limits in its use for this purpose may emerge due to potential cross-reactivity with mouse tissue samples as stated previously, and some other observations came on its inability to detect all A $\beta$  forms **[Hunter S and Brayne C, 2017]**.

In addition, we detected an increased expression of the neuroinflammation markers GFAP and CD11b, a decrease in the synaptic marker Synaptophysin, and a decrease in NRF2, a master regulator of the antioxidant response. Moreover, in accordance with our *in vitro* results, these mice had increased protein expression of SIRT2, supporting the hypothesis that in a neurodegenerative condition there is an accumulation of this protein, and strengthening our rationale to its inhibition. However, SIRT1 basal expression was apparently unaffected by the 3xTg-AD pathologic condition. This result is partially in contrast with the hypothesis of restoring a reduced SIRT1 level already associated with the human AD condition **[Cao K et al., 2018]**. Consequently, our treatment approach is likely to be considered as a boosting

of SIRT1 neuroprotective activity rather than a compensation of its deficiency, even if it cannot be excluded that we have a reduced activity of SIRT1 in a normal protein expression condition. Another point to be addressed is the early age of animals and their early neuropathological phenotype, which could be insufficient to trigger SIRT1 downregulation and so contributes to our result. In support of this observation, some literature data report a reduction of SIRT1 in old AD mice [**Rodriguez-Ortiz CJ et al., 2014**]. In addition, Bonda et al. made some considerations about the potential role of therapeutic SIRT1 upregulation for AD phenotype amelioration given its direct involvement in counteracting AD-related pathways [**Bonda DJ et al., 2011**].

The set of neuropathological features detected in these animals could therefore be responsible for the cognitive deficit at such an early age.

Starting from this characterization and from the data already available from our previous work on the inhibition of SIRT2 [**Biella G et al., 2016**], we decided to inhibit SIRT2 and activate SIRT1, with the objective of assessing the effect of the combined treatment on 3xTg-AD memory deficit and molecular alterations. As mentioned previously, SIRT2 inhibition with AK7 gave positive results on 3xTg-AD mice at 6-7 months of age, significantly increasing the non-amyloidogenic pathway through an increase in sAPP $\alpha$  and producing a marked improvement of cognitive deficit measured with NORT [**Biella G et al., 2016**].

Starting from this point, we first of all replicated the AK7 behavioural data. As expected, AK7 treatment was well tolerated, as assessed by body weight monitoring, and led to a strong cognitive deficit improvement. In fact, the mean DI of AK7-treated mice was 0.29, a value not significantly different from that of

NTg mice (mean DI = 0.39) but clearly improved with respect to untreated 3xTg-AD mice (mean DI = 0.02).

Next, we developed a 2-week acute protocol for SIRT1 activation. We selected a brain-permeable analogue of SRT1720, SRT2104, and also member of the second generation of STACs. This compound showed promising results in models of atrophy, diabetes, psoriasis and HD, and reached the clinical trial phase several times [**Mercken EM et al., 2014; Jiang M et al., 2014; Baksi A et al., 2014; Krueger JG et al., 2015**].

3xTg-AD mice treated with SRT2104 had cognitive deficit recovery, as indicated by the DI (mean DI = 0.32) that was very close to that of NTg mice (mean DI = 0.36), while 3xTg-AD mice treated with vehicle had cognitive impairment (mean DI = -0.02).

This result is in line with that reported by other groups, where SIRT1 over-expression or pharmacological activation (e.g. by resveratrol) resulted in cognitive performance improvement of AD mouse models [**Porquet D et al., 2014; Corpas R et al., 2017**].

Given the promising results obtained with the single SIRT1 or SIRT2 modulation, we moved to the main objective of the project, to modulate the two SIRTs in opposite directions.

AK7 and SRT2104 were given to 3xTg-AD mice with the same doses and routes of administration of the single treatments, and body weight was monitored during the course of the experiment. A preliminary evaluation of vehicle/DMSO toxicity following a repeated treatment was also performed prior to the double treatment, with no evidence of detrimental effects (data not shown).

In fact, the double treatment was well tolerated and significantly improved cognitive performance, as the mean DI of 3xTg-AD treated mice and NTg group was the same (NTg mean DI = 0.38; double-treated 3xTg-AD mean DI = 0.37), with a complete reversion of the vehicle-treated 3xTg-AD mice cognitive impairment (mean DI = 0.03). One experimental limit to be considered is that we excluded NTg-treated group from our analyses, to focus the attention on the improvement of the transgenic phenotype both at behavioural and biochemical level, but further analyses on the possible effect on healthy animals should be performed to draw more complete conclusions. Another important limitation that deserves attention is related to the choice of the behavioural task analysed. In fact, we measured visual recognition memory without assessing other recognition memory experimental settings (such as those discriminating the encoding, storage and retrieval of memory) or other types of memory, such as the spatial one that requires other behavioural tests (e.g. Morris Water Maze, Barnes Maze or Y-maze). Thus, the concept of complete cognitive recovery should be approached with caution. Additionally, our 24 hours test setting is a long-term memory assessment that do not give any information about the influence of the treatment on different time-point memories, such as short-term memory, a limit that could be exceeded by multiple time point behavioural analysis. NORT cognitive assessment has supporting literature regarding hippocampal involvement in object recognition, but just as much literature exists about the difficult interpretation of NORT because of multiple brain regions involvement, chiefly the perirhinal cortex that seems highly involved in memory retrieval [Broadbent NJ et al, 2009; Cohen SJ and Stackman RW, 2015; Lueptow

**LM, 2017]**. This is a reason to foresee the analysis of biochemical parameters also in other brain areas involved in recognition memory, as the experiments presented below were focused on hippocampal samples only.

As previously stated, we treated our 3xTg-AD mice in an early phase, when amyloid plaques are not evident but intracellular and oligomeric A $\beta$  forms are detectable together with other pathologic alterations, as shown in the 3xTg-AD characterization results. Moreover, A $\beta$  oligomers have been proposed as directly responsible for alterations such as synaptic damage and neuroinflammation [**Mroczko B et al., 2018**].

Consequently, we tried to correlate the recovery in mice cognitive impairment with neuropathological changes of those markers that resulted altered in 3xTg-AD mice at basal level.

We already knew that SIRT2 inhibition with AK7 acted on APP processing in hippocampus of 3xTg-AD mice by increasing the non-amyloidogenic pathway, with higher levels of the neuroprotective fragment sAPP $\alpha$  and lower levels of sAPP $\beta$  [**Biella G et al., 2016**].

Therefore, we investigated sAPP $\alpha$  levels in hippocampus of SRT2104 and double-treated mice too, and results showed that both treatments significantly increased this APP protein fragment, in accordance with our *in vitro* data and with literature about SIRT1 activation.

Another relevant parameter detected in hippocampal soluble fractions of 3xTg-AD mice was the A $\beta$  form having SDS-PAGE molecular weight of 55 kDa, which corresponds in size to a 12-mer. We hypothesize it to be the reported A $\beta$ \*56 toxic species found in Tg2576 AD mice and directly associated with memory loss [**Lesnè S et al., 2006; Amar F et al., 2017**]. Moreover, this band



was also detected in brain lysates from memory impaired 3xTg-AD mice [Billings LM et al., 2007]. We assessed the level of this oligomer after each treatment, and found that while SRT2104 alone did not affect its level, AK7 administration significantly lowered it, and the double treatment condition maintained AK7 effect, showing again a significant decrease of 55 kDa A $\beta$ .

This result could align with the A $\beta$ 42 paradoxical effect seen on AK7-treated H4-sw cells and with our hypothesis of a direct effect of AK7 on A $\beta$  aggregation dynamics.

These data strengthen the potential of SIRT2 inhibition in counteracting A $\beta$ -related pathology, acting both on APP processing and on soluble aggregated forms of A $\beta$  peptide that are generally considered the most toxic species [Verma M et al., 2015]. In fact, it is reasonable to assume that an increase in sAPP $\alpha$  production and a reduction in hippocampal A $\beta$  oligomers could give a strong contribution to mice cognitive improvement.

As stated in the Results section, despite its widespread use, the 6E10 antibody for A $\beta$ O visualization could raise some doubts related to mouse cross-reactivity, even if the absence of the 55kDa A $\beta$  form in NTg mice could suggest that we are detecting some specific signal. To eliminate this doubt and verify the identification of A $\beta$ \*56 as an oligomeric species, we could select another A $\beta$  oligomer-specific antibody instead of 6E10, such as 4G8, A11 or 82E1 clones, in parallel to an optimized extraction protocol with varying detergent concentrations [Chiang ACA et al., 2018].

Another factor to discuss is the sole analysis of soluble fractions, which on one hand we decided to select as an amount of circulating soluble A $\beta$  oligomers that can confer neurotoxicity is present [Hong W et al., 2018] and could also

constitute an interesting player in the pathogenesis of the AD early stages that we are analyzing. On the other hand, this choice may highlight a limitation of our experiments that could have been performed on the insoluble A $\beta$ O-containing pellets too, to assess both soluble and insoluble A $\beta$  forms and draw a complete picture of the situation. For future analyses, western blotting could be performed on hippocampal ultracentrifuged pellets solubilized in formic acid (FA) for detection of those insoluble A $\beta$ O species, as well as other interesting insoluble fractions.

Next, we assessed the effect of the treatments on neuroinflammation by measuring hippocampal levels of GFAP and CD11b, that were increased in 3xTg-AD mice.

Neuroinflammation is a major player in AD pathogenesis, as A $\beta$  peptide is directly responsible for glial over-activation, which is considered an early event for AD neuronal damage and synaptic failure [**Ahmad MH et al., 2019; Avila-Muñoz E and Arias C, 2014**].

We also measured the effect on the pre-synaptic marker Synaptophysin, whose basal level was decreased in 3xTg-AD mice, indicating an initial synaptic deficit.

SRT2104 administration, but not AK7, significantly reduced GFAP and CD11b levels, and increased Synaptophysin in the hippocampus of 3xTg-AD mice. This result was confirmed in mice treated with the combination of AK7 and SRT2104, indicating that SIRT1 activation effects were maintained.

Overall, one could hypothesize that decreased neuroinflammation markers lead directly to improved synaptic health that was evident through increased Synaptophysin level.

The absence of effects of AK7 on neuroinflammation markers is in accordance with our previous work on the same model **[Biella G et al., 2016]**, even if some literature data point to a role of SIRT2 inhibition in reducing reactive gliosis *in vitro* **[Scuderi C et al., 2014]**.

Another important feature of AD molecular pathology is oxidative stress and impaired antioxidant response, that are correlated with mitochondrial dysfunction and A $\beta$  accumulation. Moreover, ROS production can itself stimulate aggregation of misfolded proteins, exacerbating the toxicity status of the neuron **[Uttara B et al., 2009; Wang P and Wang ZY, 2016]**.

In our 3xTg-AD mice, we detected basal decreased levels of NRF2, a transcription factor regulating genes for the antioxidant response. Together with decreased transcription of its target genes, one important consequence of NRF2 reduction is a high intracellular iron level that can contribute to oxidative stress and cellular damage **[Yang X et al., 2017]**. Another work showed that the lack of NRF2 in an AD-NRF2 KO mouse model worsened APP and tau pathology by increasing p-tau, A $\beta$ \*56, neuroinflammation, oxidation and cognitive deficit **[Rojo AI et al., 2017]**. The levels of Nrf2 were decreased in the hippocampal neurons from AD patients and its activation has been proposed as a new goal for oxidative stress and inflammation suppression in AD pathology **[Ramsey CP et al., 2007; Kedar N Prasad, 2016]**.

Different works reported a link between NRF2 pathway and SIRT1 in different pathological contexts, including neurodegenerative disorders and AD.

As an example, Cui and colleagues reported that the antioxidant D3T exerted its neuroprotective effect on AD mice up-regulating SIRT1/NRF2 pathway, an

effect that was abolished by pharmacological inhibition of SIRT1 [Cui Y et al., 2018], thus suggesting a direct link between SIRT1 function and NRF2 beneficial effects.

SIRT2 seems to be involved in NRF2 function too, in particular by deacetylating NFR2 and favouring its degradation, with consequent decrease of iron efflux from the cell and increase in intracellular iron levels [Yang X et al., 2017], an event that if pathologically imbalanced could favour the progression of oxidative damage.

Given these assumptions, we hypothesized that with both SIRT1 activation and SIRT2 inhibition it could be possible to obtain increased NRF2 level improving the antioxidant response pathway in our pathologic context.

We decided to assess the level of NRF2 in 3xTg-AD mice treated with SRT2104 and AK7. In parallel, we assessed the level of the antioxidant enzyme SOD1, another protein that is reportedly decreased in the brain of AD patients together with SIRT1 levels [Cao K et al., 2018]. Among the different antioxidant proteins, we selected SOD1 as an example of downstream players of the antioxidant machinery connected with NRF2 activation too [Park EY and Rho HM, 2002; Mota SI et al., 2015], but the assessment of other enzymes could be useful to make more complete picture of this pathway involvement (i.e. HO-1).

The results showed that SIRT1 activation with SRT2104 significantly increased both hippocampal NRF2 and SOD1 levels, supporting the hypothesis of a SOD1 increase downstream consequence of NRF2 enhancement. In the case of SIRT2 inhibition with AK7, though, we were unable to obtain a significant NRF2 increase, and no effect on SOD1 level was appreciable too.

As for 3xTg-AD mice treated simultaneously with AK7 and SRT2104, they had increased levels of NRF2 and SOD1 as expected, indicating that with our treatment we could be able to improve the antioxidant defence machine that appears impaired in AD condition.

Overall, *in vivo* results support the objective of this work, which was to affect different AD neuropathological alterations by modulating SIRT1 and SIRT2 activity, finally obtaining a recovery of the cognitive deficit. The set of the carried-out analyses suggest that SIRT1 activation is more prone to affect different pathways and give a broader spectrum effect on neuroinflammation, synaptic function, antioxidative response and APP metabolism, while SIRT2 inhibition seems to act more specifically on APP-relevant parameters with a negligible effect on other targets, at least in our context.

However, some limitations of our main findings should be taken into account. First of all, the *in vitro* model may not be completely descriptive of the pathology, since we did not use neuronal-like cells that could have given more realistic and complete informations not only for APP metabolism, but also for other peculiar mechanisms that characterize neuronal functioning. Another point regards the key finding of sAPP $\alpha$  increase, that we obtained both *in vitro* and *in vivo* upon SIRT1 and SIRT2 treatments, as this was not paralleled by an effect on the alpha-secretase ADAM10 and this result does not reflect what has been reported in some literature works [Tippman F et al., 2009; Lee HR et al., 2014]. Anticipating that ADAM10 analysis is still lacking in *in vivo* experiments, we cannot definitely conclude that our model is inadequate for the analysis of this parameter.

*In vitro* data also showed some confounding results about the effect of the SIRT2 inhibitor AK7 on A $\beta$ 42, which need careful investigation to confirm if it could be a side effect, a model-dependent effect, or an anti-aggregant effect as hypothesized by us.

In our *in vivo* experiments, despite we had a clear indication of the pro-cognitive effect of the treatments on 3xTg-AD mice, some points need further investigation, since we described only one memory task (visual recognition memory), at one time-point and without considering other brain regions involvement other than the hippocampal one [**Cohen SJ and Stackman RW, 2015; Lueptow LM, 2017**]. Moreover, we did not compare all the experimental groups in the same behavioural and biochemical analyses, keeping each treatment as an independent experiment. These shortcomings may not make the overall *in vivo* picture complete, as it could be interesting to know if the double treatment is able to produce greater effects on all parameters (memory and protein markers) with respect to the single modulation, giving integrative informations to those obtained in this thesis.

The *in vitro* and *in vivo* data are, in our opinion, supportive of the combined approach in SIRTs modulation in AD therapy. However, several limitations are to be considered. One of these pertains to the available SIRTs modulators and their pharmacokinetic features.

For this reason, in the last part of the thesis, we focused our attention on the preliminary characterization of a controlled release system for the administration of SIRTs modulators. Despite the growing development of compounds able to modulate SIRT1 and SIRT2 and their promising biological effects, it is difficult to optimize the pharmacokinetic characteristics of the

molecule in order to permit access to the brain and simultaneously allow a prolonged effect without rapid clearance. It is the case, for example, of the SIRT1 activator SRT1720 which we used for *in vitro* experiments, that is unable to cross the BBB. Likewise, AK7, despite its brain-permeability, has a very short half-life and needs repeated administrations. Therefore, a possible application of a controlled release system could be a peripheral implantation for brain-permeable compounds with poor pharmacokinetics, a CNS direct implant for those not brain-permeable and rapidly eliminated, but also for brain-permeable molecules, to reduce the loss in other body districts and minimize associated side effects [Li J et al., 2016; Basso J et al., 2018; Garbayo E et al., 2013; Tunesi et al., 2014].

Hydrogel-based DDS are three-dimensional, biocompatible, injectable, and perform in situ gelation. These characteristics allow their use for the release of neuroactive molecules in the CNS [Khaing Z et al., 2014]. In addition, hydrogels are biodegradable, and do not require surgery for their removal [Pakulska MM et al., 2012].

Cooke et al, who developed a controlled epi-cortical DDS, proposed one promising application of hydrogel-based delivery systems. Their device consisted in a PEG-EGF-loaded hydrogel placed epicortically to treat stroke-injured brain, aiming at a local, minimally invasive and controlled delivery to the brain [Cooke MJ et al, 2011]. Caicco and colleagues successfully reproduced the same approach in 2013 [Caicco MJ et al, 2013].

For the development of our DDS, we selected a semi-interpenetrated hydrogel [Hoare TR et al., 2008] made by type I Collagen and PEG2000. The safety of this matrix was tested in cellular models of neurodegeneration and by

intracranial and subcutaneous injection in AD and PD models [Tunesi M et al., 2013]. The lack of inflammatory potential was confirmed in this thesis through the air-pouch model, where the COLL-PEG2000 hydrogel resulted safe after 24 hours of implantation in CD-1 mice.

We selected three SIRT1-2 modulators for our experiments. The first was SIRT1 activator SRT1720, which despite its higher potency respect to SRT2104 is not brain permeable. In addition, we selected AK7 SIRT2 inhibitor and AGK2, another compound that has a better IC<sub>50</sub> despite not being brain-permeable.

AGK2 is a well-documented SIRT2 inhibitor and was used for *in vitro* experiments in a previous work from our laboratory [Scuderi C et al., 2014; Biella G et al., 2016].

For modulator quantification, we chose the UV-Vis spectrophotometric technique, and identified the maximum absorbance peak ( $\lambda_{\text{max}}$ ) for each modulator. Unfortunately, AK7 did not show any absorbance peak and was excluded from further experiments.

AGK2 was not eligible for our hydrogel-based approach, due to the impossibility of detecting its presence at any time-point.

This result suggests that AGK2 is not released by the hydrogel, and could be trapped inside the matrix with some chemical or physical interaction with its components.

On the contrary, SRT1720 was released from the COLL/PEG2000 hydrogel with decreasing speed over time. After 7 days, the percentage of molecule released is 92.8% of the loaded quantity, confirming that the hydrogel-based



system has some positive features for a prospective application in a therapeutic strategy involving SIRT1 activation.

This preliminary picture needs implementation, particularly in the optimization of the release assessment for those compounds that were not suitable for our experimental setup, but also for the *in vivo* application in the 3xTg-AD mouse model to verify the efficacy of the release system.

The development of an effective delivery system of SIRT modulators could be a useful tool for *in vivo* drug-delivery, overcoming the limitations and invasiveness of conventional administrations. Moreover, this approach could potentially be of considerable impact in future clinical practice on AD, PD and other CNS disorders, as hydrogel-based DDS systems might improve the effective delivery of drugs to the target site thanks to their multiple beneficial features. However, much work will still be needed in formulation, characterization and production processes to effectively translate these systems in human CNS diseases.

## **CONCLUSIONS**

In conclusion, the results obtained in this thesis support the main objectives of the project, demonstrating the feasibility of a combined treatment targeting SIRT1 and 2 and confirming the promising role of SIRT1 and SIRT2 as therapeutic targets for cognitive recovery in AD. The combined SIRT1 activation and SIRT2 inhibition, an approach we propose for the first time in AD context, could represent a useful tool aimed at attacking the disease on multiple molecular aspects that integrate each other to ameliorate cognitive impairment (Fig. 6.1).

The most promising results have emerged with *in vivo* experiments. 3xTg-AD mice treated with a combination of SIRT1 activator and SIRT2 inhibitor had a recovery of cognitive impairment in the object recognition task, associated with hippocampal biochemical changes, such as non-amyloidogenic APP metabolism increase, reduced oligomeric A $\beta$  and neuroinflammation markers GFAP and CD11b, increased Synaptophysin and antioxidant proteins NRF2 and SOD1. Some of these changes seemed to depend on the single modulation of SIRT1, like neuroinflammation, antioxidant and synaptic markers, while A $\beta$ -related parameters seemed more linked to SIRT2 inhibition, further supporting the complementarity of the double treatment at the neuropathological level.

An important point to address is that both single treatments independently affected memory, producing a significant amelioration of object recognition performance. A possible explanation could reside in the fact that one main biochemical change shared by both SIRT1 and SIRT2 treatment is the boosting of sAPP $\alpha$  neuroprotective fragment, that alone can affect cognition. It is possible that this is the main molecular effector of the cognitive improvement, even if we cannot conclude that this is the only one.

Although the double treatment did not show a cognitive effect different from that of the single treatments, thus making its added value negligible, its importance could lie in the interesting hints obtained from biochemical analyses.

If on the one hand the increase in the  $\alpha$ -cleavage could be the most important effect for the cognitive result, on the other hand AD is not only cognitive decline. The protective effect on other pathways that we took in consideration

could help in supporting neuroprotection acting on other behavioural disturbances or even on other neuropathological aspects such as neurovascular alterations (strictly connected to neuroinflammation and oxidative stress). Thus, it cannot be excluded that, besides APP processing, the other pathways contribute to the overall phenotypic effect, maybe through some synergic mechanisms that could emerge in future experimental settings.

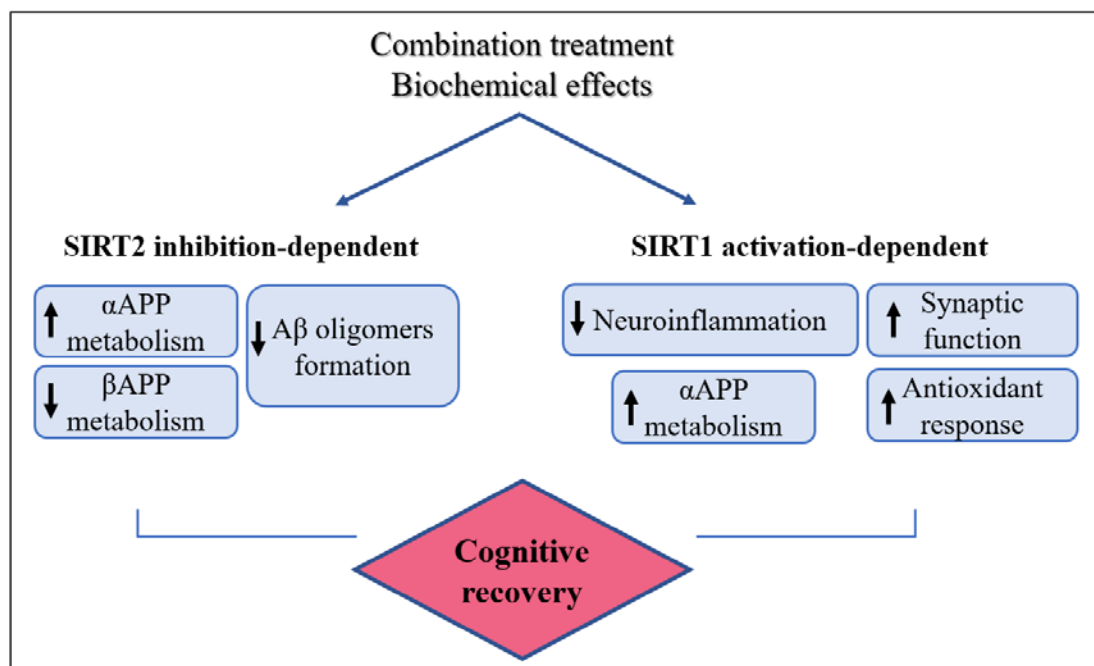


**Figure 6.1** Summary of the key findings of this work, where cognitive recovery of 3xTg-AD mice seems to be attributable to a complementary effect of SIRT1 activation and SIRT2 inhibition on different pathological pathways, supporting the potential of a multi-target strategy to counteract the multifactorial nature of AD pathogenesis.

Finally, the preliminary characterization of a hydrogel-based system for the controlled release of SIRTs modulators with poor pharmacokinetics, proved to be promising for further optimization in the neurodegeneration context, to allow a more effective delivery of neuroactive compounds to the CNS.

## FUTURE PERSPECTIVES

The future perspectives of this project will aim at overcoming the limitations described during the discussion of the obtained results.

To deepen the usefulness and clinical traslability of AK7 compound as SIRT2 inhibitor, specific experiments should be dedicated to the investigation of its effects on the A $\beta$  peptide aggregation and production, as described previously. *In vivo* behavioural analyses should focus on the memory recovery outcome comparing both NTg and 3xTg-AD mice receiving single and combined treatment, to have a quantitative measure of the memory improvement that the combination could give with respect to the single drug and to assess if the double treatment has not only complementaty, but also synergic effects.

A detailed analysis of both short-term and long-term memory, together with the parallel assessment of other memory tasks, could be very useful to draw a complete cognitive picture after SIRTs modulation.

In addition, we could propose to anticipate the timing of the pharmacological treatments in a preventive key, for mice with no cognitive deficit on which it could be interesting to see if the treatment delays it, or to postpone it in a curative key under full-blown pathology.

Future biochemical experiments should focus both on hippocampus and cortex samples and paralleled with behavioural results. Those experiments should deepen the analysis of the treatment's effect on ADAM10, clarify that on A $\beta$  oligomers with more specific antibodies and extraction protocols, but also investigate those molecular pathways that could be involved in biochemical changes seen in our results (e.g. NfkB involvement in inflammation effects, microtubules dynamics and acetylation of tau).

Further experiments will be required to evaluate the potential use of SIRTs modulator-loaded hydrogels *in vivo* and to confirm the maintenance of the biological effects of the treatment. In addition, it would be interesting to explore the physical-chemical interaction between the matrix and the active molecules to overcome the limitations in the formulation of the system.

## **7. Bibliography**

- Agostinho P, Pliássova A, Oliveira CR, Cunha RA.** Localization and Trafficking of Amyloid- $\beta$  Protein Precursor and Secretases: Impact on Alzheimer's disease. *J Alzheimers Dis.* 2015; 45(2):329-47.
- Ahmad MH, Fatima M, Mondal AC.** Influence of microglia and astrocyte activation in the neuroinflammatory pathogenesis of Alzheimer's disease: Rational insights for the therapeutic approaches. *J Clin Neurosci.* 2019 Jan; 59:6-11.
- Akhter R, Sanphui P, Biswas SC.** The essential role of p53-up-regulated modulator of apoptosis (Puma) and its regulation by FoxO3a transcription factor in  $\beta$ -amyloid-induced neuron death. *J Biol Chem* 2014; 289:10812–10822.
- Albani D, Polito L, Batelli S, De Mauro S, Fracasso C, Martelli G, Colombo L, Manzoni C, Salmona M, Caccia S, Negro A, Forloni G.** The SIRT1 activator resveratrol protects SK-N-BE cells from oxidative stress and against toxicity caused by alpha-synuclein or amyloid-beta (1-42) peptide. *J Neurochem.* 2009 Sep; 110(5):1445-56.
- Alonso Vilatela ME, López-López M, Yescas-Gómez P.** Genetics of Alzheimer's disease. *Arch Med Res.* 2012 Nov; 43(8):622-31.
- Alves L, Correia AS, Miguel R, Alegria P, Bugalho P.** Alzheimer's disease: a clinical practice-oriented review. *Front Neurol.* 2012 Apr 20; 3:63.
- Alzheimer A, Stelzmann RA, Schnitzlein HN, Murtagh FR.** An English translation of Alzheimer's 1907 paper, "Über eine eigenartige Erkankung der Hirnrinde". *Clin Anat.* 1995; 8(6):429-31.
- Amar F, Sherman MA, Rush T, Larson M, Boyle G, Chang L, Götz J, Buisson A, Lesné SE.** The amyloid- $\beta$  oligomer A $\beta$ \*56 induces specific alterations in neuronal signaling that lead to tau phosphorylation and aggregation. *Sci Signal.* 2017 May 9; 10(478).
- Anamika, Khanna A, Acharjee P, Acharjee A, Trigun SK.** Mitochondrial SIRT3 and neurodegenerative brain disorders. *J Chem Neuroanat.* 2019 Jan; 95:43-53.
- Anand R, Gill KD, Mahdi AA.** Therapeutics of Alzheimer's disease: Past, present and future. *Neuropharmacology.* 2014 Jan; 76 Pt A: 27-50.
- Arber C, Lovejoy C, Wray S.** Stem cell models of Alzheimer's disease: progress and challenges. *Alzheimers Res Ther.* 2017;9(1):42.
- Atri A.** Effective pharmacological management of Alzheimer's disease. *The American Journal of Managed Care.* 2011 Nov; 17 Suppl 13:S346-55.
- Attems J, Thomas A, Jellinger K.** Correlations between cortical and subcortical tau pathology. *Neuropathol Appl Neurobiol.* 2012; 38:582–590.
- Avila J, Pallas N, Bolós M, Sayas CL, Hernandez F.** Intracellular and extracellular microtubule associated protein tau as a therapeutic target in Alzheimer disease and other tauopathies. *Expert Opin Ther Targets.* 2016 Jun; 20(6):653-61.
- Avila-Muñoz E, Arias C.** When astrocytes become harmful: functional and inflammatory responses that contribute to Alzheimer's disease. *Ageing Res Rev* 2014; 18:29–40.
- Bagyinszky E, Youn YC, An SS, Kim S.** The genetics of Alzheimer's disease. *Clin Interv Aging.* 2014 Apr 1; 9:535-51.
- Bakota L, Brandt R.** Tau Biology and Tau-Directed Therapies for Alzheimer's Disease. *Drugs.* 2016 Mar; 76(3):301-13.

- Baksi A, Kraydashenko O, Zalevkaya A, Stets R, Elliott P, Haddad J, Hoffmann E, Vlasuk GP, Jacobson EW.** A phase II, randomized, placebo-controlled, double-blind, multi-dose study of SRT2104, a SIRT1 activator, in subjects with type 2 diabetes. *Br J Clin Pharmacol.* 2014 Jul;78(1):69-77.
- Ballard C, Gauthier S, Corbett A, Brayne C, Aarsland D, Jones E.** Alzheimer's disease. *Lancet.* 2011 Mar 19; 377(9770):1019-31.
- Barage SH, Sonawane KD.** Amyloid cascade hypothesis: Pathogenesis and therapeutic strategies in Alzheimer's disease. *Neuropeptides.* 2015 Aug; 52:1-18.
- Barnett JH, Lewis L, Blackwell AD, Taylor M.** Early intervention in Alzheimer's disease: a health economic study of the effects of diagnostic timing. *BMC Neurol.* 2014 May 7; 14:101.
- Basso J, Miranda A, Nunes S, Cova T, Sousa J, Vitorino C, Pais A.** Hydrogel-Based Drug Delivery Nanosystems for the Treatment of Brain Tumors. *Gels.* 2018 Jul 19; 4(3).
- Baumgart M, Snyder HM, Carrillo MC, Fazio S, Kim H, Johns H.** Summary of the evidence on modifiable risk factors for cognitive decline and dementia: A population-based perspective. *Alzheimers Dement.* 2015 Jun; 11(6):718-26.
- Belfiore R, Rodin A, Ferreira E, Velazquez R, Branca C, Caccamo A, Oddo S.** Temporal and regional progression of Alzheimer's disease-like pathology in 3xTg-AD mice. *Aging Cell.* 2019 Feb; 18(1):e12873.
- Bhaskar M.** Neuroinflammation in Alzheimer's disease - A review. *J Pharm Sci Technol* 2016; 2:1-6.
- Bhat KPL, Kosmeder JW 2nd, Pezzuto JM.** Biological effects of resveratrol. *Antioxid Redox Signal.* 2001 Dec; 3(6):1041-64.
- Biella G, Fusco F, Nardo E, Bernocchi O, Colombo A, Lichtenthaler SF, Forloni G, Albani D.** Sirtuin 2 Inhibition Improves Cognitive Performance and Acts on Amyloid- $\beta$  Protein Precursor Processing in Two Alzheimer's Disease Mouse Models. *J Alzheimers Dis.* 2016 Jun 30; 53(3):1193-207.
- Billiet T, Vandenhoute M, Schelfhout J, Van Vlierberghe S, Dubruel P.** A review of trends and limitations in hydrogel-rapid prototyping for tissue engineering. *Biomaterials.* 2012 Sep; 33(26):6020-41.
- Billings LM, Oddo S, Green KN, McGaugh JL, LaFerla FM.** Intraneuronal A $\beta$  causes the onset of early Alzheimer's disease-related cognitive deficits in transgenic mice. *Neuron.* 2005 Mar 3; 45(5):675-88.
- Billings LM, Green KN, McGaugh JL, LaFerla FM.** Learning decreases A $\beta$ \*56 and tau pathology and ameliorates behavioral decline in 3xTg-AD mice. *J Neurosci.* 2007 Jan 24; 27(4):751-61.
- van Bogaert MJ, Groenink L, Oosting RS, Westphal KG, van der Gugten J, Olivier B.** Mouse strain differences in autonomic responses to stress. *Genes Brain Behav.* 2006;5(2):139-149.
- Bonda DJ, Lee H-G, Camins A et al**The sirtuin pathway in ageing and Alzheimer disease: mechanistic and therapeutic considerations. *Lancet Neurol* 2011; 10:275–279.
- Breydo L, Kurouski D, Rasool S, Milton S, Wu JW, Uversky VN, Lednev IK, Glabe CG.** Structural differences between amyloid beta oligomers. *Biochem Biophys Res Commun.* 2016 Sep 2; 477(4):700-705.



- Brito-Moreira J, Lourenco MV, Oliveira MM, Ribeiro FC, Ledo JH, Diniz LP, Vital JFS, Magdesian MH, Melo HM, Barros-Aragão F, de Souza JM, Alves-Leon SV, Gomes FCA, Clarke JR, Figueiredo CP, De Felice FG, Ferreira ST.** Interaction of amyloid- $\beta$  (A $\beta$ ) oligomers with neurexin 2 $\alpha$  and neuroligin 1 mediates synapse damage and memory loss in mice. *J Biol Chem.* 2017 May 5; 292(18):7327-7337.
- Broadbent NJ, Gaskin S, Squire LR, Clark RE.** Object recognition memory and the rodent hippocampus. *Learn Mem.* 2009;17(1):5-11. Published 2009 Dec 22.
- Budayeva HG, Cristea IM.** Human Sirtuin 2 Localization, Transient Interactions, and Impact on the Proteome Point to Its Role in Intracellular Trafficking. *Mol Cell Proteomics.* 2016 Oct;15(10):3107-3125.
- Cai Z, Hussain MD, Yan LJ.** Microglia, neuroinflammation, and beta-amyloid protein in Alzheimer's disease. *Int J Neurosci.* 2014 May;124(5):307-21.
- Caicco MJ, Cooke MJ, Wang Y, Tuladhar A, Morshead CM, Shoichet MS.** A hydrogel composite system for sustained epi-cortical delivery of Cyclosporin A to the brain for treatment of stroke. *J Control Release.* 2013;166(3):197-202.
- Cao K, Dong YT, Xiang J, Xu Y, Hong W, Song H, Guan ZZ.** Reduced expression of SIRT1 and SOD-1 and the correlation between these levels in various regions of the brains of patients with Alzheimer's disease. *J Clin Pathol.* 2018 Dec; 71(12):1090-1099.
- Cavalli A, Bolognesi ML, Minarini A, Rosini M, Tumiatti V, Recanatini M, Melchiorre C.** Multi-target-directed ligands to combat neurodegenerative diseases. *J Med Chem.* 2008 Feb 14;51(3):347-72.
- Cavanaugh, S. E.** Animal models of Alzheimer disease: Historical pitfalls and a path forward. *ALTEX*, 2014, 31(3), 279–302.
- Chasseigneaux S, Allinquant B.** Functions of A $\beta$ , sAPP $\alpha$  and sAPP $\beta$ : similarities and differences. *J Neurochem.* 2012 Jan; 120 Suppl 1:99-108.
- Chen H, Ji H, Zhang M, Liu Z, Lao L, Deng C, Chen J, Zhong G.** An Agonist of the Protective Factor SIRT1 Improves Functional Recovery and Promotes Neuronal Survival by Attenuating Inflammation after Spinal Cord Injury. *J Neurosci.* 2017 Mar 15; 37(11):2916-2930.
- Chen J, Zhou Y, Mueller-Steiner S et al.** SIRT1 protects against microglia-dependent amyloid-beta toxicity through inhibiting NF-kappaB signaling. *J Biol Chem* 2005; 280:40364–40374.
- Chen J, Chan AW, To KF, Chen W, Zhang Z, Ren J, Song C, Cheung YS, Lai PB, Cheng SH, Ng MH, Huang A, Ko BC.** SIRT2 overexpression in hepatocellular carcinoma mediates epithelial to mesenchymal transition by protein kinase B/glycogen synthase kinase-3 $\beta$ / $\beta$ -catenin signaling. *Hepatology.* 2013 Jun; 57(6):2287-98.
- Chen X, Wales P, Quinti L, Zuo F, Moniot S, Herisson F, Rauf NA, Wang H, Silverman RB, Ayata C, Maxwell MM, Steegborn C, Schwarzschild MA, Outeiro TF, Kazantsev AG.** The sirtuin-2 inhibitor AK7 is neuroprotective in models of Parkinson's disease but not amyotrophic lateral sclerosis and cerebral ischemia. *PLoS One.* 2015 Jan 21;10(1):e0116919.
- Cheng IH, Scearce-Levie K, Legleiter J, Palop JJ, Gerstein H, Bien-Ly N, Puoliväli J, Lesné S, Ashe KH, Muchowski PJ, Mucke L.** Accelerating amyloid-beta fibrillization reduces oligomer levels and functional deficits in Alzheimer disease mouse models. *J Biol Chem.* 2007 Aug 17;282(33):23818-28.

- Chia PZ, Gleeson PA.** Intracellular trafficking of the  $\beta$ -secretase and processing of amyloid precursor protein. *IUBMB Life*. 2011 Sep; 63(9):721-9.
- Chiang ACA, Fowler SW, Reddy R, et al.** Discrete Pools of Oligomeric Amyloid- $\beta$  Track with Spatial Learning Deficits in a Mouse Model of Alzheimer Amyloidosis. *Am J Pathol*. 2018;188(3):739-756.
- Cho CS, Han SY, Ha JH, Kim SH, Lim DY.** Clonazepam release from bioerodible hydrogels based on semi-interpenetrating polymer networks composed of poly(epsilon-caprolactone) and poly(ethylene glycol) macromer. *Int J Pharm*. 1999 Apr 30; 181(2):235-42.
- Choi SH, Kim YH, Hebisch M, Sliwinski C, Lee S, D'Avanzo C, Chen H, Hooli B, Asselin C, Muffat J, Klee JB, Zhang C, Wainger BJ, Peitz M, Kovacs DM, Woolf CJ, Wagner SL, Tanzi RE, Kim DY.** A three-dimensional human neural cell culture model of Alzheimer's disease. *Nature*. 2014 Nov 13; 515(7526):274-8.
- Choi SS, Lee SR, Lee HJ.** Neurorestorative role of stem cells in Alzheimer's disease: astrocyte involvement. *Curr Alzheimer Res* 2016; 13:419–427.
- Choonara YE, Kumar P, Modi G, Pillay V.** Improving drug delivery technology for treating neurodegenerative diseases. *Expert Opin Drug Deliv*. 2016 Jul; 13(7):1029-43.
- Chopra V, Quinti L, Kim J, Vollor L, Narayanan KL, Egerly C, Cipicchio PM, Lauver MA, Choi SH, Silverman RB, Ferrante RJ, Hersch S, Kazantsev AG.** The sirtuin 2 inhibitor AK-7 is neuroprotective in Huntington's disease mouse models. *Cell Rep*. 2012 Dec 27; 2(6):1492-7.
- Cieřlik M, Czapski GA, Strosznajder JB** The molecular mechanism of amyloid  $\beta$ 42 peptide toxicity: the role of sphingosine kinase-1 and mitochondrial sirtuins. *PLoS ONE* 2015; 10:e0137193.
- Colombo A, Bastone A, Ploia C, Scip A, Salmona M, Forloni G, Borsello T.** JNK regulates APP cleavage and degradation in a model of Alzheimer's disease. *Neurobiol Dis*. 2009 Mar;33(3):518-25.
- Colombo A, Wang H, Kuhn PH, et al.** Constitutive  $\alpha$ - and  $\beta$ -secretase cleavages of the amyloid precursor protein are partially coupled in neurons, but not in frequently used cell lines. *Neurobiol Dis*. 2013;49:137-147.
- Colović MB, Krstić DZ, Lazarević-Pašti TD, Bondžić AM, Vasić VM.** Acetylcholinesterase inhibitors: pharmacology and toxicology. *Curr Neuropharmacol*. 2013 May; 11(3):315-35.
- Cooke MJ, Wang Y, Morshead CM, Shoichet MS.** Controlled epi-cortical delivery of epidermal growth factor for the stimulation of endogenous neural stem cell proliferation in stroke-injured brain. *Biomaterials*. 2011;32(24):5688-5697.
- Corbett NJ, Hooper NM.** Soluble Amyloid Precursor Protein  $\alpha$ : Friend or Foe? *Adv Exp Med Biol*. 2018; 1112:177-183.
- Corpas R, Revilla S, Ursulet S, Castro-Freire M, Kaliman P, Petegnief V, Giménez-Llort L, Sarkis C, Pallàs M, Sanfeliu C.** SIRT1 Overexpression in Mouse Hippocampus Induces Cognitive Enhancement Through Homeostatic and Neurotrophic Mechanisms. *Mol Neurobiol*. 2017 Sep;54(7):5604-5619.
- Costa RM, Drew C, Silva AJ.** Notch to remember. *Trends Neurosci* 2005; 28:429–435.
- Cui Y, Ma S, Zhang C, Li D, Yang B, Lv P, Xing Q, Huang T, Yang GL, Cao W, Guan F.** Pharmacological activation of the Nrf2 pathway by 3H-1, 2-dithiole-3-thione is neuroprotective in a mouse model of Alzheimer disease. *Behav Brain Res*. 2018 Jan 15; 336:219-226.

- Czeh M, Gressens P, Kaindl AM.** The yin and yang of microglia. *Dev Neurosci.* 2011; 33(3-4):199-209.
- Czvitkovich S, Duller S, Mathiesen E, et al.** Comparison of pharmacological modulation of APP metabolism in primary chicken telencephalic neurons and in a human neuroglioma cell line. *J Mol Neurosci.* 2011;43(3):257-267.
- Dai H, Sinclair DA, Ellis JL, Steegborn C.** Sirtuin activators and inhibitors: Promises, achievements, and challenges. *Pharmacol Ther.* 2018 Aug; 188:140-154.
- DaRocha-Souto B, Scotton TC, Coma M, Serrano-Pozo A, Hashimoto T, Serenó L, Rodríguez M, Sánchez B, Hyman BT, Gómez-Isla T.** Brain oligomeric  $\beta$ -amyloid but not total amyloid plaque burden correlates with neuronal loss and astrocyte inflammatory response in amyloid precursor protein/tau transgenic mice. *J Neuropathol Exp Neurol.* 2011 May; 70(5):360-76.
- Deng J, Habib A, Obregon DF, Barger SW, Giunta B, Wang YJ, Hou H, Sawmiller D, Tan J.** Soluble amyloid precursor protein alpha inhibits tau phosphorylation through modulation of GSK3 $\beta$  signaling pathway. *J Neurochem.* 2015 Nov;135(3):630-7.
- Denzer I, Münch G, Friedland K.** Modulation of mitochondrial dysfunction in neurodegenerative diseases via activation of nuclear factor erythroid-2-related factor 2 by food-derived compounds. *Pharmacol Res.* 2016 Jan; 103:80-94.
- De Oliveira RM, Sarkander J, Kazantsev AG, Outeiro TF.** SIRT2 as a Therapeutic Target for Age-Related Disorders. *Front Pharmacol.* 2012 May 3;3:82.
- De-Paula VJ, Radanovic M, Diniz BS, Forlenza OV.** Alzheimer's disease. *Subcell Biochem.* 2012; 65:329-52.
- Donmez G.** The neurobiology of sirtuins and their role in neurodegeneration. *Trends Pharmacol Sci.* 2012 Sep; 33(9):494-501.
- Donmez G, Outeiro TF.** SIRT1 and SIRT2: emerging targets in neurodegeneration. *EMBO Mol Med.* 2013 Mar; 5(3):344-52.
- Doody RS, Raman R, Sperling RA, Seimers E, Sethuraman G, Mohs R, Farlow M, Iwatsubo T, Vellas B, Sun X, Ernstrom K, Thomas RG, Aisen PS; Alzheimer's Disease Cooperative Study.** Peripheral and central effects of  $\gamma$ -secretase inhibition by semagacestat in Alzheimer's disease. *Alzheimers Res Ther.* 2015 Jun 10; 7(1):36.
- Duan CM, Zhang JR, Wan TF, Wang Y, Chen HS, Liu L.** SRT2104 attenuates chronic unpredictable mild stress-induced depressive-like behaviors and imbalance between microglial M1 and M2 phenotypes in the mice. *Behav Brain Res.* 2020;378:112296.
- Durazzo TC, Mattsson N, Weiner MW; Alzheimer's Disease Neuroimaging Initiative.** Smoking and increased Alzheimer's disease risk: a review of potential mechanisms. *Alzheimers Dement.* 2014 Jun; 10(3 Suppl):S122-45.
- Engel T, Goñi-Oliver P, Lucas JJ, Avila J, Hernández F.** Chronic lithium administration to FTDP-17 tau and GSK-3 $\beta$  overexpressing mice prevents tau hyperphosphorylation and neurofibrillary tangle formation, but pre-formed neurofibrillary tangles do not revert. *J Neurochem.* 2006 Dec; 99(6):1445-55.
- Evin G.** Future therapeutics in Alzheimer's disease: development status of BACE inhibitor. *BioDrugs.* 2016 Jun; 30(3):173-94.
- Fernandez-Martos CM, Atkinson RAK, Chuah MI, King AE, Vickers JC.** Combination treatment with leptin and pioglitazone in a mouse model of Alzheimer's disease. *Alzheimers Dement (N Y).* 2016 Dec 20; 3(1):92-106.

- Fol R, Braudeau J, Ludewig S, Abel T, Weyer SW, Roederer JP, Brod F, Audrain M, Bemelmans AP, Buchholz CJ, Korte M, Cartier N, Müller UC.** Viral gene transfer of APP<sub>sα</sub> rescues synaptic failure in an Alzheimer's disease mouse model. *Acta Neuropathol.* 2016 Feb; 131(2):247-266.
- Forloni G, Artuso V, La Vitola P, Balducci C.** Oligomeropathies and pathogenesis of Alzheimer and Parkinson's diseases. *Mov Disord.* 2016 Jun; 31(6):771-81.
- Frank EM.** Effect of Alzheimer's disease on communication function. *Journal of the South Carolina Medical Association.* 1994 Sep; 90(9):417-23.
- Furukawa K, Sopher BL, Rydel RE, Begley JG, Pham DG, Martin GM, Fox M, Mattson MP.** Increased activity-regulating and neuroprotective efficacy of alpha-secretase-derived secreted amyloid precursor protein conferred by a C-terminal heparin-binding domain. *J Neurochem.* 1996 Nov; 67(5):1882-96.
- Gameiro I, Michalska P, Tenti G, Cores Á, Buendia I, Rojo AI, Georgakopoulos ND, Hernández-Guijo JM, Teresa Ramos M, Wells G, López MG, Cuadrado A, Menéndez JC, León R.** Discovery of the first dual GSK3 $\beta$  inhibitor/Nrf2 inducer. A new multitarget therapeutic strategy for Alzheimer's disease. *Sci Rep.* 2017 Mar 31; 7:45701.
- Gan L and Mucke L** Paths of convergence: sirtuins in aging and neurodegeneration. *Neuron* 2008; 58: pp. 10-14
- Gano LB, Donato AJ, Pasha HM, Hearon CM Jr, Sindler AL, Seals DR.** The SIRT1 activator SRT1720 reverses vascular endothelial dysfunction, excessive superoxide production, and inflammation with aging in mice. *Am J Physiol Heart Circ Physiol.* 2014 Dec 15; 307(12):H1754-63.
- Gao R, Wang Y, Pan Q et al.** Fuzhisan, a chinese herbal medicine, suppresses beta-secretase gene transcription via upregulation of SIRT1 expression in N2a-APP695 cells. *Int J Clin Exp Med* 2015, 8:7231–7240
- Garbayo E, Ansorena E, Blanco-Prieto MJ.** Drug development in Parkinson's disease: from emerging molecules to innovative drug delivery systems. *Maturitas.* 2013 Nov; 76(3):272-8.
- Glampedakis E, Jean M, Amateis C, Büla C.** [Management of pneumonia in advanced stage dementia]. *Rev Med Suisse.* 2016 Nov 9; 12(538):1907-1911.
- Glenner GG, Wong CW.** Alzheimer's disease: initial report of the purification and characterization of a novel cerebrovascular amyloid protein. *Biochem Biophys Res Commun.* 1984 May 16; 120(3):885-90.
- Godyń J, Jończyk J, Panek D, Malawska B.** Therapeutic strategies for Alzheimer's disease in clinical trials. *Pharmacol Rep.* 2016 Feb; 68(1):127-38.
- Gomes P, Fleming Outeiro T, Cavadas C.** Emerging Role of Sirtuin 2 in the Regulation of Mammalian Metabolism. *Trends Pharmacol Sci.* 2015 Nov; 36(11):756-768.
- Gómez Ravetti M, Rosso OA, Berretta R, Moscato P.** Uncovering molecular biomarkers that correlate cognitive decline with the changes of hippocampus' gene expression profiles in Alzheimer's disease. *PLoS One* 2010.
- Grandal Leiros B, Pérez Méndez LI, Zelaya Huerta MV, Moreno Eguinoa L, García-Bragado F, Tuñón Álvarez T, Roldán Larreta JJ.** Prevalence and concordance between the clinical and the post-mortem diagnosis of dementia in a psychogeriatric clinic. *Neurologia.* 2018 Jan - Feb; 33(1):13-17.

- Greenfield JP, Tsai J, Gouras GK, Hai B, Thinakaran G, Checler F, Sisodia SS, Greengard P, Xu H.** Endoplasmic reticulum and trans-Golgi network generate distinct populations of Alzheimer beta-amyloid peptides. *Proc Natl Acad Sci USA*. 1999 Jan 19; 96(2):742-7.
- Greenough MA, Camakaris J, Bush AI** Metal dyshomeostasis and oxidative stress in Alzheimer's disease. *Neurochem Int* 2013; 62, 540-555.
- Grimm MO, Grimm HS, Pätzold AJ, Zinser EG, Halonen R, Duering M, Tschäpe JA, De Strooper B, Müller U, Shen J, Hartmann T.** Regulation of cholesterol and sphingomyelin metabolism by amyloid-beta and presenilin. *Nat Cell Biol*. 2005 Nov; 7(11):1118-23.
- Guan Q, Wang M, Chen H, Yang L, Yan Z, Wang X.** Aging-related 1-methyl-4-phenyl-1,2,3,6-tetrahydropyridine-induced neurochemical and behavioral deficits and redox dysfunction: improvement by AK-7. *Exp Gerontol*. 2016 Sep; 82:19-29.
- Gueguen C, Palmier B, Plotkine M, Marchand-Leroux C, Besson VC.** Neurological and histological consequences induced by in vivo cerebral oxidative stress: evidence for beneficial effects of SRT1720, a sirtuin 1 activator, and sirtuin 1-mediated neuroprotective effects of poly(ADP-ribose) polymerase inhibition. *PLoS One*. 2014 Feb 21; 9(2):e87367.
- Hansen LW, Khader A, Yang WL, Prince JM, Nicastro JM, Coppa GF, Wang P.** Sirtuin 1 activator SRT1720 protects against organ injury induced by intestinal ischemia-reperfusion. *Shock*. 2016 Apr; 45(4):359-66.
- Hardy JA, Higgins GA.** Alzheimer's disease: the amyloid cascade hypothesis. *Science*. 1992 Apr 10; 256(5054):184-5.
- Hardy J.** A hundred years of Alzheimer's disease research. *Neuron*. 2006 Oct.
- Harrison IF, Smith AD, Dexter DT.** Pathological histone acetylation in Parkinson's disease: Neuroprotection and inhibition of microglial activation through SIRT 2 inhibition. *Neuroscience letters*. 2018 Feb 14; 666:48-57.
- Harrison SM, Harper AJ, Hawkins J, Duddy G, Grau E, Pugh PL, Winter PH, Shilliam CS, Hughes ZA, Dawson LA, Gonzalez MI, Upton N, Pangalos MN, Dingwall C.** BACE1 (beta-secretase) transgenic and knockout mice: identification of neurochemical deficits and behavioral changes. *Mol Cell Neurosci*. 2003 Nov; 24(3):646-55.
- Hasebe N, Fujita Y, Ueno M, Yoshimura K, Fujino Y, Yamashita T.** Soluble  $\beta$ -amyloid Precursor Protein Alpha binds to p75 neurotrophin receptor to promote neurite outgrowth. *PLoS One*. 2013 Dec 16; 8(12):e82321.
- Herman L, Atri A, Salloway S.** Alzheimer's Disease in Primary Care: The Significance of Early Detection, Diagnosis, and Intervention. *Am J Med*. 2017 Jun; 130(6):756.
- Hickman SE, Allison EK, El Khoury J.** Microglial dysfunction and defective beta-amyloid clearance pathways in aging Alzheimer's disease mice. *J Neurosci*. 2008 Aug 13; 28(33):8354-60.
- Hishikawa N, Fukui Y, Sato K, Ohta Y, Yamashita T, Abe K.** Comprehensive effects of galantamine and cilostazol combination therapy on patients with Alzheimer's disease with asymptomatic lacunar infarction. *Geriatr Gerontol Int*. 2017 Oct; 17(10):1384-1391.
- Hoare TR e Kohane DS.** Hydrogels in drug delivery: Progress and challenges. *Polymer*. 2008. (<https://doi.org/10.1016/j.polymer.2008.01.027>).
- Holtzman DM, Morris JC, Goate AM.** Alzheimer's disease: the challenge of the second century. *Sci Transl Med*. 2011 Apr 6; 3(77):77sr1.

- Hong LTA, Kim YM, Park HH, Hwang DH, Cui Y, Lee EM, Yahn S, Lee JK, Song SC, Kim BG.** An injectable hydrogel enhances tissue repair after spinal cord injury by promoting extracellular matrix remodeling. *Nat Commun.* 2017 Sep 14; 8(1):533.
- Hong W, Wang Z, Liu W, et al.** Diffusible, highly bioactive oligomers represent a critical minority of soluble A $\beta$  in Alzheimer's disease brain. *Acta Neuropathol.* 2018;136(1):19-40.
- Horvath P, Aulner N, Bickle M, et al.** Screening out irrelevant cell-based models of disease. *Nat Rev Drug Discov.* 2016;15(11):751–769.
- Hou X, Rooklin D, Fang H, Zhang Y.** Resveratrol serves as a protein-substrate interaction stabilizer in human SIRT1 activation. *Sci Rep.* 2016 Nov 30; 6:38186.
- Howitz KT, Bitterman KJ, Cohen HY, Lamming DW, Lavu S, Wood JG, Zipkin RE, Chung P, Kisielewski A, Zhang LL, Scherer B, Sinclair DA.** Small molecule activators of sirtuins extend *Saccharomyces cerevisiae* lifespan. *Nature.* 2003 Sep 11; 425(6954):191-6.
- Huang B, Tabata Y, Gao JQ.** Mesenchymal stem cells as therapeutic agents and potential targeted gene delivery vehicle for brain diseases. *J Control Release.* 2012 Sep 10; 162(2):464-73.
- Huang X, Atwood CS, Hartshorn MA, Multhaup G, Goldstein LE, Scarpa RC, Cuajungco MP, Gray DN, Lim J, Moir RD, Tanzi RE, Bush AI** The A beta peptide of Alzheimer's disease directly produces hydrogen peroxide through metal ion reduction. *Biochemistry* 1999; 38, 7609-7616.
- Hubbard BP, Sinclair DA.** Small molecule SIRT1 activators for the treatment of aging and age-related diseases. *Trends Pharmacol Sci.* 2014 Mar; 35(3):146-54.
- Hunter S, Brayne C.** Do anti-amyloid beta protein antibody cross reactivities confound Alzheimer disease research? [published correction appears in *J Negat Results Biomed.* 2017 Mar 8;16(1):8]. *J Negat Results Biomed.* 2017;16(1):1.
- Imai S, Guarente L.** Ten years of NAD-dependent SIR2 family deacetylases: implications for metabolic diseases. *Trends Pharmacol Sci.* 2010 May; 31(5):212-20.
- Inoue T, Hiratsuka M, Osaki M, Yamada H, Kishimoto I, Yamaguchi S, Nakano S, Katoh M, Ito H, Oshimura M.** SIRT2, a tubulin deacetylase, acts to block the entry to chromosome condensation in response to mitotic stress. *Oncogene.* 2007 Feb 15; 26(7):945-57.
- Irie K, Murakami K, Masuda Y, Morimoto A, Ohigashi H, Ohashi R, Takegoshi K, Nagao M, Shimizu T, Shirasawa T.** Structure of beta-amyloid fibrils and its relevance to their neurotoxicity: implications for the pathogenesis of Alzheimer's disease. *J Biosci Bioeng.* 2005 May; 99(5):437-47.
- Isik AT.** Late onset Alzheimer's disease in older people. *Clin Interv Aging.* 2010 Oct 11; 5:307-11.
- Jawhar S, Trawicka A, Jenneckens C, Bayer TA, Wirths O.** Motor deficits, neuron loss, and reduced anxiety coinciding with axonal degeneration and intraneuronal A $\beta$  aggregation in the 5XFAD mouse model of Alzheimer's disease. *Neurobiol Aging.* 2012 Jan; 33(1):196.e29-40.
- Jeřábek J, Uliassi E, Guidotti L, Korábečný J, Soukup O, Sepsova V, Hrabínova M, Kuča K, Bartolini M, Peña-Altamira LE, Petralla S, Monti B, Roberti M, Bolognesi ML.** Tacrine-resveratrol fused hybrids as multi-target-directed ligands against Alzheimer's disease. *Eur J Med Chem.* 2017 Feb 15;127:250-262.

- Jęsko H, Wencel P, Strosznajder RP, Strosznajder JB.** Sirtuins and Their Roles in Brain Aging and Neurodegenerative Disorders. *Neurochem Res.* 2017 Mar;42(3):876-890.
- Jiang M, Zheng J, Peng Q, Hou Z, Zhang J, Mori S, Ellis JL, Vlasuk GP, Fries H, Suri V, Duan W.** Sirtuin 1 activator SRT2104 protects Huntington's disease mice. *Ann Clin Transl Neurol.* 2014 Dec;1(12):1047-52.
- Jorfi M, D'Avanzo C, Kim DY, Irimia D.** Three-Dimensional Models of the Human Brain Development and Diseases. *Adv Healthc Mater.* 2018;7(1):10.
- Julien C, Tremblay C, Emond V et al.** Sirtuin 1 reduction parallels the accumulation of tau in Alzheimer disease. *J Neuropathol Exp Neurol* 2009; 68:48–58.
- Jung YW, Hysolli E, Kim KY, Tanaka Y, Park IH.** Human induced pluripotent stem cells and neurodegenerative disease: prospects for novel therapies. *Curr Opin Neurol.* 2012 Apr; 25(2):125-30.
- Kaeberlein M, McVey M, Guarente L.** The SIR2/3/4 complex and SIR2 alone promote longevity in *Saccharomyces cerevisiae* by two different mechanisms. *Genes Dev.* 1999 Oct 1; 13(19):2570-80.
- Kaluski S, Portillo M, Besnard A, Stein D, Einav M, Zhong L, Ueberham U, Arendt T, Mostoslavsky R, Sahay A, Toiber D.** Neuroprotective Functions for the Histone Deacetylase SIRT6. *Cell Rep.* 2017 Mar 28; 18(13):3052-3062.
- Kamenetz F, Tomita T, Hsieh H, Seabrook G, Borchelt D, Iwatsubo T, Sisodia S, Malinow R.** APP processing and synaptic function. *Neuron.* 2003 Mar 27; 37(6):925-37.
- Kandalepas PC, Sadleir KR, Eimer WA, Zhao J, Nicholson DA, Vassar R.** The Alzheimer's  $\beta$ -secretase BACE1 localizes to normal presynaptic terminals and to dystrophic presynaptic terminals surrounding amyloid plaques. *Acta Neuropathol.* 2013 Sep; 126(3):329-52.
- Kedar N. Prasad,** Simultaneous activation of Nrf2 and elevation of antioxidant compounds for reducing oxidative stress and chronic inflammation in human Alzheimer's disease. *Mechanisms of Ageing and Development, Vol 153, 2016, p. 41-47.*
- Kennedy ME, Stamford AW, Chen X, Cox K, Cumming JN, Dockendorf MF, Egan M, Ereshefsky L, Hodgson RA, Hyde LA, Jhee S, Kleijn HJ, Kuvelkar R, Li W, Mattson BA, Mei H, Palcza J, Scott JD, Tanen M, Troyer MD, Tseng JL, Stone JA, Parker EM, Forman MS.** The BACE1 inhibitor verubecestat (MK-8931) reduces CNS  $\beta$ -amyloid in animal models and in Alzheimer's disease patients. *Sci Transl Med.* 2016 Nov 2; 8(363):363ra150.
- Khaing Z, Thomas RC, Geissler SA, Schmidt CE.** Advanced biomaterials for repairing the nervous system: what can hydrogels do for the brain? *Materials Today* 2014. 17(7), 332-340.
- Khanfar MA, Quinti L, Wang H, Choi SH, Kazantsev AG, Silverman RB.** Development and characterization of 3-(benzylsulfonamido)benzamides as potent and selective SIRT2 inhibitors. *Eur J Med Chem.* 2014 Apr 9; 76:414-26.
- Kim DH, Yeo SH, Park JM, Choi JY, Lee TH, Park SY, Ock MS, Eo J, Kim HS, Cha HJ.** Genetic markers for diagnosis and pathogenesis of Alzheimer's disease. *Gene.* 2014 Jul 25; 545(2):185-93.
- Kim H-S, Moon S, Paik J-H et al** Activation of the 5' -AMP-activated protein kinase in the cerebral cortex of young senescence-accelerated P8 mice and association with GSK3 $\beta$ - and PP2A-dependent inhibition of p-tau396 expression. *J Alzheimers Dis* 2015; 46:249–259.

- Kim HJ, Seo SW, Chang JW, et al.** Stereotactic brain injection of human umbilical cord blood mesenchymal stem cells in patients with Alzheimer's disease dementia: a phase 1 clinical trial. *Alzheimers Dement (N Y)* 2015; 1:95–102.
- Kim HS, Vassilopoulos A, Wang RH, Lahusen T, Xiao Z, Xu X, Li C, Veenstra TD, Li B, Yu H, Ji J, Wang XW, Park SH, Cha YI, Gius D, Deng CX.** SIRT2 maintains genome integrity and suppresses tumorigenesis through regulating APC/C activity. *Cancer Cell*. 2011 Oct 18; 20(4):487-99.
- Klar AJ, Fogel S, Macleod K.** MAR1-a Regulator of the HMa and HMalpha Loci in *Saccharomyces Cerevisiae*. *Genetics*. 1979 Sep;93(1):37-50.
- Ko, K. R., & Frampton, J. P.** Developments in 3D neural cell culture models: The future of neurotherapeutics testing? *Expert Review of Neurotherapeutics*, 2016, 16(7), 739–741.
- Kojro E, Füger P, Prinzen C, Kanarek AM, Rat D, Endres K, Fahrenholz F, Postina R.** Statins and the squalene synthase inhibitor zaragozic acid stimulate the non-amyloidogenic pathway of amyloid-beta protein precursor processing by suppression of cholesterol synthesis. *J Alzheimers Dis*. 2010; 20(4):1215-31.
- Koo JH, Kang EB, Oh YS, Yang DS, Cho JY.** Treadmill exercise decreases amyloid- $\beta$  burden possibly via activation of SIRT-1 signaling in a mouse model of Alzheimer's disease. *Exp Neurol*. 2017 Feb; 288:142-152.
- Kopecek J.** Hydrogel biomaterials: a smart future? *Biomaterials*. 2007 Dec; 28(34):5185-92.
- Krueger JG, Suárez-Fariñas M, Cueto I, Khacherian A, Matheson R, Parish LC, Leonardi C, Shortino D, Gupta A, Haddad J, Vlasuk GP, Jacobson EW.** A Randomized, Placebo-Controlled Study of SRT2104, a SIRT1 Activator, in Patients with Moderate to Severe Psoriasis. *PLoS One*. 2015 Nov 10; 10(11):e0142081.
- Kuhn PH, Wang H, Dislich B, Colombo A, Zeitschel U, Ellwart JW, Kremmer E, Rossner S, Lichtenthaler SF.** ADAM10 is the physiologically relevant, constitutive alpha-secretase of the amyloid precursor protein in primary neurons. *EMBO J*. 2010 Sep 1; 29(17):3020-32.
- Kumar P, Choonara YE, Modi G, Naidoo D, Pillay V.** Multifunctional therapeutic delivery strategies for effective neuro-regeneration following traumatic spinal cord injury. *Curr Pharm Des*. 2015; 21(12):1517-28.
- Kumar S and Walter J.** Phosphorylation of amyloid- $\beta$  (A $\beta$ ) peptides - A trigger for formation of toxic aggregates in Alzheimer's disease. *Aging*. 2011 Aug;3(8):803-12.
- Ladiwala AR, Litt J, Kane RS, Aucoin DS, Smith SO, Ranjan S, Davis J, Van Nostrand WE, Tessier PM.** Conformational differences between two amyloid  $\beta$  oligomers of similar size and dissimilar toxicity. *J Biol Chem*. 2012 Jul 13; 287(29):24765-73.
- La Ferla FM, Green KN.** Animal models of Alzheimer disease. *Cold Spring Harb Perspect Med*. 2012 Nov 1; 2(11).
- Lalla R, Donmez G.** The role of sirtuins in Alzheimer's disease. *Front Aging Neurosci*. 2013 Apr 9; 5:16.
- Lammich S, Kojro E, Postina R, Gilbert S, Pfeiffer R, Jasionowski M, Haass C, Fahrenholz F** Constitutive and regulated alpha-secretase cleavage of Alzheimer's amyloid precursor protein by a disintegrin metalloprotease. *Proc Natl Acad Sci USA* 1999; 96, 3922-3927.



- Landry J, Slama JT, Sternglanz R.** Role of NAD(+) in the deacetylase activity of the SIR2-like proteins. *Biochem Biophys Res Commun.* 2000 Nov 30; 278(3):685-90.
- Lattanzio F, Carboni L, Carretta D et al.** Treatment with the neurotoxic A $\beta$  (25–35) peptide modulates the expression of neuroprotective factors Pin1, Sirtuin 1, and brain-derived neurotrophic factor in SH-SY5Y human neuroblastoma cells. *Exp Toxicol Pathol* 2016; 68:271–276.
- Lee CW, Shih YH, Kuo YM.** Cerebrovascular pathology and amyloid plaque formation in Alzheimer's disease. *Curr Alzheimer Res.* 2014 Jan; 11(1):4-10.
- Lee HR, Shin HK, Park SY et al** Cilostazol suppresses  $\beta$ -amyloid production by activating a disintegrin and metalloproteinase 10 via the upregulation of SIRT1-coupled retinoic acid receptor- $\beta$ . *J Neurosci Res* 2014; 92:1581–1590.
- Lesné SE, Koh MT, Kotilinek L, Kaye R, Glabe CG, Yang A, Gallagher M, Ashe KH.** A specific amyloid-beta protein assembly in the brain impairs memory. *Nature.* 2006 Mar 16; 440(7082):352-7.
- Lesné SE, Sherman MA, Grant M, et al.** Brain amyloid- $\beta$  oligomers in ageing and Alzheimer's disease. *Brain.* 2013;136(Pt 5):1383-1398.
- Li J, Darabi M, Gu J, Shi J, Xue J, Huang L, Liu Y, Zhang L, Liu N, Zhong W, Zhang L, Xing M, Zhang L.** A drug delivery hydrogel system based on activin B for Parkinson's disease. *Biomaterials.* 2016 Sep; 102:72-86.
- Li J, Mooney DJ.** Designing hydrogels for controlled drug delivery. *Nat Rev Mater.* 2016 Dec;1(12). pii: 16071.
- Li S, Yin J, Nielsen M, Beach TG, Guo L, Shi J.** Sirtuin 3 Mediates Tau Deacetylation. *J Alzheimers Dis.* 2019 Apr 1.
- Li W, Luo R, Lin X, Jadhav AD, Zhang Z, Yan L, Chan CY, Chen X, He J, Chen CH, Shi P.** Remote modulation of neural activities via near-infrared triggered release of biomolecules. *Biomaterials.* 2015 Oct; 65:76-85.
- Li XY, Bao XJ, Wang RZ.** Potential of neural stem cell-based therapies for Alzheimer's disease. *J Neurosci Res* 2015; 93:1313–1324.
- Libri V, Brown AP, Gambarota G, Haddad J, Shields GS, Dawes H, Pinato DJ, Hoffman E, Elliot PJ, Vlasuk GP, Jacobson E, Wilkins MR, Matthews PM.** A pilot randomized, placebo controlled, double blind phase I trial of the novel SIRT1 activator SRT2104 in elderly volunteers. *PLoS One.* 2012; 7(12):e51395.
- Lim S, Haque MM, Kim D, Kim DJ, Kim YK.** Cell-based Models To Investigate Tau Aggregation. *Comput Struct Biotechnol J.* 2014 Oct 2; 12(20-21):7-13.
- Liu L, Arun A, Ellis L, Peritore C, Donmez G.** SIRT2 enhances 1-methyl-4-phenyl-1,2,3,6-tetrahydropyridine (MPTP)-induced nigrostriatal damage via apoptotic pathway. *Front Aging Neurosci.* 2014 Aug 11; 6:184.
- Liu Y, Cheng A, Li YJ, Yang Y, Kishimoto Y, Zhang S, Wang Y, Wan R, Raefsky SM, Lu D, Saito T, Saido T, Zhu J, Wu LJ, Mattson MP.** SIRT3 mediates hippocampal synaptic adaptations to intermittent fasting and ameliorates deficits in APP mutant mice. *Nat Commun.* 2019 Apr 23; 10(1):1886.
- Luthi-Carter R, Taylor DM, Pallos J, Lambert E, Amore A, Parker A, Moffitt H, Smith DL, Runne H, Gokce O, Kuhn A, Xiang Z, Maxwell MM, Reeves SA, Bates GP, Neri C, Thompson LM, Marsh JL, Kazantsev AG.** SIRT2 inhibition achieves neuroprotection by

- decreasing sterol biosynthesis. *Proceedings of the National Academy of Science of the USA*. 2010 Apr 27; 107(17):7927-32.
- Lutz MI, Milenkovic I, Regelsberger G, Kovacs GG** Distinct patterns of sirtuin expression during progression of Alzheimer's disease. *Neuromolecular Med* 2014; 16:405–414.
- Mahoney-Sanchez L, Belaidi AA, Bush AI, Ayton S.** The Complex Role of Apolipoprotein E in Alzheimer's Disease: an Overview and Update. *J Mol Neurosci*. 2016 Nov; 60(3):325-335.
- Mantyh PW, Ghilardi JR, Rogers S, DeMaster E, Allen CJ, Stimson ER, Maggio JE** Aluminum, iron, and zinc ions promote aggregation of physiological concentrations of beta-amyloid peptide. *J Neurochem* 1993; 61, 1171-1174.
- Marcello E, Saraceno C, Musardo S, Vara H, de la Fuente AG, Pelucchi S, Di Marino D, Borroni B, Tramontano A, Pérez-Otaño I, Padovani A, Giustetto M, Gardoni F, Di Luca M.** Endocytosis of synaptic ADAM10 in neuronal plasticity and Alzheimer's disease. *J Clin Invest*. 2013 Jun;123(6):2523-38.
- Masters CL, Bateman R, Blennow K, Rowe CC, Sperling RA, Cummings JL.** Alzheimer's disease. *Nat Rev Dis Primers*. 2015 Oct 15; 1:15056.
- Mastrangelo MA, Bowers WJ.** Detailed immunohistochemical characterization of temporal and spatial progression of Alzheimer's disease-related pathologies in male triple-transgenic mice. *BMC Neurosci*. 2008 Aug 12; 9:81.
- Matsunaga S, Kishi T, Iwata N.** Combination therapy with cholinesterase inhibitors and memantine for Alzheimer's disease: a systematic review and meta-analysis. *Int J Neuropsychopharmacol*. 2014 Dec 28;18(5).
- Mattson MP.** Cellular actions of beta-amyloid precursor protein and its soluble and fibrillogenic derivatives. *Physiol Rev*. 1997 Oct; 77(4):1081-132.
- Mawuenyega KG, Sigurdson W, Ovod V, Munsell L, Kasten T, Morris JC, Yarasheski KE, Bateman RJ.** Decreased clearance of CNS beta-amyloid in Alzheimer's disease. *Science*. 2010 Dec 24; 330(6012):1774.
- Maxwell MM, Tomkinson EM, Nobles J, Wizeman JW, Amore AM, Quinti L, Chopra V, Hersch SM, Kazantsev AG.** The Sirtuin 2 microtubule deacetylase is an abundant neuronal protein that accumulates in the aging CNS. *Hum Mol Genet*. 2011 Oct 15; 20(20):3986-96.
- McKoy AF, Chen J, Schupbach T, Hecht MH.** Structure-activity relationships for a series of compounds that inhibit aggregation of the Alzheimer's peptide, A $\beta$ 42. *Chem Biol Drug Des*. 2014 Nov; 84(5):505-12.
- Mercken EM, Mitchell SJ, Martin-Montalvo A, Minor RK, Almeida M, Gomes AP, Scheibye-Knudsen M, Palacios HH, Licata JJ, Zhang Y, Becker KG, Khraiweh H, González-Reyes JA, Villalba JM, Baur JA, Elliott P, Westphal C, Vlasuk GP, Ellis JL, Sinclair DA, Bernier M, de Cabo R.** SRT2104 extends survival of male mice on a standard diet and preserves bone and muscle mass. *Aging Cell*. 2014 Oct;13(5):787-96.
- Michan S, Sinclair D.** Sirtuins in mammals: insights into their biological function. *Biochem J*. 2007 May 15; 404(1):1-13. Review.
- Mielke MM, Vemuri P, Rocca WA.** Clinical epidemiology of Alzheimer's disease: assessing sex and gender differences. *Clin Epidemiol*. 2014 Jan 8; 6:37-48.

- Milne JC, Lambert PD, Schenk S, Carney DP, Smith JJ, Gagne DJ, Jin L, Boss O, Perni RB, Vu CB, Bemis JE, Xie R, Disch JS, Ng PY, Nunes JJ, Lynch AV, Yang H, Galonek H, Israelian K, Choy W, Iffland A, Lavu S, Medvedik O, Sinclair DA, Olefsky JM, Jirousek MR, Elliott PJ, Westphal CH.** Small molecule activators of SIRT1 as therapeutics for the treatment of type 2 diabetes. *Nature*. 2007 Nov 29; 450(7170):712-6.
- Min SW, Cho SH, Zhou Y, Schroeder S, Haroutunian V, Seeley WW, Huang EJ, Shen Y, Masliah E, Mukherjee C, Meyers D, Cole PA, Ott M, Gan L.** Acetylation of tau inhibits its degradation and contributes to tauopathy. *Neuron*. 2010 Sep 23; 67(6):953-66.
- Min SW, Chen X, Tracy TE, Li Y, Zhou Y, Wang C, Shirakawa K, Minami SS, Defensor E, Mok SA, Sohn PD, Schilling B, Cong X, Ellerby L, Gibson BW, Johnson J, Krogan N, Shamloo M, Gestwicki J, Masliah E, Verdin E, Gan L.** Critical role of acetylation in tau-mediated neurodegeneration and cognitive deficits. *Nat Med*. 2015; 21:1154–1162.
- Min SW, Sohn PD, Li Y, Devidze N, Johnson JR, Krogan NJ, Masliah E, Mok SA, Gestwicki JE, Gan L.** SIRT1 Deacetylates Tau and Reduces Pathogenic Tau Spread in a Mouse Model of Tauopathy. *J Neurosci*. 2018 Apr 11; 38(15):3680-3688.
- Minor RK, Baur JA, Gomes AP, Ward TM, Csiszar A, Mercken EM, Abdelmohsen K, Shin YK, Canto C, Scheibye-Knudsen M, Krawczyk M, Irusta PM, Martín-Montalvo A, Hubbard BP, Zhang Y, Lehrmann E, White AA, Price NL, Swindell WR, Pearson KJ, Becker KG, Bohr VA, Gorospe M, Egan JM, Talan MI, Auwerx J, Westphal CH, Ellis JL, Ungvari Z, Vlasuk GP, Elliott PJ, Sinclair DA, de Cabo R.** SIRT1720 improves survival and healthspan of obese mice. *Sci Rep*. 2011; 1:70.
- Mitchell SJ, Martin-Montalvo A, Mercken EM, Palacios HH, Ward TM, Abulwerdi G, Minor RK, Vlasuk GP, Ellis JL, Sinclair DA, Dawson J, Allison DB, Zhang Y, Becker KG, Bernier M, de Cabo R.** The SIRT1 activator SIRT1720 extends lifespan and improves health of mice fed a standard diet. *Cell Rep*. 2014 Mar 13; 6(5):836-43.
- Moghadam FH, Alaie H, Karbalaie K, Tanhaei S, Nasr Esfahani MH, Baharvand H.** Transplantation of primed or unprimed mouse embryonic stem cell-derived neural precursor cells improves cognitive function in Alzheimerian rats. *Differentiation*. 2009 Sep-Oct; 78(2-3):59-68.
- Mohamad Nasir NF, Zainuddin A, Shamsuddin S.** Emerging Roles of Sirtuin 6 in Alzheimer's Disease. *J Mol Neurosci*. 2018 Feb;64(2):157-161.
- Mondragon-Rodriguez S, Perry G, Zhu X, Moreira PI, Acevedo-Aquino MC, Williams S** Phosphorylation of tau protein as the link between oxidative stress, mitochondrial dysfunction, and connectivity failure: Implications for Alzheimer's disease. *Oxid Med Cell Longev* 2013, 940603.
- Morales I, Guzmán-Martínez L, Cerda-Troncoso C, Farías GA, Maccioni RB.** Neuroinflammation in the pathogenesis of Alzheimer's disease. A rational framework for the search of novel therapeutic approaches. *Front Cell Neurosci* 2014; 8:112.
- Mori T, Koyama N, Tan J, Segawa T, Maeda M, Town T.** Combination therapy with octyl gallate and ferulic acid improves cognition and neurodegeneration in a transgenic mouse model of Alzheimer's disease. *J Biol Chem*. 2017 Jul 7; 292(27):11310-11325.
- Mota SI, Costa RO, Ferreira IL, et al.** Oxidative stress involving changes in Nrf2 and ER stress in early stages of Alzheimer's disease. *Biochim Biophys Acta*. 2015;1852(7):1428-1441.
- Mroczo B, Groblewska M, Litman-Zawadzka A, Kornhuber J, Lewczuk P.** Amyloid  $\beta$  oligomers (A $\beta$ Os) in Alzheimer's disease. *J Neural Transm (Vienna)*. 2018 Feb; 125(2):177-191.

- Müller UC, Deller T.** Editorial: The Physiological Functions of the APP Gene Family. *Front Mol Neurosci.* 2017 Oct 23; 10:334.
- Munarin F, Petrini P, Bozzini S, Tanzi MC.** New perspectives in cell delivery systems for tissue regeneration: natural-derived injectable hydrogels. *J Appl Biomater Funct Mater.* 2012 Sep 27; 10(2):67-81.
- Murray MM, Bernstein SL, Nyugen V, Condrón MM, Teplow DB, Bowers MT.** Amyloid beta protein: Abeta40 inhibits Abeta42 oligomerization. *J Am Chem Soc.* 2009 May 13; 131(18):6316-7.
- Nguyen KT, Pham MN, Vo TV, Duan W, Tran PH, Tran TT.** Strategies of Engineering Nanoparticles for Treating Neurodegenerative Disorders. *Curr Drug Metab.* 2017; 18(9):786-797.
- Nhan HS, Chiang K, Koo EH.** The multifaceted nature of amyloid precursor protein and its proteolytic fragments: friends and foes. *Acta Neuropathol.* 2015 Jan; 129(1):1-19.
- Neu SC, Pa J, Kukull W, Beekly D, Kuzma A, Gangadharan P, Wang LS, Romero K, Arneric SP, Redolfi A, Orlandi D, Frisoni GB, Au R, Devine S, Auerbach S, Espinosa A, Boada M, Ruiz A, Johnson SC, Kosciak R, Wang JJ, Hsu WC, Chen YL, Toga AW.** Apolipoprotein E Genotype and Sex Risk Factors for Alzheimer Disease: A Meta-analysis. *JAMA Neurol.* 2017 Oct 1; 74(10):1178-1189.
- Nishida K, Matsushita T, Takayama K, Tanaka T, Miyaji N, Ibaraki K, Araki D, Kanzaki N, Matsumoto T, Kuroda R.** Intraperitoneal injection of the SIRT1 activator SRT1720 attenuates the progression of experimental osteoarthritis in mice. *Bone Joint Res.* 2018 May 5;7(3):252-262.
- Niu H, Álvarez-Álvarez I, Guillén-Grima F, Aguinaga-Ontoso I.** Prevalence and incidence of Alzheimer's disease in Europe: A meta-analysis. *Neurologia.* 2017 Oct; 32(8):523-532.
- Nobili A, Latagliata EC, Viscomi MT, Cavallucci V, Cutuli D, Giacobuzzo G, Krashia P, Rizzo FR, Marino R, Federici M, De Bartolo P, Aversa D, Dell'Acqua MC, Cordella A, Sancandi M, Keller F, Petrosini L, Puglisi-Allegra S, Mercuri NB, Coccurello R, Berretta N, D'Amelio M.** Dopamine neuronal loss contributes to memory and reward dysfunction in a model of Alzheimer's disease. *Nat Commun.* 2017 Apr 3; 8:14727.
- North BJ, Marshall BL, Borra MT, Denu JM, Verdin E.** The human Sir2 ortholog, SIRT2, is an NAD<sup>+</sup>-dependent tubulin deacetylase. *Mol Cell.* 2003 Feb; 11(2):437-44.
- Nunomura A, Perry G, Aliev G, Hirai K, Takeda A, Balraj EK, et al.** Oxidative damage is the earliest event in Alzheimer disease. *J Neuropathol Exp Neurol* 2001; 60:759–67.
- Obregon D, Hou H, Deng J, Giunta B, Tian J, Darlington D, Shahaduzzaman M, Zhu Y, Mori T, Mattson MP, Tan J.** Soluble amyloid precursor protein- $\alpha$  modulates  $\beta$ -secretase activity and amyloid- $\beta$  generation. *Nat Commun.* 2012 Apr 10; 3:777.
- O'Brien JT, Markus HS.** Vascular risk factors and Alzheimer's disease. *BMC Med.* 2014 Nov 11; 12:218.
- Oddo S, Caccamo A, Shepherd JD, Murphy MP, Golde TE, Kaye R, Metherate R, Mattson MP, Akbari Y, LaFerla FM.** Triple-transgenic model of Alzheimer's disease with plaques and tangles: intracellular Abeta and synaptic dysfunction. *Neuron.* 2003 Jul 31; 39(3):409-21.
- Oddo S, Caccamo A, Tran L, Lambert MP, Glabe CG, Klein WL, LaFerla FM.** Temporal profile of amyloid-beta (Abeta) oligomerization in an in vivo model of Alzheimer disease. A link between Abeta and tau pathology. *J Biol Chem.* 2006 Jan 20;281(3):1599-604.

- O'Loughlin A, Kulkarni M, Creane M, Vaughan EE, Mooney E, Shaw G, Murphy M, Dockery P, Pandit A, O'Brien T.** Topical administration of allogeneic mesenchymal stromal cells seeded in a collagen scaffold augments wound healing and increases angiogenesis in the diabetic rabbit ulcer. *Diabetes*. 2013 Jul; 62(7):2588-94.
- Olsson B, Lautner R, Andreasson U, Öhrfelt A, Portelius E, Bjerke M, Hölttä M, Rosén C, Olsson C, Strobel G, Wu E, Dakin K, Petzold M, Blennow K, Zetterberg H.** CSF and blood biomarkers for the diagnosis of Alzheimer's disease: a systematic review and meta-analysis. *Lancet Neurol*. 2016 Jun; 15(7):673-684.
- Ordóñez-Gutiérrez L, Antón M, Wandosell F.** Peripheral amyloid levels present gender differences associated with aging in A $\beta$ PP/PS1 mice. *J Alzheimers Dis*. 2015; 44(4):1063-8.
- Oset-Gasque MJ, Marco-Contelles J.** Alzheimer's Disease, the "One-Molecule, One-Target" Paradigm, and the Multitarget Directed Ligand Approach. *ACS Chem Neurosci*. 2018 Mar 21;9(3):401-403.
- Ou L, Li W, Zhang Y, Wang W, Liu J, Sorg H, Furlani D, Gäbel R, Mark P, Klopsch C, Wang L, Lützow K, Lendlein A, Wagner K, Klee D, Liebold A, Li RK, Kong D, Steinhoff G, Ma N.** Intracardiac injection of matrigel induces stem cell recruitment and improves cardiac functions in a rat myocardial infarction model. *J Cell Mol Med*. 2011 Jun; 15(6):1310-8.
- Outeiro TF, Kontopoulos E, Altmann SM, Kufareva I, Strathearn KE, Amore AM, Volk CB, Maxwell MM, Rochet JC, McLean PJ, Young AB, Abagyan R, Feany MB, Hyman BT, Kazantsev AG.** Sirtuin 2 inhibitors rescue alpha-synuclein-mediated toxicity in models of Parkinson's disease. *Science*. 2007 Jul 27; 317(5837):516-9.
- Pajak B, Kania E, Orzechowski A. Killing Me Softly: Connotations to Unfolded Protein Response and Oxidative Stress in Alzheimer's Disease.** *Oxid Med Cell Longev*. 2016; 2016:1805304.
- Pakulska MM, Ballios BG, Shoichet MS.** Injectable hydrogels for central nervous system therapy. *Biomed Mater*. 2012 Apr; 7(2):024101.
- Pandithage R, Lilischkis R, Harting K, Wolf A, Jedamzik B, Lüscher-Firzlaff J, Vervoorts J, Lasonder E, Kremmer E, Knöll B, Lüscher B.** The regulation of SIRT2 function by cyclin-dependent kinases affects cell motility. *J Cell Biol*. 2008 Mar 10; 180(5):915-29.
- Park EY, Rho HM.** The transcriptional activation of the human copper/zinc superoxide dismutase gene by 2,3,7,8-tetrachlorodibenzo-p-dioxin through two different regulator sites, the antioxidant responsive element and xenobiotic responsive element. *Mol Cell Biochem*. 2002;240(1-2):47-55.
- Pasciuto E, Ahmed T, Wahle T, Gardoni F, D'Andrea L, Pacini L, Jacquemont S, Tassone F, Balschun D, Dotti CG, Callaerts-Vegh Z, D'Hooge R, Müller UC, Di Luca M, De Strooper B, Bagni C.** Dysregulated ADAM10-Mediated Processing of APP during a Critical Time Window Leads to Synaptic Deficits in Fragile X Syndrome. *Neuron*. 2015 Jul 15; 87(2):382-98.
- Peppas NA, Bures P, Leobandung W, Ichikawa H.** Hydrogels in pharmaceutical formulations. *Eur J Pharm Biopharm*. 2000 Jul; 50(1):27-46.
- Perez FP, Bose D, Maloney B et al** Late-onset Alzheimer's disease, heating up and foxed by several proteins: pathomolecular effects of the aging process. *J Alzheimers Dis* 2014; 40:1–17.
- Perl DP.** Neuropathology of Alzheimer's disease. *The Mount Sinai journal of medicine, New York*. 2010 Jan-Feb;77(1):32-42.

- Pfister JA, Ma C, Morrison BE, D'Mello SR.** Opposing effects of sirtuins on neuronal survival: SIRT1-mediated neuroprotection is independent of its deacetylase activity. *PLoS One*. 2008; 3(12):e4090.
- Picard F, Kurtev M, Chung N, Topark-Ngarm A, Senawong T, Machado De Oliveira R, Leid M, McBurney MW, Guarente L.** Sirt1 promotes fat mobilization in white adipocytes by repressing PPAR-gamma. *Nature*. 2004 Jun 17; 429(6993):771-6. Epub 2004 Jun 2. Erratum in: *Nature*. 2004 Aug 19; 430(7002):921.
- Pietrzak K, Czarnecka K, Mikiciuk-Olasik E, Szymanski P.** New Perspectives of Alzheimer Disease Diagnosis - the Most Popular and Future Methods. *Med Chem*. 2018; 14(1):34-43.
- Polito L, Kehoe PG, Davin A, Benussi L, Ghidoni R, Binetti G, Quadri P, Lucca U, Tettamanti M, Clerici F, Bagnoli S, Galimberti D, Nacmias B, Sorbi S, Guaita A, Scarpini E, Mariani C, Forloni G, Albani D.** The SIRT2 polymorphism rs10410544 and risk of Alzheimer's disease in two Caucasian case-control cohorts. *Alzheimers Dement*. 2013 Jul; 9(4):392-9.
- Porquet D, Griñán-Ferré C, Ferrer I, Camins A, Sanfeliu C, Del Valle J, Pallàs M.** Neuroprotective role of trans-resveratrol in a murine model of familial Alzheimer's disease. *J Alzheimers Dis*. 2014; 42(4):1209-20.
- Prati F, Bottegoni G, Bolognesi ML, Cavalli A.** BACE-1 Inhibitors: From Recent Single-Target Molecules to Multitarget Compounds for Alzheimer's Disease. *J Med Chem*. 2018 Feb 8; 61(3):619-637.
- Prince M, Guerchet M, Prina M.** Alzheimer's disease international policy brief for heads of government: the global impact of dementia 2013–2050. *Alzheimer's Disease International (ADI)*. 2013.
- Puente P, Fettig N, Luderer MJ, Jin A, Shah S, Muz B, Kapoor V, Goddu SM, Salama NN, Tsien C, Thotala D, Shoghi K, Rogers B, Azab AK.** Injectable Hydrogels for Localized Chemotherapy and Radiotherapy in Brain Tumors. *J Pharm Sci*. 2018 Mar; 107(3):922-933.
- Purushotham A, Schug TT, Xu Q, Surapureddi S, Guo X, Li X.** Hepatocyte-specific deletion of SIRT1 alters fatty acid metabolism and results in hepatic steatosis and inflammation. *Cell Metab*. 2009 Apr; 9(4):327-38.
- Puzzo D, Gulisano W, Palmeri A, Arancio O.** Rodent models for Alzheimer's disease drug discovery. *Expert Opin Drug Discov*. 2015 Jul; 10(7):703-11.
- Qin W, Yang T, Ho L, Zhao Z, Wang J, Chen L, Zhao W, Thiyagarajan M, MacGrogan D, Rodgers JT, Puigserver P, Sadoshima J, Deng H, Pedrini S, Gandy S, Sauve AA, Pasinetti GM.** Neuronal SIRT1 activation as a novel mechanism underlying the prevention of Alzheimer disease amyloid neuropathology by calorie restriction. *J Biol Chem*. 2006 Aug 4; 281(31):21745-54.
- Qiu T, Liu Q, Chen YX, Zhao YF, Li YM.** A $\beta$ 42 and A $\beta$ 40: similarities and differences. *J Pept Sci*. 2015 Jul; 21(7):522-9.
- Quinti L, Casale M, Moniot S, Pais TF, Van Kanegan MJ, Kaltenbach LS, Pallos J, Lim RG, Naidu SD, Runne H, Meisel L, Rauf NA, Leyfer D, Maxwell MM, Saiah E, Landers JE, Luthi-Carter R, Abagyan R, Dinkova-Kostova AT, Steegborn C, Marsh JL, Lo DC, Thompson LM, Kazantsev AG.** SIRT2- and NRF2-Targeting Thiazole-Containing Compound with Therapeutic Activity in Huntington's Disease Models. *Cell Chem Biol*. 2016 Jul 21; 23(7):849-861.

- Ramadori G, Lee CE, Bookout AL, Lee S, Williams KW, Anderson J, Elmquist JK, Coppari R.** Brain SIRT1: anatomical distribution and regulation by energy availability. *J Neurosci.* 2008 Oct 1; 28(40):9989-96.
- Ramesh S, Govindarajulu M, Lynd T, Briggs G, Adamek D, Jones E, Heiner J, Majrashi M, Moore T, Amin R, Suppiramaniam V, Dhanasekaran M.** SIRT3 activator Honokiol attenuates  $\beta$ -Amyloid by modulating amyloidogenic pathway. *PLoS One.* 2018 Jan 11; 13(1):e0190350.
- Ramsey CP, Glass CA, Montgomery MB, Lindl KA, Ritson GP, Chia LA, et al** Expression of Nrf2 in neurodegenerative diseases *J. Neuropathol. Exp. Neurol.*, 66 (1) (2007), pp. 75-85
- Ranjan VD, Qiu L, Tan EK, Zeng L, Zhang Y.** Modelling Alzheimer's disease: Insights from in vivo to in vitro three-dimensional culture platforms. *J Tissue Eng Regen Med.* 2018;12(9):1944–1958.
- Reed MN, Hofmeister JJ, Jungbauer L, et al.** Cognitive effects of cell-derived and synthetically derived A $\beta$  oligomers. *Neurobiol Aging.* 2011;32(10):1784-1794.
- Reitz C, Mayeux R.** Alzheimer disease: epidemiology, diagnostic criteria, risk factors and biomarkers. *Biochem Pharmacol.* 2014 Apr 15; 88(4):640-51.
- Ren Y, Du C, Shi Y, Wei J, Wu H, Cui H.** The Sirt1 activator, SRT1720, attenuates renal fibrosis by inhibiting CTGF and oxidative stress. *Int J Mol Med.* 2017 May; 39(5):1317-1324.
- Revett TJ, Baker GB, Jhamandas J, Kar S.** Glutamate system, amyloid  $\beta$  peptides and tau protein: functional interrelationships and relevance to Alzheimer disease pathology. *J Psychiatry Neurosci.* 2013 Jan; 38(1):6-23.
- Rice HC, de Malmazet D, Schreurs A, Frere S, Van Molle I, Volkov AN, Creemers E, Vertkin I, Nys J, Ranaivoson FM, Comoletti D, Savas JN, Remaut H, Balschun D, Wierda KD, Slutsky I, Farrow K, De Strooper B, de Wit J.** Secreted amyloid- $\beta$  precursor protein functions as a GABA(B)R1a ligand to modulate synaptic transmission. *Science.* 2019 Jan 11; 363(6423).
- Rodriguez-Ortiz CJ, Baglietto-Vargas D, Martinez-Coria H, LaFerla FM, Kitazawa M.** Upregulation of miR-181 decreases c-Fos and SIRT-1 in the hippocampus of 3xTg-AD mice. *J Alzheimers Dis.* 2014;42(4):1229-1238.
- Rojo AI, Pajares M, Rada P, Nuñez A, Nevado-Holgado AJ, Killik R, Van Leuven F, Ribe E, Lovestone S, Yamamoto M, Cuadrado A.** NRF2 deficiency replicates transcriptomic changes in Alzheimer's patients and worsens APP and TAU pathology. *Redox Biol.* 2017 Oct; 13:444-451.
- Rossner S, Lange-Dohna C, Zeitschel U, Perez-Polo JR.** Alzheimer's disease b secretase BACE1 is not a neuronal-specific enzyme. *J Neurochem* 2005; 92:226–34.
- Saftig P, Lichtenthaler SF.** The alpha secretase ADAM10: A metalloprotease with multiple functions in the brain. *Prog Neurobiol.* 2015 Dec; 135:1-20.
- Salminen A, Kaarniranta K** AMP-activated protein kinase (AMPK) controls the aging process via an integrated signaling network. *Ageing Res Rev* 2012; 11:230–241.
- Saraiva C, Praça C, Ferreira R, Santos T, Ferreira L, Bernardino L.** Nanoparticle-mediated brain drug delivery: Overcoming blood-brain barrier to treat neurodegenerative diseases. *J Control Release.* 2016 Aug 10; 235:34-47.

- Sawda C, Moussa C, Turner RS.** Resveratrol for Alzheimer's disease. *Ann N Y Acad Sci.* 2017 Sep; 1403(1):142-149. doi: 10.1111/nyas.13431. Epub 2017 Aug 16.
- Sayre LM, Perry G, Harris PL, Liu Y, Schubert KA, Smith MA** In situ oxidative catalysis by neurofibrillary tangles and senile plaques in Alzheimer's disease: A central role for bound transition metals. *J Neurochem* 2000; 74, 270-279.
- Sauve AA, Wolberger C, Schramm VL, Boeke JD.** The biochemistry of sirtuins. *Annu Rev Biochem.* 2006; 75:435-65. Review.
- Scheltens P, Blennow K, Breteler MM, de Strooper B, Frisoni GB, Salloway S, Van der Flier WM.** Alzheimer's disease. *Lancet.* 2016 Jul 30; 388(10043):505-17.
- Scuderi C, Stecca C, Bronzuoli MR, Rotili D, Valente S, Mai A, Steardo L.** Sirtuin modulators control reactive gliosis in an in vitro model of Alzheimer's disease. *Front Pharmacol.* 2014 May 13; 5:89.
- Selkoe DJ e Hardy J.** 2016. The amyloid hypothesis of Alzheimer's disease at 25 years. *EMBO Molecular Medicine.* 2016. Review.
- Shen J, Wu J.** Nicotinic Cholinergic Mechanisms in Alzheimer's disease. *Int Rev Neurobiol.* 2015; 124:275-92.
- Shen Z, Li X, Bao X, et al.** Microglia-targeted stem cell therapies for Alzheimer disease: a preclinical data review. *J Neurosci Res* 2017; 95:2420–2429.
- Shin J, Yu SB, Yu UY, Jo SA, Ahn JH.** Swedish mutation within amyloid precursor protein modulates global gene expression towards the pathogenesis of Alzheimer's disease. *BMB Rep.* 2010 Oct; 43(10):704-9.
- Sierra A, Encinas JM, Deudero JJ, Chancey JH, Enikolopov G, Overstreet-Wadiche LS, Tsirka SE, Maletic-Savatic M.** Microglia shape adult hippocampal neurogenesis through apoptosis-coupled phagocytosis. *Cell Stem Cell.* 2010 Oct 8; 7(4):483-95.
- Silberman DM.** Metabolism, neurodegeneration and epigenetics: Emerging role of Sirtuins. *Neural Regen Res.* 2018 Mar; 13(3):417-418.
- Simoni E, Bartolini M, Abu IF, Blockley A, Gotti C, Bottegoni G, Caporaso R, Bergamini C, Andrisano V, Cavalli A, Mellor IR, Minarini A, Rosini M.** Multitarget drug design strategy in Alzheimer's disease: focus on cholinergic transmission and amyloid- $\beta$  aggregation. *Future Med Chem.* 2017 Jun; 9(10):953-963.
- Sinclair DA, Guarente L.** Extrachromosomal rDNA circles--a cause of aging in yeast. *Cell.* 1997 Dec 26; 91(7):1033-42.
- Silva DF, Esteves AR, Oliveira CR, Cardoso SM.** Mitochondrial Metabolism Power SIRT2-Dependent Deficient Traffic Causing Alzheimer's-Disease Related Pathology. *Mol Neurobiol.* 2017 Aug; 54(6):4021-4040.
- Small GW, Greenfield S.** Current and future treatments for Alzheimer disease. *The American Journal of Geriatric Psychiatry.* 2015 Nov; 23(11):1101-5.
- Smith JJ, Kenney RD, Gagne DJ, Frushour BP, Ladd W, Galonek HL, Israelian K, Song J, Razvadauskaite G, Lynch AV, Carney DP, Johnson RJ, Lavu S, Iffland A, Elliott PJ, Lambert PD, Elliston KO, Jirousek MR, Milne JC, Boss O.** Small molecule activators of SIRT1 replicate signaling pathways triggered by calorie restriction in vivo. *BMC Syst Biol.* 2009 Mar 10; 3:31.
- Spires-Jones TL, Fox LM, Rozkalne A, Pitstick R, Carlson GA, Kazantsev AG.** Inhibition of Sirtuin 2 with Sulfobenzoic Acid Derivative AK1 is Non-Toxic and Potentially



- Neuroprotective in a Mouse Model of Frontotemporal Dementia. *Front Pharmacol*. 2012 Mar 12; 3:42.
- Spires-Jones TL, Hyman BT.** The intersection of amyloid beta and tau at synapses in Alzheimer's disease. *Neuron*. 2014 May 21; 82(4):756-71.
- Stamatovic SM, Martinez-Revollar G, Hu A, Choi J, Keep RF, Andjelkovic AV.** Decline in Sirtuin-1 expression and activity plays a critical role in blood-brain barrier permeability in aging. *Neurobiol Dis*. 2018 Sep 6.
- Takahashi RH, Nam EE, Edgar M, Gouras GK.** Alzheimer beta-amyloid peptides: normal and abnormal localization. *Histol Histopathol*. 2002 Jan; 17(1):239-46.
- Takahashi K, Yamanaka S.** Induction of pluripotent stem cells from mouse embryonic and adult fibroblast cultures by defined factors. *Cell*. 2006;126(4):663–676.
- Tarasoff-Conway JM, Carare RO, Osorio RS, Glodzik L, Butler T, Fieremans E, Axel L, Rusinek H, Nicholson C, Zlokovic BV, Frangione B, Blennow K, Ménard J, Zetterberg H, Wisniewski T, de Leon MJ.** Clearance systems in the brain-implications for Alzheimer disease. *Nat Rev Neurol*. 2015 Aug; 11(8):457-70.
- Tarawneh R, Holtzman DM.** The clinical problem of symptomatic Alzheimer disease and mild cognitive impairment. *Cold Spring Harb Perspect Med*. 2012 May; 2(5):a006148.
- Tayeb HO, Yang HD, Price BH, Tarazi FI.** Pharmacotherapies for Alzheimer's disease: beyond cholinesterase inhibitors. *Pharmacol Ther*. 2012 Apr; 134(1):8 25.
- Taylor CJ, Ireland DR, Ballagh I, Bourne K, Marechal NM, Turner PR, Bilkey DK, Tate WP, Abraham WC.** Endogenous secreted amyloid precursor protein-alpha regulates hippocampal NMDA receptor function, long-term potentiation and spatial memory. *Neurobiol Dis*. 2008 Aug; 31(2):250-60.
- Taylor DM, Balabadra U, Xiang Z, Woodman B, Meade S, Amore A, Maxwell MM, Reeves S, Bates GP, Luthi-Carter R, Lowden PA, Kazantsev AG.** A brain-permeable small molecule reduces neuronal cholesterol by inhibiting activity of sirtuin 2 deacetylase. *ACS Chem Biol*. 2011 Jun 17; 6(6):540-6.
- Thal DR and Braak H.** [Post-mortem diagnosis of Alzheimer's disease]. *Der pathologe*. 2005 May; 26(3):201-13.
- Tippmann F, Hundt J, Schneider A et al.** Up-regulation of the alpha-secretase ADAM10 by retinoic acid receptors and acitretin. *FASEB J* 2009; 23:1643–1654.
- Todd S, Barr S, Roberts M, Passmore AP.** Survival in dementia and predictors of mortality: a review. *Int J Geriatr Psychiatry*. 2013 Nov; 28(11):1109-24.
- Tönnies E, Trushina E.** Oxidative Stress, Synaptic Dysfunction, and Alzheimer's Disease. *J Alzheimers Dis*. 2017; 57(4):1105-1121.
- Tougu V, Karafin A, Palumaa P** Binding of zinc(II) and copper(II) to the full-length Alzheimer's amyloid-beta peptide. *J Neurochem* 2008; 104, 1249-1259.
- Tramutola A, Lanzillotta C, Perluigi M, Butterfield DA.** Oxidative stress, protein modification and Alzheimer disease. *Brain Res Bull*. 2017 Jul; 133:88-96.
- Tree J, Kay J.** Longitudinal assessment of short-term memory deterioration in a logopenic variant primary progressive aphasia with post-mortem confirmed Alzheimer's disease pathology. *Journal of neuropsychology*. 2015 Sep; 9(2):184-202.

- Trinchese F, Liu S, Battaglia F, Walter S, Mathews PM, Arancio O.** Progressive age-related development of Alzheimer-like pathology in APP/PS1 mice. *Ann Neurol.* 2004 Jun; 55(6):801-14.
- Tunesi M, Batelli S, Rodilossi S, Russo T, Grimaldi A, Forloni G, Ambrosio L, Cigada A, Gloria A, Albani D, Giordano C.** Development and analysis of semi-interpenetrating polymer networks for brain injection in neurodegenerative disorders. *Int J Artif Organs.* 2013 Nov; 36(11):762-74.
- Tunesi M, Prina E, Munarin F, Rodilossi S, Albani D, Petrini P, Giordano C.** Cross-linked poly(acrylic acids) microgels and agarose as semi-interpenetrating networks for resveratrol release. *J Mater Sci Mater Med.* 2015 Jan; 26(1):5328.
- Uttara B, Singh AV, Zamboni P, Mahajan RT** Oxidative stress and neurodegenerative diseases: A review of upstream and downstream antioxidant therapeutic options. *Curr Neuropharmacol* 2009, 7, 65-74.
- Vandenberghe R, Rinne JO, Boada M, Katayama S, Scheltens P, Vellas B, Tuchman M, Gass A, Fiebich JB, Hill D, Lobello K, Li D, McRae T, Lucas P, Evans I, Booth K, Luscan G, Wyman BT, Hua L, Yang L, Brashear HR, Black RS** Bapineuzumab 3000 and 3001 Clinical Study Investigators. Bapineuzumab for mild to moderate Alzheimer's disease in two global, randomized, phase 3 trials. *Alzheimers Res Ther.* 2016 May 12; 8(1):18.
- Vaquero A, Scher MB, Lee DH, Sutton A, Cheng HL, Alt FW, Serrano L, Sternglanz R, Reinberg D.** SirT2 is a histone deacetylase with preference for histone H4 Lys16 during mitosis. *Genes Dev.* 2006 May 15; 20(10):1256-61.
- Verma M, Vats A, Taneja V.** Toxic species in amyloid disorders: Oligomers or mature fibrils. *Ann Indian Acad Neurol.* 2015 Apr-Jun; 18(2):138-45.
- Villalba JM, Alcaín FJ.** Sirtuin activators and inhibitors. *Biofactors.* 2012 Sep-Oct;38(5):349-59.
- Vinet J, Weering HR, Heinrich A, Kälin RE, Wegner A, Brouwer N, Heppner FL, Rooijen Nv, Boddeke HW, Biber K.** Neuroprotective function for ramified microglia in hippocampal excitotoxicity. *J Neuroinflammation.* 2012 Jan 31; 9:27.
- Viola KL, Klein WL.** Amyloid  $\beta$  oligomers in Alzheimer's disease pathogenesis, treatment, and diagnosis. *Acta Neuropathol.* 2015 Feb;129(2):183-206.
- Walsh DM, Klyubin I, Fadeeva JV, et al.** Naturally secreted oligomers of amyloid beta protein potently inhibit hippocampal long-term potentiation in vivo. *Nature.* 2002;416(6880):535-539.
- Wang B, Zhang Y, Cao W, Wei X, Chen J, Ying W.** SIRT2 Plays Significant Roles in Lipopolysaccharides-Induced Neuroinflammation and Brain Injury in Mice. *Neurochem Res.* 2016 Sep; 41(9):2490-500.
- Wang F, Nguyen M, Qin FX, Tong Q.** SIRT2 deacetylates FOXO3a in response to oxidative stress and caloric restriction. *Aging Cell.* 2007 Aug; 6(4):505-14.
- Wang J, Fivecoat H, Ho L, Pan Y, Ling E, Pasinetti GM.** The role of Sirt1: at the crossroad between promotion of longevity and protection against Alzheimer's disease neuropathology. *Biochim Biophys Acta.* 2010 Aug; 1804(8):1690-4.
- Wang P, Wang ZY** Metal ions influx is a double-edged sword for the pathogenesis of Alzheimer's disease. *Ageing Res Rev* 2016.

- Wang SM, Lee CU, Lim HK.** Stem cell therapies for Alzheimer's disease: is it time? *Curr Opin Psychiatry.* 2019 Mar; 32(2):105-116.
- Wang X, Guan Q, Wang M, Yang L, Bai J, Yan Z, Zhang Y, Liu Z.** Aging-related rotenone-induced neurochemical and behavioral deficits: role of SIRT2 and redox imbalance, and neuroprotection by AK-7. *Drug Des Devel Ther.* 2015 May 7; 9:2553-63.
- Wątroba M, Szukiewicz D.** The role of sirtuins in aging and age-related diseases. *Adv Med Sci.* 2016 Mar; 61(1):52-62.
- Wątroba M, Dudek I, Skoda M, Stangret A, Rzodkiewicz P, Szukiewicz D.** Sirtuins, epigenetics and longevity. *Ageing Res Rev.* 2017 Nov; 40:11-19.
- Wei W, Xu X, Li H, Zhang Y, Han D, Wang Y, Yan W, Wang X, Zhang J, Liu N, You Y.** The SIRT2 polymorphism rs10410544 and risk of Alzheimer's disease: a meta-analysis. *Neuromolecular Med.* 2014 Jun; 16(2):448-56.
- Wen MM, El-Salamouni NS, El-Refaie WM, Hazzah HA, Ali MM, Tosi G, Farid RM, Blanco-Prieto MJ, Billa N, Hanafy AS.** Nanotechnology-based drug delivery systems for Alzheimer's disease management: Technical, industrial, and clinical challenges. *J Control Release.* 2017 Jan 10; 245:95-107.
- Wencel PL, Lukiw WJ, Strosznajder JB, Strosznajder RP.** Inhibition of Poly(ADP-ribose) Polymerase-1 Enhances Gene Expression of Selected Sirtuins and APP Cleaving Enzymes in Amyloid Beta Cytotoxicity. *Mol Neurobiol.* 2018 Jun; 55(6):4612-4623.
- Wood JG, Rogina B, Lavu S, Howitz K, Helfand SL, Tatar M, Sinclair D.** Sirtuin activators mimic caloric restriction and delay ageing in metazoans. *Nature.* 2004 Aug 5; 430(7000):686-9.
- Xu J, Jackson CW, Khoury N, Escobar I, Perez-Pinzon MA.** Brain SIRT1 Mediates Metabolic Homeostasis and Neuroprotection. *Front Endocrinol (Lausanne).* 2018 Nov 23; 9:702.
- Xue F, Huang JW, Ding PY, Zang HG, Kou ZJ, Li T, Fan J, Peng ZW, Yan WJ.** Nrf2/antioxidant defense pathway is involved in the neuroprotective effects of Sirt1 against focal cerebral ischemia in rats after hyperbaric oxygen preconditioning. *Behav Brain Res.* 2016 Aug 1; 309:1-8.
- Yamasaki TR, Blurton-Jones M, Morrisette DA, Kitazawa M, Oddo S, LaFerla FM.** Neural stem cells improve memory in an inducible mouse model of neuronal loss. *J Neurosci.* 2007 Oct 31; 27(44):11925-33.
- Yan J, Hu J, Liu A, He L, Li X, Wei H.** Design, synthesis, and evaluation of multitarget-directed ligands against Alzheimer's disease based on the fusion of donepezil and curcumin. *Bioorg Med Chem.* 2017 Jun 15; 25(12):2946-2955.
- Yang X, Park SH, Chang HC, Shapiro JS, Vassilopoulos A, Sawicki KT, Chen C, Shang M, Burridge PW, Epting CL, Wilsbacher LD, Jenkitkasemwong S, Knutson M, Gius D, Ardehali H.** Sirtuin 2 regulates cellular iron homeostasis via deacetylation of transcription factor NRF2. *J Clin Invest.* 2017 Apr 3; 127(4):1505-1516.
- Yang W, Zou Y, Zhang M et al** Mitochondrial Sirt3 expression is decreased in APP/PS1 double transgenic mouse model of Alzheimer's disease. *Neurochem Res* 2015; 40:1576–1582.
- Yu JT, Tan L, Hardy J.** Apolipoprotein E in Alzheimer's disease: an update. *Annu Rev Neurosci.* 2014; 37:79-100.

- Yuan XZ, Sun S, Tan CC, Yu JT, Tan L.** The Role of ADAM10 in Alzheimer's disease. *J Alzheimers Dis.* 2017; 58(2):303-322.
- Zhang H, Ma Q, Zhang YW, Xu H.** Proteolytic processing of Alzheimer's  $\beta$ -amyloid precursor protein. *J Neurochem.* 2012 Jan; 120 Suppl 1:9-21.
- Zhang YW, Thompson R, Zhang H, Xu H.** APP processing in Alzheimer's disease. *Mol Brain.* 2011 Jan 7; 4:3.
- Zheng W, Tsai MY, Wolynes PG.** Comparing the Aggregation Free Energy Landscapes of Amyloid Beta (1-42) and Amyloid Beta (1-40). *J Am Chem Soc.* 2017 Nov 22; 139(46):16666-16676.
- Zoratto N, Matricardi P.** Semi-IPN- and IPN-Based Hydrogels. *Advances in experimental medicine and biology.* 2018; 1059:155-188.